UNIVERSIDADE FEDERAL DO PARANÁ

MARINES MARIA WILHELM

PANORAMA HISTÓRICO DAS MUDANÇAS AMBIENTAIS NO COMPLEXO ESTUARINO DE PARANAGUÁ, PR, BRASIL: UMA ABORDAGEM GEOQUÍMICA PARA INTERPRETAR AS MUDANÇAS AMBIENTAIS RECENTES

PONTAL DO PARANÁ

2023

MARINES MARIA WILHELM

PANORAMA HISTÓRICO DAS MUDANÇAS AMBIENTAIS NO COMPLEXO ESTUARINO DE PARANAGUÁ, PR, BRASIL: UMA ABORDAGEM GEOQUÍMICA PARA INTERPRETAR AS MUDANÇAS AMBIENTAIS RECENTES

Tese apresentada ao curso de Pós-Graduação em Sistemas Costeiros e Oceânicos, Centro de Estudos do Mar, Universidade Federal do Paraná, como requisito parcial à obtenção do título de Doutor em Sistemas Costeiros e Oceânico.

Orientador: Prof. Dr. César de Castro Martins

PONTAL DO PARANÁ

2023

FICHA CATALOGRÁFICA

DADOS INTERNACIONAIS DE CATALOGAÇÃO NA PUBLICAÇÃO (CIP)
UNIVERSIDADE FEDERAL DO PARANÁ
SISTEMA DE BIBLIOTECAS – BIBLIOTECA DO CENTRO DE ESTUDOS DO MAR

Wilhelm, Marines Maria
Panorama histórico das mudanças ambientais no Complexo Estuarino de Paranaguá, PR, Brasil: uma abordagem geoquímica para interpretar as mudanças ambientais recentes / Marines Maria Wilhelm. – Pontal do Paraná, 2023.
1 recurso on-line : PDF.

Tese (Doutorado) – Universidade Federal do Paraná, Campus Pontal do Paraná, Centro de Estudos do Mar, Programa de Pós-Graduação em Sistemas Costeiros e Oceânicos.

Orientador: Prof. Dr. César de Castro Martins.

1. Sedimentos estuarinos. 2. Carbono. 3. Nitrogênio. I. Martins, César de Castro. II. Universidade Federal do Paraná. Programa de Pós-Graduação em Sistemas Costeiros e Oceânicos. III. Título.

Bibliotecária: Fernanda Pigozzi CRB-9/1151

TERMO DE APROVAÇÃO

MINISTÉRIO DA EDUCAÇÃO
REITORIA
UNIVERSIDADE FEDERAL DO PARANÁ
PRÓ-REITORIA DE PESQUISA E PÓS-GRADUAÇÃO
PROGRAMA DE PÓS-GRADUAÇÃO SISTEMAS COSTEIROS E OCEÂNICOS - 40001016054P6

TERMO DE APROVAÇÃO

Os membros da Banca Examinadora designada pelo Colegiado do Programa de Pós-Graduação SISTEMAS COSTEIROS E OCEÂNICOS da Universidade Federal do Paraná foram convocados para realizar a arguição da tese de Doutorado de **MARINES MARIA WILHELM** intitulada: **PANORAMA HISTÓRICO DAS MUDANÇAS AMBIENTAIS NO COMPLEXO ESTUARINO DE PARANAGUÁ, PR, BRASIL: UMA ABORDAGEM GEOQUÍMICA PARA INTERPRETAR AS MUDANÇAS AMBIENTAIS RECENTES.**, sob orientação do Prof. Dr. CÉSAR DE CASTRO MARTINS, que após terem inquirido a aluna e realizada a avaliação do trabalho, são de parecer pela sua APROVAÇÃO no rito de defesa.

A outorga do título de doutora está sujeita à homologação pelo colegiado, ao atendimento de todas as indicações e correções solicitadas pela banca e ao pleno atendimento das demandas regimentais do Programa de Pós-Graduação.

Pontal do Paraná, 28 de Setembro de 2023.

Assinatura Eletrônica
03/10/2023 12:28:58.0
CÉSAR DE CASTRO MARTINS
Presidente da Banca Examinadora

Assinatura Eletrônica
09/10/2023 10:28:59.0
CASSIA DE OLIVEIRA FARIAS
Avaliador Externo (UNIVERSIDADE DO ESTADO DO RIO DE JANEIRO)

Assinatura Eletrônica
31/10/2023 08:43:21.0
ANA CECILIA RIZZATTI DE ALBERGARIA BARBOSA
Avaliador Externo (UNIVERSIDADE FEDERAL DA BAHIA)

Assinatura Eletrônica
03/10/2023 14:03:39.0
RENATA HANAE NAGAI
Avaliador Interno (UNIVERSIDADE FEDERAL DO PARANÁ)

AGRADECIMENTOS

A Deus. Onipresente em todos os caminhos que decidi seguir. Onisciente de todas as minhas aspirações.

Agradeço à Coordenação de Aperfeiçoamento de Pessoal de Nível Superior (CAPES) e ao Ministério da Ciência, Tecnologia e Inovação por intermédio do Conselho Nacional de Desenvolvimento Científico e Tecnológico (CNPq) por todo suporte financeiro e material provido através de bolsa de estudo e recursos através do projeto EQCEP (Baías do Brasil, 441265/2017-0 – Coordenador: Prof. Dr. Michel Michaelovitch de Mahiques, IO/USP).

A toda equipe do projeto EQCEP, em particular, Paulo Alves de Lima Ferreira, Tailisi Hoppe Trevizani, Italo Martins Paladino, Edilson de Oliveira Faria, Samara Cazzoli y Goya, Satie Taniguchi e aos Professores Renata Hanae Nagai e Rubens Cesar Lopes Figueira pelo apoio nas inúmeras análises realizadas e discussões.

Ao Professor César de Castro Martins pela orientação acadêmica paciente, presente, transparente e criteriosa. Por ser um orientador fiel e sensível, pelas vezes que foi além da sua profissão escutando (chorar) e aconselhando quando necessário. Que confiou no meu trabalho, mesmo quando eu não estava confiante, que me incentivou e apoiou ao longo desses 8 anos. Estou muito grata por sua orientação e incentivo.

Aos revisores das semanas acadêmicas, qualificação, da presente Tese e da revista cientifica em que meu primeiro artigo foi aceito. Seus comentários foram essenciais para a melhoria do trabalho.

Aos professores e funcionários da Pós-Graduação em Sistemas Costeiros e Oceânicos (PGSISCO) e do Centro de Estudos do Mar (CEM), que me proporcionaram uma educação de qualidade e que sempre me incentivaram a aprender. Pelas lições aprendidas e pelas conversas de corredor. Mesmo em dias difíceis, um sorriso ou um cumprimento pôde fazer toda a diferença.

Às LaGPoM *girls* super parceiras que passaram pelo laboratório em algum momento desses 8 anos: Amanda, Ana Caroline (Carol), Ana Lúcia, Fernanda I. (Fer), Josilene (Josi), Marina R. e ao Bruno, um afortunado que nos aturou... e que sempre posso contar com meus amigos, seja no laboratório ou em qualquer outro lugar. Nós conseguimos formar e manter um time. Tenho muito orgulho de fazer parte desse time! A solicitude define esse grupo!

Ao meu pai (*in memorian*), minha mãe e irmãos, que acompanharam meu encanto e dedicação ao estudo e meu desejo de aprender sempre mais todos os dias. Obrigada pelo incentivo, por entender os momentos de ausência ou desânimo e vibrar junto com as conquistas!

Em especial a minha mãe Neli, que me deu suporte para realizar esse sonho. Aos meus irmãos (Alceu, Dirceu e Dorinda), pelo apoio e ajuda incondicional. Meus cunhados (Reinaldo, Patrícia e Junior) pelo companheirismo. Ao Reinaldo meu obrigada, pelas seções de "terapia" e pelas palavras de encorajamento.

Por fim, obrigada a todos que de uma forma ou outra contribuíram para o desenvolvimento deste trabalho!

O RIO E O OCEANO

Diz-se que, mesmo antes de um rio cair no oceano ele treme de medo.
Olha para trás, para toda a jornada, os cumes, as montanhas,
o longo caminho sinuoso através das florestas, através dos
povoados, e vê à sua frente um oceano tão vasto que entrar
nele nada mais é do que desaparecer para sempre.
Mas não há outra maneira. O rio não pode voltar.
Ninguém pode voltar. Voltar é impossível na existência. Você
pode apenas ir em frente.
O rio precisa se arriscar e entrar no oceano.
E somente quando ele entra no oceano é que o medo
desaparece.
Porque apenas então o rio saberá que não se trata de
desaparecer no oceano, mas tornar-se oceano.
Por um lado, é desaparecimento e por outro lado é
renascimento.
Assim somos nós.
Só podemos ir em frente e arriscar.
Coragem! Avance firme e torne-se Oceano!

OSHO

RESUMO

O Complexo Estuarino de Paranaguá (CEP) é um importante ecossistema costeiro brasileiro com rica biodiversidade e importância econômica. O CEP abriga remanescentes de Mata Atlântica, Patrimônio Mundial da UNESCO, e possui o maior terminal graneleiro e o primeiro terminal de movimentação de contêineres da América Latina. O objetivo do presente estudo é realizar a caracterização da MO sedimentar (carbono e nitrogênio nas formas elementares e isotópicas e marcadores orgânicos geoquímicos), em amostras de sedimentos superficial e de testemunhos, a fim de estabelecer o panorama histórico e atual do CEP quanto as mudanças das condições ambientais, e relacionar os resultados obtidos com processos naturais e antrópicos associados às mudanças ambientais em diferentes escalas de tempo. A matéria orgânica sedimentar (MOS) no CEP é predominantemente de origem terrígena, proveniente de afluentes fluviais. A contribuição fluvial, juntamente com as correntes de maré, domina a hidrodinâmica local. No entanto, a região da foz do estuário e o sector norte são fortemente influenciados pela MO marinha. As atividades antrópicas, como a transposição do rio Capivari para o rio Cachoeira e a dragagem no leito e foz do estuário, estão provocando alterações significativas nos sedimentos do sistema e no armazenamento de matéria orgânica local. Estas mudanças podem impactar negativamente a biodiversidade, a qualidade da água e a ciclagem de nutrientes. Os efeitos climáticos de eventos periódicos, como o El Niño-Oscilação Sul, não parecem ter imposto mudanças perceptíveis na MO sedimentar no CEP durante o século passado. Em vez disso, as variações da MO podem responder a mudanças na bacia de drenagem ou a atividades humanas locais específicas. O CEP é um ecossistema complexo que está a ser influenciado por uma variedade de fatores, incluindo atividades humanas e eventos climáticos. Compreender as fontes e processos que controlam a MO sedimentar no CEP é essencial para avaliar a qualidade ambiental da região e desenvolver estratégias de gestão ambiental.

Palavras-chave: Marcadores orgânicos geoquímicos; Composição elementar e isotópica; Carbono. Nitrogênio; Sedimentos estuarinos.

ABSTRACT

The Paranaguá Estuarine System (PES) is an important Brazilian coastal ecosystem with rich biodiversity and economic significance. It houses remnants of the Atlantic Forest, a UNESCO World Heritage Site, and boasts the largest bulk terminal and the first container handling terminal in Latin America. This study aims to characterize sedimentary organic matter (OM) in surface sediment samples and cores through analyzing carbon and nitrogen in elemental and isotopic forms and organic geochemical markers. By doing so, we seek to establish a historical and current perspective on environmental changes within the PES and correlate the obtained results with natural and anthropogenic processes associated with environmental change on different timescales. Sedimentary organic matter (SOM) in the PES predominantly originates from riverine inputs, indicating a terrigenous origin. The fluvial contribution, along with tidal currents, governs local hydrodynamics. However, the estuary mouth region and the northern sector are heavily influenced by marine OM. Anthropogenic activities, such as the diversion of the Capivari River to the Cachoeira River and dredging in the estuary bed and mouth, are causing significant alterations to the system's sediments and the storage of local organic matter. These changes can have negative consequences for biodiversity, water quality, and nutrient cycling. Climatic effects, such as those arising from the El Niño-Southern Oscillation, do not appear to have had noticeable impacts on sedimentary OM in the PES during the past century. Instead, variations in OM may be more responsive to changes within the drainage basin or specific local human activities. The PES is a complex ecosystem influenced by a multitude of factors, including human activities and climate events. Understanding the sources and processes governing sedimentary OM in the PES is crucial for evaluating the region's environmental quality and developing effective environmental management strategies.

Keywords: Geochemical organic markers; Elemental and isotopic composition; Carbon; Nitrogen; Estuarine sediments.

LISTA DE FIGURAS

CAPÍTULO I

CAPÍTULO II

CAPÍTULO III

LISTA DE TABELAS

SUMÁRIO

1 INTRODUÇÃO GERAL

O estuário é um corpo aquoso litorâneo, parcialmente fechado, que recebe aporte de água doce de rios, a qual se mistura com a água salgada do mar, criando uma massa de água salobra com circulação mais ou menos restrita, que mantém comunicação constante com o oceano aberto (Suguio 2003; Gianesella & Saldanha-Corrêa, 2013).

Os estuários são sistemas complexos, devido à circulação que é controlada por diferentes fatores como: vazão dos rios que desaguam no estuário, correntes de marés, rotação da Terra, forças atmosféricas e pelos efeitos da batimetria (geomorfologia de fundo do estuário) (Kowalewska-Kalkowska & Marks, 2015). Além disso, o intemperismo e erosão resultante das bacias de drenagens, originam os sedimentos (partículas inorgânicas) e material orgânico, (detritos de vegetais e organismos), que são transportados pelo escoamento superficial ao leito dos rios que deságuam nos estuários. Ao se depositar, estas partículas constroem o substrato sedimentar, que vão atuar como reservatórios de armazenamento temporário e/ou permanente de resíduos biológicos e químicos, podendo preservar o histórico das transformações do ecossistema, devido a influência dos diferentes tipos de aporte e das interferências causada pela região geográfica que se encontra (Patchineelam, Soares & Calliari, 2008; Manahan, 2013).

Os estuários são zonas de transição entre os ambientes terrestre e marinho. São ecossistemas vulneráveis, pois o desenvolvimento humano está fortemente ligado aos recursos (vivos, minerais e econômicos) que estes ambientes proporcionam. Além disso, o aumento populacional nas últimas décadas tem perturbado a dinâmica natural, fazendo com que o uso e a ocupação do solo sejam alterados, causando mudanças na qualidade das águas e sedimentos e no aporte de matéria orgânica (MO) (Canuel & Hardison, 2016).

Esses ambientes funcionam como uma armadilha de sedimentos, devido às características geomorfológicas e aos processos hidrodinâmicos, associados às interações do sistema de drenagem das bacias que desaguam no estuário, e do regime de marés, criando locais propícios para o acúmulo de material fino e lamoso. Além disso, os estuários estão entre os ecossistemas mais produtivos do mundo, o que favorece a biodiversidade ambiental, além de atuar como um excelente reservatório natural de uma variada gama de elementos de origem biogênica e antrópica, incluindo contaminantes orgânicos e inorgânicos (Brownawel & Farrington, 1986; Odum & Barrett, 2015; Pérez-Fernández et al., 2020). Essas substâncias se aderem ou são adsorvidas ao material particulado devido a sua natureza hidrofóbica, sendo posteriormente incorporadas ao sedimento, permitindo um registro da qualidade ambiental do estuário (Neto, Pozi & Sichel, 2004; Eglinton & Eglinton, 2008).

O processo digenético, responsável pela transformação da MO, tem início logo após a morte (senescência) do organismo que a sintetizou os compostos que formam a MO. Quando de origem terrígena, a MO será retrabalhada, podendo atingir um corpo d'água e alcançar um estuário pela drenagem continental (material alóctone), ou poderá ser reciclada em águas superficiais dentro da alça microbiana, sendo decomposta, remineralizando nutrientes orgânicos e servindo de alimento aos organismos de níveis tróficos superiores (material autóctone) (Azam et al., 1983; Pomeroy et al., 2007). Uma pequena fração desse total pode ser depositado nos sedimentos superficiais, onde continuará o processo diagenético por via biótica ou abiótica (Didyk et al., 1978; Meyers & Ishiwatari, 1993). Em geoquímica orgânica, o termo diagênese é aplicado aos processos que afetam a produção e o consumo de substâncias que ocorrem antes da deposição e durante os estágios iniciais do soterramento do material particulado sob condições de baixa temperatura e pressão, ao contrário da transformação ocorrida em escala geológica (pressões e temperaturas mais altas) (Killops & Killops, 2005).

O aporte de material continental nas zonas costeiras pode ser afetado por fatores antrópicos, que alteram a dinâmica natural de uma região quando a vegetação é removida, aumentando as taxas de erosão, alterações no padrão de vazão, aumento do aporte de MO, nutrientes, contaminantes, e deposição de sedimentos, influenciado pela alteração no uso e ocupação do solo (Cullen, 2008; Calijuri et al., 2013). Isso pode desencadear uma série de mudanças nas condições naturais aos corpos d`água alterando a qualidade ambiental de todo um ecossistema (Odum & Barrett, 2015). Condições que se aproximam dos limites de tolerância de um organismo em seu meio são limitantes, pois desencadeiam alterações ambientais (Calijuri et al., 2013).

Os estuários são amplamente explorados pelo homem, necessitando de uma gestão cuidadosa e monitoramento contínuo dos processos ambientais que neles ocorrem. Por exemplo a deterioração da qualidade da água, devido ao aumento da carga sedimentar, de nutrientes e substâncias contaminantes, causando mudanças nos fluxos das águas, tipos de sedimentos e matéria orgânica (MO) dos rios que desaguam nos estuários. A determinação da saúde do estuário é fundamental para a gestão eficaz dos impactos antropogênicos atuais e futuros dos sistemas costeiros (Hirst, 2004; Birch, 2011; Canuel & Hardison, 2016). Os resultados das mudanças ambientais, naturais e antrópicas podem ser identificados a partir de um estudo criterioso da distribuição, composição e qualidade da MO presente nos sedimentos estuarinos. Em razão da composição da MO estuarina ser uma mistura complexa em diferentes estados de degradação, caracterizada principalmente por material terrígeno oriundo das bacias de drenagem (áreas urbanas, agrícolas e naturais) e insumos marinhos, como organismos aquáticos

(do fento- ao macroplâncton, bactérias, algas entre outros) (Sikes et al., 2009; Canuel & Hardison, 2016; Volkman & Smittenberg, 2017), a MO torna-se um importante componente no estudo das condições atuais e da evolução histórica de um ambiente (Meyers, 1994; 1997; Killops & Killops, 2005; Schulz & Zabel, 2006).

Entre os processos influenciados pelas atividades antrópicas, destaca-se a ciclagem da MO nos diferentes ambientes costeiros. A caracterização da MO em estuários é desafiadora, pois existem inúmeras fontes contribuindo com diferentes proporções para o reservatório de MO (Canuel & Hardison, 2016). Além disso, os processos que afetam a MO atuam de maneira diferente entre materiais de qualidades distintas (Tremblay & Gagné, 2009).

Para compreender e distinguir as principais fontes que contribuem para composição da MO, pode-se empregar ferramentas geoquímicas, como os marcadores moleculares e indicadores da composição elementar e isotópica (Meyers, 1997). Os marcadores moleculares têm estabilidade química e origem definida e, portanto, podem auxiliar no entendimento dos ciclos da MO, desde sua origem até o estado diagenético atual, bem como na identificação de alterações antropogênicas e dos efeitos causados por estressores químicos (Meyers, 1997; Canuel & Hardison, 2016; Filimonova, et al., 2016).

Durante a sedimentação da MO e a incorporação nos sedimentos de fundo, mais de 90% do material inicial é remineralizado (Eadie et al., 1984, Meyers, 2003). Desse modo, é necessário o uso de múltiplos *proxies*, para entender os vários processos ativos de alterações ambientais em um sistema estuarino, tanto para reconstrução das mudanças de um ecossistema, como para entender as transformações atuais na composição do sedimento superficial. Dentre as principais classes de marcadores moleculares presentes nos sedimentos podemos citar os *n*-alcanos, *n*-alcanóis e esteróis, que são diretamente relacionados com organismos aquáticos, bactérias, algas, fungos e plantas superiores, compondo a MO sedimentar (Harwood & Russel 1984; Meyers, 1997; Volkman, 2006; Libes, 2011). Eles podem ser aplicados desde a reconstrução paleoambiental, com foco nas mudanças climáticas regionais, e para estudar ambientes modernos, para distinguir as diferentes fontes de carbono, alóctone, autóctone e de origem antrópica com base nos diferentes grupos de compostos geoquímicos (Martins et al. 2023; Liu & Liu, 2016).

Os *n*-alcanos são hidrocarbonetos alifáticos, de cadeia linear aberta e sem ramificações, classificados pelo comprimento de suas cadeias carbônicas: cadeias curtas (*n*-C_{15}, *n*-C_{17} e *n*-C_{19}), que ocorrem em algas e bactérias, destacando-se o *n*-C_{17} em sedimentos contemporâneos (Meyers & Eadie, 1993; Volkman et al., 1998); cadeias médias (*n*-C21, *n*-C_{23} e *n*-C_{25}), que estão relacionadas a macrófitas emersas e flutuantes, e as cadeias longas (*n*-C_{27}, *n*-C_{29} e *n*-C_{31}), que

predominam nas ceras epicuticulares das folhas das plantas superiores (Meyers & Eadie, 1993; Meyers, 1997).

Os *n*-alcanóis apresentam estrutura semelhante aos *n*-alcanos, porém contêm um grupo funcional hidroxila (-OH) ligado a um carbono terminal, sendo utilizados de forma complementar aos *n*-alcanos. No material terrígeno, predominam os *n*-alcanóis de cadeias longas (*n*-C_{22}-OH, *n*-C_{24}-OH, *n*-C_{26}-OH, *n*-C_{28}-OH e *n*-C_{30}-OH), enquanto algas e bactérias apresentam *n*-alcanóis de cadeias curtas (*n*-C_{16}-OH a *n*-C_{22}-OH) e o *n*-C_{24}-OH também é um biomarcador proveniente de macrófitas submersas e cianobactérias (Meyers, 2003).

Os esteróis são triterpenóides construídos a partir de unidades de isopreno, que é um hidrocarboneto alifático e insaturado contendo 5 átomos de carbono, responsável por formar uma diversidade de compostos cíclicos e acíclicos devido a ligações duplas e a capacidade de polimerização, formando anéis ou cadeias abertas. São moléculas essenciais aos organismos vivos, pois estão presentes em suas membranas celulares dando rigidez a esta estrutura (Killops & Killops, 2005; Peters et al., 2005). Os esteróis sintetizados por organismos fotossintéticos, os fitoesteróis, são comumente utilizados para verificar as mudanças no aporte de MO de origem terrígena nas áreas costeiras, sendo os esteróis sitosterol (24-etil-colest-5-en-3β-ol, $C_{29}\Delta^5$) e estigmasterol (24-etilcolest-5,22E-dien-3β-ol, $C_{29}\Delta^{5,22E}$) frequentemente associados com plantas superiores (Killops & Killops, 1993; Bianchi & Canuel, 2011). Já o esterol brassicasterol (24-metilcolest-5,22E-dien-3β-ol, $C_{28}\Delta^{5,22E}$) é associado a diatomáceas e cocolitoforideos, o colesterol a algas e animais (Meyers, 1997).

As principais aplicações dos marcadores moleculares, vão além da especificidade de fonte, podendo ser empregados para verificar a qualidade nutricional do ambiente e perturbações antrópicas (uso e ocupação do solo, descarga de esgotos *in natura*, eutrofização, derrames de petróleo, introdução de estressores químicos como metais e pesticidas, entre outros). Auxiliam também como parâmetro de avaliação do nível de degradação e preservação da MO, possibilitando um estudo da evolução ambiental da MO em diferentes escalas de tempo, facilitando a compreensão do ciclo biogeoquímico local do carbono e a disponibilidade de componentes essenciais para a manutenção da biota associada (Peters & Moldowan, 1993; Meyers, 1994; 1997; Freeman & Pancost, 2014).

O litoral paranaense passou por vários cenários econômicos, desde o ciclo do ouro de aluviões (século XVI) até despontar no cenário nacional e internacional em função da atividade portuária (década de 1970) (Pierri et al., 2006; Chemin & Abrahão, 2014). Após a Segunda Guerra Mundial, houve a modernização do Porto de Paranaguá para suportar navios com maior calado, buscando adequar-se à demanda mundial. Com isso, houve a necessidade de aprofundar

o canal de acesso ao porto e com o passar do tempo, tornou-se o maior porto graneleiro da América Latina e atualmente destaca-se pelo maior Terminal de Contêineres da América do Sul (TCP, 2020).

Paralelamente, houve um aumento populacional na região, passando de 167.231 habitantes, no ano de 2010, para 171.350 em 2022. Esta população está distribuída de forma desigual entre os três municípios que margeiam o Complexo Estuarino de Paranaguá (CEP): 85,1 % pertencente a Paranaguá, 10,6 % a Antonina e 4,3 % a Guaraqueçaba (Pierri et al., 2006; Chemin & Abrahão, 2014; IBGE, 2023). O município de Paranaguá possui 44,1 % de esgotamento sanitário adequado e Guaraqueçaba até 91,5 %, enquanto Antonina coleta, mas não trata seu esgoto (ANA, 2022).

Como consequência das atividades portuárias, agrícolas e de uso e ocupação do solo, os impactos ambientais na bacia de drenagem resultam em maior aporte de sedimentos e MO para o estuário, bem como a ressuspensão do sedimento de fundo quando o canal de acesso ao porto necessita de dragagem, além do impacto causado pelo transporte marítimo, atividades de lazer e turismo, bem como o uso e extração dos recursos naturais (Marone et al., 2005).

Desse modo, faz-se necessário entender os componentes da MO que chegam aos estuários, e os ciclos biogeoquímicos da MO nesses ambientes e suas alterações, com base nas análises elementares, isotópicas e moleculares da MO sedimentar. A integração destas ferramentas biogeoquímicas com a geocronologia e a sedimentologia do estuário permite entender as alterações ambientais ocorridas em uma determinada escala de tempo, refletindo não apenas o impacto recente das atividades humanas, mas também a variabilidade natural condicionada, por exemplo, por processos climáticos.

Considerando a versatilidade desses marcadores moleculares, podemos empregá-los para elucidar diferentes questões, relacionadas a origem do material orgânico introduzido no ambiente estuarino, como os constituintes moleculares da MO sedimentar que fornece detalhes da produção, distribuição e preservação (Meyers, 1997). Podemos citar exemplos específicos dessa utilização como: o uso de *n*-alcanos para distinguir a contribuição de fontes especificas da MO, onde cadeias curtas e ímpares ocorrem em algas e bactérias, cadeias médias estão relacionadas a macrófitas emersas e flutuantes, e cadeia longas predominam nas ceras epicuticular das folhas nas plantas superiores. Além disso, eles são utilizados para identificar a presença de petróleo e derivados; a predominância de cadeias carbônicas longas e pares de *n*-alcanóis é utilizada para identificar a contribuição de material terrígeno (Eglinton & Eglinton, 1967; Meyers et al., 2003; Alfaro et al., 2006; Martins et al., 2010; Volkman & Smittenberg, 2017).

1.1 Justificativa

O presente estudo elucidou o panorama atual e histórico do CEP no que diz respeito a qualidade ambiental local, através da análise detalhada de MO nas suas principais componentes (elementar, isotópica e molecular) presentes em sedimentos superficiais e testemunhos. Desta forma, esta Tese contribui para o entendimento das alterações locais nos ciclos, através de informações biogeoquímicas que permitiram entender os processos de transferência de materiais entre continente e estuário, relacionando-as com a mudança climática e a ação antrópica em diferentes escalas de tempo. As informações geradas contribuem para a gestão sustentável do Complexo Estuarino de Paranaguá, para o entendimento dos efeitos das mudanças climáticas e para a tomada de decisões sobre a conservação e o uso sustentável dos ambientes costeiros e dos recursos marinhos.

Este estudo fornece informações relevantes para o cumprimento dos Objetivos do Desenvolvimento Sustentável (ODS), da Agenda 2030 da ONU (https://www.agenda2030.com.br/) no que se refere aos oceanos e sistemas costeiros, a citar: (i) ODS 6: Assegurar a disponibilidade e gestão sustentável de água e saneamento para todos; (ii) ODS 13: Tomar medidas urgentes para combater a mudança climática e seus impactos; (iii) ODS 14: Conservação e uso sustentável dos oceanos, dos mares e dos recursos marinhos para o desenvolvimento sustentável (UN, 2015).

Os objetivos desse estudo contribuíram para as metas dos ODS citados anteriormente, sendo que os dados gerados poderão auxiliar na identificação da poluição oriunda das atividades terrestres, agrícola, despejos de esgoto urbanos e industriais, além de contribuir com indicadores da mudança climática. Além disso, esta Tese apresenta informações para o gerenciamento dos oceanos de forma sustentável, tendo em vista a integração entre a ciência e a política, por meio dos tomadores de decisões locais e nacionais em consonância aos objetivos gerais de fortalecimento da Ciência Oceânica ao longo da próxima década (https://en.unesco.org/ocean-decade).

1.2 Objetivos

1.2.1 Objetivo geral

Realizar a caracterização da MO sedimentar (carbono e nitrogênio nas formas elementares e isotópicas e marcadores orgânicos geoquímicos), em amostras de sedimentos superficial e de testemunhos, a fim de estabelecer o panorama histórico e atual do CEP quanto as mudanças das condições ambientais, e relacionar os resultados obtidos com processos naturais e antrópicos associados às mudanças ambientais em diferentes escalas de tempo.

1.2.2 Objetivos específicos

→ Fazer um diagnóstico espacialmente detalhado e recente da qualidade ambiental e da natureza da composição orgânica dos sedimentos recentes do CEP por meio da determinação da composição elementar e isotópica da MO e de marcadores moleculares como os n-alcanos e n-alcanóis em sedimentos superficiais (Capítulo I);

→ Avaliar possíveis alterações no ciclo biogeoquímico da MO sedimentar e possíveis alterações composicionais em função da variabilidade climática e da ação antrópica, através da determinação da composição elementar e isotópica da MO em testemunhos sedimentares (Capítulo II);

→ Relacionar geocronologicamente os resultados dos parâmetros geoquímicos determinados com eventos naturais e antrópicos a fim de estabelecer um histórico das alterações ambientais ocorridas na região, e (Capítulo II e Capítulo III);

1.3 Hipóteses

H_1: Se houve alteração no ciclo biogeoquímico da MO ao longo do período estudado, então a composição elementar e isotópica da MO e o fluxo de carbono sequestrado pelo sedimento devem ser maiores que os fluxos de carbono pré-industriais para a região.

H_1: Se a intensificação das atividades humanas na costa paranaense gerou um aumento no aporte de material oriundo de áreas urbanas e agrícolas, então as concentrações dos marcadores moleculares serão maiores nas regiões mais urbanizadas.

Referências

Alfaro, A.C., Thomas, F., Sergent, L., & Duxbury, M. 2006. Identification of trophic interactions within an estuarine food web (northern New Zealand) using fatty acid biomarkers and stable isotopes. *Estuarine, Coastal and Shelf Science*, *70*(1-2), 271-286.

ANA (Agência Nacional de Águas). 2022. Atlas esgotos: despoluição de bacias hidrográficas. Mapas interativos. Disponível em < http://atlasesgotos.ana.gov.br/> Acesso em: nov/2022.

Azam, F., Fenchel, T., Field, J. G., Gray, J. S., Meyer-Reil, L. A., Thingstad, F. 1983. The ecological role of water-column microbes in the sea. *Marine ecology progress series*, 257-263.

Bianchi, T.S.; Canuel, E.A. 2011. Chemical biomarkers in aquatic ecosystems. Princeton, NJ: Princeton University Press, 392p.

Birch, G.F. 2011. Indicators of anthropogenic change and biological risk in coastal aquatic environments. Wolanski E, McLusky DS. Treatise on estuarine and coastal science. Ed. Waltham: Academic Press. Publisher: Elsevier, 235-270.

Brownawell, B. J., Farrington, J. W. 1986. Biogeochemistry of PCBs in interstitial waters of a coastal marine sediment. *Geochimica et Cosmochimica Acta*, *50*(1), 157-169.

Calijuri, M. D. C., Cunha, D. G. F., Moccellin, J. 2013. Fundamentos ecológicos e ciclos naturais. *Engenharia Ambiental: Conceitos, Tecnologia e Gestão. São Paulo: Elsevier Editora Ltda.*

Canuel, E. A., Hardison, A. K. 2016. Sources, ages, and alteration of organic matter in estuaries. *Annual Review of Marine Science*, *8*, 409-434.

Chemin, M., Abrahão, C. M. 2014. Integração territorial do litoral do Estado do Paraná (Brasil): transportes, balnearização e patrimonialização na formação e dinâmica do espaço turístico. *Raega-O Espaço Geográfico em Análise*, *32*, 212-239.

Cullen, P. 2008. Water in the landscape: The coupling of aquatic ecosystems and their catchments. *Managing and Designing Landscapes for Conservation: Moving from Perspectives to Principles*, 458.

Didyk, B. M., Simoneit, B. R. T., Brassell, S. T., Eglinton, G. 1978. Organic geochemical indicators of palaeoenvironmental conditions of sedimentation. *Nature*, *272*(5650), 216-222.

Eadie, B. J., Chambers, R. L., Gardner, W. S., Bell, G. L. 1984. Sediment trap studies in Lake Michigan: Resuspension and chemical fluxes in the southern basin. *Journal of Great Lakes Research*, *10*(3), 307-321.

Eglinton, G., Hamilton, R. J. 1967. Leaf Epicuticular Waxes: The waxy outer surfaces of most plants display a wide diversity of fine structure and chemical constituents. *science*, *156*(3780), 1322-1335.

Eglinton, T. I., Eglinton, G. 2008. Molecular proxies for paleoclimatology. *Earth and Planetary Science Letters*, *275*(1-2), 1-16.

Filimonova, V., Goncalves, F., Marques, J. C., De Troch, M., Goncalves, A. M. 2016. Fatty acid profiling as bioindicator of chemical stress in marine organisms: a review. *Ecological indicators*, *67*, 657-672.

Freeman, K. H., Pancost, R. D. 2014. Biomarkers for terrestrial plants and climate. In *Organic Geochemistry* (pp. 395-416). Elsevier Inc..

Gianesella, S.M.F., Saldanha-Corrêa, F.M.P. 2013. Oceanos e áreas costeiras. Engenharia Ambiental: Conceitos, Tecnologia e Gestão. São Paulo: Elsevier Editora Ltda.

Harwood, J. L., Russell, N. J. 1984. Lipids in plants and microbes Allen and Unwin.

Hirst, A. J. 2004. Broad-scale environmental gradients among estuarine benthic macrofaunal assemblages of south-eastern Australia: implications for monitoring estuaries. Marine and Freshwater Research, 55(1), 79-92.

IBGE (Instituto Brasileiro de Geografia e estatística). 2023. Densidade populacional estimada. Disponível em: https://cidades.ibge.gov.br. Acesso em: Out/2023.

Killops, S.D., Killops, V.J. 1993. An introduction to organic geochemistry. New York: Longman Scientific &Technical,. 265 p..

Killops, V. J., Killops, S. D. 2005. Introduction to organic geochemistry. Blackwell Science Ltda, p.406.

Kowalewska-Kalkowska, H., Marks, R. 2015. Estuary, estuarine hydrodynamics. Encykl. Mar. Geosci, 1, 235-238.

Libes, S. 2011. Introduction to marine biogeochemistry. Academic Press.

Liu, H., Liu, W. 2016. n-Alkane distributions and concentrations in algae, submerged plants and terrestrial plants from the Qinghai-Tibetan Plateau. Organic geochemistry, 99, 10-22.

Manahan, S.E. 2013. Química Ambiental. 9.ed. Porto Alegre: Bookman, 912 p.

Marone, E., Machado, E. C., Lopes, R. M., Silva, E. T. D. 2005. Land-ocean fluxes in the Paranaguá Bay estuarine system, southern Brazil. *Brazilian Journal of Oceanography*, *53*, 169-181.

Martins, C. C., Braun, J. A., Seyffert, B. H., Machado, E. C., Fillmann, G. 2010. Anthropogenic organic matter inputs indicated by sedimentary fecal steroids in a large South American tropical estuary (Paranaguá estuarine system, Brazil). *Marine Pollution Bulletin*, *60*(11), 2137-2143.

Martins, C. C., Adams, J. K., Yang, H., Shchetnikov, A. A., Di Domenico, M., Rose, N. L., & Mackay, A. W. 2023. Earthquake, floods and changing land use history: A 200-year overview of environmental changes in Selenga River basin as indicated by n-alkanes and related proxies in sediments from shallow lakes. *Science of The Total Environment*, *873*, 162245.

Meyers, P. A. 1994. Preservation of elemental and isotopic source identification of sedimentary organic matter. *Chemical geology*, *114*(3-4), 289-302.

Meyers, P. A. 1997. Organic geochemical proxies of paleoceanographic, paleolimnologic, and paleoclimatic processes. *Organic geochemistry*, *27*(5-6), 213-250.

Meyers, P. A. 2003. Applications of organic geochemistry to paleolimnological reconstructions: a summary of examples from the Laurentian Great Lakes. *Organic geochemistry*, *34*(2), 261-289.

Meyers, P. A., Eadie, B. J. 1993. Sources, degradation and recycling of organic matter associated with sinking particles in Lake Michigan. *Organic Geochemistry*, *20*(1), 47-56.

Meyers, P. A., Ishiwatari, R. 1993. Lacustrine organic geochemistry—an overview of indicators of organic matter sources and diagenesis in lake sediments. *Organic geochemistry*, *20*(7), 867-900.

Neto, J. B., Ponzi, V. R. A., Sichel, S. E. 2004. Introdução à geologia marinha. Editora Interciência, 279.

Odum, E.P., Barrett, G.W. 2015. Fundamentos de ecologia. São Paulo: Cengage Learning, p. 611.

Patchineelam, S.M., Soares, C.R., Calliari, L.J. 2008. Assoreamento, aterros e dragagens. *Poluição Marinha.* Rio de Janeiro: Editora Interciência.

Pérez-Fernández, B., Viñas, L., Besada, V. 2020. Concentrations of organic and inorganic pollutants in four Iberian estuaries, North Eastern Atlantic. Study of benchmark values estimation. *Marine Chemistry*, *224*, 103828.

Peters, K. E., Moldowan, J. M. 1993. The biomarker guide: interpreting molecular fossils in petroleum and ancient sediments.

Peters, K. E., Walters, C. C., Moldowan, J. M. 2005. The biomarker guide: Volume 1, Biomarkers and isotopes in the environment and human history. Cambridge University Press.

Pierri, N., Angulo, R. J., de SOUZA, M. C., Kim, M. K. 2006. A ocupação e o uso do solo no litoral paranaense: condicionantes, conflitos e tendências. *Desenvolvimento e Meio Ambiente*, *13*.

Pomeroy, L. R., WILLIAMS, P. J., Azam, F., Hobbie, J. E. 2007. The microbial loop. *Oceanography*, *20*(2), 28-33.

Sikes, E. L., Uhle, M. E., Nodder, S. D., Howard, M. E. 2009. Sources of organic matter in a coastal marine environment: evidence from n-alkanes and their δ13C distributions in the Hauraki Gulf, New Zealand. *Marine Chemistry*, *113*(3-4), 149-163.

Suguio, K. 2003. Geologia sedimentar. Editora Blucher.

Schulz, H.D.; Zabel, M. 2006. Marine Geochemistry. 2.ed. Berlin: Springer, p. 574.

Schwarzbauer, J., & Jovančićević, B. 2016. From biomolecules to chemofossils. Springer International Publishing.

TCP (Terminal de Contêineres de Paranaguá). 2020. TCP quebra recordes de movimentações. Disponível em: <https://www.tcp.com.br/tcp-quebra-recordes-de-movimentacoes/>. Acesso em: Out/2020.

Tremblay, L., & Gagné, J. P. 2009. Organic matter distribution and reactivity in the waters of a large estuarine system. Marine Chemistry, 116(1-4), 1-12.

Volkman, J. K., Smittenberg, R. H. 2017. Lipid biomarkers as organic geochemical proxies for the paleoenvironmental reconstruction of estuarine environments. *Applications of paleoenvironmental techniques in estuarine studies*, 173-212.

Volkman, J. K. 2006. Lipid markers for marine organic matter. *Marine organic matter: biomarkers, isotopes and DNA*, 27-70.

Volkman, J. K., Barrett, S. M., Blackburn, S. I., Mansour, M. P., Sikes, E. L., Gelin, F. 1998. Microalgal biomarkers: a review of recent research developments. *Organic Geochemistry*, *29*(5-7), 1163-1179.

2 CAPÍTULO I

Geochemical mapping of modern sedimentary organic matter deposited on a subtropical estuary affected by human activities: stable isotopes and molecular approaches

Marines M. Wilhelm[1,2,*], Ana Caroline Cabral[1], Ana Lúcia L. Dauner[3], The LaGPoM Group [2,$], Renata H. Nagai[2,4], Rubens C.L. Figueira[4], Michel M. Mahiques[4], César C. Martins[2,4,*]

[1] Graduate Program in Coastal and Oceanic Systems, Federal University of Paraná, Pontal do Paraná, PR, Brazil.

[2] Center of Marine Studies, Campus Pontal do Paraná, Federal University of Paraná, Pontal do Paraná, PR, Brazil.

[3] Ecosystems and Environment Research Program, University of Helsinki, Helsinki, Finland.

[4] Oceanographic Institute, University of São Paulo, São Paulo, SP, Brazil.

Corresponding authors: * wilhelm.marines@gmail.com (M.M. Wilhelm)
* ccmart@ufpr.br (C.C. Martins)

[$] The LaGPoM Group included the following co-authors: Amanda Câmara de Souza, Bruno Martins Gurgatz, Fernanda Kassumi Ishii, Marina Reback Garcia.

Abstract

The Paranaguá Estuarine System (PES) plays an important ecological and economic role in the coastal zone of Brazil. It is home to relevant remaining areas of the Atlantic rainforest, considered a World Heritage Site by UNESCO. At the same time, PES accommodates the largest grain bulk terminal and is the first place in container handling in Latin America. In this study, we combined elemental and isotopic composition, and molecular markers (n-alkanes and n-alkanols) to understand and distinguish the primary sources of sedimentary organic matter (OM) to evaluate the environmental quality of a WHS under human pressure. Composition was carried out using a wide sample set of surface sediments of the PES, to provide a geochemical mapping of the OM. A mapping of the different sectors of the estuarine system based on the predominance of terrigenous and marine source materials in sediments was purposed. Primary OM origin is the terrigenous contribution from fluvial inputs. The fluvial contribution, together with tidal currents, dominates the local hydrodynamics. However, the estuarine mouth region and north sector are strongly influenced by marine OM. It was also observed that the hydrodynamics controls the OM deposition in Antonina Bay due to the low energy, favouring the deposition of fine sediments. In Paranaguá Bay, due to the presence of a mixing zone with intrusion of fresh- and marine waters, there are sites of preferential accumulation of OM caused by the flocculation of fine particles. This geochemical mapping of sedimentary OM composition may be important in the future scenarios of environmental changes to track the deposition and accumulation of anthropogenic residues from the continental basin and port activities.

Keywords: Organic matter; Molecular markers; Atlantic Rainforest; Sediments**;** Organic carbon; Nitrogen; Phosphorus.

2.1 Introduction

The organic matter (OM) present in estuarine sediments is a complex mixture of aquatic and continental material in different states of degradation. Terrestrial material comes from runoff of drainage basins that includes agricultural, forestry and urban inputs (Canuel and Hardison, 2016). Several classes of biomolecules make up the OM, including polysaccharides (cellulose, hemicellulose, chitin), proteins, lipids/aliphatic materials (fatty acids, waxes, cutin, suberin, and terpenoids), and lignin (De Leeuw and Largeau, 1993; Baldock et al., 2004). To understand and distinguish the primary sources of sedimentary OM, geochemical tools such as molecular markers and the elemental (carbon, nitrogen, and phosphorus) and isotopic ($\delta^{13}C$ and $\delta^{15}N$) composition of the OM has been applied over decades (Meyers, 1997).

The organic carbon found in the estuary is derived from allochthonous sources and autochthonous primary production, as a main component of OM. Despite being abundant in the atmosphere as $N_{2\,(g)}$, nitrogen is not very bioavailable in this form. Some organisms, especially bacteria, may convert N_2 into more bioavailable forms, such as NH_4^+ and NO_3^-, making nitrogen more available in soils and aquatic environments (Kuypers et al., 2018). Phosphorus is derived from continental rocks weathering, and it can be transported to marine environments by river input or by atmospheric deposition of mineral aerosols, such as dust and ash from forest fires (Calijuri et al., 2013; Peñuelas et al., 2013). Primary producers require essential nutrients as NO_3^- and PO_4^{3-}, that reach the aquatic systems from the drainage basins and degradation of labile autochthonous OM, promoting the maintenance of organic carbon cycle (Meyers, 1997).

In the last 50 years, the changes in land use and coastal human occupation, the increased fertilizer uses in agriculture and the discharge of domestic and industrial sewage into rivers and estuaries, have increased the transport of phosphorus and nitrogen to the aquatic environment (Vieira Filho, 2016; Dan et al., 2020). This anthropogenic contribution may potentially change the chemical composition of estuarine waters, the structure and composition of biotic communities and, consequently, the sediments (Daniel et al., 2002; Piola et al., 2006; Barros et al., 2010).

Molecular markers are compounds produced by living organisms, that present little or no changes in the chemical structure after deposition and may reflect both the source and the biogeochemical processes involved in OM diagenesis and water column and sediments (Eganhouse, 1997; Peters et al., 2005). In addition, molecular markers can be applied to assess the nutritional quality of the environment and anthropogenic disturbances, related to sewage

discharge, eutrophication, and agriculture residues (Meyers, 1997; Canuel and Hardison, 2016; Filimonova et al., 2016).

The Paranaguá Estuarine System (PES) plays an important ecological and economic role in the coastal zone of Brazil. It encompasses relevant remaining areas of the Atlantic rainforest, considered a World Natural Heritage Site since 1999 (UNESCO, 1999). The PES hosts the largest maritime grain bulk terminal and is the main container handling in South America (TCP, 2020). Thus, the discrimination of the primary sources of sedimentary OM becomes essential to understand the current environmental quality and predict changes in the organic carbon cycle of a subtropical estuarine system under increased human influence over natural conditions.

This study presents a set of different approaches to categorize the spatial distribution of sedimentary OM based on the elementary, isotopic, and molecular analyses of modern sediment of PES. Biogeochemical studies of OM composition in estuarine South Hemisphere environments are limited and the results may purpose strategies to understand the local alterations in organic carbon cycle and the processes of land-sea material transfer, fully applicable in a global perspective.

2.2 Study Area

The PES is located on the north-central coast of the state of Paraná (25°00'S – 25°35'S; 48°15'W – 48°40'W) in Southern Brazil and covers an area of approximately 622 km^2 (Fig. 1). The PES is subdivided into two axes. The main axis is positioned at an 'E–W' direction, about 56 km length, comprising the Antonina (west inner portion) and Paranaguá (central portion) bays where human occupation and port activities are intensively developed. The 'N–S' axis includes the Laranjeiras, Guaraqueçaba, and Pinheiros bays (north inner portion), about 30 km long, and it is considered the most preserved area of PES, with the occurrence of artisanal fishing and local farming activities as the subsistence human activities (Marone et al., 2005; Lamour et al., 2007; Martins et al., 2010; 2015).

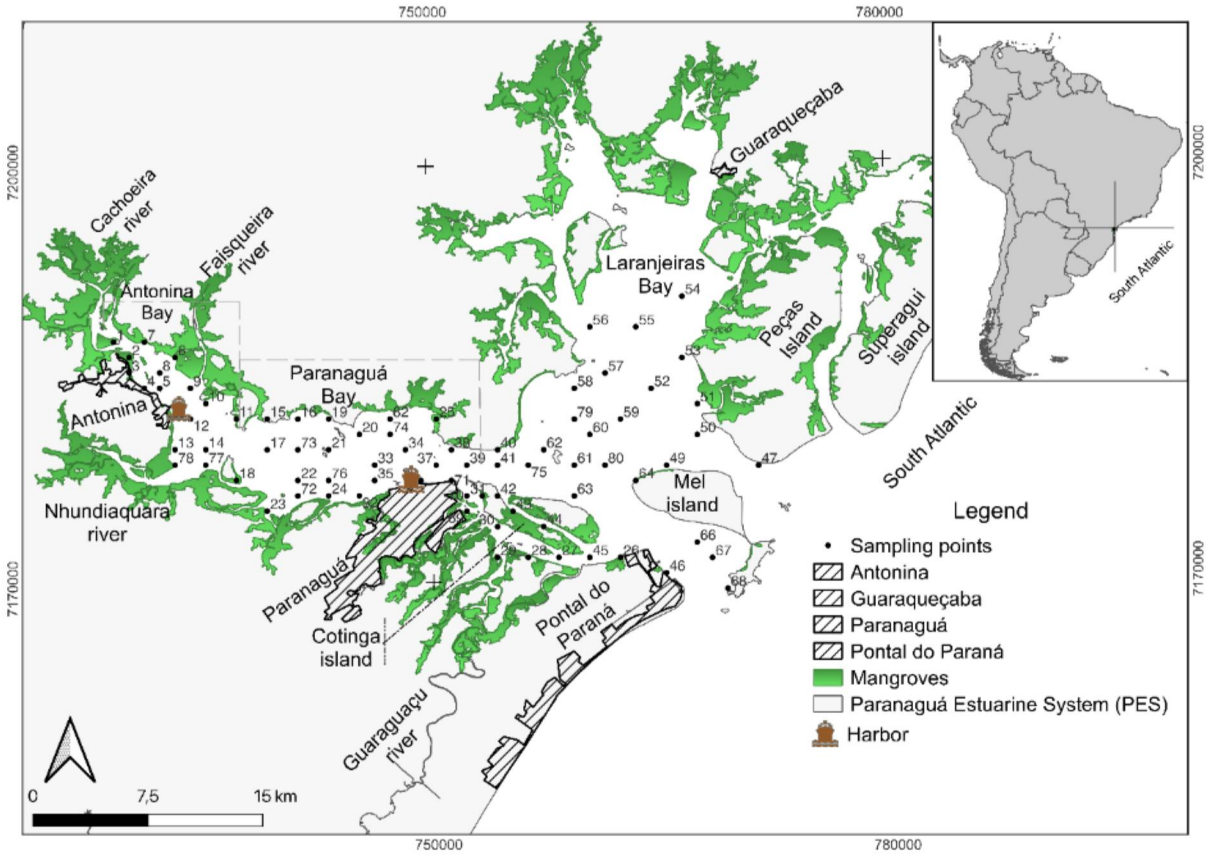

Figure 1-Map of the studied area: Paranaguá Estuarine System, South Atlantic, and sampling points.

The 'E–W' axis has a more significant human influence due to commercial fishing, urban occupation, tourist activities, and the presence of fertilizer industries, fuel terminals and the ports of Antonina and Paranaguá (Martins et al., 2015; Cardoso et al., 2016). The primary sources of dissolved inorganic nitrogen for PES are river input and sewage disposal from Paranaguá city (Mizerkowski et al., 2012), while dissolved inorganic phosphorus input is associated with port activities and riverine input. Conversely, the 'N–S' axis is characterized by large extensions of Environmental Protection Areas (Lana et al., 2001; Martins et al., 2012).

The sedimentary processes present in PES are affected by fluvial freshwater discharge and currents generated by waves and tides. Antonina Bay is dominated by river flows, favouring the deposition of fine sediments and, consequently, the accumulation of OM. At the mouth of the estuary (i.e., the east outer portion), currents generated by offshore waves and tides predominate and promote the deposition of coarse sediments (Angeli et al., 2020; Paladino et al., 2022).

127 The PES is surrounded by a mountainous region called 'Serra do Mar'. With more than
128 1000 m slope between the plateau and sea level, the intense wind current support the mountain
129 erosion, generating materials that reach the coastal basins (Angulo et al., 2006). An example of
130 this potential erosion is observed in the drainage basins that flow into Antonina Bay, presenting
131 diverse contributions. The northern margin receives about 82.7 ton km^{-2} a^{-1} of continental
132 material via the Cachoeira and Faisqueira rivers, while the southern margin receives
133 approximately 176 ton km^{-2} a^{-1} via the Nhundiaquara river (Cattani and Lamour, 2016).
134 According to the physicochemical characteristics of the water column, this estuary is classified
135 as partially mixed with lateral heterogeneities. The geomorphology of the margins and the water
136 circulation determine ecological gradients, and an estuarine sectorization (Marone et al., 2005;
137 Martins et al., 2011; Lessa et al., 2018). The geomorphology of the estuary bottom is mainly
138 composed of sandy sediments with static and mobile wave-shaped features. The movement of
139 the estuary bottom is uneven, with speeds of 0.17 to 1.29 meters per day for the moving sand
140 waves in the channels. After eliminating anthropogenic factors such as human errors, dredging,
141 and severe weather events, the most likely hypothesis is that seabed morphodynamics are
142 responsible for the movement of bottom features (Alves et al., 2017). River flow plays a crucial
143 role in the renewal of CEP waters, particularly in areas near tributaries. Hydrodynamic studies
144 have demonstrated that incorporating river flow into models substantially enhances renewal
145 rates compared to scenarios that solely consider tidal influence. In contrast, wind exerted a
146 minimal impact on the water renewal process compared to river flow (Dalazen et al., 2020).
147 The Paranaguá estuary can be categorized into three distinct zones based on the salinity of the
148 waters. The inner region, with lower salinity, is more susceptible to seasonal fluctuations owing
149 to the impact of rainfall. This area also exhibits elevated concentrations of fine sediment and
150 nutrients. The middle zone, with intermediate salinity, exhibits polyhaline traits, where the
151 maximum turbidity zone is situated. The outer region, with higher salinity, is distinguished by
152 heightened energy and diminished concentrations of fine sediments (Amorin et al., 2020; Lana
153 et al., 2001)
154 The climate in the region is humid and temperate, with hot and rainy summers and cold
155 and less rainfall winters (Lana et al., 2001; IPARDES, 2001). The humid climate favours the
156 existence of the Atlantic Rainforest, which is preserved especially within protected areas, such
157 as the 'Guaraqueçaba Environmental Protection Area' and the 'Superagui National Park'.
158 Mangroves are very well developed in the margins of PES. The tidal plains and streams are
159 colonized by saltmarshes formed by *Spartina alterniflora*, which constitute narrow,

160 monospecific, and discontinuous belts in front of the mangrove forests (Lana et al., 2001;
161 Garcia et al., 2019).
162
163 ## 2.3 Material and Methods

164 ### 2.3.1 Sampling

165 A total of 82 surface sediments (0 – 3 cm) from the PES were collected in two sampling
166 campaigns occurred in March 2018, and April 2019 (Fig. 1). The sediments were sampled with
167 a Van Veen-type grab, placed in aluminium containers (previously calcined in a high
168 temperature furnace 400 ºC for 4 h), and then frozen at –20 ºC. The samples were then freeze-
169 dried, gently macerated, and stored in previously decontaminated glass vials according to the
170 procedure adopted to the aluminium containers.
171
172 ### 2.3.2 Particle size, elemental and isotopic analysis

173 The grain size analyses were carried out in a Malvern Hydro 2000 granulometer, using 2
174 g of sediment from each sample. Firstly, carbonate was removed with 10% HCl solution. Next,
175 the OM was removed with 10% H_2O_2 solution. The two steps were performed on a plate heated
176 to 65 ºC (Angeli et al., 2020; Paladino et al., 2022). The data obtained from the granulometer
177 are presented in the φ (phi) scale, and the Sysgran 3.2 Software (Camargo, 2006) was used to
178 obtain the percentages of gravel, sand, silt, and clay in each sample.
179 Inorganic carbon, assumed as predominantly in the form of calcium carbonate, was
180 calculated by the weighting 1 g of dry sediment sample before and after exposing about to 10%
181 HCl solution. The contents of total organic carbon (TOC) and total nitrogen (TN) and their
182 respective isotopic compositions ($\delta^{13}C$ and $\delta^{15}N$) were determined using a Costech Elemental
183 Analyzer Combustion System, coupled to the with a Thermo Scientific Delta V Advantage
184 Isotope Ratio Mass Spectrometer detector.
185 The initial pulses of the runs were analysed to assess the stability of the equipment. At
186 least ten sample-free runs were performed for each compound.
187 The standard used for quantifying the percentages was Soil LECO 402-309 from LECO
188 Corporation. The carbon content of this standard is 13.77%, and the nitrogen content is 0.092%.
189 To evaluate the calibration of the equipment, two certified standards are injected for each
190 run of 40 samples. One of them is the USGS-40, with values of $\delta^{13}C$ = -26.388‰ and $\delta^{15}N$ =
191 -4.5‰. The other is the IAEA-600, with $\delta^{13}C$ = -27.777‰ and $\delta^{15}N$ = +1.0‰.
192 To assess the repeatability of the measurements, a sediment sample used by the laboratory
193 as a secondary standard was injected every ten samples.

2.3.3 Determination of organic markers

The laboratory method for determining organic markers is described in Dauner et al. (2019) (Fig. S1, Supplementary Information). The *n*-alkanes and *n*-alkanols were extracted from 5 g of sediments with 25 mL of a mixture of methanol:dichoromethane (MeOH: DCM; 1:9; v:v) using an ultrasonic bath for 20 min. This process was repeated three more times for each sample, resulting 100 mL of total organic extract. The resulting extract was concentrated to 2 mL in a vacuum rotary evaporator in a water bath at a temperature of 40 °C (bulk extract). To each extracted sample, 100 µL of a mixture of surrogate standards containing 1–eicosene (5 ng μL^{-1}) and 5α-androstanol (2 ng μL^{-1}) was added, for evaluation of the analytical recoveries and quantification of compounds. Activated copper was also added to remove the sulphur possibly present in the samples.

The bulk extract were dried in a nitrogen flow and saponified for two hours at 70 °C, with 2 mL of a 0.1 mol L^{-1} solution of KOH in MeOH:H_2O (9:1; v:v). Then, 1 mL of *n*-hexane was added to obtain the neutral fraction from the saponified extract. This process was repeated more four times for each sample, resulting about 5 mL of neutral fraction extract.

The neutral fraction extracts were dried under a nitrogen flow and then dissolved in 1 mL of *n*-hexane before clean up step. Next, the extracts were purified, passing through a silica gel column (1% deactivated with Milli–Q® water), and eluted with 4 mL of *n*-hexane (F1 fraction, containing *n*-alkanes), 4 mL of *n*-hexane: DCM (1:2; v:v) (Fraction F2, containing ketone (not used in this study) and 4 mL of DCM: MeOH (1:1; v:v) (Fraction F3, containing *n*-alkanols).

Fraction F1 was transferred to glass vials, concentrated under nitrogen flow until 450 µL and added with 50 µL of internal standard solution (1–tetradecane, 5 ng μL^{-1}), totalizing 500 µL as final volume. Fraction F3 was also dried under nitrogen flow and added with 25 mL of pyridine and acetic anhydride for a derivatization reaction (1 h, 60 °C). The excess of reagents was dried with nitrogen, and the resulting solid was resuspended in *n*-hexane and then transferred to glass vials. Finally, 50 µL of internal standard solution (5α-cholestane, 2 ng μL^{-1}) and *n*-hexane was added until reaching a final volume of 500 µL.

The determination of aliphatic hydrocarbons from fraction F1 was performed from a 2 µL aliquot of organic extract into a gas chromatograph (GC) (Agilent GC System 7890A Series) equipped with a flame ionization detector (FID), in the splitless injection mode, and using hydrogen as carrier gas. The chromatographic column used was Agilent HP-5 19091J-413 (with dimensions of 30.0 m x 0.32 mm x 0.25 □m). The determination of *n*-alkanols from fraction F3 was performed from a 2 µL aliquot of organic extract into a GC (Agilent GC System 7890A Series) coupled to a mass spectrometer (MS) (Agilent 5975C inert MSD with Triple-

Axis Detector). The chromatographic column used was the Agilent HP-5 19091-J-433 (with dimensions of 30.0 m x 0.25 mm x 0.25 □m), in splitless injection mode. Helium was used as carrier gas. The oven temperature to both equipment's was programmed to start at 40 °C, holding for 1 min, 40–60 °C at 20 °C min^{-1}, then to 290 °C at 5 °C min^{-1}, and finally to 300 °C at 5 °C min^{-1}, where the temperature was maintained for 10 min. Data acquisition was performed in the selected ion monitoring mode (SIM). Detailed information regarding quality assurance procedures are presented as Supplementary Information (Sections 1).

2.3.4 Diagnostic ratios for OM source identification

The percentages of TOC and TN from the sediment samples were used to calculate the TOC/TN ratio (represented as C/N), which was multiplied by 1.167 (the balance of the atomic masses of nitrogen and carbon) to obtain the C/N atomic ratios (Equation I) (Meyers and Teranes, 2002).

Equation I: C/N={(TOC/TN) * (1.167)}

Different diagnostic OM sources ratios were applied between individual *n*-alkanes, such as Carbon Preference Index (CPI, Equation II; Aboul-Kassim and Simoneit, 1996), Terrestrial Aquatic Ratio (TAR, Equation III; Chevalier et al., 2015), Proxy aquatic ratio (P_{aq}, Equation IV; Ficken et al., 2000), and Average Chain Length (ACL, Equation V; Freeman and Pancost, 2014).

Equation II: $CPI = \{½ * (([n\text{-}C_{25}] + [n\text{-}C_{27}] + [n\text{-}C_{29}] + [n\text{-}C_{31}] + [n\text{-}C_{33}]) / ([n\text{-}C_{24}] + [n\text{-}C_{26}] + [n\text{-}C_{28}] + [n\text{-}C_{30}] + [n\text{-}C_{32}])) + (([n\text{-}C_{25}] + [n\text{-}C_{27}] + [n\text{-}C_{29}] + [n\text{-}C_{31}] + [n\text{-}C_{33}]) / ([n\text{-}C_{26}] + [n\text{-}C_{28}] + [n\text{-}C_{30}] + [n\text{-}C_{32}] + [n\text{-}C_{34}]))\}$

Equation III: $TAR = (([n\text{-}C_{25}] + [n\text{-}C_{27}] + [n\text{-}C_{29}] + [n\text{-}C_{31}] + [n\text{-}C_{33}]) / ([n\text{-}C_{15}] + [n\text{-}C_{17}] + [n\text{-}C_{19}] + [n\text{-}C_{21}] + [n\text{-}C_{23}]))$

Equation IV: $P_{aq} = (([n\text{-}C_{23}] + [n\text{-}C_{25}])) / (([n\text{-}C_{23}] + [n\text{-}C_{25}] + [n\text{-}C_{29}] + [n\text{-}C_{31}]))$

Equation V: $ACL = \{(25 * [n\text{-}C_{25}]) + (27 * [n\text{-}C_{27}]) + (29 * [n\text{-}C_{29}]) + (31 * [n\text{-}C_{31}]) + (33 * [n\text{-}C_{33}])\} / \{[n\text{-}C_{25}] + [n\text{-}C_{27}] + [n\text{-}C_{29}] + [n\text{-}C_{31}] + [n\text{-}C_{33}]\}$

2.3.5 Data analysis

The spatial distribution maps of grain size (% silt + clay), elementary and isotopic composition and molecular markers and their diagnostic ratios were generated by the QGIS Software v. 3.26.1, using the interpolation from vector points map by splines (sectioned polynomials) technique.

A spatial pattern representing the distribution of sedimentary OM in the study area was obtained by multivariate analyses considering only samples in which more than 50% of

262 individual *n*-alkanes and *n*-alkanols presented concentrations above the detection level (0.020
263 □g g^{-1}). Cluster analysis was carried out to verify whether there is sectorization in the estuary
264 according to the distribution of the studied parameters. Statistical analyses were carried out
265 within R environment (version 4.2.2), using the following variables: percentage of fine
266 sediments (% silt + clay), TOC, TN, $\delta^{13}C$, $\delta^{15}N$, *n*-alkanes, and *n*-alkanols. The same set of data
267 was used to perform a principal component analysis (PCA) to evaluate how the spatial
268 distribution may be affected by the variation of these geochemical parameters.
269 In addition, the Spearman correlation between TOC and TN was calculated and a strong
270 correlation ($\rho = 0.97$; $p < 0.005$) was observed, corroborating the application of the atomic C/N
271 ratio as source proxy of sedimentary OM to the PES sediment samples (Meyers, 1997; Bianchi
272 and Canuel, 2011).
273

274 ## 2.4 Results

275 ### 2.4.1 Grain size

276 Sand was the predominant grain fraction in the analysed samples, followed by silt and
277 clay. The percentages varied between 1.0 and 100.0% (mean = 55.1 □ 30.8), 0.0 to 77.0% (mean
278 = 35.2 □ 24.5), and 0.0 to 45.3% (mean = 9.73 □ 7.88) for sand, silt and clay, respectively.
279

280 2.4.2 Elementary and isotopic composition of sedimentary OM of PES

281

282 The values related to the elementary and isotopic composition, as C/N ratio to the
283 analysed sediments are shown in Table S1 ('S' denotes Supplementary Information). The TOC,
284 TN, levels ranged from 0.10 to 4.70 (mean = 1.60 □ 1.27), 0.02 to 0.43 (mean = 0.15 □ 0.12),
285 respectively (Table S1). The C/N ratio ranged from 4.98 to 17.9 (mean = 11.3 □ 2.80), while
286 the N/P ratio ranged from 1.39 to 19.8 (mean = 10.7 □ 3.88). The $\delta^{13}C$ and $\delta^{15}N$ ranged from
287 −27.15 to −22.88 ‰ (mean = −25.24 □ 0.93) and from 1.99 to 12.96‰ (mean = 5.15 □ 2.14),
288 respectively (Table S1).

289

290 2.4.3 Molecular markers

291

292 Total *n*-alkane concentrations and individual concentrations of analysed compounds are
293 shown in Table S2. Total *n*-alkane concentrations ranged from 0.76 to 50.3 μg g^{-1} (mean = 8.48
294 □ 8.40). The distribution of individual *n*-alkanes and outliers, considering all analysed samples,
295 are shown in Fig. S2. The predominant *n*-alkane was *n*-C_{29}, being the most abundant compound
296 in around 85 % of the analysed samples, followed by the other long-chain *n*-alkanes with an
297 odd number of carbon atoms, particularly, the *n*-C_{25} that was the main *n*-alkane in 13% of the
298 analysed samples.

299 The sum of short- (Σ *n*-C_{15} + *n*-C_{17} + *n*-C_{19}), mid- (Σ *n*-C_{21} + *n*-C_{23} + *n*-C_{25}) and long
300 chain (Σ *n*-C_{27} + *n*-C_{29} + *n*-C_{31}) *n*-alkanes varied from < LD to 0.19 μg g^{-1} (mean = 0.05 □ 0.05),
301 0.03 and 13.0 μg g^{-1} (mean = 1.58 □ 2.17), and 0.29 to 12.3 μg g^{-1} (mean = 3.59 □ 2.80),
302 respectively. The values of CPI, TAR, P_{aq}, and ACL ranged between 1.17 and 5.62 (mean =
303 3.19 □ 1.22), 4.13 and 64.9 (mean = 17.6 □ 11.8), between 0.08 and 0.74 (mean = 0.31 □ 0.15),
304 and between 26.86 and 30.20 (mean = 28.74 □ 0.67), respectively (Table S2).

305 Total *n*-alkanol concentrations ranged from 0.57 to 1271.5 μg g^{-1} (mean = 46.4 □ 143.9;
306 Table S3). The distribution of individual *n*-alkanols, considering all analysed samples, is shown
307 in Fig. S3. The most abundant *n*-alkanol was *n*-C_{30}-OH, followed by the other long-chain *n*-
308 alkanols with an even number of carbon atoms, with emphasis on *n*-C_{28}-OH and *n*-C_{32}-OH. The
309 sum of short- (Σ *n*-C_{16}-OH + *n*-C_{18}-OH + *n*-C_{20}-OH), mid- (Σ *n*-C_{22}-OH + *n*-C_{24}-OH + *n*-C_{26}-
310 OH) and long chain (Σ *n*-C_{28}-OH + *n*-C_{30}-OH + *n*-C_{32}-OH) *n*-alkanols varied between 0.09 and
311 20.2 μg g^{-1} (mean = 1.36 □ 2.52), between 0.07 and 49.4 μg g^{-1} (mean = 3.40 □ 6.22) and
312 between 0.19 and 998.1 μg g^{-1} (mean = 32.8 □ 114.4), respectively.

2.4.4 Multivariate analysis

The cluster analysis (Fig. S4) separated the sites in three groups according to their geochemical parameters analysed. However, once one of the groups was formed only by one sample (site 8), this group was not included in the following analysis and this sample was included in group 1 only to perform PCA (Fig. 2). Thus, in the discussion section, the sites were grouped into two groups (C1 and C2; Fig. 2), following the result of the dendrogram.

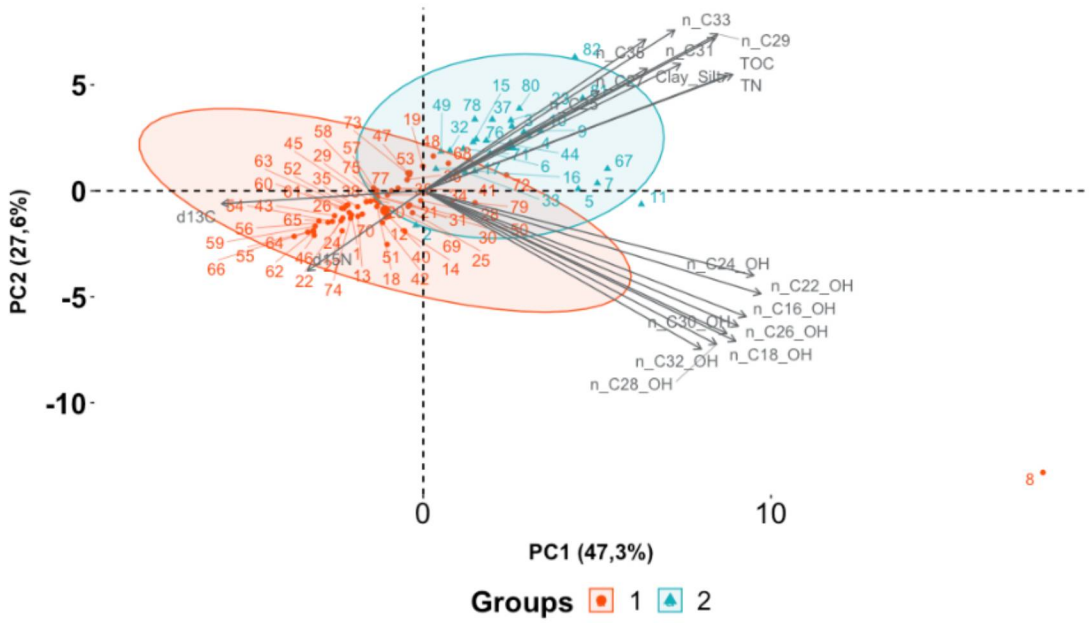

Figure 2. Principal component analysis of parameters studied in surface sediments from the Paranaguá Estuarine System, South Atlantic.

The PCA resulted in 74.9% of explanation to the total data variance according to the two first components (PC1: 47.3% and PC2: 27.6%; Fig. 2). PC1 was positively correlated with n-alkanes, n-alkanols, % fine sediments (silt + clay), TOC and TN, while its was negatively correlated with $\delta^{13}C$ and $\delta^{15}N$. PC2 was negatively correlated with $\delta^{15}N$, and *n*-alkanols and positively correlated with % fine sediments, TOC, TN, and *n*-alkanes. Based on the cluster analyses and PCA, it was observed that sites from Group C1 are characterized by lower % fine sediments, TN, TOC, *n*-alkanes, *n*-alkanols and enriched of lighter isotopes ^{12}C and ^{14}N. Group C2 was composed of sediments enriched of the heaviest isotopes (^{13}C and ^{15}N) and TN, TOC, fine sediments, *n*-alkanes, and *n*-alkanols (Fig. S5, S6, S15 and S16). The map with integration of bulk parameters and molecular markers, following the groups C1 and C2, is shown in Fig. 3.

2.5 Discussion

The two groups formed by PCA and cluster analyses distinguished sites under higher (Group 1) and lower (Group 2) energy based on sedimentary and hydrodynamics features, due higher percentage of fine sediments and higher levels of TN, TOC, and *n*-alkanes, that were related to Group 2 (Fig. 3, S5, S6 and S15). Characterizing a predominance of OM from a terrigenous source corroborated by the isotopic ratio of $\delta^{13}C$, with depleted values (Fig. S5).

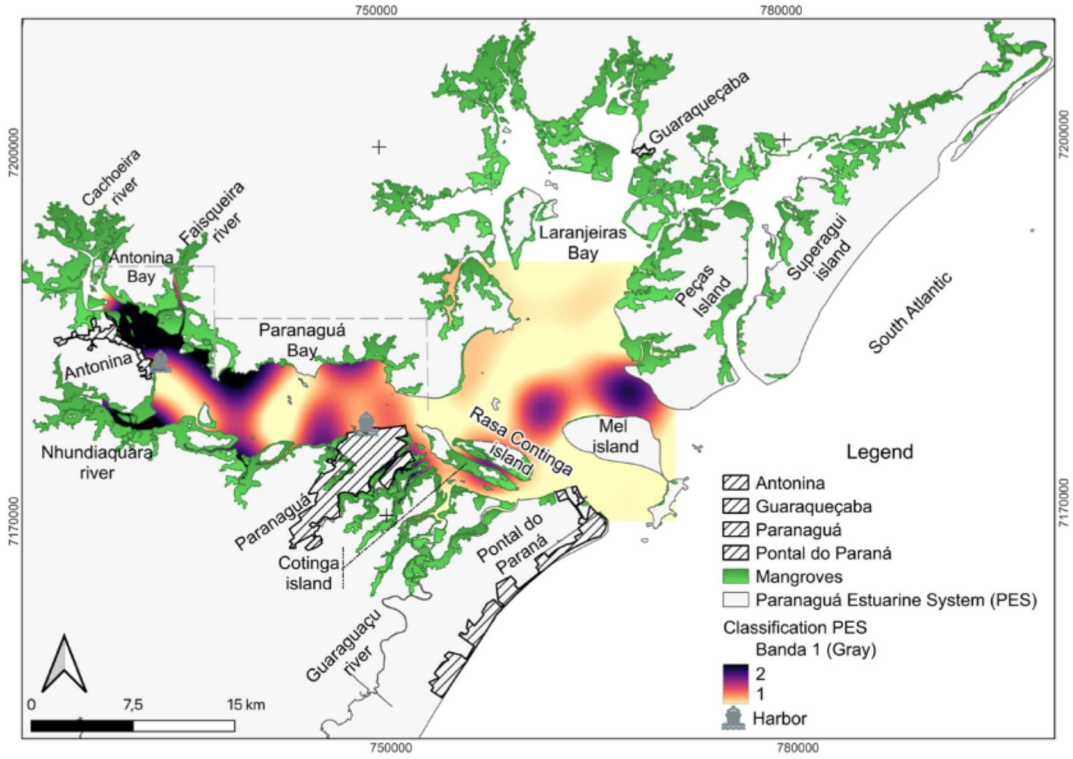

Figure 3.Sectorization map of the Paranaguá Estuarine System in terms of types of sedimentary OM, following the groups (1 and 2) from the cluster analysis.

The inner sector of the 'E-W' axis (Antonina Bay) is under more significant fluvial influence, with contribution of the Faisqueira, Nhundiaquara and Cachoeira rivers (Fig. 1). Consequently, this area has a higher content of fine sediments than the outer sectors (Paladino et al., 2022). This grain size pattern can also be observed at the mouths of rivers on the western margin of Peças Island (Fig. S7). Previous studies have been found that a mixture of fluvial and marine contribution predominates in the central sector (Paranaguá Bay) (Cardoso et al., 2016 e Cattani and Lamour, 2016), promoting a maximum mixing zone that acts as barrier for the transport of fine particles, and favouring its deposition, resulting in an area of relatively fine sediments content.

356 The sites located in the estuarine channels close to the city of Paranaguá and north of the
357 Mel Island may also present a low energy environment (Garcia and Martins, 2021; Fig. 3 and
358 S7). In these locations, the water flow by preferential paths, reducing the energy of the ebb
359 currents and promoting sedimentation near the banks. According to Lamour et al. (2004), the
360 increase in the depth of the estuarine entrance channel forces the ebb flow to the north mouth,
361 influencing the depositional processes in the area. This change in circulation reduced the bottom
362 currents' speed, allowing larger transport of suspended material in the north mouth, which thus
363 favours the deposition of fine sediments in this region (Paladino et al., 2022). The outer sector
364 has a stronger marine influence (Garcia and Martins, 2021), and consequently, there is a
365 predominance of fine to very fine sands (Fig. S7, also observed by Angeli et al. (2020).
366 The 'N-S' axis has less influence from river basins than the 'E-W' axis (Soares &
367 Barcelos, 1995; Noernberg et al., 2008). This is why the transport capacity is greater near the
368 Peças island, due to the ebb tide presenting a circulation with greater energy, giving rise to
369 preferential routes in the downstream direction, as North Channel (Angulo et al., 2006;
370 Bigarella et al., 2008) (Fig. S8). On the west bank (Saco da Tambarutaca), in front of the Peças
371 island, there is the presence of the Perigo shoal, which was formed in the convergence zone of
372 the tidal currents coming from the Laranjeiras and Paranaguá Bays (Soares & Barcelos, 1995;
373 Bigarella et al., 2008). The shallows in the interior of Laranjeiras bay originated due to areas of
374 weak currents or calm waters, topographically protected, which favour deposition (Soares &
375 Barcelos, 1995; Bigarella et al., 2008) (Fig. S8). Therefore, the integration of grain size data
376 and hydrodynamic features indicated that PES presents intrinsic characteristics for each bay.
377 The highest values of TOC, TN, TP, *n*-alkanes and *n*-alkanols showed spatial distribution
378 in agreement to fine sediments (Fig. S9–S14), indicating a correspondence between its
379 distribution and the local hydrodynamics. In fact, TOC, TN and TP were accumulated mainly
380 on the north bank of the 'E-W' axis of the estuary, which are places of favoured deposition due
381 low energy (Fig. 3; also described by Cattani and Lamour, 2016; Paladino et al., 2022).
382 Furthermore, strong positive correlations between fine sediments, carbon and nutrients contents
383 and molecular markers are frequently found in estuarine sediments, once silt and clay particles
384 exhibit larger surface area and greater capacity for OM adsorption (Hedges and Keil, 1999;
385 Mertz et al., 2005).
386 The C/N ratio have been extensively used to identify OM sources in the South Atlantic
387 (e.g., Mahiques et al., 2007; Nagai et al., 2010). Factors as the absence of cellulose and high
388 amount of protein in algae and bacteria, as well the abundance of cellulose in vascular plants
389 promotes differentiation in elemental compositions of each organism (Meyers, 1997; Das et al.,

2008). Thus, in general, C/N ratios ranging between 4 and 6 is related to bacteria, 4 and 10 to algae (indicating marine OM), and C/N ratio greater than 20 to vascular land plants (indicating terrigenous OM) (Meyers,1997; Khan et al., 2015). Accordingly, to C/N ratio, it is suggested that a mixture of autochthonous and allochthonous sources was predominant in PES (C/N between 10.0 and 17.9; Table S1; Fig. S12), especially in the location between north and south margins of Antonina and Paranaguá Bays (Fig. 5 and S12). The sedimentary OM of marine origin (algae, phyto - and zooplankton) predominated at the Laranjeiras Bay ('N-S' axis) and at PES mouth, a place of high energy and close to the continental shelf (Fig. 5 and S8). Therefore, inner bay areas, in general, presented results that suggested a stronger influence of continental apportions (i.e., high C/N), which terrigenous OM are quickly deposited due to the lower energy depositional environment. In contrast, the lowest average C/N ratio were observed in the outer area, suggesting a higher energy depositional environment exposed to a stronger marine influence. A mixture source signature is expected between these two areas once it is characterized by the presence of a maximum mixing zone (Cattani and Lamour, 2016; Paladino et al., 2022). Also, the strong positive correlation between TOC and TN suggesting that the detected TN is predominantly from organic source (Bergamaschi et al., 1997) and that both TOC and TN are originated from similar sources and presents same distribution trends and preferential depositional sites.

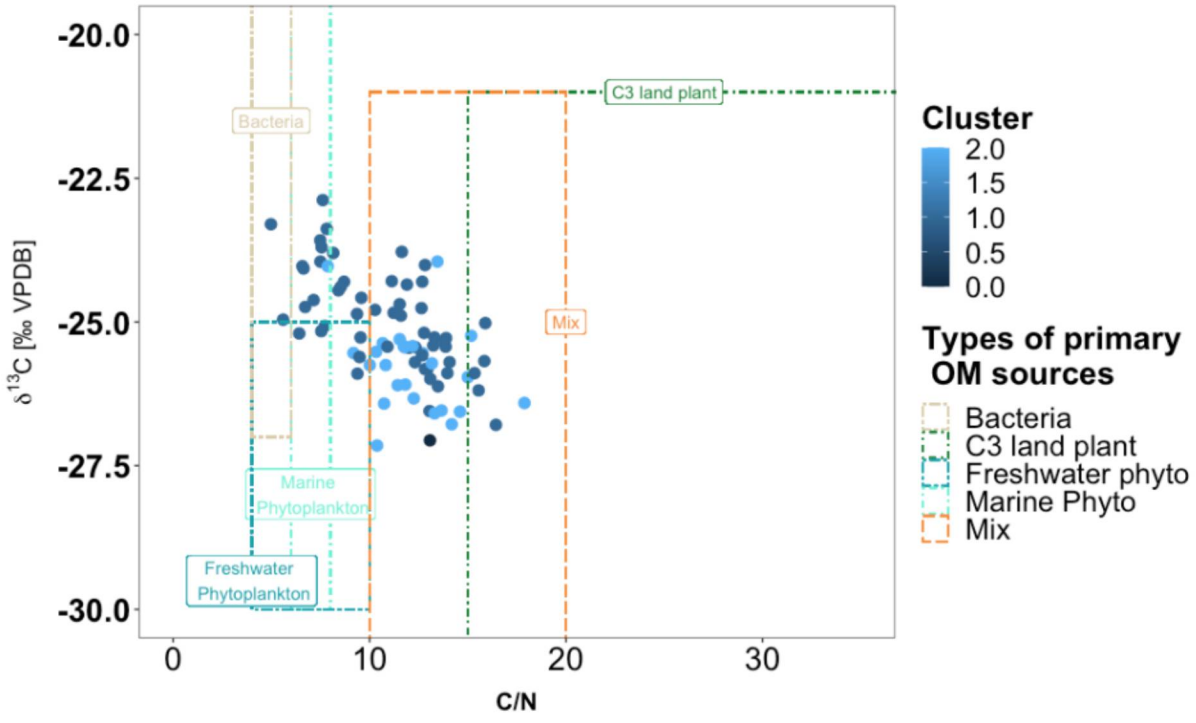

Figure 4. Scatterplot of $\delta^{13}C$ vs C/N proxies to the distribution of the main types of OM sources presented in the Paranaguá Estuarine System, South Atlantic.

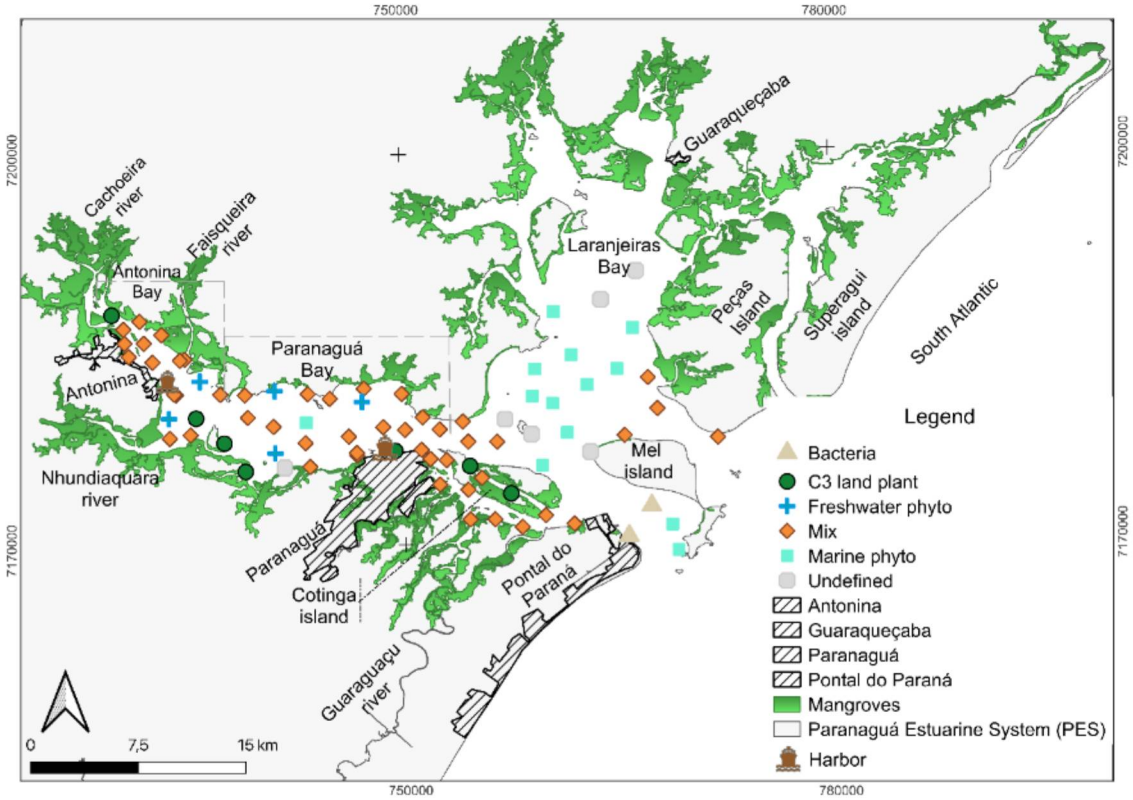

411 Figure 5. Spatial distribution of the main sources of OM presented in the Paranaguá Estuarine System, South
412 Atlantic, based on $\delta^{13}C$ vs C/N proxies.

413

414 In addition to C/N ratio, carbon and nitrogen isotopic signatures of sedimentary OM are
415 also typically used to confirm and distinguish between marine, terrestrial and another specific
416 allochthonous sources (Meyers, 1997; Vaalgamaa et al., 2013; Zhang et al., 2020). The $\delta^{13}C$
417 ranges of each OM source are mainly a result of the specific process of carbon assimilation
418 during photosynthesis of each primary producer group and the isotopic compositions of the
419 carbon source (Meyers, 1997). Thus, even with some variability, specific ranges can be related
420 to marine phytoplankton (−24 to −18 ‰), freshwater phytoplankton (−30 to −25 ‰) and
421 terrestrial plants utilizing C3 (−32 to −21 ‰), C4 (−17 to −9 ‰) or Crassulacean Acid
422 Metabolism (−28 to −10 ‰) paths (Meyers, 1997; Khan et al., 2015). According to these
423 variations, it is possible to consider a $\delta^{13}C$ signal around −27 ‰ to terrigenous source and
424 between up to −24 ‰ to marine source (corroborating e.g., Cabral et al., 2019).

425 The PES presented $\delta^{13}C$ values between −27 and −23 ‰, an intermediate range between
426 marine and riverine/terrestrial endmembers, that was similar to that found in tidal-dominated
427 estuaries (between −26 and −24 ‰) (Middelburg and Herman, 2007). The PES mouth and
428 Laranjeiras Bay were the areas with the most important contribution from autochthonous
429 marine OM, indicated by the enrichment of $\delta^{13}C$, that is related to a marine phytoplankton
430 signature (Fig. S13).

Sites located in the estuarine channels close to the cities of Antonina, Paranaguá and Peças Island showed lower values of $\delta^{13}C$ ($\delta^{13}C < -24$ ‰), indicating a relative more influence of terrigenous sources (Fig. S13). Garcia and Martins (2021) have found the same $\delta^{13}C$ range in mangrove sediments from PES (−28.4 to −23.1 ‰), suggesting the mangrove vegetation established in the estuary margins as an important source of terrigenous OM to the PES estuarine sediments (Fig. 5). The cross plot of $\delta^{13}C$ vs C/N, evidenced a large area of terrigenous and marine sources mixing covering almost the entire 'E-W' axis, with some sites presenting specific signals for freshwater, C3 plants and marine phytoplankton (Fig. 5). However, two sites from the PES mouth (P46 and P66) showed microbial signature with C/N ratio values (5.4 and 5.8, respectively) lower than expected for sedimentary OM from marine planktonic organisms (between 4.0 and 10.0) (Table S1 and Fig. 4 and 5). Once this is the main access channel to the port, with intense vessel traffic and constant dredging, some disturbance of the bottom sediments area expected, favouring the aerobic degradation of the OM and reducing the values of the C/N ratio, making those present values compatible with the presence of bacteria.

Sedimentary $\delta^{15}N$ variations tend to be more complex, once it is influenced by a variety of biological and environmental factors related to the selective assimilation of the ^{14}N and/or ^{15}N forms by living organisms and processes like biological nitrogen fixation and nitrogen cycling in sediments (Meyers, 1997; Bueno et al., 2018). However, despite contributions from multiple nutrient sources, $\delta^{15}N$ signatures may indicate different sources of OM to estuarine sediments, especially when analysed together with other proxies, as $\delta^{13}C$ and C/N (Vaalgamaa et al., 2013). In general, marine OM are enriched in ^{15}N ($\delta^{15}N \sim 8.0$ ‰) relative to the main compounds related to terrestrial OM, as lignin and lipids ($\delta^{15}N \sim 3.0$ ‰, when not impacted by agriculture runoff). In addition, $\delta^{15}N$ is even lower in raw sewage ($\delta^{15}N \sim 2.0$ ‰) but may be enriched when sewage effluent receives tertiary treatment ($\delta^{15}N \sim 15.0$ ‰) (Meyers and Ishiwatari, 1993; Vaalgamaa et al., 2013; Savage et al., 2010). About 80% of the analysed samples from PES showed a range of $\delta^{15}N$ values compatible to a mixture of terrigenous and marine sources (2.0 – 7.3 ‰; Table S1). This range is common for estuarine sediments (e.g., Middelburg and Nieuwenhuize, 1998), once is interpreted as characteristic of residual anthropogenic nitrogen delivered by rivers and diffuse runoff (Voss et al., 2005). However, higher $\delta^{15}N$ values (> 7.5 ‰) were recorded in about 9% of the samples, in punctual areas from PES (Fig. S13). These higher $\delta^{15}N$ values can be related to greater marine influence (at the southern mouth; Fig. S13) or a possible punctual denitrification process (at Cachoeira River mouth and middle region of Paranaguá Bay), which occurs in the subsurface sediment layer

464 during low oxygen conditions leading to a selective release of ^{14}N (Vaalgamaa et al., 2013)
465 (Fig. S14). The lower $\delta^{15}N$ values recorded in this study could not be related to raw sewage
466 influence, once samples presenting $\delta^{15}N \sim 2.0$ ‰ are distant from Paranaguá and Antonina
467 cities (Fig. S14), the main sources of sewage input (Martins et al., 2010; Cabral et al., 2018). In
468 addition, $\delta^{15}N$ is considered an inconclusive proxy for sewage contamination for PES region
469 (Cabral et al., 2019), once the signatures for raw sewage and terrigenous OM are overlapped
470 (Vaalgamaa et al., 2013; Savage et al., 2010).
471 The distribution of $\delta^{15}N$ presented the same range of values for sites from different sectors
472 of PES; so it is not feasible to use this proxy sole to distinguish the OM sources in PES. The
473 combination of $\delta^{15}N$ and $\delta^{13}C$ data also evidenced values within the mixed source range (or
474 estuarine; Fig. 6 and 7). Still, it was possible to identify specific C3 plants signatures in about
475 10% of the sites, located mainly near to rivers mouth (Fig. 7). Thus, this signature may be
476 related to OM from mangrove trees established in the banks of the estuary, but also to OM from
477 other Atlantic Forest C3 species that border the main rivers that flow into PES, as Cachoeira
478 and Faisqueira rivers (Branco, 2008; Paula et al., 2021). Some sites in this area have been
479 undefined (Fig. 5), which may be related to anthropogenic activities influence, once these rivers
480 drain areas with larger urban and agricultural occupations (Branco, 2008; Paula et al., 2021). In
481 these outflow areas, tidal flats were also observed, being vegetated by saltmarshes of *Spartina*
482 *alterniflora*, and presenting predominance of fine sediment deposition (Netto and Lana, 1997).
483 These ecosystems exhibit a highly efficient (around 50%) root system that captures sediments
484 and organic carbon from external sources, as they slow down the water and retain the particles,
485 storing them in the sediment (Duarte et al., 2005; Mcleod et al., 2011). Both autochthonous and
486 allochthonous OM can be retained in this system, promoting ambiguous signals for sources.
487 Molecular markers such as n-alkanes and n-alkanols, along with variations in their chain
488 lengths, predominance, and even-to-odd carbon chain ratios, are typically employed to
489 differentiate between marine and terrestrial organic matter sources. (Meyers, 1997; Carreira et
490 al., 2016; Brandini et al., 2022; Albergaria-Barbosa et al., 2023). Short chains (until *n*-C_{19} or *n*-
491 C_{20}-OH) are associated to marine biogenic origins, such as marine phyto- and zooplankton and
492 benthic algae; the mid chains (between *n*-C_{21} and *n*-C_{25} or *n*-C_{22}-OH and *n*-C_{26}-OH) are
493 associated to aquatic plants, i.e., submerged and floating macrophytes, and non-emergent
494 vascular plants and; the long chains (between *n*-C_{27} and *n*-C_{31} or *n*-C_{28}-OH and *n*-C_{32}-OH) are
495 associated to biogenic contribution of terrigenous origin, once are predominant in the
496 epicuticular waxes of vascular plants(Meyers, 1997; Ficken et al., 2000).

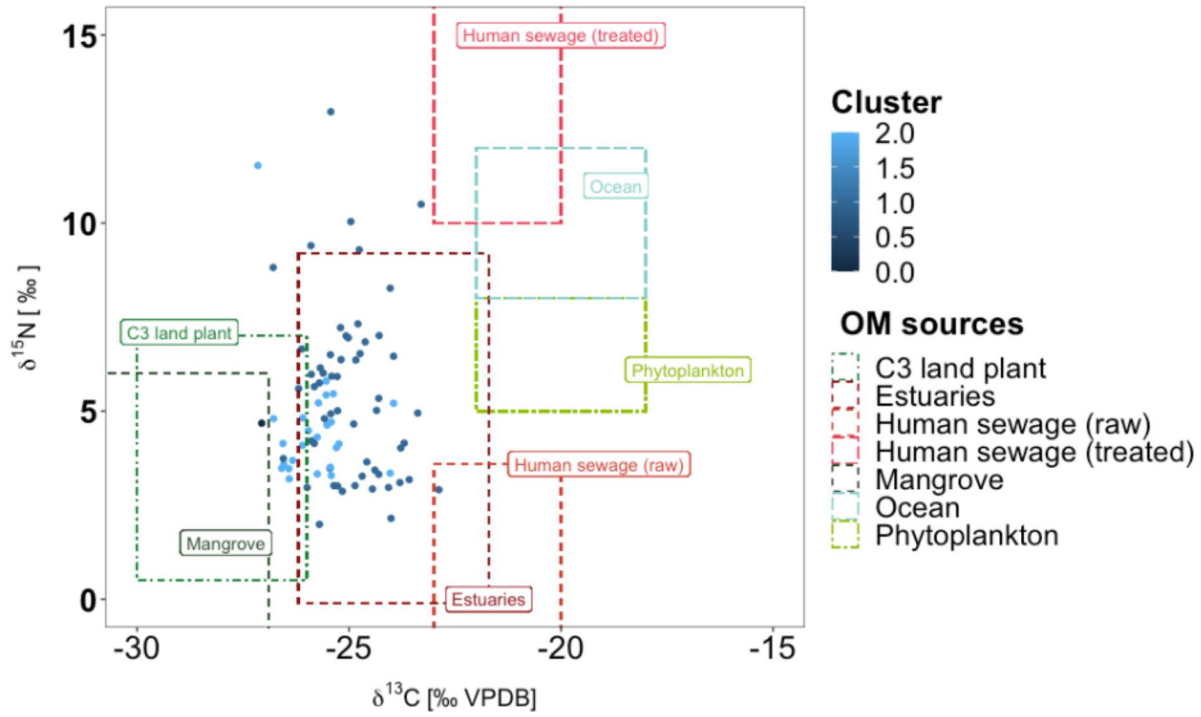

497

498 Figure 6.Scatterplot of $\delta^{15}N$ vs $\delta^{13}C$ to the distribution of the main types of OM sources presented in the Paranaguá
499 Estuarine System, South Atlantic.

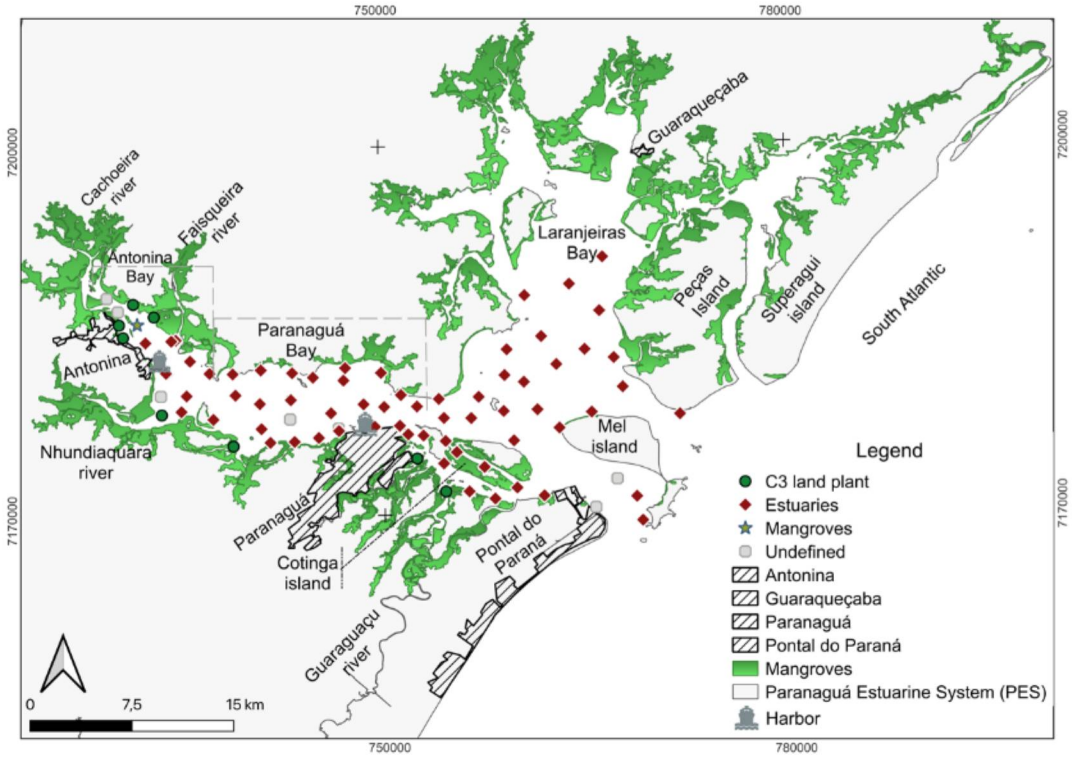

500

501 Figure 7.Spatial distribution of the main sources of OM presented in the Paranaguá Estuarine System, South
502 Atlantic, based on $\delta^{15}N$ vs $\delta^{13}C$.

503

504 The terrigenous-to-aquatic, proxy aquatic and average chain length ratios are based on
505 the above statement, considering the relative amounts of different length homologues (Meyers,
506 1997; Ficken et al., 2000; Freeman and Pancost, 2014). Accordingly, terrigenous source
507 predominance is indicated by TAR > 3.0, Paq < 0.1 and higher ACL values; mixed sources by
508 Paq between 0.1 and 0.4 and; autochthonous OM (macrophytes) when Paq > 0.4 (Ficken et al.,
509 2000; Sikes et al., 2009; Freeman and Pancost, 2014). Higher concentrations of *n*-alkanes and
510 *n*-alkanols were found in the sites of group C2 (Fig. S15 and S16). It was expected once group
511 C2 is also characterized by higher percentage of fine sediments and TOC (Fig. 2), that favour
512 the adsorption and accumulation of hydrophobic compounds such as these molecular markers
513 (Hedges and Keil, 1999; Brandini et al., 2022).
514 There was a predominance of *n*-alkanes and *n*-alkanols long chains in both sample groups
515 (C1 and C2) prevailing the odd chains for *n*-alkanes and even chains for the *n*-alkanols (Fig.
516 S15 and S16). The most abundant compounds were *n*-C_{29} and *n*-C_{30}-OH (Fig. S15 and S16),
517 suggesting predominance of terrigenous material over marine contributions.
518 Predominance of terrigenous OM was also verified by the high values of TAR (mean of
519 17.6 ± 11.8) and ACL (mean of 28.7 ± 0.67), while mixed sources was indicated by Paq (mean
520 of 0.31 ± 0.15) (Fig. S17 and Table S2). The abundance of long-chain *n*-alkanes in the
521 epicuticular waxes of higher vascular plants serves the physiological function of protective
522 barrier to regulate water loss, whether through transpiration processes or another stressful
523 conditions, such as tidal flooding, high soil salinity, and nutrient limitation (Meyers, 1997;
524 Sachse et al., 2006), that are predominant conditions of estuarine environments (Rivera-Monroy
525 et al., 2017). In addition to the vascular plant's contributions originating from the Cachoeira
526 and others rivers, the PES is featured with a densely mangrove area, and the OM provided by
527 this vegetation contributes to the signals of terrigenous material indicated by diagnostic ratios.
528 Moreover, recent studies have found values for *n*-alkane ratios in mangrove leaves similar to
529 those found here for sediments (e.g., Belligotti et al., 2007; Ceccopieri et al., 2021; Albergaria-
530 Barbosa et al., 2023). Finally, it is observed a more expressive signal of terrigenous OM at
531 group C2, due to higher CPI and TAR values at (Fig. S17). It may indicate a more significant
532 terrigenous contribution close to the estuary margins (Fig. 3), where tidal flats tend to decrease
533 the system's energy, become easy the deposition of finer sediments and, thus, OM
534 accumulation.
535 In marine environment under influence of anthropogenic activities, especially urban and
536 harbour's regions, the concentrations of total n-alkanes can be used to identify OM inputs
537 associated with the petroleum and by-products input (Volkman et al., 1992; Bícego et al., 2006).

Accordingly, the overall low concentrations of *n*-alkanes levels (about 70% of the samples with total *n*-alkanes < 10.0 μg g^{-1}) combined with the predominance of odd chains *n*-alkanes found here (Table S2 and Fig. S2) suggest an uncontaminated environment with a significant contribution of biogenic hydrocarbons to the PES, regarding petrogenic sources. Despite these low total n-alkanes levels, some sites located in Antonina Bay (e.g., sites 2, 4 and 10), Paranaguá Bay (e.g., sites 32, 37 and 69) and in the surroundings of Peças Island (e.g., sites 50 and 53) presented relatively high levels of total *n*-alkanes (> 13.0 μg g^{-1}), suggesting those as 'hot spot' areas of OM, accumulation, that may include contaminants deposition, due to low hydrodynamics, low depth and fast sedimentation of suspended particles, as discussed above.

A variety of hydrocarbons that cannot be easily separated or identified using standard analytical methods, such as GC, appears as a hump in the chromatograms, being named "Unresolved Complex Mixture" (UCM) (Volkman et al., 1992; Bouloubassi and Saliot, 1993). These mixtures are often found in crude oil and other complex environmental samples, and UCM has been used as an indicator of chronic oil input when concentrations of total *n*-alkanes are higher than 10.0 μg g^{-1} (Farrington et al., 1977; Readman et al., 2002). About 18.0% of the PES sites did not show detectable UCM while 46.4% showed low concentrations and it has been associated with the OM degradation. However, 35.7% of the sites presented UCM and total *n*-alkanes > 10 μg g^{-1}, although only one site (P21) presented a high UCM concentration (68.0 μg g^{-1}). This apparent local oil contamination has been related to the depositional conditions in this site, placed in the maximum turbidity zone of estuary and due the proximity to the Paranaguá port. The UCM/Σ *n*-alk ratio suggest oil contamination to values greater than 10.0 (Tolosa et al., 2009; Bet et al., 2015; Dauner et al., 2018); however, the observed values in PES indicate aliphatic hydrocarbons from degraded biogenic OM, once virtually all samples showed UCM/Σ *n*-alk ratio < 10.0 (Table S2).

The Carbon Preference Index (CPI) indicates the extent to which *n*-alkane distributions reflect the biological preference for odd chain lengths (Freeman and Pancoast, 2014), where CPI index values > 4.00 indicate a predominance of terrigenous material and between 1.0 and 3.0 to marine OM contribution. The CPI values close to 1.00 might suggest OM either from algae and bacteria (Bray and Evans, 1961; Freeman and Pancost, 2014) or the presence of oil and derivatives (Bray and Evans, 1961; Abreu-Mota et al., 2014; Martins et al., 2015). In the PES, more than half of the samples had CPI < 4.00, and almost 20% of the samples had CPI < 2.00 (Table S2). As the concentrations of total *n*-alkanes and UCM were low, the low values of the CPI index are probably associated with intense microbial activity at the time of OM deposition.

When comparing the values obtained in this study with previous studies carried out in the PES, an increase in the concentrations of total *n*-alkanes has been observed over the last decade (Table S4). This variation may be associated with population growth, and changes in land use and occupation (Martins et al., 2015; Wilhelm et al., 2022). In addition, extreme events of high rainfall increase the erosion potential of the rivers that drain the hydrographic basin of the coast of Paraná, which has a steep slope (Amorin et al., 2020). In March, 2011, for example, precipitation accumulation reached values of 235 mm in 48 h, which corresponds to an average of almost 5 mm h^{-1}, but reached 40 mm h^{-1} during the heaviest rain period (Defesa Civil do Paraná, 2011). Extreme rainfall events like that carry more material to the estuary and increase the concentrations of molecular markers observed in surface sediments.

2.6 Conclusion

In this study, an integrated evaluation of the distribution of molecular markers (*n*-alkanes and *n*-alkanols), elemental and isotopic OM composition was carried out using surface sediments of the Paranaguá Estuarine System. This environment is characterized by anthropic activity related to agriculture, tourism, and port activities, although it is part of the Atlantic Rainforest, a Biosphere Reserve from UNESCO. Terrigenous contribution from fluvial inputs, the estuarine margins and the tidal currents that dominates the estuary hydrodynamics, both have an important role to define the geochemical mapping denoting a mixture of allochthonous and marine OM sources along the 'E-S' PES axis. The local hydrodynamics also controls the OM deposition in Antonina and Paranaguá Bays due to the low energy and the presence of a mixing zone between freshwater and marine waters, respectively, creating sites of preferential accumulation of OM caused by the flocculation of fine materials. The estuarine mouth region and Laranjeiras Bay, however, are strongly influenced by marine OM.

It is expected that such results have the potential to guide the public policies proposed by the Coastal Basin Committee and consequently collaborate for the goals of the Sustainable Development Goals, as this study allowed identifying areas prone to nutrient accumulation.

Acknowledgements

This work was carried out with the support of the Coordination for the Improvement of Higher Education Personnel – Brazil (CAPES) – Financing Code 001. C.C. Martins and M.M. Mahiques would like to thank CNPq (Brazilian National Council for Scientific and Technological Development) for financial support (441265/2017-0). Finally, this work results from the EQCEP project (Historical input and future perspectives related to the occurrence of

the chemical stressors in the Paranaguá Estuarine System) sponsored by CNPq and the Brazilian Ministry of Science, Technology, Innovation and Communication. This work is a Brazilian contribution, via CNPq funds, to the United Nation Sustainable Development Goals. Finally, this study was developed as part of a graduate course on Coastal and Ocean Systems at the Federal University of Paraná (PGSISCO - UFPR).

CRediT authorship contribution statement

Marines Maria Wilhelm: Data acquisition, Formal analysis, Methodology, Writing - original draft, review & editing. Ana Caroline Cabral: Supervision, Writing - review & editing. Ana Lucia Lindroth Dauner: Methodology, Writing - review & editing. Renata Hanae Nagai: Conceptualization, Writing - review & editing, Project administration. Rubens C. L. Figueira: Data acquisition, Formal analysis, Methodology, Writing – review. Michel Michaelovitch de Mahiques: conceptualization, Writing – review. Funding acquisition, Project administration. César C. Martins: Formal supervision, Conceptualization, Writing – review & editing, Project administration.

Declaration of competing interest

The authors declare that they have no known competing financial interests or personal relationships that could have appeared to influence the work reported in this paper.

Appendix A. Supplementary data

Supplementary data to this article can be found online at: https://doi.org/10.1016/j.XXXXXXX.2023.XXXXXX.

631 References
632
633 Aboul-Kassim, T.A.T., Simoneit, B.R.T., 1996. Lipid geochemistry of surficial sediments from
634 the coastal environment of Egypt I. Aliphatic hydrocarbons – characterization and
635 sources. Marine Chemistry, 54, 135–158.

636 Abreu-Mota, M.A., Barboza, C.A.M, Bícego, M.C., Martins, C.C., 2014. Sedimentary
637 biomarkers along a contamination gradient in a human-impacted sub-estuary in
638 Southern Brazil: a multi-parameter approach based on spatial and seasonal variability.
639 Chemosphere, 103, 156-163.

640 Albergaria-Barbosa, A.C.R., Schefuß, E., Taniguchi, S., Santos, P.S., Cunha-Lignon, M.,
641 Tassoni-Filho, M., Figueira, R.C.L., Mahiques, M.M., Bícego, M.C., 2023.
642 Characterization of the organic matter produced by Atlantic Rainforest plants and its
643 influence in the surface sediments deposited in a protected subtropical Estuarine–
644 Lagoon system. Regional Studies in Marine Science, 57, 102728

645 Amorim, A.C.B., Scudelari, A.C., Cunha, C., Gonçalves, J.E., 2020. Eventos Extremos de
646 Precipitação no Litoral do Paraná (Baía de Paranaguá). Revista Brasileira de
647 Meteorologia, 35, 563-575.

648 Angeli, J.L.F., Trevizani, T.H., Nagai, R.H., Martins, C.C., Figueira, R.C.L., Mahiques, M.M.,
649 2020. Geochemical mapping in a subtropical estuarine system influenced by large grain-
650 shipping terminals: Insights using Metal/Metal ratios and multivariate analysis.
651 Environmental Earth Sciences, 79, 1-15.

652 Angulo, R.J., Soares, C.R., Marone, E., Souza, M.C., Odreski, L.L.R., Noernberg, M.A., 2006.
653 Paraná. In: Erosão e progradação do litoral brasileiro. Muehe, D. (org.). Brasília:
654 Ministério do Meio Ambiente, 476p.

655 Baldock, J.A., Masiello, C.A., Gelinas, Y., Hedges, J.I., 2004. Cycling and composition of
656 organic matter in terrestrial and marine ecosystems. Marine Chemistry, 92, 39-64.

657 Barros, G.V., Martinelli, L.A., Novais, T.M.O., Ometto, J.P.H., Zuppi, G.M., 2010. Stable
658 isotopes of bulk organic matter to trace carbon and nitrogen dynamics in an estuarine
659 ecosystem in Babitonga Bay (Santa Catarina, Brazil). Science of the Total Environment,
660 408, 2226-2232.

661 Belligotti, F.M., Carreira, R.S., Soares, M.L.G., 2007. Contribuição ao estudo do aporte de
662 matéria orgânica em sistemas costeiros: hidrocarbonetos biogênicos em folhas de
663 mangue. Geochimica Brasiliensis, 21, 71-85.

664 Bergamaschi, B.A., Tsamakis, E., Keil, R.G., Eglinton, T.I., Montluçon, D.B., Hedges, J.I.,
665 1997. The effect of grain size and surface area on organic matter, lignin and
666 carbohydrate concentration, and molecular compositions in Peru Margin sediments.
667 Geochimica et Cosmochimica Acta, 61, 1247–1260.

668 Bet, R., Bícego, M.C., Martins, C.C., 2015. Sedimentary hydrocarbons and sterols in a South
669 Atlantic estuarine/shallow continental shelf transitional environment under oil terminal
670 and grain port influences. Marine Pollution Bulletin, 95, 183-194.

671 Bianchi, T.S., Canuel, E.A., 2011. Chemical biomarkers in aquatic ecosystems. Chemical
672 Biomarker Applications to Ecology and Paleoecology. Princeton University Press,
673 Princeton.

674 Bícego, M.C., Taniguchi, S., Yogui, G.T., Montone, R.C., da Silva, D.A.M., Lourenço, R.A.,
675 Martins, C.C., Sasaki, S.T., Pellizari, V.H., Weber, R.R., 2006. Assessment of

676 contamination by polychlorinated biphenyls and aliphatic and aromatic hydrocarbons in
677 sediments of the Santos and São Vicente Estuary System, São Paulo, Brazil. Marine
678 Pollution Bulletin, 52, 1804-1816.

679 Bigarella, J.J., Klein R., Silva, J.L, Passos, E. 2008. A serra do Mar e planície costeira do
680 Paraná: um problema de segurança ambiental e nacional. Florianópolis:
681 UFSC/CFH/GCN.

682 Bouloubassi, I., Saliot, A., 1993. Investigation of anthropogenic and natural organic inputs in
683 estuarine sediments using hydrocarbon markers (NAH, LAB, PAH). Oceanologica
684 Acta, 16, 145–161.

685 Branco, J.C., 2008. Variação morfológica dos ecossistemas de planície de maré na Foz do Rio
686 Cachoeira, PR. Caminhos de Geografia, 9, 12–23.

687 Brandini, N., da Costa Machado, E., Sanders, C.J., Cotovicz Jr, L.C., Bernardes, M.C.,
688 Knoppers, B.A., 2022. Organic matter processing through an estuarine system:
689 Evidence from stable isotopes (δ13C and δ15N) and molecular (lignin phenols)
690 signatures. Estuarine, Coastal and Shelf Science, 265, 107707.

691 Bray, E.E., Evans, E.D., 1961. Distribution of *n*-paraffin as a clue to recognition of source beds.
692 Geochimica et Cosmochimica Acta, 22, 2-15.

693 Bueno, C., Brugnoli, E., Bergamino, L., Muniz, P., García-Rodríguez, F., Figueira, R., 2018.
694 Anthropogenic and natural variability in the composition of sedimentar organic matter
695 of the urbanised coastal zone of Montevideo (Río de la Plata). Marine Pollution Bulletin,
696 126, 197–203.

697 Cabral, A.C., Stark, J.S., Kolm, H.E., Martins, C.C., 2018. An integrated evaluation of some
698 faecal indicator bacteria (FIB) and chemical markers as potential tools for monitoring
699 sewage contamination in subtropical estuaries. Environmental Pollution, 235, 739-749.

700 Cabral, A.C., Wilhelm, M.M., Figueira, R.C., Martins, C.C., 2019. Tracking the historical
701 sewage input in South American subtropical estuarine systems based on faecal sterols
702 and bulk organic matter stable isotopes ($\delta^{13}C$ and $\delta^{15}N$). Science of The Total
703 Environment, 655, 855-864.

704 Calijuri, M.D.C., Cunha, D.G.F., Moccellin, J., 2013. Fundamentos ecológicos e ciclos
705 naturais. Engenharia Ambiental: Conceitos, Tecnologia e Gestão. São Paulo: Elsevier
706 Editora Ltda.

707 Camargo, M.G., 2006. Sysgran: um sistema de código aberto para análises granulométricas.
708 Revista Brasileira de Geofísica, 2, 371–378.

709 Canuel, E.A., Hardison, A.K., 2016. Sources, ages, and alteration of organic matter in estuaries.
710 Annual Review of Marine Science, 8, 409-434.

711 Cardoso, F.D., Dauner, A.L.L., Martins, C.C., 2016. A critical and comparative appraisal of
712 polycyclic aromatic hydrocarbons in sediments and suspended particulate material from
713 a large south american subtropical estuary. Environmental Pollution, 214, 219–229.

714 Carreira, R.S., Cordeiro, L.G.M.S., Bernardes, M.C., Hatje, V., 2016. Distribution and
715 characterization of organic matter using lipid biomarkers: A case study in a pristine
716 tropical bay in NE Brazil. Estuarine, Coastal and Shelf Science, 168, 1–9.

717 Cattani, P.E., Lamour, M.R., 2016. Considerations regarding sedimentation rates along the EW
718 axis of the Paranaguá Estuarine Complex, Brazil: a bathymetric approach. Journal of
719 Coastal Research, 32, 619-628.

720 Ceccopieri, M., Scofield, A.L., Almeida, L., Araújo, M.P., Hamacher, C., Farias, C.O., Soares,
721 M.L.G., Wagner, A.L., 2021. Carbon isotopic composition of leaf wax n-alkanes in
722 mangrove plants along a latitudinal gradient in Brazil. Organic Geochemistry, 161,
723 104299.

724 Chevalier, N., Savoye, N., Dubois, S., Lama, M.L., David, V., Lecroart, P., Menach, K.L.,
725 Budzinski, H.J., 2015. Precise indices based on n-alkane distribution for quantifying
726 sources of sedimentary organic matter in coastal systems. Organic Geochemistry, 88,
727 69–77.

728 Dan, S.F., Liu, S.M., Yang, B., 2020. Geochemical fractionation, potential bioavailability, and
729 ecological risk of phosphorus in surface sediments of the Cross River estuary system
730 and adjacent shelf, South East Nigeria (West Africa). Journal of Marine Systems, 201,
731 103244.

732 Daniel, M.H., Montebelo, A.A., Bernardes, M.C., Ometto, J.P., Camargo, P.B.D., Krusche,
733 A.V., Ballester, M.V., Victoria, R.L., Martinelli, L.A., 2002. Effects of urban sewage
734 on dissolved oxygen, dissolved inorganic and organic carbon, and electrical
735 conductivity of small streams along a gradient of urbanization in the Piracicaba River
736 basin. Water, Air, and Soil Pollution, 136, 189-206.

737 Das, S.K., Routh, J., Roychoudhury, A.N., Klump, J.V., 2008. Elemental (C, N, H and P) and
738 stable isotope ($\delta^{15}N$ and $\delta^{13}C$) signatures in sediments from Zeekoevlei, South Africa: a
739 record of human intervention in the lake. Journal of Paleolimnology, 39, 349–360.

740 Dauner, A.L., Dias, T.H., Ishii, F.K., Libardoni, B.G., Parizzi, R.A., Martins, C.C., 2018.
741 Ecological risk assessment of sedimentary hydrocarbons in a subtropical estuary as tools
742 to select priority areas for environmental management. Journal of Environmental
743 Management, 223, 417-425.

744 Dauner, A.L.L., Mollenhauer, G., Bícego, M.C., de Souza, M.M., Nagai, R.H., Figueira, R.C.
745 L., Mahiques, M.M., Souza, S.H.M., Martins, C.C., 2019. Multi-proxy reconstruction
746 of sea surface and subsurface temperatures in the western South Atlantic over the last~
747 75 kyr. Quaternary Science Reviews, 215, 22-34.

748 De Leeuw, J.W., Largeau, C., 1993. A review of macromolecular organic compounds that
749 comprise living organisms and their role in kerogen, coal, and petroleum formation. In:
750 Organic Geochemistry, 23-72.

751 Defesa Civil do Paraná. 2011. Webpage: https://www.defesacivil.pr.gov.br/sites/defesa-
752 civil/arquivos_restritos/files/documento/2019-05/desastre_de_2011_-
753 _aguas_de_marco.pdf. Accessed on March 05, 2023.

754 Duarte, C.M., Middelburg, J.J., Caraco, N., 2005. Major role of marine vegetation on the
755 oceanic carbon cycle. Biogeosciences, 2, 1-8.

756 Eganhouse, R.P., 1997. Molecular markers in environmental geochemistry. American
757 Chemical Society Symposium Series 671.

758 Farrington, J.W., Frew, N.M., Geshwend, P.M., Tripp, R.W., 1977. Hydrocarbons in cores of
759 northwestern Atlantic coastal and continental margin sediments. Estuarine and Coastal
760 Marine Science, 5, 793–808

761 Ficken, K.J., Li, B., Swain, D.L., Eglinton, G., 2000. An *n*-alkane proxy for the sedimentary
762 input of submerged/ floating freshwater aquatic macrophytes. Organic Geochemistry
763 31, 745-749.

764 Filimonova, V., Goncalves, F., Marques, J.C., De Troch, M., Goncalves, A.M., 2016. Fatty acid
765 profiling as bioindicator of chemical stress in marine organisms: a review. Ecological
766 Indicators, 67, 657-672.

767 Freeman, K.H., Pancost, R.D., 2014. Biomarkers for terrestrial plants and climate. In: Organic
768 Geochemistry. Elsevier Inc. pp. 395-416.

769 Garcia, M.R., Cattani, A.P., Lana, P.C., Figueira, R.C.L., Martins, C.C., 2019. Petroleum
770 biomarkers as tracers of low-level chronic oil contamination of coastal environments: A
771 systematic approach in a subtropical mangrove. Environmental Pollution, 249, 1060-
772 1070.

773 Garcia, M.R., Martins, C.C., 2021. A systematic evaluation of polycyclic aromatic
774 hydrocarbons in South Atlantic subtropical mangrove wetlands under a coastal zone
775 development scenario. Journal of Environmental Management, 277, 111421.

776 Hedges, J.I., Keil, R.G., 1999. Organic geochemical perspectives on estuarine processes:
777 sorption reactions and consequences. Marine Chemistry, 65, 55–65.

778 Hedges, J.I., Keil, R.G., 1999. Organic geochemical perspectives on estuarine processes:
779 sorption reactions and consequences. Marine Chemistry, 65, 55–65.

780 IPARDES (Instituto Paranaense de Desenvolvimento Econômico e Social). 2001. Zoneamento
781 da Área de Proteção Ambiental de Guaraqueçaba. Curitiba: IPARDES, p. 150.

782 Khan, N.S., Vane, C.H., Horton, B.P., Hillier, C., Riding, J.B., Kendrick, C.P., 2015. The
783 application of $\delta^{13}C$, TOC and C/N geochemistry to reconstruct Holocene relative sea
784 levels and paleoenvironments in the Thames Estuary, UK. Journal of Quaternary
785 Science, 30, 417–433.

786 Kuypers, M.M.M., Marchant, H.K., Kartal, B., 2018. The microbial nitrogen-cycling network.
787 Nature Reviews Microbiology, 16, 263-276.

788 Lamour, M.R., Angulo, R.J., Soares, C.R., 2007. Bathymetrical evolution of critical shoaling
789 sectors on Galheta Channel, navigable access to Paranaguá Bay, Brazil. Journal of
790 Coastal Research, 23, 49-58.

791 Lamour, M.R., Soares, C.R., Carrilho, J.C., 2004. Mapas de parâmetros texturais de sedimentos
792 de fundo do complexo estuarino de Paranaguá PR. Boletim Paranaense de Geociências,
793 55, 77-82.

794 Lana, P.C., Marone, E., Lopes, R.M., Machado, E.C., 2001. The subtropical estuarine complex
795 of Paranaguá Bay, Brazil. In: Coastal marine ecosystems of Latin America. Springer,
796 Berlin, Heidelberg. pp. 131-145.

797 Lessa, G.C., Santos, F.M., Souza Filho, P.W., Corrêa-Gomes, L.C., 2018. Brazilian estuaries:
798 A geomorphologic and oceanographic perspective. In: Brazilian Estuaries. Springer,
799 Cham. pp. 1-37.

800 Mahiques M. M., Fukumoto M. M., Silveira I. C. A., Figueira R. C. L., Bícego M. C., Lourenço
801 R. A., et al. (2007). Sedimentary changes on the southeastern Brazilian upper slope
802 during the last 35,000 years. Anais da Academia Brasileira de Ciências 79, 171–181.

803 Marone, E., Machado, E.C., Lopes, R.M., Silva, E.T.D., 2005. Land-ocean fluxes in the
804 Paranaguá Bay estuarine system, southern Brazil. Brazilian Journal of Oceanography,
805 53, 169-181.

806 Martins, C.C., Bícego, M.C., Figueira, R.C., Angelli, J.L.F., Combi, T., Gallice, W.C., Mansur,
807 E.N., Rocha, M.L., Wisnieski, E., Ceschim, L.M.M., Ribeiro, A.P., 2012. Multi-

808 molecular markers and metals as tracers of organic matter inputs and contamination
809 status from an Environmental Protection Area in the SW Atlantic (Laranjeiras Bay,
810 Brazil). Science of the Total Environment,417, 158-168.

811 Martins, C.C., Braun, J.A., Seyffert, B.H., Machado, E.C., Fillmann, G., 2010. Anthropogenic
812 organic matter inputs indicated by sedimentary fecal steroids in a large South American
813 tropical estuary (Paranaguá estuarine system, Brazil). Marine Pollution Bulletin, 60,
814 2137-2143.

815 Martins, C.C., Doumer, M.E., Gallice, W.C., Dauner, A.L.L., Cabral, A.C., Cardoso, F.D.,
816 Dolci, N.N., Camargo, L.M. Ferreira, P.A.L., Figueira, R.C.L. Mangrich, A.S., 2015.
817 Coupling spectroscopic and chromatographic techniques for evaluation of the
818 depositional history of hydrocarbons in a subtropical estuary. Environmental Pollution,
819 205, 403-414.

820 Martins, C.C., Seyffert, B.H., Braun, J.A., Fillmann, G., 2011. Input of organic matter in a large
821 South American tropical estuary (Paranaguá Estuarine System, Brazil) indicated by
822 sedimentary sterols and multivariate statistical approach. Journal of the Brazilian
823 Chemical Society, 22, 1585-1594.

824 Mcleod, E., Chmura, G.L., Bouillon, S., Salm, R., Björk, M., Duarte, C.M., Lovelock, C.E.,
825 Schlesinger, W.H., Silliman, B.R., 2011. A blueprint for blue carbon: toward an
826 improved understanding of the role of vegetated coastal habitats in sequestering CO_2.
827 Frontiers in Ecology and the Environment, 9, 552-560.

828 Mertz, C., Kleber, M., Jahn, R., 2005. Soil organic matter stabilization pathways in clay sub-
829 fractions from a time series of fertilizer deprivation. Organic. Geochemistry 36, 1311–
830 1322.

831 Meyers, P.A., 1994. Preservation of elemental and isotopic source identification of sedimentary
832 organic matter. Chemical Geology, 114, 289-302.

833 Meyers, P.A., 1997. Organic geochemical proxies of paleoceanographic, paleolimnologic, and
834 paleoclimatic processes. Organic Geochemistry, 27, 213-250.

835 Meyers, P.A., Ishiwatari, R., 1993. Lacustrine organic geochemistry — an overview of
836 indicators of organic matter sources and diagenesis in lake sediments. Organic
837 Geochemistry, 20, 867-900.

838 Meyers, P.A., Teranes, J.L., 2002. Sediment organic matter. In: Tracking environmental change
839 using lake sediments. Springer, Dordrecht. pp. 239-269.

840 Middelburg, J.J., Herman, P.M.J., 2007. Organic matter processing in tidal estuaries. Marine
841 Chemistry 106, 127–147.

842 Middelburg, J.J., Nieuwenhuize, J., 1998. Carbon and nitrogen stable isotopes in suspended
843 matter and sediments from the Schelde Estuary. Marine Chemistry, 60, 217-225.

844 Mizerkowski, B.D., Hesse, K.J., Ladwig, N., Machado, E.C., Rosa, R., Araujo, T., Koch, D.,
845 2012. Sources, loads and dispersion of dissolved inorganic nutrients in Paranaguá Bay.
846 Ocean Dynamics, 62, 1409-1424.

847 Noernberg, M. A., Angelotti, R., Caldeira, G. A., & Ribeiro de Sousa, A. F. 2008. Determinação
848 da sensibilidade do litoral paranaense à contaminação por óleo. Brazilian Journal of
849 Aquatic Science and Technology, 12(2), 49-59.

850 Nagai R. H., Sousa S. H. M., Lourenço R. A., Bícego M. C., Mahiques M. M. (2010).
851 Paleoproductivity changes during the late quaternary in the southeastern Brazilian upper

852 continental margin of the southwestern Atlantic. Brazilian Journal of Oceanography, 58,
853 31–41.

854 Netto, S.A., Lana, P.C., 1997. Influence of *Spartina alterniflora* on superficial sediment
855 characteristics of tidal flats in Paranagua Bay (South-eastern Brazil). Estuarine, Coastal
856 and Shelf Science, 44, 641-648.

857 Paladino, I.M., Mengatto, M.F., Mahiques, M.M., Noernberg, M.A., Nagai, R.H., 2022. End-
858 member modeling and sediment trend analysis as tools for sedimentary processes
859 inference in a subtropical estuary. Estuarine, Coastal and Shelf Science, 108126.

860 Paula, E.V., Paz, O.L.S., Pai, M.O., Oliveira, M., 2021. Sustaining port activities through nature
861 conservation: the case of Paraná Coast in Southern Brazil. In: Practices in Regional
862 Science and Sustainable Regional Development. https://doi.org/10.1007/978-981-16-
863 2221-2_720

864 Peñuelas, J., Poulter, B., Sardans, J., Ciais, P., Van Der Velde, M., Bopp, L., Boucher, O.,
865 Godderis, Y., Hinsinger, P., Lusia, J., Nardin, E., Vicca, S., Obersteiner, M., Janssens,
866 I.A., 2013. Human-induced nitrogen–phosphorus imbalances alter natural and managed
867 ecosystems across the globe. Nature Communications, 4, 1-10.

868 Peters, K.E., Walters, C.C., Moldowan, J.M., 2005. The biomarker guide: Volume 1 -
869 Biomarkers and isotopes in the environment and human history. Cambridge University
870 Press.

871 Piola, R.F., Moore, S.K., Suthers, I.M., 2006. Carbon and nitrogen stable isotope analysis of
872 three types of oyster tissue in an impacted estuary. Estuarine, Coastal and Shelf Science,
873 66, 255-266.

874 Readman, J.W., Fillmann, G., Tolosa, I., Bartocci, J., Villeneuve, J.-P., Catinni, C., Mee, L.D.,
875 2002. Petroleum and PAH contamination of the Black Sea. Marine Pollution Bulletin,
876 44, 48–62.

877 Rivera-Monroy, V.H., Lee, S.Y., Kristensen, E., Twilley, R.R., 2017. Mangrove Ecosystems:
878 A Global Biogeographic Perspective. Springer.

879 Sachse, D., Radke, J., Gleixner, G., 2006. δD values of individual *n*-alkanes from terrestrial
880 plants along a climatic gradient - implications for the sedimentary biomarker record.
881 Organic Geochemistry, 37, 469–483.

882 Savage, C., Leavitt, P.R., Elmgren, R., 2010. Effects of land use, urbanization, and climate
883 variability on coastal eutrophication in the Baltic Sea. Limnology and Oceanography,
884 55, 1033–1046.

885 Sikes, E.L., Uhle, M.E., Nodder, S.D., Howard, M.E., 2009. Sources of organic matter in a
886 coastal marine environment: evidence from n-alkanes and their δ13C distributions in
887 the Hauraki Gulf, New Zealand. Marine Chemistry 113, 149-163.

888 Soares, C. R., & Barcelos, J. H. 1995. Considerações sobre os sedimentos de fundo das baías
889 de Laranjeiras e de Guaraqueçaba, Complexo Estuarino da Baía de Paranaguá (Paraná,
890 Brasil). Boletim Paranaense de Geociências, 43, 41-60.

891 Tolosa, I., Mesa-Albernas, M., Alonso-Hernandez, C.M., 2009. Inputs and sources of
892 hydrocarbons in sediments from Cienfuegos bay, Cuba. Marine Pollution Bulletin, 58,
893 1624-1634.

894 UNESCO (United Nations Educational Scientific and Cultural Organization). 1999.
895 Convention concerning the protection of the world cultural and natural heritage: Atlantic
896 forest south/ east Brazil. Brazil, March, p. 257.

897 USEPA. (1996). Method 3050B. Acid digestion of sediments, sludges and soil. Revision 2,
898 December, 1996.

899 USEPA. (2007). SW-846 test methods for evaluating solid waste, physical/chemical methods,
900 method 6010C: Inductively coupled plasma-atomic emission spectrometry. Revision 3,
901 February, 2007.

902 Vaalgamaa, S., Sonninen, E., Korhola, A., Weckström, K. 2013. Identifying recent sources of
903 organic matter enrichment and eutrophication trends at coastal sites using stable
904 nitrogen and carbon isotope ratios in sediment cores. Journal of Paleolimnology, 50,
905 191-206.

906 Vieira Filho, J.E.R., 2016. Expansão da fronteira agrícola no Brasil: desafios e perspectivas.
907 IPEA. p. 1-28.

908 Villeneuve, J.P., de Mora, S.J., Cattini, C., Carvalho, F.P., 2000. Determination of
909 organochlorinated compounds and petroleum hydrocarbons in sediment sample IAEA-
910 408. Results from a world-wide intercalibration exercise. Journal of Environmental
911 Monitoring, 2, 524-528.

912 Volkman, J.K., Holdsworth, D.G., Neill, G.P., Bavor Jr, H.J., 1992. Identification of natural,
913 anthropogenic and petroleum hydrocarbons in aquatic sediments. Science of the Total
914 Environment, 112, 203-219.

915 Voss, M., Emeis, K.-C., Hille, S., Neumann, T., Dippner, J.W., 2005. Nitrogen cycle of the
916 Baltic Sea from an isotopic perspective. Global Biogeochemical Cycles, 19, 1–15,
917 GB3001.

918 Wilhelm, M.M., Cabral, A.C., Dauner, A.L.L., Garcia, M.R., Figueira, R.C.L., Martins, C.C.,
919 2023. Variability of sedimentary organic matter in subtropical estuarine systems due to
920 anthropogenic and climatic events. Environmental Earth Sciences, 82, 22.

921 Wisnieski, E., Ceschim, L.M., Martins, C.C., 2016. Validation of an analytical method for
922 geochemical organic markers determination in marine sediments. Química Nova, 39,
923 1007-1014.

924 Zhang, S., Liang, C., Xian, W., 2020. Spatial and temporal distributions of terrestrial and marine
925 organic matter in the surface sediments of the Yangtze River estuary. Continental Shelf
926 Research, 203, 104158.

927

3 CAPÍTULO II

1.

Mudanças históricas na composição da matéria orgânica sedimentar revelam o impacto humano e a variabilidade climática em um estuário subtropical no Atlântico Sul

Marines M. Wilhelm[1,2,*], Ana Lúcia L. Dauner[3], Ana Caroline Cabral[1,2], Marina Reback Garcia [2], Renata H. Nagai[2,4], Rubens C. L. Figueira [4], Michel M. Mahiques[4], César C. Martins [1,*]

[1] Centro de Estudos do Mar, Campus Pontal do Paraná, Universidade Federal do Paraná. Caixa Postal 61, 83255-976, Pontal do Paraná, PR, Brasil.

[2] Programa de Pós-Graduação em Sistemas Costeiros e Oceânicos (PGSISCO), Universidade Federal do Paraná, Caixa Postal 61, 83255-976, Pontal do Paraná, PR, Brasil.

[3] Programa de Pesquisa em Ecossistemas e Meio Ambiente, Universidade de Helsinque, Finlândia.

[4] Instituto Oceanográfico, Universidade de São Paulo, Praça do Oceanográfico, 191, 05508-900, São Paulo, SP, Brasil.

[*]Autores correspondentes: wilhelm.marines@gmail.com (M.M. Wilhelm)
ccmart@ufpr.br (C.C. Martins)

Resumo

Os estuários desempenham um papel fundamental na ciclagem da matéria orgânica, pois são ambientes dinâmicos que recebem contribuições de múltiplas fontes. Eles também funcionam como uma interface entre o continente e o oceano costeiro, onde ocorre a desaceleração das correntes fluviais, a floculação da matéria orgânica devido à diferença de salinidade e a sedimentação. O Complexo Estuarino de Paranaguá (CEP) é um importante ecossistema costeiro brasileiro, com rica biodiversidade e importância econômica. O CEP abriga remanescentes de Mata Atlântica, considerada Patrimônio Mundial pela UNESCO, e possui o maior terminal graneleiro e o primeiro em movimentação de contêineres da América Latina. O objetivo deste estudo foi avaliar possíveis alterações no ciclo biogeoquímico da matéria orgânica sedimentar, bem como as alterações composicionais que estas alterações podem causar. Para isso, foi determinada a composição elementar e isotópica da matéria orgânica em testemunhos sedimentares. Os resultados foram relacionados geocronologicamente com eventos naturais e antrópicos, a fim de estabelecer um histórico das alterações ambientais ocorridas na região. O entendimento das fontes de matéria orgânica sedimentar (MOS) é essencial para a avaliação da qualidade ambiental dos ambientes costeiros e marinhos em todo o mundo. As mudanças climáticas e a atividade humana estão causando alterações no ciclo biogeoquímico da MO, o que pode ter impactos significativos na saúde e na biodiversidade desses ambientes. O estudo forneceu importantes insights sobre os impactos das atividades humanas no meio ambiente, como a transposição do rio Capivari para o rio Cachoeira e as dragagens no leito do estuário e na desembocadura, causando mudanças significativas nos sistemas sedimentares e no armazenamento de material orgânico local. Essas mudanças podem ter impactos negativos na biodiversidade, na qualidade da água e no ciclo de nutrientes. Além disso, o estudo forneceu uma visão abrangente dos impactos das atividades humanas, gerando dados concretos, e visa auxiliar com recomendações para a gestão ambiental na região.

Palavras-chave: Impacto antropogênico; Matéria orgânica; Composição elementar e isotópica; Ciclagem; Mudanças ambientais.

3.1 Introdução

A matéria orgânica (MO) tem um fluxo cíclico e pode ser reaproveitada repetidamente em cada nível trófico devido às alterações das moléculas que a compõem (Calijuri et al., 2013). Esse fluxo dinâmico ocorre em múltiplos compartimentos ao longo de vários estágios de biossíntese, metabolismo e degradação, através de reações espontâneas ou por intervenção biológica (Harvey, 2006; Summons, 1993).

Os principais elementos constituintes da MO de importância ecológica são o carbono, o nitrogênio, o enxofre e o fósforo, uma vez que estes elementos se distribuem em todos os compartimentos bióticos e abióticos e através de diferentes ciclos biogeoquímicos, determinando a composição e a distribuição da MO no ambiente terrestre e marinho (Peñuelas et al., 2019; Fernández-Martines et al., 2021).

O principal componente elementar da MO é o carbono, que está sujeito aos processos físicos, químicos, biológicos e geológicos que atuam em diferentes escalas de tempo, sendo estas desde dias e semanas quando envolve a reciclagem biológica, ou mais longas quando envolvem rochas sedimentares e a geração dos combustíveis fósseis (Killops & Killops, 2005).

Processos naturais e antropogênicos, associados a mudanças do clima, podem alterar fluxo de carbono da bacia de drenagem para o estuário e o oceano costeiro, graças as mudanças no balanço hídrico (variabilidade nas taxas de precipitação e evapotranspiração), práticas agrícolas, supressão de áreas alagadas, entre outros eventos (Bauer et al., 2013).

Os estuários desempenham um papel fundamental na ciclagem da MO, pois: são ambientes dinâmicos que recebem contribuições de múltiplas fontes de MO; por funcionar como um ambiente de transição entre o continente e o oceano costeiro, pelo papel fundamental no aprisionamento de partículas fluviais devido a desaceleração das correntes, pela floculação causada pela diferença de salinidade no interior do estuário e consequente sedimentação, pela respiração microbiana e a foto-oxidação (Postacchini et al., 2023; Khan et al., 2014; Bauer et al., 2013; Killops & Killops, 2005).

Uma das lacunas que precisa ser compreendida é como cada sistema estuarino com suas peculiaridades, fatores físicos, geológicos e biológicos controlam a ciclagem da MO nesses ambientes ao longo de uma escala de tempo (Goñi et al., 2003). Com esse intuito, o objetivo deste trabalho é avaliar as possíveis alterações no ciclo biogeoquímico da MO, em função da variabilidade climática e da ação antrópica, além de estimar a contribuição de MO alóctone no para o Complexo Estuarino de Paranaguá (CEP), através da determinação da composição elementar e isotópica da MO em testemunhos sedimentares.

3.2 Área de estudo

O Complexo Estuarino de Paranaguá (CEP) está localizado no litoral centro-norte do estado do Paraná (25°00'S–25°35'S; 48°15'W–48°40'W), na costa sul do Brasil e abrange uma área de aproximadamente 622 Km^2. O CEP pode ser subdividido em dois eixos principais, denominados 'Leste–Oeste', compreendendo as Baías de Antonina e de Paranaguá, e dois portos situados em suas margens, e 'Norte–Sul', que compreende as Baías das Laranjeiras, Guaraqueçaba e Pinheiros, onde a pesca artesanal e a agropecuária são as atividades humanas mais importantes (Fig. 1) (Marone et al., 2005; Martins et al., 2010; 2015).

As Baías de Antonina e de Paranaguá estão sob maior influência antrópica, devido as atividades pesqueiras, urbanas e turísticas em suas margens e entorno, a presença de fábricas de fertilizantes, terminais de combustíveis e os Portos de Antonina e de Paranaguá, esse último considerado o maior porto graneleiro da América Latina (Gurgatz et al., 2023, Garcia & Martins, 2021).

O clima da região é classificado como Cfa, o que significa que é subtropical úmido. A precipitação média anual é de 2.500 mm, com máximos de 5.300 mm. A umidade média do ar de 85%. A estação chuvosa começa no final da primavera e dura a maior parte do verão. A estação seca dura do final do outono até o final do inverno, mas geralmente é interrompida por um período chuvoso curto e fraco no início do inverno (IPARDES, 2001; Lana et al., 2001). As temperaturas médias são elevadas, com o mês mais quente com média superior a 22° C e o mês mais frio com média entre 3 °C e 18°C. Devido à baixa altitude nessas regiões, as geadas são pouco frequentes (IPARDES, 2001). Essas condições climáticas da planície costeira são um recurso natural importante para a região. Devido ao fornecimento de água para o abastecimento doméstico e geração de energia elétrica, além de contribuir para a biodiversidade local.

O uso e a ocupação dos solos nas margens do CEP datam de meados do século XVI, impulsionada pela busca de mão-de-obra indígena e pela descoberta de ouro nos rios que desaguam nas baías, o que ocasionou um movimento migratório para o litoral paranaense, com posterior declínio devido ao término do ciclo do ouro (Pierri et al., 2006; Chemin & Abrahão, 2014). Com a fixação e aumento da população na região, iniciou-se o desmatamento de áreas de vegetação nativa para o cultivo e criação de animais (Pierri et al., 2006).

Com a implantação da estrada da Graciosa (1873) e de uma estrada de ferro (1885), tem-se o início do ciclo de extração de madeira (*Araucária angustifólia*; *Ilex paraguariensis*) e consequente exportação pelos portos de Antonina e Paranaguá (Chemin & Abrahão, 2014; IPARDES, 1989). Devido à proximidade com a cidade de Curitiba, a capital do estado do

Paraná, Antonina torna-se, entre 1930 e 1950, o principal porto do estado e o 4º maior do país em exportação (Estades, 2003).

Mudanças nas atividades econômicas nos cenários nacional e mundial ao término da Segunda Guerra Mundial fizeram com que Paranaguá se tornasse o porto mais importante do estado a partir da década de 1950 e com a ampliação de suas instalações no início da década de 1970, passou a receber navios mais modernos utilizados para o transporte de grãos, consolidando-se nas décadas subsequentes como o maior porto graneleiro da América Latina (Martins et al., 2015 Pierri et al., 2006).

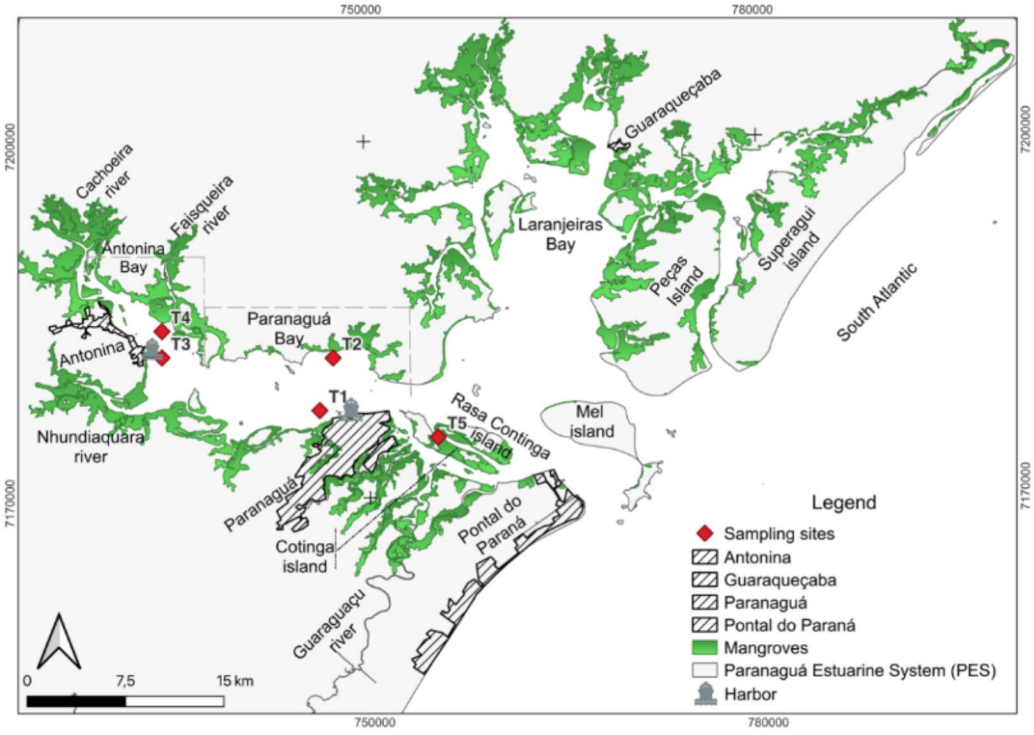

Figura 1.Área de estudo: Complexo Estuarino de Paranaguá e pontos amostrais dos cinco testemunhos.

1.Área de estudo: Complexo Estuarino de Paranaguá e pontos amostrais dos cinco testemunhos.

A dinâmica demográfica do litoral paranaense é definida principalmente pelas variações nas atividades econômicas regionais, em destaque, as atividades portuárias, o turismo, a pesca artesanal, a aquicultura, a agricultura e as indústrias petroquímicas e de fertilizantes (Azevedo, 2016; Pierri et al., 2006). Dados do IBGE mostram o crescimento demográfico de Antonina e Paranaguá entre o ano de 1872 (4.795 e 7.519 habitantes por município, respectivamente) e o último censo demográfico, realizado em 2022, mostrando uma população local com 18.091 e 145.829 habitantes, respectivamente (IBGE, 2023).

3.3 Material e Métodos

3.3.1 Amostragem

Cinco testemunhos sedimentares foram coletados ao longo do mês de abril de 2019, com auxílio de um *gravity corer* nos locais indicados na Fig. 1. Os testemunhos foram abertos longitudinalmente e sub-amostrados em parcelas de 2 cm até 120 cm, sendo armazenados em recipientes de alumínio previamente calcinados em forno mufla por 4 h, 400 °C. Em seguida, as amostras foram congeladas a –20 °C e então, liofilizadas, pesadas, homogeneizadas/maceradas e acondicionadas em frascos de vidro limpos até posterior análise.

3.3.2 Datação dos testemunhos

A geocronologia dos sedimentos foi estabelecida através da determinação do ^{210}Pb, utilizando um detector de germânio hiper puro, tipo GMX 25190P acoplado a um analisador multicanal SPECTRUM MASTER™, modelo 92XII, da EG&G/ORTEC. A determinação do ^{210}Pb foi realizada nas camadas mais superficiais dos testemunhos, isso é, nos primeiros 100 cm de cada coluna sedimentar, visto a detecção do ^{210}Pb para fins geocronológicos é viável apenas para intervalos entre 100 e 150 anos após deposição do material sedimentar e que dados prévios de taxa de sedimentação no CEP indicaram valores em torno de 0,5 até 1,0 cm ano^{-1}, o que poderia refletir a deposição dos últimos 50 a 100 anos.

O modelo geocronológico pelo ^{210}Pb foi gerado a partir da medição deste radionuclídeo em diferentes camadas de cada testemunho, gerando perfis de distribuição vertical (Fig. S1- S2) ('S' denota Informação Suplementar), através do cálculo denominado CRS (da sigla em inglês, *Constant Rate of Supply*, proposto por Appleby & Oldfield, 1978), no qual o fluxo de entrada do radionuclídeo (isso é, taxa de deposição de ^{210}Pb em função do tempo e da profundidade) no ambiente é constante. Desse modo, o excesso de atividade de ^{210}Pb diminuirá exponencialmente com a profundidade do sedimento, dificultando sua detecção, necessitando extrapolar os dados do modelo utilizado para obter a datação do perfil sedimentar (Lubis, 2006).

3.3.3 Análises granulométricas, elementares e isotópicas

As análises granulométricas foram realizadas em um granulomêtro *Malvern Hydro 2000*. Utilizou-se 2,000 g de sedimento de cada amostra, a qual foi realizada a descarbonatação com HCl a 10 % em água (v:v) e na sequência foi realizada a remoção de MO com auxílio de peróxido de hidrogênio (H_2O_2) a 10% em água (v:v), sendo as duas etapas realizadas sobre chapa aquecida (65 °C) (Angeli et al., 2020; Paladino et al., 2022). Os dados obtidos na escala *φ (phi)* foram transformados em porcentagens de cascalho, areia, silte e argila utilizando o *Software Sysgran 3.2* (Camargo, 2006).

O conteúdo de carbono inorgânico total (CIT), correspondente ao carbonato de cálcio, foi determinado por diferenças de massa através de pesagem antes e após a exposição de cerca de 1,000 g de sedimento seco a solução de HCl diluída a 10 % em água (v:v).

Os conteúdos de carbono orgânico total (COT) e nitrogênio total (NT) e a razão entre os respectivos isótopos estáveis ($^{13}C/^{12}C$, $\delta^{13}C$ e $^{15}N/^{14}N$, $\delta^{15}N$) foram determinados com auxílio

do analisador elementar (EA) *Costech Elemental Combustion System*, acoplado ao detector de espectrometria de massas com razão isotópica *Thermo Scientific Delta V Advantage Isotope Ratio MS* (IRMS).

3.3.4 Razão C/N e Análise de Dados

As porcentagens em peso de carbono e nitrogênio das amostras de sedimentos são usadas para o cálculo da razão de massa C/N, que são multiplicados por 1,167 (i.e., a razão das massas atômicas do nitrogênio e carbono) para a obtenção das razões atômicas C/N (equação I) (Meyers & Teranes, 2002).

Equação I: $$C/N = \{(C/N) * (1{,}167)\}$$

As análises estatísticas foram realizadas no ambiente R (versão 4.3.0) (Juggins, 2017; Montero & Vilar, 2014; Okesanen et al., 2022). A representação SAX (Aproximação Agregada Simbólica) do pacote 'TSclust' foi utilizada para criar a matriz de dissimilaridade, enquanto o pacote 'vegan', foi empregado para criar os *clusters* restritos com base nas distancias euclidianas dos dados normalizados (i.e., subtração do valor pela média e divisão pelo desvio padrão), e a análise de agrupamento restrita foi realizada pelo pacote 'rioja', para definir as zonas estratigráficas (Dauner et al., 2019; 2022). O pacote *broken stick*, que possui funções para descrição de curvas individuais de um modelo linear misto usando *B-splines* de 2ª ordem, foi utilizado com o intuito de definir o número de agrupamentos do *cluster* (zonas) que melhor explicasse os dados analisados (van Buuren, 2023) (Fig. S3).

3.4 Resultados e discussão

3.4.1 Granulometria

No testemunho T1, o diâmetro médio do grão variou entre à areia muito fina (φ = 3–4) a média (φ = 1–2), com as maiores porcentagens de areia fina (φ = 2–3) sendo verificadas entre a base do testemunho e 47 cm, oscilando para areia média. A partir desta profundidade o diâmetro médio passa para areia muito fina (entre 45 e 31 cm), alternando para areia fina e depois retornando para areia muito fina (15 e 3 cm), com o topo do testemunho sendo constituído de silte grosso (Fig. S4).

O diâmetro médio do grão para o testemunho T2 variou entre silte fino (φ = 7–8) a areia grossa (φ = 0–1). Entre a base do testemunho e 69 cm, o diâmetro médio dos sedimentos oscilou entre silte fino (φ = 7–8) e silte médio (φ = 6–7), com presença de areia fina (φ = 2–3) em 65 cm, voltando a oscilar de silte grosso (φ = 5–6) a silte médio e grosso novamente até 57 cm. As

amostras entre 55 a 29 cm não foram analisadas no granulomêtro a laser, em função de limitações instrumentais associadas ao tipo de grão (areia grossa a cascalho) (Fig. S5). A partir de 27 até 15 cm, o diâmetro médio voltou a oscilar entre areia fina a média (φ = 1–2). Desta profundidade até o topo deste testemunho, o diâmetro médio oscilou entre silte fino e areia muito fina (φ = 3–4). As maiores porcentagens de silte foram observadas entre a base do testemunho e 59 cm e depois próximo ao topo do testemunho, com predomino de areia somente no intervalo de 27 a 15 cm (Fig. S5).

No testemunho T3, o diâmetro médio do grão variou entre silte fino (φ = 7–8) a areia fina (φ = 2–3). As maiores porcentagens de areia foram observadas entre a base do testemunho e 63 cm, oscilando com silte grosso. A partir desta profundidade o diâmetro médio passou para silte (fino, médio e grosso) até o topo do testemunho (Fig. S6).

No testemunho T4, o diâmetro médio do grão variou entre argila grossa (φ = 8–9) à silte grosso (φ = 5–6). Há o predomínio de silte da base do testemunho até 27 cm, variando o diâmetro médio entre silte grosso, médio, fino para muito fino. A partir de 25 cm, há predomínio de argila grossa até o topo do testemunho (Fig. S7).

O diâmetro médio do testemunho T5 variou entre silte grosso (φ = 5–6) à areia muito fina (φ = 3–4). Entre a base do testemunho até 61 cm, ocorreu predomínio de areia fina. A partir desta profundidade até o topo, houve alternância de areia fina a muito fina, com exceção nas profundidades 35 cm e 27 cm, que apresentaram silte grosso como diâmetro médio do grão (Fig. S8).

Os valores da contribuição percentual de sedimentos finos (% silte + argila) variaram entre 0,0 e 34,7 (média 13,2 □ 7,6), 11,7 e 95,6 (média 69,3 □ 26,4), 11,7 e 97,3 (média 61,0 □ 31,3); 46,6 e 99,9 (média 76,3 □ 15,7); e 6,5 e 38,6 % (média 13,7 □ 6,8) para os testemunhos T1 até T5, respectivamente (Fig. S4–S8; Tabelas S1–S5).

241 3.4.2 Geocronologia

242 Os resultados dos modelos de idade dos testemunhos analisados são apresentados na
243 Tabela S6. O método adotado foi o CRS, em que o testemunho T1 cobre até o ano de 1820, o
244 Testemunho T2 até 1762, o testemunho T3 até 1917, o testemunho T4 até 1861 e o testemunho
245 T5 até 1876 (Tabela 1).

246 Com base na atividade do radionuclídeo ^{210}Pb para cada seção dos testemunhos
247 analisados, foram estimadas as seguintes taxas de sedimentação, conforme abaixo:

248 (i) Testemunho T1 com taxa de sedimentação variável entre 0,20 e 1,39 cm ano^{-1} (média
249 = 0,83 □ 0,29). As taxas de sedimentação variaram desde 0,20 ± 0,02 cm ano^{-1} na base, com um
250 máximo de 1,39 ± 0,14 cm ano^{-1} em 49 cm chegando a 0,80 ± 0,08 cm ano^{-1} no topo da coluna
251 sedimentar.

252 (ii) Testemunho T2 com taxa de sedimentação variável entre 0,11 e 3,18 cm ano^{-1} (média
253 = 1,11 □ 0,85). As taxas de sedimentação variaram ao longo da coluna sedimentar, com valores
254 mínimos de 0,11 ± 0,01 cm ano^{-1} na base, alcançando um máximo de 3,18 ± 0,32 cm ano^{-1} em
255 47 cm e 1,08 ± 0,11 cm ano^{-1} no topo do testemunho.

256 (iii) Testemunho T3 com taxa de sedimentação variável entre 0,54 e 6,73 cm ano^{-1} (média
257 = 1,90 □ 1,59). As taxas de sedimentação variaram de 0,62 ± 0,06 cm ano^{-1} na base, com um
258 máximo de 6,73± 0,67 cm ano^{-1} em 31 cm chegando a 0,78 ± 0,08 cm ano^{-1} no topo da coluna
259 sedimentar.

260 (iv) Testemunho T4 com taxa de sedimentação variável entre 0,26 e 1,62 cm ano^{-1} (média
261 = 0,82 □ 0,45). As taxas de sedimentação apresentaram valor de 0,34 ± 0,03 cm ano^{-1} na base,
262 com um máximo de 1,62 ± 0,16 cm ano^{-1} em 45 cm e 1,46 ± 0,15 cm ano^{-1} no topo do
263 testemunho.

264 (iv) Testemunho T5 com taxa de sedimentação variável entre 0,16 e 5,25 cm ano^{-1} (média
265 = 1,67 □ 1,38). As taxas de sedimentação variaram ao longo do testemunho de 0,16 ± 0,02 cm
266 ano^{-1} na base, com um máximo de 5,25 ± 0,53 cm ano^{-1} em 25 cm, chegando a 1,83 ± 0,18 cm
267 ano^{-1} no topo da coluna sedimentar.

268

Tabela 1.Dados de taxa de sedimentação ao longo dos cinco testemunhos e suas respectivas idades estimadas.

	T1	**T2**	**T3**	**T4**	**T5**
Localização	Próximo ao porto de Paranaguá	Margem norte da Baía de Paranaguá, ou seja, oposto ao porto de Paranaguá	Próximo ao porto de Antonina	Próximo à desembocadura do rio Faisqueira	Entre a Ilha Rasa da Cotinga e a Ilha da Cotinga
Latitude / Longitude	(-25,5026; -48,5458)	(-25,45815; -48,54112)	(-25,46232; -48,67268)	(-25,43875; -48,66883)	(-25,51817; -48,45812)
Idade estimada	2019 – 1820	2019 – 1762	2019 – 1917	2019 - 1861	2019 –1876
Intervalo da taxa de sedimentação	0,20 –1,39	0,11 – 3,18	0,54 – 6,73	0,26 – 1,62	0,16 – 5,25
Taxa de sedimentação média	0,83 ± 0,29	1,11 ± 0,85	1,90 ± 1,59	0,82 ± 0,45	1,67 ± 1,38
Taxa de sedimentação na base	0,20 ± 0,02	0,11 ± 0,01	0,62 ± 0,06	0,34 ± 0,03	0,16 ± 0,02
Taxa de sedimentação máxima	1,39 ± 0,14	3,18 ± 0,32	6,73± 0,67	1,62 ± 0,16	5,25 ± 0,53
(profundidade /ano)	49cm / 1953	47cm / 1956	31cm / 1989	45cm / 1967	25cm / 2003
Taxa de sedimento no topo	0,80 ± 0,08	1,08 ± 0,11	0,78 ± 0,08	1,46 ± 0,15	1,83 ± 0,18

269

3.4.3 Composição elementar e isotópica

Os valores determinados em cada testemunho para a composição elementar e isotópica da MO sedimentar podem ser vistos nas Tabelas S1 a S5.

Os teores de COT e NT nas amostras do testemunho T1 variaram entre 0,09 e 2,26% (média = 0,94 ± 0,56) e 0,01 a 0,19 % (média = 0,07 ± 0,05), respectivamente (Fig. 2). Os valores das razões $\delta^{13}C$ e $\delta^{15}N$ variaram de –27,18 a –24,57 ‰ (média = –26,19 ± 0,40 ‰) e 1,33 a 26,37 ‰ (7,67 ± 6,56 ‰), respectivamente (Fig. 2 e 3).

No testemunho T2, os teores de COT e NT nas amostras variaram entre 0,22 e 4,17% (média = 1,58 ± 1,04) e 0,02 a 0,29 % (média = 0,14 ± 0,09), respectivamente (Fig. 3). Os valores das razões $\delta^{13}C$ e $\delta^{15}N$ variaram de –27,00 a –25,30 ‰ (média = –26,05 ± 0,37‰) e –2,15 a 18,22 ‰ (4,98 ± 3,58‰), respectivamente (Fig. 2 e 3).

Nas amostras do T3, os teores de COT e NT variaram entre 0,19 a 2,84% (média = 1,37 ± 0,95); 0,01 a 0,31 % (média = 0,14 ± 0,11), respectivamente (Fig. 2 e 3). Os valores das razões $\delta^{13}C$ e $\delta^{15}N$ variaram de –27,11 a –25,02 ‰ (média = –25,83 ± 0,34‰) e 1,67 a 41,12 ‰ (média = 8,86 ± 7,60‰), respectivamente (Fig. 2 e 3).

No testemunho T4, os teores de COT e NT nas amostras do variaram entre 0,75 e 4,19% (média = 1,77 ± 1,10); 0,06 a 0,34 % (média = 0,14 ± 0,10), respectivamente (Fig. 2 e 3). Os valores das razões $\delta^{13}C$ e $\delta^{15}N$ variaram de –26,10 a –23,80 ‰ (média = –25,05 ± 0,57‰) e 1,81 a 12,62 ‰ (6,39 ± 1,93‰), respectivamente (Fig. 2 e 3).

Por fim, os valores encontrados no testemunho T5 referente a COT e NT variaram entre 0,44 a 3,24 % (média = 0,85 ± 0,42); 0,02 a 0,09 % (média = 0,04 ± 0,02), respectivamente (Fig. 2 e 3). Os valores das razões $\delta^{13}C$ e $\delta^{15}N$ variaram de –27,69 a –14,72 a ‰ (média = –25,69 ± 1,51‰) e 3,69 a 10,63 ‰ (7,33 ± 1,60‰), respectivamente (Fig. 2 e 3).

Usando *box-plots* para comparação entre os cinco testemunhos, nota-se que os dados de COT que apresentaram maior amplitude interquartil foi para os testemunhos T2 e T3, seguido de T4, T1 e T5 (Fig. 4). O NT segue um padrão semelhante com as maiores amplitudes observadas nos testemunhos T2, T3 e T4, seguida de T1 e T5. Os três testemunhos com as maiores amplitude interquartil para o conteúdo de sedimentos finos (silte + argila) são T3, T2 e T4, seguido de T1 e T5. Para a razão $\delta^{15}N$, os dois testemunhos com maior amplitude de valores foram o T1 e T3, e apresentaram valores discrepantes (*outlier*), enquanto para a razão $\delta^{13}C$, a maior amplitude interquartil foi para o testemunho T4. Por fim, a razão C/N mostrou maior amplitude interquartil para o testemunho T5.

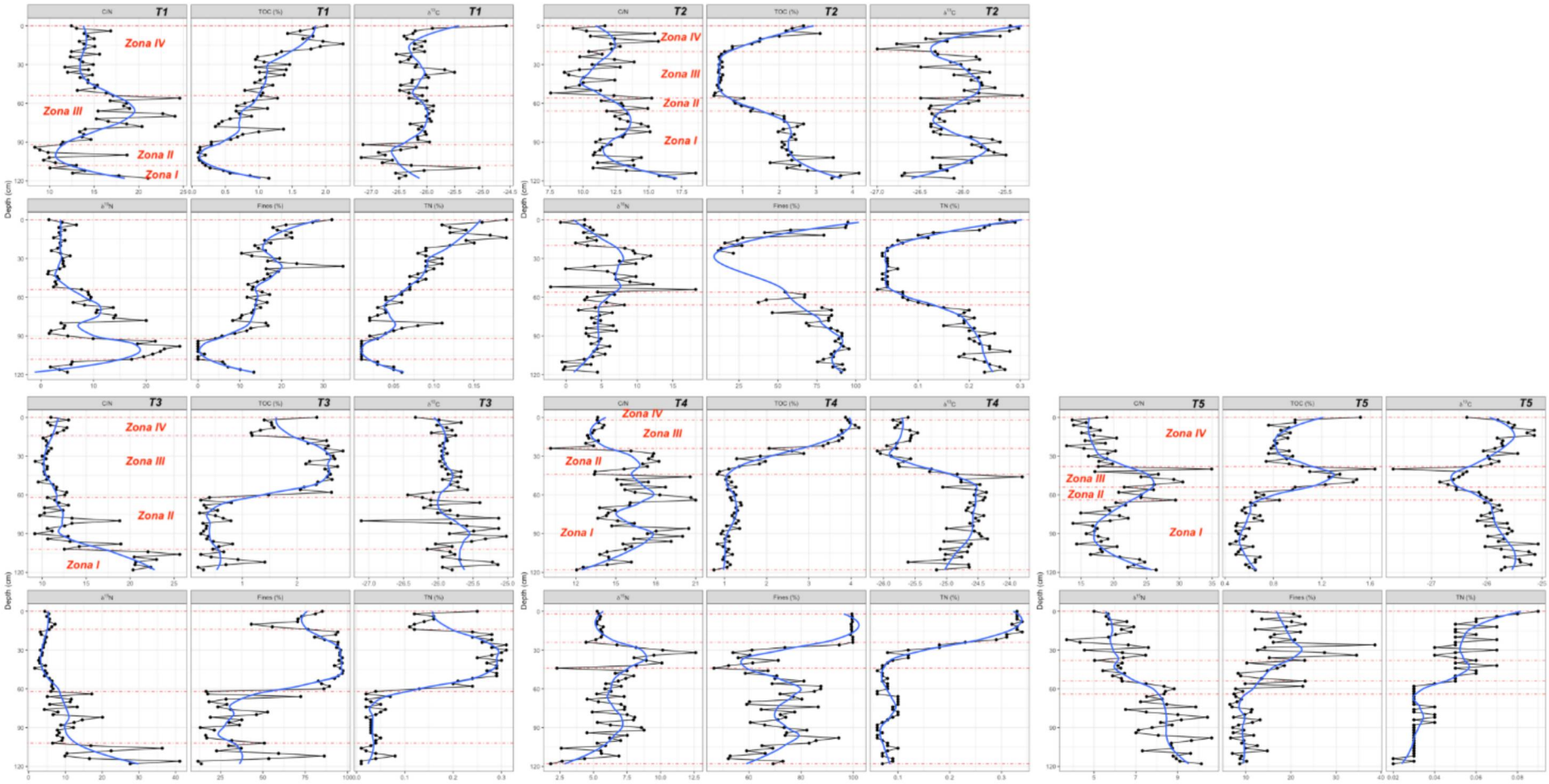

302

303 Figura 2.Testemunho T1 – T5: razão C/N, COT, $\delta^{13}C$, $\delta^{15}N$, finos (argila + silte) e NT. Os pontos ligados pela linha preta foram os valores encontrados para cada parâmetro, a
304 linha azul representa a média móvel entre 3 pontos, linha pontilhada vermelha separa cada perfil em duas zonas conforme descrito nos perfis sedimentares

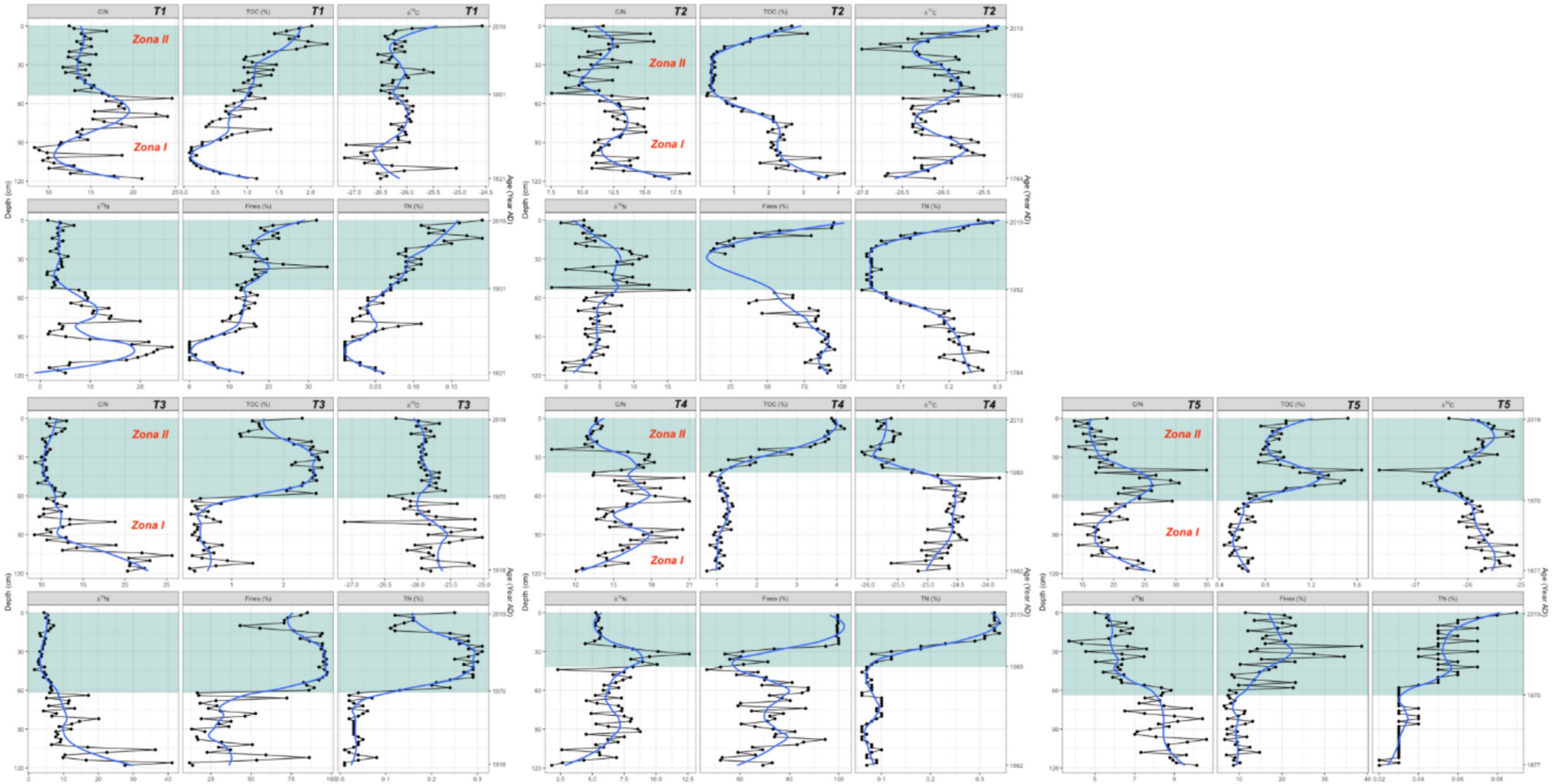

Figura 3.Testemunho T1 – T5: razão C/N, COT, $\delta^{13}C$, $\delta^{15}N$, finos (argila + silte) e NT. Os pontos ligados pela linha preta foram os valores encontrados para cada parâmetro, a linha azul representa a média móvel entre 3 pontos, faixa verde separa cada perfil em duas zonas conforme descrito nos perfis sedimentares

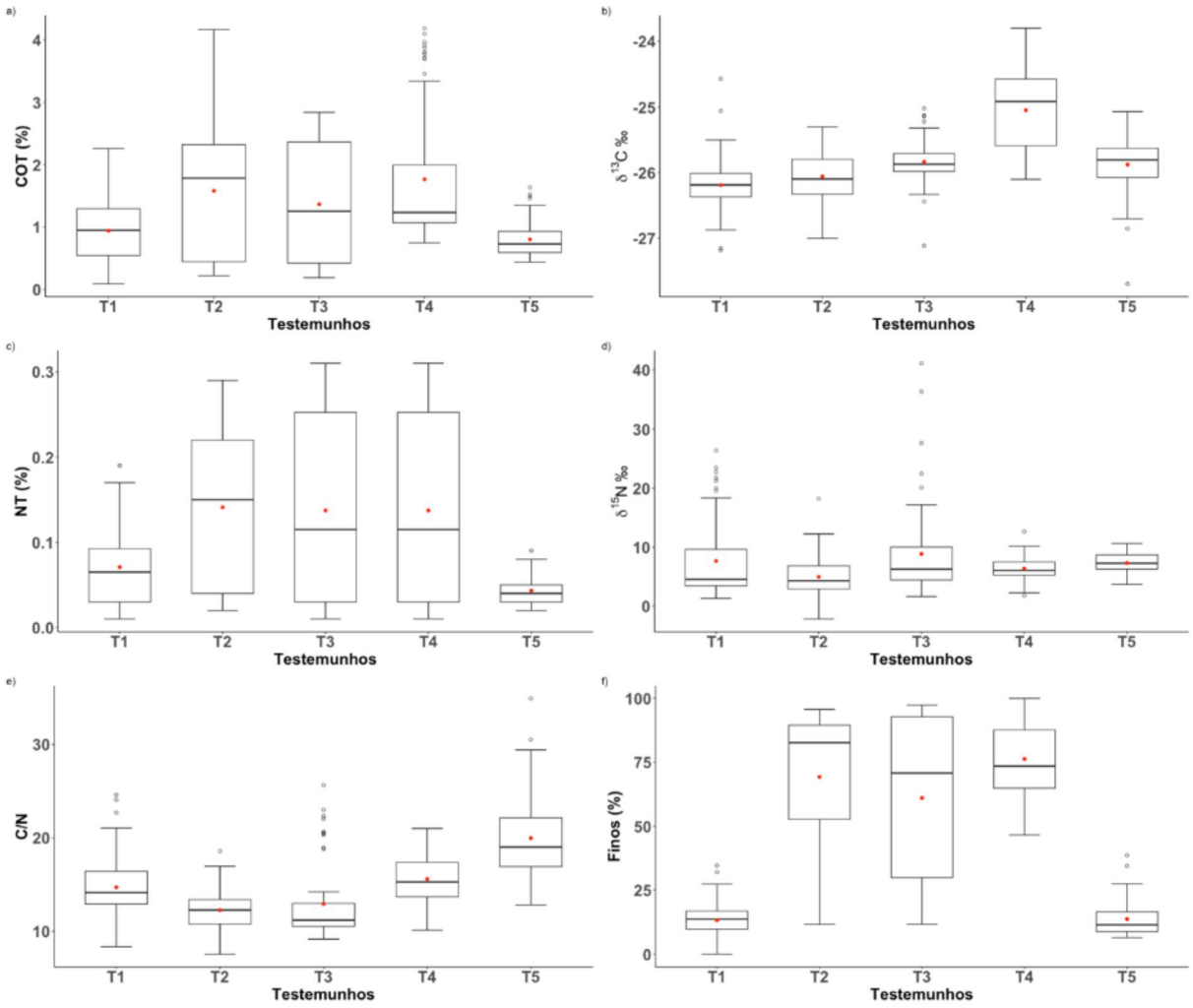

Figura 4. *Box plot* da distribuição dos parâmetros analisados nos testemunhos coletados no Complexo Estuarino de Paranaguá (SPE). Pontos abertos → *outliers*; Barras → limite inferior e superior.

A comparação dos valores dos parâmetros de COT, NT, razão C/N e $\delta^{13}C$ do CEP com diferentes estuários da costa brasileira, a citar, os estuários de Santos (SP), Caravelas (BA), Guanabara (RJ) e Guaratuba (PR) indica que todos possuem contribuição similares de material orgânico como o presente estudo, sendo que a variabilidade de valores que ocorre em pequena proporção, pode ser justificada em termos de peculiaridades de cada estuários (Tabela S7). No contexto da ocupação urbana, a população que vive nas bacias de drenagem que desaguam no CEP é superior apenas a Baia de Guaratuba e Caravelas (BA), o que define indiretamente o grau de impacto humano em comparação aos demais estuários brasileiros (Fig. S9).

323 3.4.4 Correlação entre COT e NT e razão C/N

324 Dados de correlação de Spearman entre COT e NT indicou correlação linear ao nível de
325 significância ($\alpha = 0,05$), com $r = 0,96$; $r = 0,94$; $r = 0,97$; $r = 0,86$; $r = 0,80$ ($p < 0,005$) para os
326 testemunhos T1 a T5, respectivamente. Uma moderada correlação linear ocorreu entre COT e
327 NT para amostras do testemunho T5 ao nível de significância ($\alpha = 0,05$), com $r = 0,50$ ($p <$
328 0,005). Desta forma, os valores da razão C/N atômica podem ser utilizados para avaliação de
329 fontes de MO (Meyers & Teranes, 2002) e variaram de 8,3 a 24,6 (média = 14,7 ± 3,5), de 7,6
330 a 18,6 (média = 12,3 ± 2,2), de 9,2 a 25,6 (média = 12,9 ± 4,0), de 10,1 a 21,0 (média = 15,6 ±
331 2,4) e de 12,8 a 34,9 (média = 19,9 ± 4,6), para os testemunhos T1 a T5, respectivamente.
332
333 3.4.5 Mudanças nos parâmetros indicadores da matéria orgânica sedimentar ao longo dos anos

334 O testemunho T1, coletado nas proximidades do porto de Paranaguá, apresentou quatro
335 zonas distintas de variação de valores dos parâmetros estudados, de acordo com a análise
336 *broken stick* e a separação do cluster restritivo para os parâmetros mostrou dois grupos distintos
337 de variáveis: grupo 1: NT e COT, finos e $\delta^{13}C$ e grupo 2: $\delta^{15}N$ e a razão C/N (Fig. S10). As
338 variações dos perfis verticais para estes parâmetros indicam valores menores na base,
339 aumentando em direção ao topo do testemunho para o grupo 1, enquanto o grupo 2 apresenta
340 maior oscilação na base do testemunho e valores constantes até as seções mais próximas do
341 topo do testemunho (Fig. 2).

342 Conforme verificado pela correlação de Spearman, os perfis verticais para COT e NT
343 apresentaram distribuições verticais visualmente similares, com valores aumentando da base
344 em direção ao topo do testemunho, sugerindo remineralização de material orgânico presente
345 (Fig. 2). O gráfico de dispersão $\delta^{13}C$ *vs* C/N mostra que predomínio de amostras sujeitas a
346 mistura de fontes terrígenas e marinhas, plantas C3, bem como material oriundo de fitoplâncton
347 de água doce (Fig. S11).

348 A hidrodinâmica controla o transporte de sedimentos e consequentemente seleciona o
349 tamanho do grão, evidenciando que no período coberto pelas zonas I, II e III, a energia local
350 era maior devido a fração groseira predominante, mudando gradativamente na zona IV (Fig. 2).
351 Portanto, estes resultados sugerem uma mudança quanto ao predomínio de material de origem
352 marinha nas zonas I, II e III para um ambiente com maior influência terrígena nas seções mais
353 próximas ao topo do testemunho, ou seja, zona IV. Embora tenha um leve enriquecimento nos
354 teores de ^{13}C e, portanto, valores menos negativos de $\delta^{13}C$, este parâmetro indica MO de origem
355 terrígena ao longo de todo o perfil.

O testemunho T2, coletado na margem norte da Baía de Paranaguá, ou seja, oposto ao porto de Paranaguá, apresentou quatro zonas de variação de valores dos parâmetros estudados, que mostrou dois grupos distintos de variáveis: grupo 1: % silte + argila, NT, COT e a razão C/N e grupo 2: $\delta^{13}C$ e $\delta^{15}N$. As variações dos perfis verticais dos parâmetros do grupo 1 indicam valores maiores na base do testemunho, e diminuem nas zonas II e III, e aumentam na zona IV (Fig. 2). A hidrodinâmica local é influenciada pela dinâmica fluvial, que altera significativamente a deposição dos sedimentos e MO ao longo do tempo. As atividades de dragagem no Canal da Galheta, que permitem o aumento na profundidade média do canal de navegação dando passagem segura para os navios que alcançam no porto de Paranaguá, afetam deposição de sedimentos e MO, favorecendo a deposição de sedimentos mais grosseiros e reduzindo os teores de COT e NT devido à alta remobilização do sedimento. Já os parâmetros do grupo 2, indicam valores relativamente constantes na maior parte do testemunho, e diminuindo nas seções de topo.

O gráfico de dispersão $\delta^{13}C$ *vs* C/N das amostras do testemunho T2 mostram fontes similares as aquelas verificadas para o testemunho T1, ou seja, mistura de fontes (marinhas e terrígenas), plantas C3 e de material oriundo de água doce (Fig. S11- S12).

O Testemunho T3, coletado nas proximidades do porto de Antonina, apresentou quatro zonas de variação de valores dos parâmetros estudados, que mostrou dois grupos distintos de variáveis: grupo 1: % silte + argila, NT e COT e grupo 2: $\delta^{13}C$, $\delta^{15}N$ e razão C/N. Os perfis verticais dos parâmetros do grupo 1 apresentaram baixos valores nas zonas I e II, com aumento abrupto na zona III, seguido de leve decréscimo na zona IV, próximo ao topo do testemunho (Fig. 2). Já os parâmetros do grupo 2, a razão C/N e $\delta^{15}N$ foram elevados na zona I, diminuindo na zona II e se mantendo constantes até o topo do testemunho, enquanto o $\delta^{13}C$ manteve-se constante desde a base até o topo desta coluna sedimentar.

No gráfico de dispersão entre $\delta^{13}C$ *vs* C/N das amostras do testemunho T3, amostras associadas a contribuições de plantas C3 ocorreram, porém, mistura de fontes (marinhas e terrígenas) predominou ao longo do perfil e poucas amostras foram associadas com MO autóctone de água doce (Fig. S13).

As alterações na composição da MO ao longo do testemunho T3 se deve a transposição do rio Capivari para o leito do rio Cachoeira, o que aumentou sua vazão em 33 % fazendo com que os sedimentos fossem revolvidos e sedimentados em novos locais de acordo com a nova hidrodinâmica (Branco, 2008).

A transposição pode ter contribuído para aumentar a capacidade de carga do rio, gerando depósitos no leito do rio a serem transportados para porções internas da baía (Branco, 2008). Essa alteração ambiental é claramente identificada nas variações na % silte + argila, COT e NT.

O Testemunho T4, coletado próximo à desembocadura do rio Faisqueira, na Baia de Antonina, apresentou quatro zonas de variação de valores dos parâmetros estudados, que mostrou dois grupos distintos de variáveis: grupo 1: COT, NT e % silte + argila e grupo 2: razão C/N, $\delta^{13}C$ e $\delta^{15}N$. Os perfis dos parâmetros do grupo 1 são similares com valores mais baixos nas zonas I e II, aumentando na Zona III e em direção ao topo do testemunho (Fig. 2). Já os parâmetros do grupo 2, apresentaram valores mais elevados nas zonas I e II, diminuindo na Zona III e em direção ao topo do testemunho.

A variação nos valores de COT e NT desde a base até topo do testemunho reflete a remineralização da MO, mais efetiva nas camadas mais profundas da coluna sedimentar, enquanto o gráfico de dispersão $\delta^{13}C$ *vs* C/N apresentou amostras sob influência de mistura de fontes terrígenas e marinhas bem como de plantas C3 (Fig. S14).

A influência da transposição do rio Capivari para o leito do rio Cachoeira, evidenciada no testemunho T3 parece ter pouco impacto na variabilidade dos parâmetros estudados para o testemunho T4, mesmo sendo na mesma margem que a desembocadura do rio. O aumento de vazão do rio Cachoeira não teve ação direta da capacidade de carga do rio Capivari, o que foi evidenciado pelo aumento gradativo da % silte + argila e no aumento dos teores de COT e NT.

O Testemunho T5, coletado entre a Ilha Rasa da Cotinga e a Ilha da Cotinga apresentou quatro zonas de variação de valores dos parâmetros estudados, que mostrou dois grupos distintos de variáveis: grupo 1: $\delta^{13}C$ e $\delta^{15}N$ e o grupo 2: COT, NT, razão C/N e % silte + argila. Os perfis dos parâmetros do grupo 1 apresentam valores mais baixos (i.e., enriquecimento dos isótopos mais pesados) na Zona I, enquanto o perfil do $\delta^{15}N$ indica um empobrecimento do ^{15}N em direção ao topo do testemunho nas zonas II, III e IV. Já o perfil do $\delta^{13}C$ indica um empobrecimento do ^{13}C na zona II e III e volta a ser mais enriquecido em ^{13}C na zona IV em direção ao topo do testemunho (Fig. 2). Os perfis dos parâmetros NT, COT e % silte + argila apresentam perfil similares, com valores baixos na zona I e II com leve aumento na zona III e IV, no topo do testemunho, enquanto a razão C/N apresentou oscilação nas zonas I, II e III valores constantes na zona 4 topo do testemunho.

No gráfico de dispersão $d^{13}C$ *vs* C/N (Fig.S15), o testemunho T5 apresentou uma oscilação das zonas I e IV com maior concentração de amostras na faixa de mistura de fontes (mix) e a zona II e III na faixa de plantas C3, mostrando que houve alterações nas fontes.

3.4.6 Histórico deposicional do Complexo Estuarino de Paranaguá

O histórico de uso e ocupação do solo da região sugere que o baixo aporte terrígeno apresentado na zona I (1821 a 1951) (Fig. 3), próximo ao Porto de Paranaguá no Testemunho T1, nos perfis de COT e NT é devido a corrida pelo ouro de aluvião que acontecia na época, pelos bandeirantes que desbravavam a região, os quais se utilizavam dos próprios leitos dos rios e suas margens para encontrar o ouro, sem a remobilização de terra ou supressão vegetal, com posterior declínio devido ao término do ciclo do ouro de aluvião, por ser pouco eficiente (Pierri et al., 2006; Chemin & Abrahão, 2014).

Com a implantação da Estrada da Graciosa (1873) e da Estrada de Ferro (1885), ambas ligando o planalto até o litoral, tem-se início o ciclo de extração de madeira (*Araucária angustifólia*) e de erva mate (*Ilex paraguariensis*), e exportação pelos portos de Antonina e Paranaguá (Chemin & Abrahão, 2014; IPARDES, 1989), o que explica o aumento gradativo nos valores de COT durante a Zona I dos Testemunhos.

Na margem norte da baía de Paranaguá, a zona de máxima turbidez possui um papel importante na deposição de sedimentos finos ao longo dos anos sendo a Zona I (1763 a 1952) predominando com sedimentos finos (alta % silte +argila) e COT (Fig. 3), decrescendo à medida que se aproxima da Zona II até o topo do Testemunho T2 (1952-2019), devido a dragagem do Canal da Galheta (1968), que muda a hidrodinâmica local, aumentando a energia e consequentemente o tipo de sedimento. Tal processo antrópico favorece o retrabalhamento do sedimento, reduzindo o teor de COT a ser depositado e preservado nesse ambiente. O aumento da população local não teve grande influência nas mudanças ocorridas na região antes de 1960. Após II Guerra Mundial, houve a estruturação e ampliação do Porto de Paranaguá, no período chamado de transição econômica, levando ao aumento na infraestrutura local, nas instalações portuárias e de marinas e das atividades de dragagem.

Na margem oposta ao porto de Antonina, o registro deposicional mostra a mudança na hidrodinâmica local devido a interferência humana, causada pela transposição do rio Capivari e construção da Represa Pedro Viriato Parigot de Souza, para gerar energia no litoral paranaense. A central de máquinas e os vertedouros das turbinas desaguando no rio Cachoeira, aumentou a vazão do mesmo em 33%, aumentando transporte da carga sedimentar no leito do rio, que antes continha bancos de areia, que, portanto, foram carreados baía adentro.

Tal processo é bem definido nos registros sedimentares e de MO (i.e., COT, NT e % silte +argila) entre a zona I (1918 a 1970) e II (1970 a 2019), graças a um aumento na zona II para os três parâmetros no Testemunho T3 (Fig. 3) e também próximo à desembocadura do rio Faisqueira, onde os parâmetros $\delta^{13}C$, COT e % silte +argila foram afetados pela influência da hidrodinâmica local, porém em menor intensidade, como verificado na Zona II (1970 a 2019) do Testemunho T4 (Fig. 3).

O subestuário da Cotinga é um dos locais mais abrigados do CEP e, consequentemente, recebe pouca ou nenhuma influência humana direta; entretanto, a variabilidade dos parâmetros sedimentares ao longo da Zona II (1970 a 2019) sugere uma maior entrada e abrupta de água doce, carreando material terrígeno para a baía, conforme verifica-se nos perfis do isótopo $\delta^{13}C$, COT e razão C/N (Fig. 3).

3.5 Considerações Finais

Através do estudo de parâmetros sedimentares e da composição em nível elementar e isotópica da matéria orgânica no Complexo Estuarino de Paranaguá, foi possível verificar que, como a maior parte dos sistemas estuarinos do planeta, a área de estudo sofre influências múltiplas de atividades humanas em diferentes escalas de tempo. As mudanças ambientais desempenham transformações significativas nos sistemas deposicionais e influenciam o armazenamento do material orgânico local. A interferência humana nos registros sedimentares da região foi significativa. A transposição do rio Capivari para o rio Cachoeira e as dragagens no leito do estuário, principalmente o aprofundamento do canal da Galheta, alteraram a deposição dos proxies devido à mudança na hidrodinâmica local.

A matéria orgânica sedimentar é constituída de uma mistura complexa de fontes marinhas e terrígenas, sendo destacado o predomínio de material terrígeno em todos os locais estudados e na escala de tempo estabelecida quando se utiliza o *proxy* de $\delta^{13}C$.

480 **Referências**
481
482 Angeli, J. L. F., Trevizani, T. H., Nagai, R. H., Martins, C. C., Figueira, R. C. L., Mahiques, M.
483 M. 2020. Geochemical mapping in a subtropical estuarine system influenced by large
484 grain-shipping terminals: Insights using Metal/Metal ratios and multivariate
485 analysis. Environmental Earth Sciences, 79(19), 1-15.

486 Appleby, P. G., Oldfield, F. 1978. The calculation of lead-210 dates assuming a constant rate
487 of supply of unsupported 210Pb to the sediment. Catena, 5(1), 1-8.

488 Azevedo, N.T. 2016. A vulnerabilidade social dos municípios do litoral do Paraná: construção
489 do Índice de Vulnerabilidade Social (IVS) com base nos dados dos setores censitários
490 IBGE 2010. Guaju - Matinhos 2, 89-124.

491 Bauer, J. E., Cai, W. J., Raymond, P. A., Bianchi, T. S., Hopkinson, C. S., Regnier, P. A. 2013.
492 The changing carbon cycle of the coastal ocean. Nature, 504(7478), 61-70.
493 Branco, J. C. 2008. Ecossistemas de Planície de Maré e Alterações Morfológicas na Foz do Rio
494 Cachoeira, Paraná. Publicação UEPG: Ciências Exatas e da Terra, Agrárias e
495 Engenharias-ATIVIDADES ENCERRADAS, 14(01).

496 Camargo, M. G. 2006. SysGran: um sistema de código aberto para análises granulométricas do
497 sedimento. Revista Brasileira de Geociências, 36(2), 371-378.

498 Calijuri, M. D. C., Cunha, D. G. F., Moccellin, J. 2013. Fundamentos ecológicos e ciclos
499 naturais. Engenharia Ambiental: Conceitos, Tecnologia e Gestão. São Paulo: Elsevier
500 Editora Ltda.
501 Chemin, M., Abrahão, C. M. 2014. Integração territorial do litoral do Estado do Paraná (Brasil):
502 transportes, balnearização e patrimonialização na formação e dinâmica do espaço
503 turístico. Raega-O Espaço Geográfico em Análise, 32, 212-239.
504 Dauner, A. L. L., Mollenhauer, G., Bícego, M. C., de Souza, M. M., Nagai, R. H., Figueira, R.
505 C. L., Mahiques, M.M., Souza, S.H.M., Martins, C. C. 2019. Multi-proxy reconstruction
506 of sea surface and subsurface temperatures in the western South Atlantic over the last~
507 75 kyr. Quaternary Science Reviews, 215, 22-34.
508 Dauner, A. L. L., Mollenhauer, G., Bicego, M. C., & Martins, C. C. 2020. Cluster analysis for
509 time series based on organic geochemical proxies. Organic Geochemistry, 145, 104038.
510 Estades, N.P., 2003. O litoral do Paraná: entre a riqueza natural e a pobreza
511 social. Desenvolvimento e meio ambiente, 8(1), 25-41.

512 Fernández-Martínez, M. 2022. From atoms to ecosystems: elementome diversity meets
513 ecosystem functioning. New Phytologist, 234(1), 35-42.

514 Garcia, M. R., & Martins, C. C. 2021. A systematic evaluation of polycyclic aromatic
515 hydrocarbons in South Atlantic subtropical mangrove wetlands under a coastal zone
516 development scenario. Journal of Environmental Management, 277, 111421.

517 Goñi, M. A., Teixeira, M. J., Perkey, D. W. 2003. Sources and distribution of organic matter in
518 a river-dominated estuary (Winyah Bay, SC, USA). Estuarine, Coastal and Shelf
519 Science, 57(5-6), 1023-1048.
520 Gurgatz, B. M., Garcia, M. R., Cabral, A. C., de Souza, A. C., Nagai, R. H., Figueira, R. C.,
521 Mahiques, M.M., Martins, C. C. 2023. Polycyclic aromatic hydrocarbons in a Natural
522 Heritage Estuary influenced by anthropogenic activities in the South Atlantic:
523 Integrating multiple source apportionment approaches. Marine Pollution Bulletin, 188,
524 114678.

525 Harvey, H. R. 2006. Sources and cycling of organic matter in the marine water column. Marine
526 organic matter: biomarkers, isotopes and DNA, 1-25.
527 IBGE (Instituto Brasileiro de Geografia e Estatística. 2023. Censo 2022. Disponível em
528 <https://cidades.ibge.gov.br/brasil/pr/paranagua/panorama> Acesso em agos/2023.
529 IPARDES (Instituto Paranaense de Desenvolvimento Econômico e Social). 2001. Zoneamento
530 da Área de Proteção Ambiental de Guaraqueçaba. Curitiba: IPARDES, p. 150.
531 IPARDES (Instituto Paranaense de Desenvolvimento Econômico e Social). 1989. APA de
532 Guaraqueçaba: caracterização socioeconômica dos pescadores artesanais e pequenos
533 produtores rurais. Curitiba: IPARDES, 87 p.
534 Juggins, S. 2017. Rioja: analysis of Quaternary science data, R package version (0.9-15.1).
535 Khan, M. B., Masiol, M., Hofer, A., & Pavoni, B. 2014. Harmful elements in estuarine and
536 coastal systems. PHEs, Environment and Human Health: Potentially harmful elements
537 in the environment and the impact on human health, 37-83.
538 Killops, V. J., Killops, S. D. 2005. Introduction to organic geochemistry. Blackwell Science
539 Ltda, p.406.
540 Lana, P. C., Marone, E., Lopes, R. M., Machado, E. C. 2001. The subtropical estuarine complex
541 of Paranaguá Bay, Brazil. In Coastal marine ecosystems of Latin America (pp. 131-
542 145). Springer, Berlin, Heidelberg.
543 Lubis, A. A. 2006. Constant rate of supply (CRS) model for determining the sediment
544 accumulation rates in the coastal area using 210Pb. Journal of Coastal
545 Development, 10(1), 9-18.
546 Marone, E., Machado, E. C., Lopes, R. M., Silva, E. T. D. 2005. Land-ocean fluxes in the
547 Paranaguá Bay estuarine system, southern Brazil. Brazilian Journal of
548 Oceanography, 53, 169-181.
549 Martins, C. C., Braun, J. A., Seyffert, B. H., Machado, E. C., Fillmann, G. 2010. Anthropogenic
550 organic matter inputs indicated by sedimentary fecal steroids in a large South American
551 tropical estuary (Paranaguá estuarine system, Brazil). Marine Pollution
552 Bulletin, 60(11), 2137-2143.
553 Martins, C. C., Doumer, M. E., Gallice, W. C., Dauner, A. L. L., Cabral, A. C., Cardoso, F. D.,
554 Dolci, N.N., Camargo, L.M., Ferreira, P. A.L., Figueira, R.C.L., Mangrich, A. S. 2015.
555 Coupling spectroscopic and chromatographic techniques for evaluation of the
556 depositional history of hydrocarbons in a subtropical estuary. Environmental
557 Pollution, 205, 403-414.
558 Meyers, P. A., Teranes, J. L. 2002. Sediment organic matter. In Tracking environmental change
559 using lake sediments (pp. 239-269). Springer, Dordrecht.
560 Montero, P., Vilar, J.A. 2015. TSclust: um pacote R para clustering de séries temporais. Jornal
561 de Software Estatístico , 62 , 1-43.
562 Oksanen, J., Simpson, G. L., Blanchet, F. G., Kindt, R. et al., 2022. Package 'vegan'
563 Community Ecology Package. Disponível em <
564 https://cran.ism.ac.jp/web/packages/vegan/vegan.pdf>. Acesso em jun/2023.
565 Paladino, Í. M., Mengatto, M. F., Mahiques, M. M., Noernberg, M. A., Nagai, R. H. 2022. End-
566 member modeling and sediment trend analysis as tools for sedimentary processes
567 inference in a subtropical estuary. Estuarine, Coastal and Shelf Science, 108126.
568 Peñuelas, J., Fernández-Martínez, M., Ciais, P., Jou, D., Piao, S., Obersteiner, M., Vicca, S.,
569 Janssens, I.A., Sardans, J. 2019. The bioelements, the elementome, and the
570 biogeochemical niche. Ecology, 100(5), e02652.

571 Pierri, N., Angulo, R. J., de SOUZA, M. C., Kim, M. K. 2006. A ocupação e o uso do solo no
572 litoral paranaense: condicionantes, conflitos e tendências. Desenvolvimento e Meio
573 Ambiente, 13.
574 Postacchini, M., Manning, A. J., Calantoni, J., Smith, J. P., & Brocchini, M. 2023. A storm
575 driven turbidity maximum in a microtidal estuary. Estuarine, Coastal and Shelf
576 Science, 288, 108350.
577 Summons, R. E. 1993. Biogeochemical Cycles A Review of Fundamental Aspects of Organic
578 Matter. Organic Geochemistry: Principles and Applications, 11, 1.
579 van Buuren, S. (2023). Broken Stick Model for Irregular Longitudinal Data. Journal of
580 Statistical Software, 106(7), 1–51. doi:10.18637/jss.v106.i07
581

4 CAPÍTULO III

2.

Variability of sedimentary organic matter in subtropical estuarine systems due to anthropogenic and climatic events

Marines M. Wilhelm [1,2], Ana Caroline Cabral [1], Ana Lúcia L. Dauner [1], Marina Reback Garcia [1], Rubens C.L. Figueira [3], César C. Martins [2]

[1] Programa de Pós-Graduação em Sistemas Costeiros e Oceânicos (PGSISCO). Universidade Federal do Paraná. Caixa Postal 61. 83255-976. Pontal do Paraná. PR. Brasil.

[2] Centro de Estudos do Mar, Campus Pontal do Paraná. Universidade Federal do Paraná. Caixa Postal 61. 83255-976. Pontal do Paraná. PR. Brasil.

[3] Instituto Oceanográfico. Universidade de São Paulo. Praça do Oceanográfico, 191. 05508-900. São Paulo, SP, Brasil.

* Corresponding authors: wilhelm.marines@gmail.com (M.M. Wilhelm)
ccmart@ufpr.br (C.C. Martins)

Status do artigo:

Publicado: https://doi.org/10.1007/s12665-022-10704-2

Environmental Earth Sciences (2023) 82:22. Springer Nature.

Abstract

Estuaries are ecosystems that have been changed by climatic and anthropogenic events, and subtropical estuaries located in the Southern Hemisphere are important examples of historical human occupation, land use and recent degradation. This study aims to assess whether climatic and anthropogenic events promoted the variability of sedimentary organic matter (OM) in two estuarine systems, the Paranaguá Estuarine System and Guaratuba Bay, Brazil, using geochemical multiproxies. In this approach, bulk elementary and isotopic properties were integrated with specific molecular biomarkers (*n*-alkanes, *n*-alkanol and sterols) detected in the sedimentary OM from sediment cores. Our results showed a predominance of terrigenous OM in both estuarine systems over the last century. However, sterols proved to be a more robust proxy for indicating changes in the autochthonous input of sedimentary OM, especially in the core top sections. Based on the molecular biomarkers and total annual precipitation data, the climatic effects of periodic events (e.g., El Niño–Southern Oscillation) that occurred during the last century did not seem to have imposed noticeable changes in the sedimentary OM over the period covered by the cores (e.g., between 1912 and 2010 for the Paranaguá Estuarine System). Instead, OM variations may respond to changes in the drainage basin or to specific local human activities. Plant extraction in the drainage basin was recorded in Guaratuba Bay before the 1960s, and the intensification of human occupation after the 1950s was recorded in the Paranaguá Estuarine System. The multiproxy approach demonstrated that local environmental changes related to regional anthropogenic events in the adjacent drainage basin of estuaries may be considered for identifying human impacts in coastal zones.

Keywords: Estuaries; Molecular biomarkers; Stable isotopes; Sediment; Population growth; Terrigenous organic matter.

4.1 Introduction

Estuaries are vulnerable ecosystems located between terrestrial and marine environments. Increased population density around these areas has disturbed natural dynamics due to intensive land use. Human settlements result in changes in the water and sediment properties and in the load of organic matter (OM) on the coasts (Canuel and Hardison 2016). Local geomorphology, relief, altitude, climatic aspects (temperature and precipitation rate variability), soil composition, and other secondary factors engrave signatures in the receiving sedimentary systems that can be altered by regional climatic and anthropogenic events (Rullkötter 2006). Estuarine sediments consist of sedimentary OM derived mainly from terrigenous material originating from drainage basins (e.g., urban areas, agriculture, pastures, and natural vegetation inputs) and from marine inputs such as aquatic organisms (zooplankton and bacteria, among other sources) (Sikes et al. 2009).

The OM input and composition in estuaries may present variations over time that can be associated with historical environmental changes, and the application of geochemical multiproxies (such as the elemental, isotopic and molecular compositions of OM) may reveal the contributions of anthropogenic processes to ecosystem modification (Meyers 1997; Bianchi and Canuel 2011; Lacey et al. 2018).

Molecular biomarkers are organic compounds that provide information about the environmental conditions during the deposition, burial and preservation of OM in sediments. These molecules act as fingerprints of environmental processes, having a traceable origin and high resistance to bacterial degradation and physicochemical transformations (Peters et al. 2005). N-alkanes, n-alkanols and sterols are traditional classes of molecular biomarkers found in estuaries (Meyers 1997). N-alkanes are linear aliphatic hydrocarbons that are abundant in the natural environment. Short carbon chain n-alkanes (< n-C20) predominate in algae and bacteria, mid-chain n-alkanes are related to macrophytes, and long-chain n-alkanes (> n-C26) are abundant in the epicuticular waxes of plants (Eglinton and Hamilton 1967; Ficken et al. 2000; Freeman and Pancost 2013). Sterols are very specific and refractory geochemical proxies used to trace a wide range of OM sources. Sitosterol (29Δ5), campesterol (28Δ5) and stigmasterol (29Δ5,22E) are often associated with higher plants and are commonly used to study changes in OM from terrigenous sources. Brassicasterol (28Δ5,22E) is usually associated with diatoms and coccolithophores; dehydrocholesterol (27Δ5,22E) is associated with phytoplankton; and cholesterol (27Δ5) is produced mainly by algae, zooplankton and other animals (Meyers 1997). N-alkanols are chemically and structurally similar to n-alkanes except for the presence of a

hydroxyl functional group (-OH) attached to a terminal carbon. They can also be used to distinguish between marine and terrestrial OM inputs based on the length of their carbon chain (Hu et al. 2009).

Subtropical estuaries located in the Southern Hemisphere, especially along the Brazilian coast, provide important records of human occupation, land use and recent environmental degradation (e.g., Egres et al. 2012; Dauner et al. 2018; Cabral et al. 2020). In addition, estuaries are subject to periodic climatic events, such as the El Niño–Southern Oscillation, which is a combined ocean–atmosphere irregular cycle that is mainly reflected by sea surface temperature in the Pacific Ocean. These ocean–atmospheric interactions can reach the upper layers of the atmosphere, resulting in climatic reflexes at the regional and global scales and causing changes in the precipitation regimes at mid-latitudes (30°N–30°S) (Grimm and Tedeschi 2009). The evaluation of local environmental changes related to regional climatic and anthropogenic events using a geochemical multiproxy approach has been less explored, especially in the Southern Hemisphere. This geochemical approach is relevant to the environmental sciences since it allows us to combine a range of indicators with the evolution of human activities in estuaries.

In this context, the aims of this study were (i) to identify whether the evolution of human occupation and anthropogenic activities developed during the last century in adjacent land areas has changed the sedimentary OM composition presented in these estuaries; (ii) to evaluate whether periodic climatic events such as the El Niño–Southern Oscillation cause noticeable changes in the OM composition; and (iii) to determine the adequacy of molecular biomarkers as indicators of local environmental estuarine changes on short time scales. For these goals, vertical variations in bulk elementary (TOC and TN) and isotopic properties (δ13C and δ15N), molecular biomarkers (n-alkanes, n-alkanols and sterols) and their related ratios were evaluated in three sediment cores from two estuaries located in the South Atlantic.

4.2 Study Area

The study was performed in the Paranaguá Estuarine System (PES) and Guaratuba Bay (GB), two subtropical estuaries on the Brazilian coast (Fig. 1A). The climate is wet and warm, with 2500 mm of mean annual rainfall, which is more intense during the austral summer (maximum of 5300 mm), when the highest atmospheric temperatures are recorded (mean between 29 and 30 °C) (Lana et al. 2001; Vanhoni and Mendonça 2008). Both estuaries are surrounded by preserved and modified mangroves/salt marshes (213 km² in PES vs. 63 km² in GB) (Pires et al. 2005).

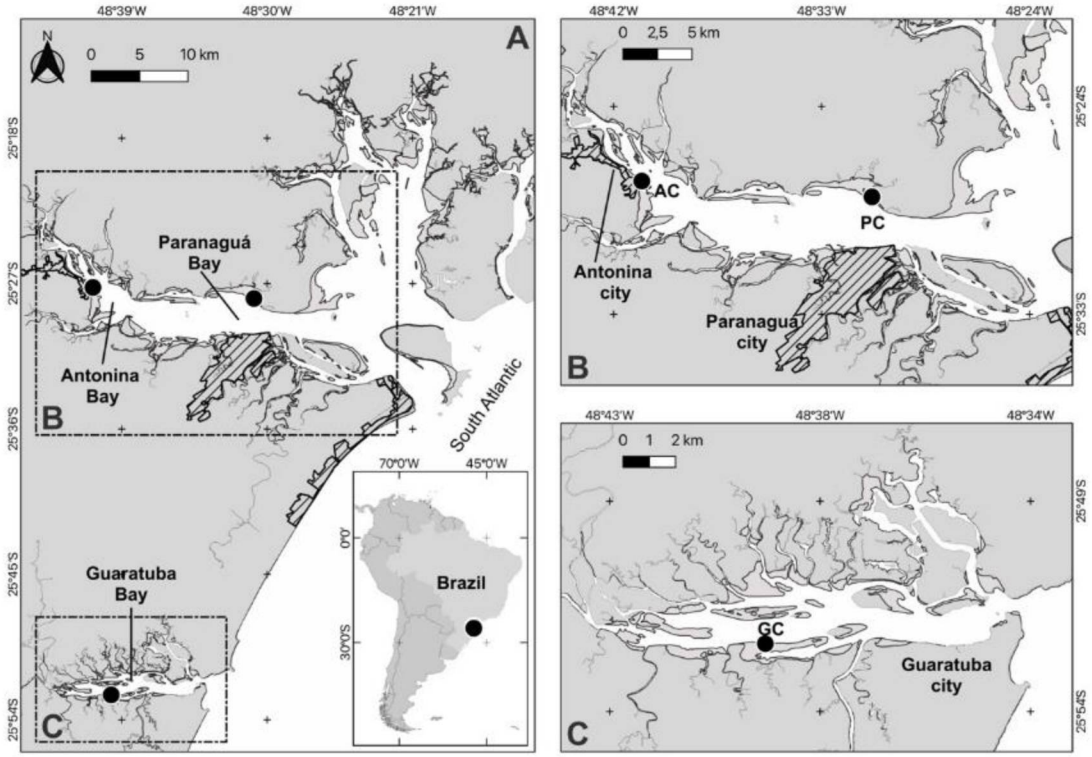

115 Figure 1. Map of the study area indicating southern Brazil with two subtropical estuaries (subset A). Sampling
116 sites (black circles) where the cores were collected in the respective bays: Antonina core (AC) and Paranaguá
117 core (PC) (subset B) and Guaratuba core (GC) (subset C). Cities are shown as shaded areas.
118

119 The PES is considered a natural heritage site by the United Nations Educational,
120 Scientific and Cultural Organization (Lana et al. 2001) and the major estuary of the Paraná coast
121 (552 km²). According to hydrodynamics and geographic features, the PES can be divided into
122 the North–South (N–S) sector and the East–West (E–W) sector (Fig. 1A and B) (Martins et al.
123 2015). The E–W sector was analysed in this study. It comprises the Antonina and Paranaguá
124 bays and hosts two harbours (Fig. 1B). One of these ports, Paranaguá Port, is the largest Latin
125 American port for grain exportation (Cardoso et al. 2016). The E–W sector has approximately
126 450 km² of surface water area and is 46 km long and 10 km wide (maximum), with
127 approximately three days of water residence time (Bigarella 2001; Lana et al. 2001; Marone et
128 al. 2005). The hydrodynamic pattern is influenced mainly by Cachoeira and Nhundiaquara river
129 runoff (more intense during summer) and by the asymmetric variation in tides (semidiurnal with
130 diurnal irregularities) (Mantovanelli et al. 2004). The neap and spring tide heights are 1.3 and
131 1.7 m, respectively, in the entrance of the bay and 2.0 and 2.7 m, respectively, in Antonina Bay
132 (Lana et al. 2001).

GB is part of the Guaratuba Environmental Protection Area (Sutilli et al. 2020) and the RAMSAR's list of wetlands of international importance (nº 2317) (https://rsis.ramsar.org/) (Fig. 1C). Agriculture, fisheries, and tourism are the main economic activities developed in the area (Pietzsch et al. 2010; Dauner and Martins 2015). The surface water area is approximately 50.2 km² and is 15 km long and 5 km wide (maximum), with approximately nine days of water residence time (Marone et al. 2006). The hydrodynamics are mainly governed by Cubatão and São João river flows and by tides (semidiurnal with diurnal irregularities) (Marone et al. 2006). The mean tidal range is 1.50 and 0.65 m during spring and neap tides, respectively (Marone et al. 2006).

4.3 Material and Methods

4.3.1 Sampling

Three short sediment cores were obtained along the Paraná coast (i) Antonina core (AC; in November 2010; diameter = 10 cm; length = 27 cm); (ii) Paranaguá core (PC; in November 2010; diameter = 10 cm; length = 27 cm) and Guaratuba core (GC; in November 2013; diameter = 7 cm; length = 32 cm). The three cores were collected by scuba diving with aluminium tubes for molecular biomarkers, bulk properties, grain size and dating.

Each sediment cores were subsampled every 2 cm. Each subsample was stored in aluminium containers and plastic bags at -20 °C. Next, the sediments were freeze-dried, weighed, homogenized and stored in cleaned glass bottles until laboratory analysis.

4.3.2 Bulk organic matter proxies

Around 6 – 8 mg of acid treated sediment (Costa et al. 2016) was weighed to determine total organic carbon (TOC) and the carbon isotope ratio ($\delta^{13}C$); the same amount of sediment (bulk sediment) was weighed to determine total nitrogen (TN) and nitrogen isotope ratio ($\delta^{15}N$).

Samples and calibration standards were analysed using a Costech elemental analyser coupled to a Thermo Scientific Delta V Advantage isotope ratio mass spectrometer. The analytical accuracy was measured using the USGS-40 (glutamic acid, United States Geological Survey) and IAEA-600 (caffeine, International Atomic Energy Agency) analysed to each group of 40 samples, with a precision (reproducibility) of 0.1% for the TOC and TN, 0.03% for $\delta^{13}C$ and 0.09‰ for $\delta^{15}N$. The analytical accuracy for the determination of TOC and TN was evaluated by the analyses of Soil LECO standard (LECO Corporation USA), with estimated values of 13.6 and 0.81%, respectively.

166 Grain size distributions were measured by laser granulometry, in the size range between
167 0.02 and 2000 μm, using a Microtrac Bluewave S3500 instrument. As described in Martins et
168 al. (2015), 1.0 g of each dry sediment sample was treated sequentially with 10% hydrogen
169 peroxide and 10% hydrochloric acid, in order to remove OM and carbonates, respectively.
170 Small aliquots of this treated material were taken from the previously shaken bottles and
171 repeatedly injected into the dispersion module of the analyzer. The instrument reproducibility
172 varied from 0.6 to 4.0%. The method described by Folk and Ward (1957) was used to estimate
173 the sediment parameters.
174
175 4.3.3 Molecular biomarkers
176 The analytical procedure for the determination of *n*-alkanes, *n*-alkanols and sterols was
177 based on the method described by Wisnieski et al. (2016). Approximately 10 to 20 g of dry
178 sediment was extracted for 8 hours in a Soxhlet apparatus with 80 mL of a mixture of *n*-hexane
179 and dichloromethane (DCM) (1:1, v/v) and copper to eliminate elementary sulphur. A mixture
180 of surrogate standards (100 μL) containing 1-eicosene and 1-hexadecene (50 ng μL^{-1}) and 5α–
181 androstanol (20 ng μL^{-1}) was added to each sample and blank before extraction.
182 The extract was concentrated to *ca.* 2 mL on a rotary vacuum evaporator, followed by
183 adsorption liquid chromatography in a glass column containing 5% water-deactivated silica (3.2
184 g) and alumina (1.8 g) and sodium sulphate. The *n*-alkanes (fraction 1) were eluted with 10 mL
185 of *n*-hexane, while polycyclic aromatic hydrocarbons (presented by Sutilli et al. 2020) were
186 eluted with 15 mL of a mixture of DCM and *n*-hexane (3:7, v/v). Sterols and *n*-alkanols (fraction
187 3) were obtained by the elution of 5 mL of ethanol and DCM (1:9, v/v) followed by 15 mL of
188 ethanol. The fraction 1 extracts were concentrated to 400 μL, and 100 μL of an internal standard
189 solution (1-tetradecene, 50 ng μL^{-1}) was added. The fraction 3 extracts were dried with a gentle
190 stream of nitrogen and derivatized using 50 μL of N,O-bis(trimethylsilyl)trifluoroacetamide
191 with 1% trimethylchlorosilane for 90 min at 65 °C. The extracts were dried again, and 100 μL
192 of internal standard (5*α*-cholestane, 20 ng μL^{-1}) was added. The final extracts were injected into
193 a gas chromatograph (Agilent 7890A Series) equipped with a flame ionization detector.
194 The quality control was based on blank samples and on the recovery of the surrogates
195 for each fraction. The blank samples did not present interferences in the chromatographic peaks
196 of the target compounds at levels higher than acceptable (3 times the limit of detection of the
197 method, LDM). The recovery of surrogates ranged from 56 to 125% (mean 81 ± 14%) for 1-
198 hexadecane, 53 to 106% (mean 87 ± 12%) for 1-eicosene, and 66 to 125% (mean 88 ± 13%)
199 for 5*α*-androstanol. The adopted LDM in this study were 0.007 ± 0.002 μg g^{-1} for the *n*-alkanes,

200 0.018 ± 0.007 μg g^{-1} for *n*-alkanols and 0.005 ± 0.002 μg g^{-1} for the sterols (Wisnieski et al.
201 2016). The precision was evaluated by analysing the standard reference materials (IAEA-408
202 and IAEA-417; International Atomic Energy Agency) to hydrocarbons available in the IAEA
203 reference sheet (e.g., *n*-C_{17}, *n*-C_{18} and Total *n*-alkanes (*n*-C_{14}-*n*-C_{34})). Precision was within the
204 target (<15% of the average values), and hydrocarbons concentrations presented recoveries in
205 agreement to ±20% within the certified values.
206
207 4.3.4 Sedimentation rates and dating
208 The sedimentation rates were obtained by the determination of lead-210 (^{210}Pb) and
209 caesium-137 (^{137}Cs) radionuclides by gamma spectrometry with a superpure Ge detector (GMX
210 25190P) and Spectrum Master 92XII software from EG&G/ORTEC. The gamma spectra were
211 analysed using Maestro v.6 software (EG&G/ORTEC), and the photopeaks used in this analysis
212 were 46.52 keV for ^{210}Pb and 609.31 keV for radium-226 (^{226}Ra) (gamma-ray emissions of a
213 ^{226}Ra daughter, bismuth-214). Based on the vertical profiles of the unsupported ^{210}Pb activity
214 (Fig. S1, where 'S' refers to Supplementary Data) and the application of the constant initial
215 concentration (CIC) model (Robbins and Edgington 1975), the linear sedimentation rates were
216 0.49 ± 0.05 (AC core), 0.26 ± 0.03 (PC core) and 0.36 ± 0.02 cm y^{-1} (GC core) as previously
217 presented by Martins et al. (2015) and Combi et al. (2013). The estimated period for each
218 sediment section was calculated according to the linear sedimentation rate of the sediment core
219 (cm y^{-1}) and the depth of the section (cm). The periods covered by each sediment core were *ca.*
220 1960 – 2012 (AC core), *ca.* 1912 – 2010 (PC core) and *ca.* 1925 – 2008 (GC core).
221
222 4.3.5 Diagnostic ratios for OM source identification
223 The carbon preference index (CPI), terrestrial-to-aquatic ratio (TAR), and aquatic proxy
224 (P_{aq}) for *n*-alkanes were calculated in this study (Table S1). The CPI is a diagnostic ratio based
225 on the predominance of odd/even carbon chains in the distribution of *n*-alkanes. CPI values >
226 4 indicate a predominance of terrestrial material, while lower values (1–3) may suggest a marine
227 OM contribution (Bray and Evans 1961; Aboul-Kassim and Simoneit 1996). The TAR is
228 obtained from the ratio between long chain *n*-alkanes (*n*-C_{27}+*n*-C_{29}+*n*-C_{31}, associated with
229 terrigenous sources) and short chain *n*-alkanes (*n*-C_{15}+*n*-C_{17}+*n*-C_{19}, related to marine origin). A
230 TAR > 3 indicates terrigenous source predominance (Bourbonniere and Meyers 1996; Meyers
231 1997). The P_{aq} index is calculated by the ratio between mid-chain *n*-alkanes of even carbon
232 number (*n*-C_{23} and *n*-C_{25}), typically from macrophytes (terrestrial) and algae (marine
233 environments), and mid- and long-chain ones (*n*-C_{23} to *n*-C_{31}), characteristic of higher plants

(Ficken et al. 2000). P_{aq} values lower than 0.1 are associated with terrestrial OM; values between 0.1 and 0.4 suggest mixed sources; and values higher than 0.4 are typical of autochthonous OM (submerged and floating macrophytes) (Ficken et al. 2000).

The ratios between individual *n*-alkanols (*n*-C_{22}-OH/*n*-C_{24}-OH, *n*-C_{24}-OH/*n*-C_{26}-OH and *n*-C_{26}-OH/*n*-C_{30}-OH) were also applied to verify precipitation trends (Table S1). For instance, *n*-C_{24}-OH/*n*-C_{26}-OH is higher if the precipitation in the considered period is low (Zheng et al. 2009).

4.3.6 Statistical analysis

Correlation analysis was performed to analyse the dependence among the proxies and their relationship with population growth. Because of the nonnormal distribution of the dataset ($p > 0.05$; Shapiro–Wilk normality test), a nonparametric correlation analysis, Spearman rank test, was applied. The Spearman coefficient is represented as ρ (rho) and ranges from -1 to +1. When ρ is close to zero, there is no association between the variables. Values close to +1 indicate a positive monotonic relationship, while values close to -1 indicate a negative monotonic relationship (Queen et al. 2002; Jafarabadi et al. 2019). For this analysis, the following variables were used: % fine sediments (% fine), TOC, TN, $\delta^{13}C$, $\delta^{15}N$, long-chain odd *n*-alkanes (*n*-C_{27}, *n*-C_{29} and *n*-C_{31}; Alk_L), mid-chain odd *n*-alkanes (*n*-C_{21}, *n*-C_{23} and *n*-C_{25}; Alk_M), short-chain odd *n*-alkanes (*n*-C_{15}, *n*-C_{17} and *n*-C_{19}; Alk_S), long-chain even *n*-alkanols (*n*-C_{26}-OH, *n*-C_{28}-OH and *n*-C_{30}-OH; OH_L), mid-chain even *n*-alkanols (*n*-C_{20}-OH, *n*-C_{22}-OH and *n*-C_{24}-OH; OH_M), short-chain even *n*-alkanols (*n*-C_{14}-OH, *n*-C_{16}-OH and *n*-C_{18}-OH; OH_S), dehydrocholesterol (cholesta-5,22E-dien-3β-ol, 27Δ□□□), cholesterol (cholest-5-en-3β-ol, 27Δ□), campesterol (24-methyl-cholest-5-en-3β-ol, 28Δ□), stigmasterol (24-ethylcholesta-5,22E-dien-3β-ol, 29Δ□□□), sitosterol (24-ethyl-cholest-5-en-3β-ol, 29Δ□), population (pop) and total annual precipitation (prec).

Principal component analysis (PCA) was performed to investigate the main sources of OM and how they varied over the analysed period in each sediment core. PCA is a multivariate approach that reduces the data dimensionality within a lower group of factors (principal components), providing more effective data to interpret environmental variations without losing the main information of the original data (Reimann et al. 2011; Jolliffe and Cadima 2016). As a result, PCA has been widely applied to find and interpret variations and sources of contaminants and geochemical markers determined in environmental samples (e.g., Bern et al. 2019; Cabral et al. 2018; Yang et al. 2020; Timoszczuk et al. 2021). Before performing the PCA, the data were standardized to allow comparisons among properties with different units

and ranges, and the nondetectable values were reassigned as "zero" (Reimann et al. 2011). PCA calculation was based on Euclidean distances. The results are presented as biplots, in which the loadings (eigenvectors or variables) derived from the PCA are plotted as arrows simultaneously with the points (plotted according to sample coordinates with regard to these eigenvectors) that represent the "observations" (Gabriel, 1971). The sediment layers were used as "observations", while the following parameters were used as "variables": %-fine, $\delta^{13}C$, $\delta^{15}N$, Alk_L, Alk_S, OH_L OH_S, terrigenous sterols (sum of 29Δ and 29Δ), marine sterols (sum of 27Δ and 27Δ), pop, prec, the carbon preference index (CPI) and the sterol index (29Δ/(27Δ+ 29Δ)).

All statistical analyses were performed in the R environment (R Core Team 2020) using the packages stats (correlation analysis and PCA) and pracma (Borchers, 2019; PCA). The TOC, $\delta^{13}C$ and $\delta^{15}N$ results were previously presented in Cabral et al. (2019). Grain size (% fine sediments represented by silt and clay) was previously presented in Martins et al. (2015) for the AC and PC cores and Combi et al. (2013) for the GC core, and these data were used in this study for statistical purposes. The population data were acquired from IBGE (2017), and total annual precipitation was obtained from ANA (2017).

4.4 Results

4.4.1 Bulk organic matter proxies and grain size

The bulk elementary and isotopic composition and grain size data in the analysed cores are presented in Table S1 and Fig. 2. Briefly, the total organic carbon (TOC) in the AC core was higher than that obtained in the PC and GC cores, with averages of 3.65 ± 0.13, 0.92 ± 0.18 and 1.05 ± 0.14%, respectively. The AC core also presented a slight increase in % TOC since the 1980s, which was not clear in the PC and GC profiles. Total nitrogen (TN) levels presented no marked variation in any of the cores, with only the PC core showing a slight upwards trend towards the core. A period of lower values of TOC and TN in the 1990s was observed in the GC core, followed by a recent increased level. The AC core had higher and constant values of TN (mean 0.30 ± 0.01%), followed by the PC core (mean 0.14 ± 0.03%) and GC core (mean 0.12 ± 0.02%). The δ15N values were constant in the AC core until the 1980s, when they decreased until ca. 1996 and then remained constant thereafter. The PC and GC cores presented more variable δ15N values but with no clear trend, except for the two top layers, which showed more 15N enrichment. The δ13C values were relatively constant over the three cores, being less negative in the PC core (mean -25.25 ± 0.24‰) and more negative in the AC and GC cores (-26.31 ± 0.11 and -27.09 ± 0.20‰, respectively). Regarding grain size data, there was a

predominance of the sand fraction in the PC and GC cores (68-92% and 61-93%, respectively) (Table S1). The sand fraction was less pronounced in the AC core (22-72%), especially in ca. 1977 and ca. 1960, when silt predominated (78 and 77% of silt contents, respectively). Excluding these two 'peaks' in silt content, the AC core had a slightly higher average fine sediment content (36.8 ± 1.92%), followed by the GC and PC cores (29.4 ± 9.2 and 20.2 ± 7.1%, respectively). The GC and PC cores presented constant and more variable values of fine sediments (between 7.2 and 39.2%), with a slight upwards trend towards the top sections of the cores (Fig. 2).

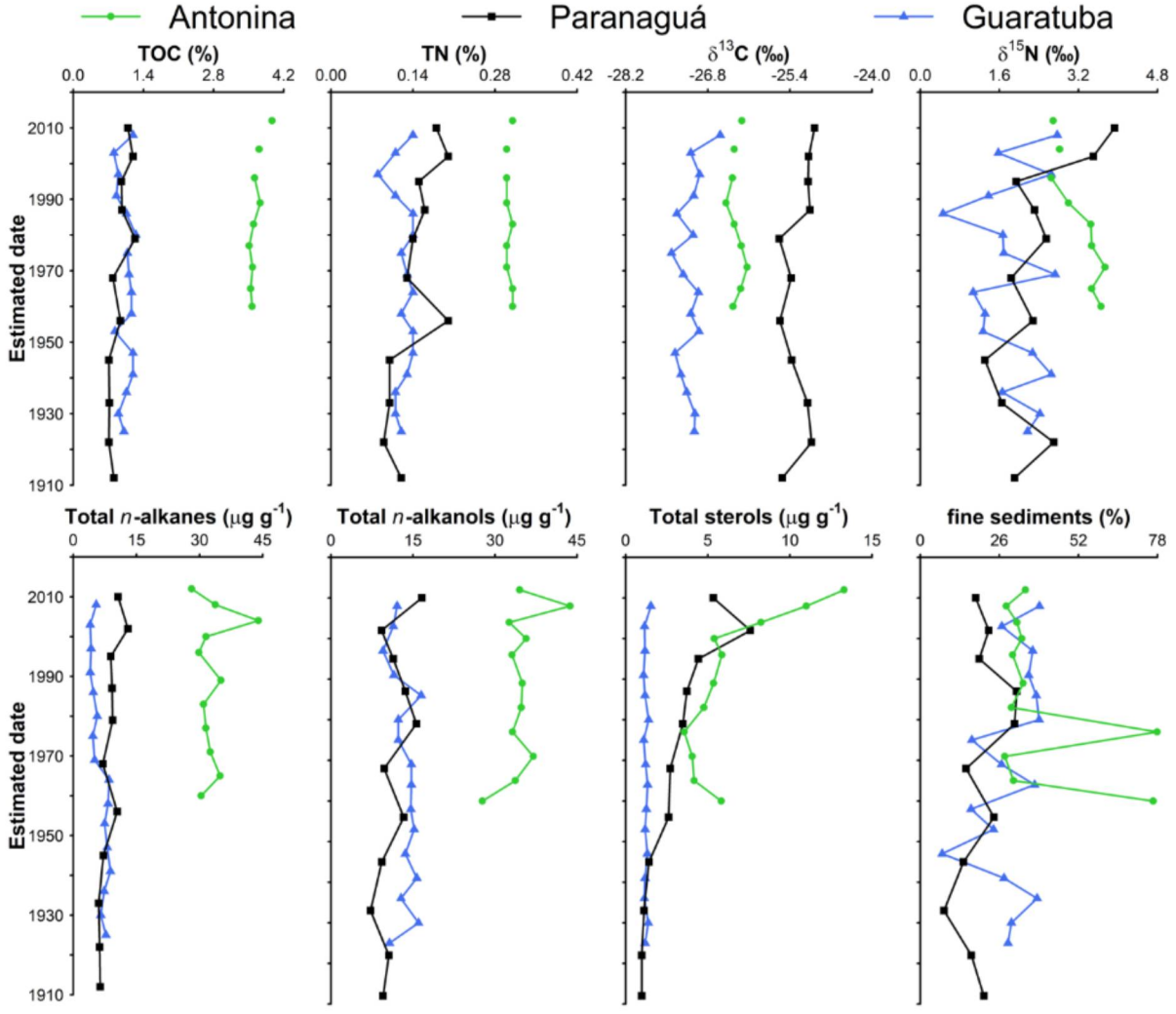

Figure 2. Profiles of bulk organic matter proxies, % fine sediments (silt + clay) and total organic proxies (n-alkanes, n-alkanols, and sterols) for the three sediment cores analysed. Abbreviations: TOC = total organic carbon and TN = total nitrogen.

4.4.2 Total molecular biomarker levels and vertical distribution

The highest values for total *n*-alkanes were found in the AC core (28.1 to 44.0 μg g^{-1}; mean 33.0 ± 4.0), followed by the PC core (6.0 to 13.0 μg g^{-1}; mean 8.6 ± 2.1; previously

317 presented by Martins et al. 2015) and GC core (4.0 to 8.8 μg g^{-1}; mean 6.3 ± 1.7; previously
318 presented by Sutilli et al. 2020) (Fig. 2; Tables S2–S4). The *n*-alkanes in all cores had a
319 predominance of odd long-chain *n*-alkanes, particularly *n*-C_{29} (Fig. 3). The concentrations of
320 total *n*-alkanols in the AC, PC and GC cores ranged from 27.7 to 43.7 μg g^{-1} (mean 34.6 ± 3.7),
321 from 7.2 to 16.6 μg g^{-1} (mean 11.5 ± 2.8) and from 9.5 to 16.5 μg g^{-1} (mean 13.4 ± 2.0),
322 respectively (Fig. 2; Tables S5–S7). The most abundant *n*-alkanols in the three cores were *n*-
323 C_{28}-OH and *n*-C_{30}-OH. *n*-C_{28}-OH was slightly more abundant in the AC and GC cores, whereas
324 *n*-C_{30}-OH was generally more abundant in the PC core (Fig. 3). The vertical distributions of the
325 total *n*-alkanes and *n*-alkanols for the PC and GC cores were similar, with low concentrations
326 and variability with depth when compared to the AC core (Fig. 2). In the AC core, the total *n*-
327 alkanes presented a 'peak' concentration in *ca.* 2004, whereas the total *n*-alkanols presented a
328 'peak' concentration in *ca.* 2008.

329 The total sterol concentrations varied from 3.56 to 13.3 μg g^{-1} (mean 6.50 ± 2.95), from
330 0.97 to 7.59 μg g^{-1} (mean 3.12 ± 1.99), and from 0.93 to 1.34 μg g^{-1} (mean 1.07 ± 0.11 μg g^{-1})
331 for the AC, PC and GC cores, respectively (Fig. 2, Tables S8–S10). Unsaturated sterols were
332 predominant in all cores analysed, particularly 29Δ^5, 29$\Delta^{5,22E}$ and 27Δ^5 (Fig. S2). The PC and
333 GC cores presented similar and low concentrations of total sterol until *ca.* 1950, when a slight
334 increase in the concentrations was noted in the PC core. In the GC core, total sterols remained
335 low until the top layer. The PC core showed a second increase in the total sterol levels since *ca.*
336 1980, which was also observed in the AC core, pointing to an overall trend in the PES area. In
337 recent layers, the AC core presented a sharp increase in total sterols from *ca.* 2000 to the top
338 layer, while the PC core had a 'peak' concentration in ca. 2002 (Fig. 2).

339 In general, the concentrations of total *n*-alkanes, *n*-alkanols and sterols in the bottom
340 layers remained relatively constant and low, while their highest concentrations were found in
341 the top core sections, especially in the PC and AC cores (Fig. 2). The same vertical variation
342 pattern was observed for the predominant 'groups' of these biomarkers, such as odd long-chain
343 *n*-alkanes and *n*-alkanols and terrigenous sterols (sum of 29Δ^5 and 29$\Delta^{5,22E}$) (Fig. 4).
344

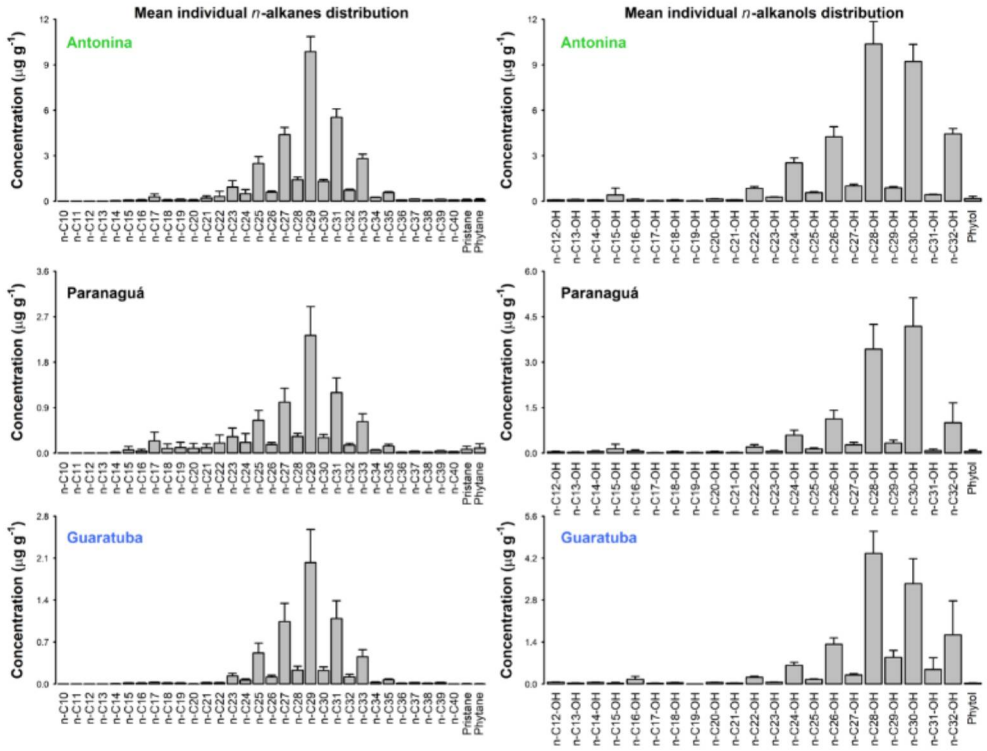

345

346 Figure 3. Mean concentrations of individual n-alkanes and n-alkanols, both in µg g-1. The error bars reflect the
347 standard deviations of the compounds among the depths from each sediment core.

348

349 4.4.3 Diagnostic ratios for OM source identification

350 In this study, the CPI values ranged from 5.46 to 6.14 (mean 5.72 ± 0.21), from 4.33 to
351 6.08 (mean 5.35 ± 0.54) and from 6.37 to 8.31 (mean 7.05 ± 0.44) for the AC, PC and GC cores,
352 respectively; the TAR values in the AC, PC and GC cores ranged from 20.5 to 97.4 (mean 54.2
353 ± 20.1), from 5.22 to 214.2 (mean 38.1 ± 61.9) and from 36.2 to 131.2 (mean 85.4 ± 24.6),
354 respectively; and P_{aq} values found in the three cores were mostly in a range of 0.14 to 0.31 (Fig.
355 4, Table S1).

356 The *n*-C_{22}-OH/*n*-C_{24}-OH ratio varied from 0.32 to 0.39 (mean 0.33 ± 0.02) in the AC
357 core, from 0.24 to 0.39 (mean 0.33 ± 0.05) in the PC core, and from 0.30 to 0.39 (mean 0.35 ±
358 0.02) in the GC core. The *n*-C_{24}-OH/*n*-C_{26}-OH ratio varied between 0.52 and 0.64 (mean 0.60
359 ± 0.03), 0.44 and 0.57 (mean 0.52 ± 0.03), and 0.41 and 0.50 (mean 0.47 ± 0.02) in the AC, PC
360 and GC cores, respectively. The *n*-C_{26}-OH/*n*-C_{30}-OH ratio also remained in restricted ranges:
361 0.34 to 0.57 (mean 0.46 ± 0.07) in the AC core, 0.22 to 0.33 (mean = 0.27 ± 0.03) in the PC
362 core, and 0.27 to 0.60 (mean 0.41 ± 0.10) in the GC core (Table S1). These low and relatively
363 constant values along the cores indicate climatic stability of predominantly wet conditions.

364

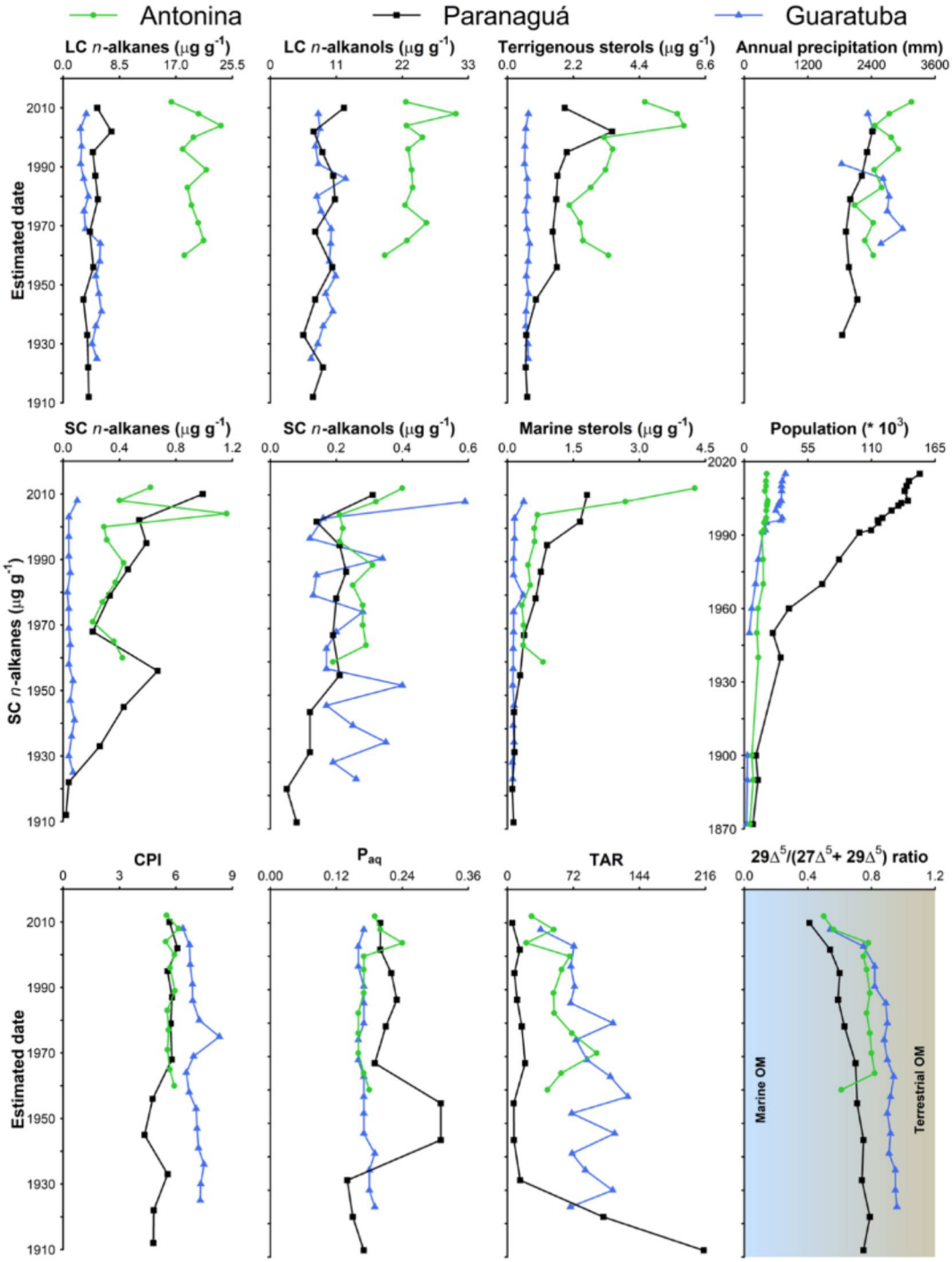

Figure 4. Profiles of terrestrial OM indicators (long chain n-alkanes, long chain n-alkanols and terrigenous sterols, i.e. 29Δ5,22 and 29Δ5), marine OM indicators (short chain n-alkanes, short chain n-alkanols and marine sterols, i.e. $27\Delta^{5,22E}$ and $27\Delta^{5}$), diagnostic ratios, precipitation and population for the three sediment cores analysed. Abbreviations: LC = long chain, SC = short chain, CPI = carbon preference index, Paq = aquatic proxy, TAR = terrigenous-to-aquatic ratio.

372 4.4.4 Spearman correlation and principal component analysis

373 In the AC core, TOC was positively correlated with $28\Delta^5$ and $29\Delta^{\square}$ ($\rho > 0.90$; *p value* <
374 0.05). Conversely, $\delta^{15}N$ presented strong negative correlations with these same variables ($\rho <$ -
375 0.75; *p value* < 0.05). Additionally, high positive correlations ($\rho > 0.70$) were observed between
376 all sterols, despite their different sources. Population was not significantly correlated with any
377 of the OM proxies, while precipitation correlated positively with TOC ($\rho = 0.78$; *p value* < 0.05)
378 and with all sterols ($\rho > 0.72$; *p value* < 0.05), except for $29\Delta^{5,22}$ (Table S11).

379 In the PC core, TOC was positively correlated with long-chain *n*-alkanes ($\rho = 0.96$; *p*
380 *value* < 0.05) and with unsaturated sterols from aquatic organisms ($27\Delta^{5,22E}$ and $27\Delta^5$) ($\rho >$
381 0.80; *p value* < 0.05). TN was positively correlated with almost all organic proxies, except for
382 long chain *n*-alkanols, whereas $\delta^{15}N$ presented a positive correlation with long-chain *n*-alkanes
383 ($\rho = 0.76$; *p value* < 0.05) (Table S12). Additionally, a high correlation between sterols from
384 aquatic organisms ($27\Delta^{5,22E}$ and $27\Delta^5$) and molecular biomarkers associated with terrestrial
385 sources (long-chain *n*-alkanes) was detected. Population was positively correlated with bulk
386 proxies (TN, $\delta^{13}C$ and $\delta^{15}N$) ($\rho > 0.72$; *p value* < 0.05) and sterols ($27\Delta^{5,22E}$, $27\Delta^5$, $28\Delta^5$ and
387 $29\Delta^5$; $\rho > 0.93$; *p value* < 0.05). Precipitation correlated positively with TN ($\rho = 0.81$; *p value*
388 < 0.05) and all sterols, except for $29\Delta^{5,22}$ (Table S12).

389 In the GC core, there were few significant correlations among the molecular biomarkers,
390 such as the long-chain *n*-alkanes with $28\Delta^5$ ($\rho = 0.72$) and $29\Delta^5$ ($\rho = 0.74$; *p value* < 0.05) (Table
391 S13). The number of inhabitants correlated negatively with the mid- and long-chain *n*-alkanes
392 (ρ = -0.73 and ρ = -0.78, respectively; *p value* < 0.05) and positively with $27\Delta^5$ ($\rho = 0.94$; *p*
393 *value*< 0.05). Precipitation was positively correlated only with $27\Delta^{5,22}$ ($\rho = 0.80$; *p value*< 0.05)
394 (Table S13).

395 Finally, almost no significant correlations were observed between % fine sediments and
396 bulk and molecular proxies, and precipitation was not significantly correlated with long-chain
397 *n*-alkanes or long-chain *n*-alkanols in any of the records (Tables S11–S13).

398 Regarding PCA, the first two components of the AC, PC and GC cores explained 52.9,
399 69.8 and 47.4% of the data variability, respectively (Fig. 5). In general, PC1 from the AC and
400 PC cores presented a gradient of population growth (with increases towards the top sections;
401 Fig. 5 and Table S14). PC1 from the AC core explained 33.4% of the variability and was mainly
402 associated with marine sterols ($27\Delta^{5,22E}$ and $27\Delta^5$), precipitation, short-chain *n*-alkanols,
403 terrigenous sterols ($29\Delta^{5,22}$ and $29\Delta^5$), $\delta^{15}N$, and population. PC1 from the PC core explained
404 50.9% of the variability and was mainly associated with marine sterols, population, odd long-

405 chain *n*-alkanes, terrigenous sterols and $\delta^{15}N$. Last, PC1 from the GC core explained 27.2% of
406 the data variability, and its main contributors were $\delta^{13}C$, marine sterols, short-chain *n*-alkanols,
407 short-chain *n*-alkanes and CPI (Table S14). Regarding PC2, short- and long-chain *n*-alkanes
408 were the main representative variables in the AC core; sterol index, % fine sediments and $\delta^{13}C$
409 were the main variables in the PC core; and long-chain *n*-alkanes, sterol index and terrigenous
410 sterols were the main variables in the GC core.
411
412 ## 4.5 Discussion

413 ### 4.5.1 Sources of sedimentary organic matter

414 The general predominant terrigenous OM or a mixture of sources were verified in the
415 sites of the three cores analysed. Specifically, the AC core presented predominant terrigenous
416 sources, while terrigenous or mixed sources were verified in the PC and GC cores, depending
417 on the analysed proxy. The AC core is under great fluvial influence due to its proximity to the
418 main riverine inputs in the E–W sector of the PES (Fig. 1B) and thus receives a large amount
419 of terrestrial material. On the other hand, the PC core may also receive a significant amount of
420 terrestrial OM but presents a higher marine influence than the AC core due to the proximity of
421 the estuary mouth, explaining the terrestrial/mixed source OM pattern. Similarly, the GC core
422 is under mixed influence, since it was collected from the mid-sector of Guaratuba Bay,
423 presenting more marine influence than the AC core but less than the PC core.

424 Total organic carbon (TOC) (for the AC and PC cores) and total nitrogen (TN) values
425 (for the PC core) increased throughout the cores (Fig. 2), indicating a slight increase in OM
426 input in the PES in recent years. In the PC core, there was no evidence of a predominant source
427 acting in the recent increase in OM input (Table S12). On the other hand, terrigenous OM was
428 the main contributor in recent years in the AC core, according to the positive correlations of
429 TOC with terrigenous sterols ($29\Delta^{\square\square\square}$ and $29\Delta^{\square}$) and precipitation and the negative correlation
430 of TOC with $\delta^{15}N$ (Table S11). Terrestrial contributions from drainage basins may increase with
431 precipitation and consequently increase the levels of molecular biomarkers such as sterols (e.g.,
432 campesterol and sitosterol) (Mudge and Lintern 1999). This terrestrial contribution was
433 corroborated by the decrease in $d^{15}N$ values. On the other hand, the relatively large availability
434 of nutrients provided by increased terrestrial OM may have favoured phytoplankton abundance,
435 explaining the observed increase in dehydrocholesterol (Mudge and Lintern 1999).
436

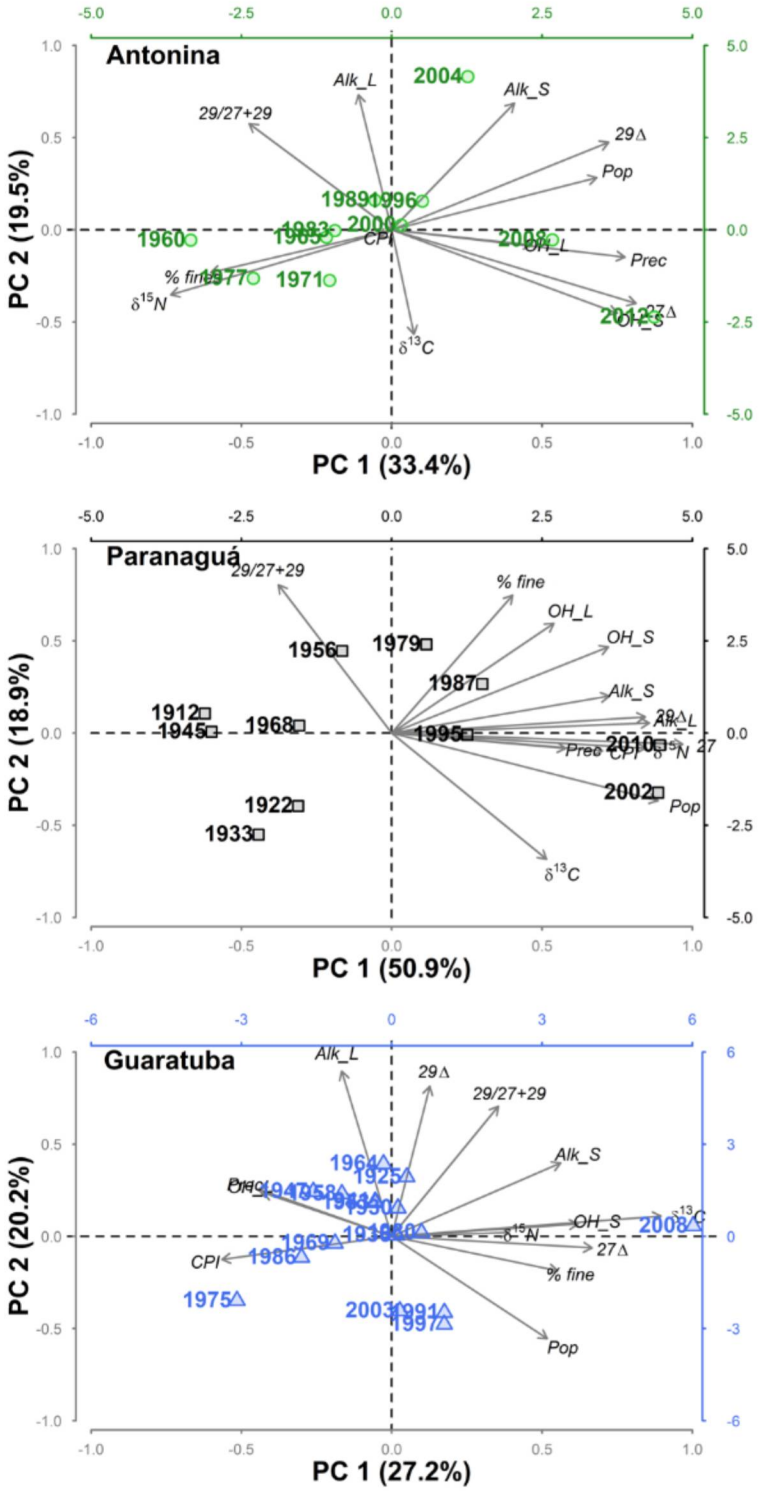

Figure 5. PCA biplots for the three sediment cores analysed. Variables: fine sediment (% fine), $\delta^{13}C$, $\delta^{15}N$, long-chain *n*-alkanes (Alk_L), short-chain *n*-alkanes (Alk_S), long-chain *n*-alkanols (OH_L), short-chain *n*-alkanols (OH_S), terrigenous sterols (29Δ: $29\Delta^{5,22}$ and $29\Delta^{5}$), marine sterols (27Δ: $27\Delta^{5,22}$ and $27\Delta^{5}$), CPI and the sterol index (29/27+29: $29\Delta^{5}/(27\Delta^{5} + 29\Delta^{5})$).

In Fig. 6, it is possible to distinguish the sediment cores according to their δ13C values, with only the PC core presenting values compatible with marine phytoplankton (-26 to -18‰). However, all cores presented values in the same range as those related to freshwater phytoplankton (-30 to -24‰) and terrestrial plants utilizing C3 (-32 to -24‰) and crassulacean acid metabolism (CAM) (-30 to -12‰). Regarding δ15N, the AC core presented relatively higher values than the PC and GC cores. The three cores may have received material from benthic phytoplankton (0 to 5‰), C3 freshwater marshes (3.5 to 5.5 ‰) and C4 salt marshes (3 to 7‰). However, some layers in the PC and GC cores presented δ15N values lower than 2.0 ‰, suggesting a contribution from vascular plants (-2 to 2‰), indicating periods with a greater influence of terrigenous OM input (Bianchi and Canuel 2011, Chikaraishi 2013).

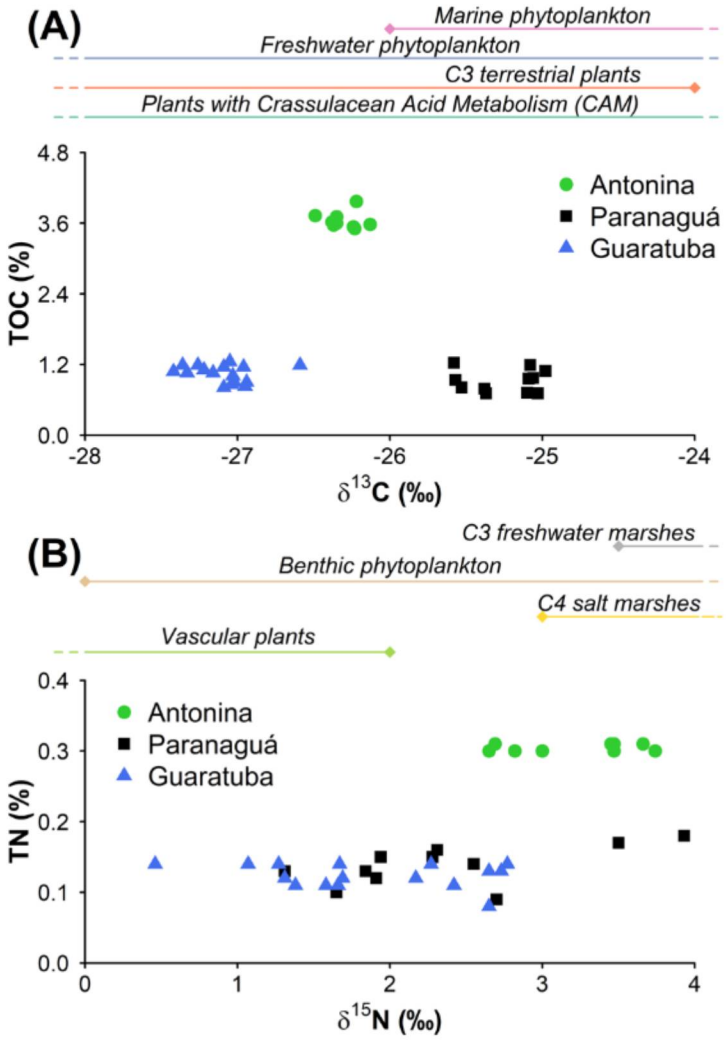

Figure 6. Cross-plot between bulk organic matter properties, grouping samples from the three sediment cores analysed: (A) Total organic carbon (TOC) *vs* $\delta^{13}C$; (B) total nitrogen (TN) *vs* $\delta^{15}N$ Reference values were obtained from Chikaraishi (2013) ($\delta^{13}C$) and Bianchi and Canuel (2011) ($\delta^{15}N$).

459 The most abundant organic biomarkers determined in the three cores were *n*-C_{29}, *n*-C_{28}-
460 OH, *n*-C_{30}-OH, $29\Delta^5$ and $29\Delta^{5,22E}$. The odd long-chain *n*-alkanes have also been the main
461 molecular biomarkers reported in the PES (Abreu-Mota et al. 2014; Bet et al. 2015). Together
462 with the long-chain *n*-alkanols, they suggest terrigenous sources in the cores (Fig. 3), as they
463 are related to the epicuticular waxes of higher plants (Eglinton and Hamilton 1967; Logan et al.
464 1995). However, the positive correlation between aquatic sterols and long-chain *n*-alkanes
465 suggests a mixture of terrestrial and marine contributions. An increase in primary production
466 may be expected as a result of the nutrients from terrigenous OM input. Once the distribution
467 of molecular biomarkers may be affected by rainfall and soil management, the transport of rich
468 OM soil to estuaries by surface runoff may affect marine OM production.
469 In the AC core, for instance, $28\Delta^5$, 29Δ□ and TOC seemed to be of common terrigenous
470 origin. The positive correlation between sterols of aquatic and terrestrial sources (Table S11)
471 and their similar contribution to PC1 in the PCA (Fig. 5) suggests that the input of terrigenous
472 OM may influence the autochthonous production of OM. In this way, the negative correlation
473 between $\delta^{15}N$ and 29Δ□ suggests an aquatic source of nitrogen (Bianchi and Canuel 2011).
474 In the PC core, the correlation between TOC and long-chain *n*-alkanes indicated a
475 primary contribution from terrestrial OM. However, the contribution of autochthonous OM was
476 also noticeable due to the correlation obtained between TOC and unsaturated sterols from
477 aquatic organisms ($27\Delta^{5,22E}$ and $27\Delta^5$) (Mudge and Lintern 1999), whose concentrations
478 increased through the core (Fig. 4). The positive correlation between sterols from aquatic
479 organisms and molecular markers associated with terrestrial sources (long-chain *n*-alkanes)
480 again suggests that the input of allochthonous OM may have influenced the production of
481 aquatic OM. This was also observed in the PCA (Fig. 5), where terrigenous and marine markers
482 followed the same orientation.
483 In the GC core, the few significant correlations between the molecular markers indicated
484 sedimentary terrigenous OM. This was also observed in the PCA, where most samples were
485 grouped with terrestrial-source biomarkers (left quadrants) rather than with marine-source
486 biomarkers (right quadrants) (Fig. 5).
487 The *n*-alkane and *n*-alkanol indices indicated mixed sources (P_{aq} index = 0.1–0.4) or
488 terrestrial sources (CPI > 4, TAR >> 3) along the three core sections analysed. The sterol
489 diagnostic ratio $29\Delta^5/(27\Delta^5 + 29\Delta^5)$, based on terrestrial ($29\Delta^5$) and marine ($27\Delta^5$) biomarkers,
490 may be proposed to corroborate the *n*-alkane and *n*-alkanol indices once sterols are less labile
491 than short-chain *n*-alkanes. In all cores, this ratio also indicated a large predominance of

492 terrigenous OM. The marine OM influence was observed in sections of the AC and GC cores
493 and mainly in the surface layers of the PC core, where $27\Delta^5$ was detected at higher
494 concentrations (Fig. 4). These increases may be associated with increased urban occupation,
495 combined with high local rainfall (*ca.* 1800 mm $year^{-1}$), releasing nutrients through coastal
496 erosion due to urbanization, mangrove exploration and basin drainage, which may have
497 promoted a slight increase in primary production in recent years (Fig. 7 and Fig. 8).
498
499 4.5.2 Land uses and soil occupation
500 Soil use and human occupation in the surrounding areas may affect allochthonous OM
501 inputs to water bodies (e.g., Carreira et al., 2002; Martins et al., 2010). Regarding the population
502 growth in the study area, the city of Paranaguá had the most significant population growth,
503 mainly beginning in the 1950s. The population sizes in Antonina and Guaratuba were more
504 stable, with a slight leap in Guaratuba in the mid-1990s and stabilization later (Fig. 4). However,
505 although the concentrations of some biomarkers and bulk properties presented some variation
506 in recent decades (Figs. 2 and 4), none of these variables showed a conclusive relationship with
507 population growth evolution.
508 Although PC1 of the PCAs for the AC and PC cores reflected population growth
509 followed by both terrigenous and marine indicators, the population vector was only close to
510 terrigenous sterols (29Δ5,22 and 29Δ5) in the AC core and had unclear relationships with the
511 other variables in the PC and GC cores (Fig. 5). Therefore, the variation obtained for the
512 biomarkers and bulk properties may reflect other events in addition to the local population
513 increase. In the PES (which includes the Paranaguá and Antonina bays), an increase in the
514 supply of terrigenous material was observed since ca. 1945, indicated by the increase in
515 terrestrial sterols (sum of 29Δ5,22E and 29Δ5) and long-chain n-alkanes (Fig. 4), marked as an
516 economic transition period after the end of World War II. The installation of marinas and yacht
517 clubs on the banks of the estuary, as well as the improvement of the Paranaguá port and dredging
518 activities, contributed to the environmental changes in the region (Pierri et al. 2006; Martins et
519 al. 2015). Dredging activities were also responsible for imposing changes on sediment flux and
520 deposition into the estuary. For example, the local dredging in Antonina Bay in ca. 2001–2002,
521 coupled with an increase in terrestrial drainage due to seasonal rainfall, may have favoured the
522 dispersion of the sediment dredge plume to other regions of the PES, carrying previously
523 accumulated terrigenous material from the inner sectors to the outer zones of this estuarine
524 system, such as Paranaguá Bay (Lamour and Soares 2007).

525

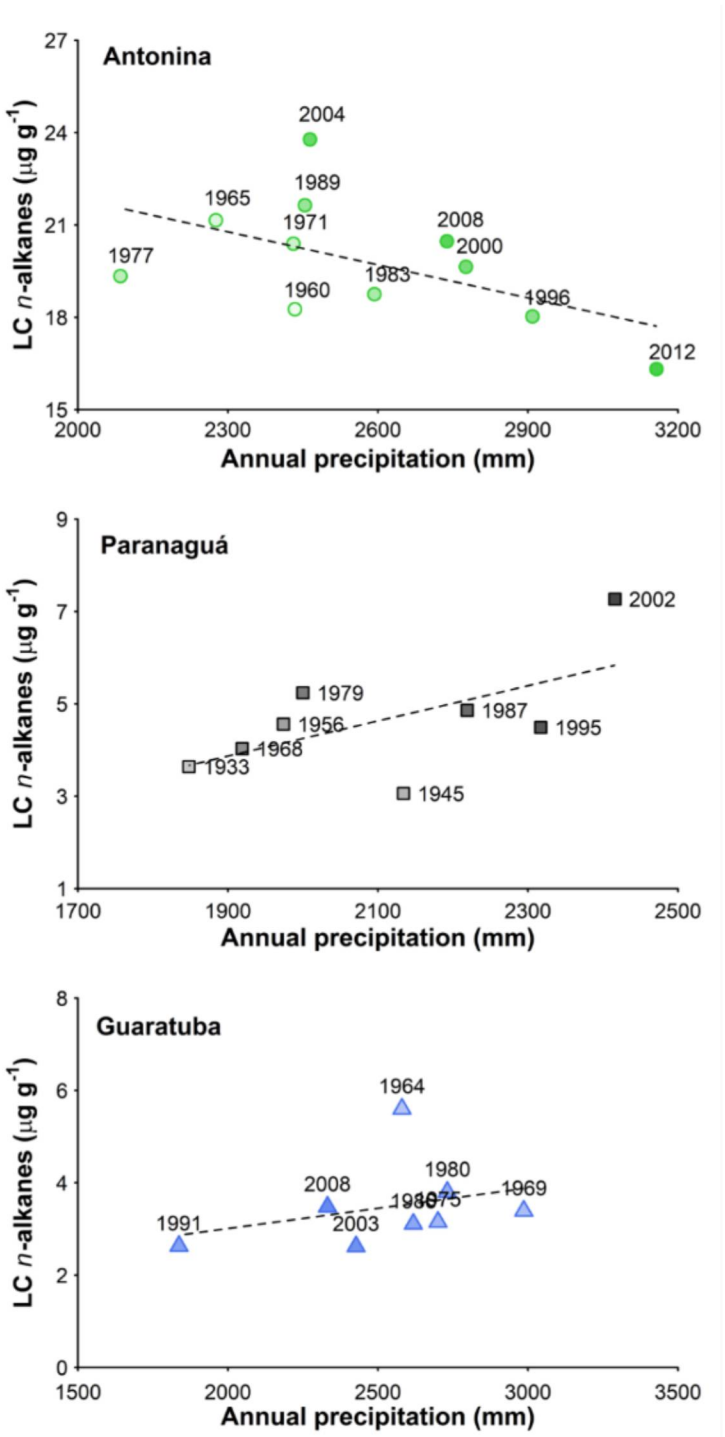

526 Figure 7. Relationship between annual precipitation (in mm) and long-chain *n*-alkanes (LC *n*-alkanes = *n*-C_{27} + *n*-
527 C_{29} + *n*-C_{31}, in µg g^{-1}) for the three sediment cores analysed. Darker colours indicate the top core samples, whereas
528 more transparent colours indicate the top bottom samples. A dashed line indicates a nonsignificant Spearman
529 correlation (*p*-value > 0.05).

530

531

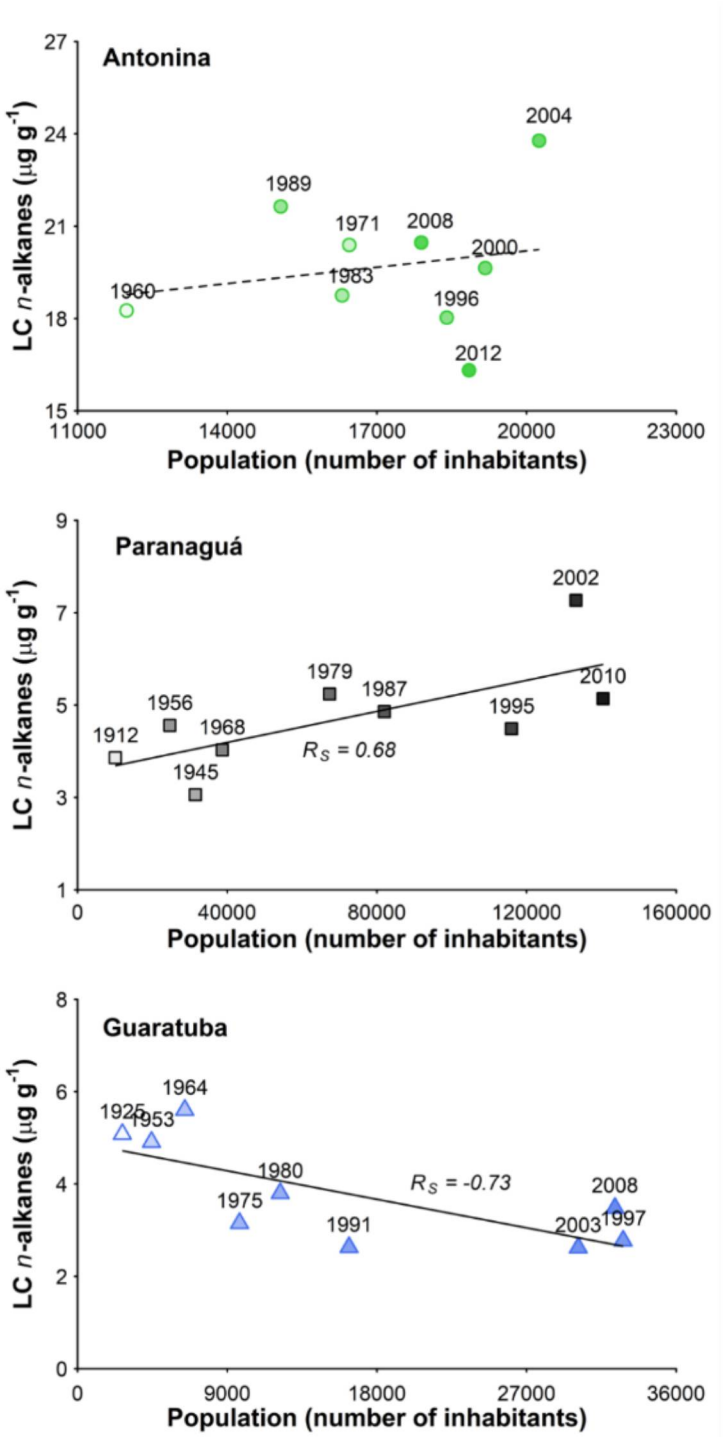

532 Figure 8. Relationship between population growth (in number of inhabitants) and long-chain *n*-alkanes (LC *n*-
533 alkanes = *n*-C_{27} + *n*-C_{29} + *n*-C_{31}, in µg g^{-1}) for the three sediment cores analysed. Darker colours indicate the top
534 core samples, whereas more transparent colours indicate the top bottom samples. A dashed line indicates a
535 nonsignificant Spearman correlation (p-value > 0.05), whereas a continuous line indicates a significant Spearman
536 correlation (p-value < 0.05).

537

538 An increase in precipitation was observed after ca. 2000 in the AC core, with 'peaks' of
539 some biomarkers of OM in ca. 2002, such as total sterols, total n-alkanes and terrigenous sterols,
540 29Δ□□□□ and 29Δ□□In addition, increases in the precipitation rate and drainage in the PES tend
541 to promote the availability of nutrients that may favour aquatic OM production (Cabral and
542 Martins 2018), as shown by the sterol ratio in Fig. 4.
543 The population growth observed in the last decades in the study area did not have the
544 same magnitude as observed in other very populated estuaries located in the Brazilian coast
545 (e.g., Guanabara Bay and Santos estuary; Fig. S3), what may not let us identify notable changes
546 in the organic matter deposition. In addition, the estuaries in Paraná coastline present large areas
547 of tidal flats covered by mangroves, saltmarshes, swamps and seagrass beds, which form a
548 complex ecosystem structure (Angulo, 2004). These ecosystems are extremely efficient at
549 sequestering and burying sediments and organic carbon from external sources (Duarte et al.,
550 2005; Mcleod et al., 2011), contributing to promote lower bottom shear stresses, hence lowering
551 erosion rates (Leonard and Luther, 1995; Middelburg et al., 1997).
552 For the GC core, the lack of estimated population data in some years between *ca.* 1910
553 and 1990 limits us to only a qualitative evaluation of the trends. The large inputs of long-chain
554 *n*-alkanes before *ca.* 1965 may be related to the removal of *Ilex paraguariensis* vegetation for
555 economic purposes, which was prominent between *ca.* 1930 and *ca.* 1950. This change did not
556 result in a noticeable population increase (Fig. 8) but caused extensive deforestation prior to *ca.*
557 1960, which may have been related to the decrease in terrestrial OM inputs in the following
558 years (> 1970s) (Chemin and Abrahão 2014). This decrease may be evidenced by the constant
559 value patterns observed for terrestrial sterols and in the PCA (Fig. 4 and Fig. 5).
560
561 4.5.3 El Niño–Southern Oscillation events
562 In El Niño–Southern Oscillation (ENSO) years, when increases in temperature and
563 rainfall may occur (Camilloni and Barros 2000), an increase in terrigenous OM input is
564 expected due to increased continental runoff. The ENSO starts in August (year 0) and extends
565 to July (year +1) of the following year (Grimm and Tedeschi 2009).
566 The AC and PC cores present significant positive correlations between precipitation and
567 both marine (e.g., $27\Delta^{5,22}$ and $27\Delta^{5}$) and terrigenous (e.g., $28\Delta^{5}$ and $29\Delta^{5}$) sterols (Tables S11
568 and S12; Fig. 5). In the GC core, precipitation is in the same PCA quadrant as terrigenous
569 proxies (e.g., terrigenous sterols and long-chain *n*-alkanes and *n*-alkanols) (Fig. 5). However, it
570 did not contribute significantly to PC1 or PC2 (Tables S13 and S14), indicating a lack of
571 influence of precipitation on the contribution of terrestrial OM in these estuaries. Nevertheless,

572 the virtually constant and low *n*-C_{24}-OH/*n*-C_{26}-OH ratio values (Table S1) suggest that the OM
573 was produced under warm and humid conditions in the periods represented by the cores, as this
574 restricted differentiation in *n*-alkanol production and thus indicated low climatic variability
575 (Zheng et al. 2009). This is corroborated by the other indices that did not indicate changes in
576 the types of OM contributions to the estuaries. Therefore, considering the temporal resolution
577 of the records and the available total annual precipitation data series, the ENSO events that
578 occurred within the time span covered by the cores did not appear to have a clear influence on
579 the rates of terrestrial input to the sediments in the studied estuaries. This was also evidenced
580 by the absence of a correlation between precipitation and long-chain *n*-alkanes (Fig. 7) in all
581 cores studied.
582 Moreover, the intensity of ENSO in South America depends on a multitude of factors,
583 including the impact of other modes of climatic variability and interactions between the Pacific
584 and Atlantic basins. Climatic variability can also modify ENSO impacts directly, either
585 reinforcing corresponding anomalies or muting them (Cai et al. 2020). The study area is located
586 between the Atlantic Ocean and the "Serra do Mar" mountain range, with heights reaching up
587 to 1800 m (Angulo, 1999). The interaction with this geographical location with atmospheric
588 systems may affect rainfall dynamics and the local thermal amplitude (Vanhoni and Mendonça,
589 2008; Reboita et al., 2010) (Fig. S4). The main atmospheric systems acting on the region are
590 the South Atlantic Convergence Zone (ZCAS in Fig. S4) and the South Atlantic High (ASAS
591 in Fig. S4), in addition to the mesoscale convective complexes (CCM in Fig. S4), atmospheric
592 blocking and the passage of warm and cold fronts (FQ and FF in Fig. S4) (Angulo et al., 2006;
593 Grimm et al., 1998; Reboita et al., 2010). The interaction of these several static and dynamic
594 features ends up masking and weakening the ENSO signal.
595
596 4.6 Conclusions

597 Coastal ecosystems have been historically disturbed due to intensive land use and
598 human occupation and are under the influence of climatic events. The application of a
599 geochemical multiproxy approach was tested in two subtropical estuaries located on the
600 Brazilian coast in the South Atlantic to characterize the OM input and composition variations
601 under a scenario of environmental changes. In general, terrigenous OM was predominant over
602 the time scale studied in the Paranaguá Estuarine System (Paranaguá and Antonina bays) and
603 in Guaratuba Bay. However, marine influence was detected in some sections of the Guaratuba
604 and Paranaguá cores, indicating mixed sources of sedimentary OM, especially in the surface
605 layers of the Paranaguá core.

606 Recent anthropogenic activities interfered with the composition and input of
607 sedimentary OM to the Antonina and Paranaguá bays during the last century. The variation in
608 the molecular biomarker concentrations after *ca.* the 1950s along the Antonina and Paranaguá
609 cores may be associated with land uses due to the intensification of human occupation in coastal
610 and adjacent basin drainages, as well as port activities. An unexpected negative correlation
611 between increased population and long-chain *n*-alkanes was found in the Guaratuba core,
612 suggesting moderate impacts of vegetal extraction and land use by the population near this bay.
613 Regarding climatic events, the effects of the periodic event considered (i.e., El Niño–
614 Southern Oscillation) did not seem to have imposed noticeable changes in the sedimentary OM
615 during the last century in either estuary, as indicated by the virtually constant diagnostic ratio
616 values in all cores and by the absence of substantial changes in the types of contributions in the
617 two estuaries.
618 This study represents a scientific contribution in addressing environmental changes
619 (climatic and anthropic) in subtropical estuaries using bulk properties and biomarkers. Factors
620 of different scales that comprise local features (i.e., geomorphology of the region), events of
621 the regional economic cycles, local climatic variability, and interactions between the Pacific
622 and Atlantic basins (i.e., El Niño–Southern Oscillation) were considered in this study. Variations
623 that stood out in the beginnings and ends of the different cycles of the predominant economic
624 activities along the short time scale (approximately one century) covered by the cores were
625 observed in most biomarkers and bulk properties analysed, with sterols seeming to be a more
626 robust proxy for indicating changes in the autochthonous contribution to sedimentary OM.
627 Therefore, the tested multiproxy approach demonstrated that local environmental changes
628 related to anthropogenic events in the adjacent drainage basin may be considered a potential
629 stratigraphic tool for identifying human impacts in coastal zones.
630

631 **Author Contributions**

632 Marines M. Wilhelm: Formal analysis, Writing - Original Draft, Review & Editing; Ana
633 Caroline Cabral: Writing - Original Draft, Review & Editing; Ana Lúcia L. Dauner: Writing -
634 Review & Editing, Visualization; Marina Reback Garcia: Writing – Review; Rubens C.L.
635 Figueira: Formal analysis, Writing – Review; César C. Martins: Resources, Writing - Review;
636 Funding acquisition.
637

638 **Acknowledgements**

M.M. Wilhelm would like to thank CAPES (Coordenação de Aperfeiçoamento de Pessoal de Ensino Superior). C.C. Martins would like to thank CNPq (Brazilian National Council for Scientific and Technological Development) and Fundação Araucária de Apoio ao Desenvolvimento Científico e Tecnológico do Estado do Paraná. We are grateful to A. Salaroli for assistance with bulk organic matter analysis. Also, this work contributed to the EQCEP project (*Historical input and future perspectives related to the chemical stressors occurrence in the Paranaguá Estuarine System*) sponsored by CNPq and Brazilian Ministry of Science, Technology, Innovation and Communication and coordinated by Professor M.M. Mahiques. This study was developed as part of a graduate course on estuarine and ocean systems at the Federal University of Paraná (PGSISCO-UFPR).

Funding

We would like to thank CNPq (448945/2014-2; 305734/2014-8; 441265/2017-0) and Fundação Araucária de Apoio ao Desenvolvimento Científico e Tecnológico do Estado do Paraná (401/12, 15.078) for research grants received.

Declarations

The authors declare no competing interests.

Supplementary data

Supplementary data to this article can be found online

660 **References**
661
662 Aboul-Kassim, T.A.T. and B.R.T. Simoneit. 1996. Lipid geochemistry of surficial sediments
663 from the coastal environment of Egypt I. Aliphatic hydrocarbons-characterization and
664 sources. *Marine Chemistry* 54: 135–158.
665 https://doi.org/10.1016/0304-4203(95)00098-4
666 Abreu-Mota, M.A., C.A.M. Barboza, M.C. Bícego and C.C. Martins. 2014. Sedimentary
667 biomarkers along a contamination gradient in a human-impacted sub-estuary in
668 Southern Brazil: A multi-parameter approach based on spatial and seasonal variability.
669 *Chemosphere* 103: 156–163.
670 https://doi.org/10.1016/j.chemosphere.2013.11.052
671 ANA (Agência Nacional de Águas). 2017. Relatório de Alturas mensais de precipitação.
672 Available in: http://www.sih-web.aguasparana.pr.gov.br/sih-
673 web/gerarRelatorioAlturasAnuaisPrecipitacao.do?action=carregarInterfaceInicial. (in
674 Portuguese). Accessed in March/2017.
675 Angulo, R.J. 1999. Morphological characterization of the tidal deltas on the coast of the State
676 of Paraná. *Anais da Academia Brasileira de Ciências* 71: 935-960.
677 Angulo, R.J. 2004. Mapa do Cenozóico do litoral do Estado do Paraná. *Boletim Paranaense de*
678 *Geociências* 55: 25-42.
679 Angulo, R.J., C.R. Soares, E. Marone, M.C. Souza, L.L.R. Odreski, M.A. Noernberg. 2006.
680 Paraná. *In*: Muehe, D., Erosão e progradação do litoral brasileiro. Brasília: Ministério
681 do Meio Ambiente, 1, 475.
682 Bern, C.R., K. Walton-Day and D.L. Naftz. 2019. Improved enrichment factor calculations
683 through principal component analysis: Examples from soils near breccia pipe uranium
684 mines, Arizona, USA. *Environmental Pollution* 248: 90–100.
685 https://doi.org/10.1016/j.envpol.2019.01.122
686 Bet, R., M.C. Bícego and C.C. Martins. 2015. Sedimentary hydrocarbons and sterols in a South
687 Atlantic estuarine/shallow continental shelf transitional environment under oil terminal
688 and grain port influences. *Marine Pollution Bulletin* 95: 183-194.
689 https://doi.org/10.1016/j.marpolbul.2015.04.024
690 Bianchi, T.S. and E.A. Canuel. 2011. *Chemical biomarkers in aquatic ecosystems*. Chemical
691 Biomarker Applications to Ecology and Paleoecology. Princeton University Press,
692 USA.
693 Bigarella, J.J. 2001. Contribuição ao estudo da planície litorânea do Estado do Paraná. *Brazilian*
694 *Archives of Biology and Technology* Jubilee Volume (1946-2001): 65-110.
695 Borchers, H.W., 2019. pracma: Practical Numerical Math Functions. R package version 2.2.5.
696 Bourbonniere, R.A. and P.A. Meyers. 1996. Anthropogenic influences on hydrocarbon contents
697 of sediments deposited in eastern Lake Ontario since 1800. *Environmental Geology* 28:
698 22–28.
699 https://doi.org/10.1007/s002540050074
700 Bray, E.E. and E.D. Evans. 1961. Distribution of n-paraffins as a clue to recognition of source
701 beds. *Geochimica et Cosmochima Acta* 22: 2–15.

https://doi.org/10.1016/0016-7037(61)90069-2

Cabral, A.C., Stark, J.S., Kolm, H.E., Martins, C.C., 2018. An integrated evaluation of some faecal indicator bacteria (FIB) and chemical markers as potential tools for monitoring sewage contamination in subtropical estuaries. *Environmental Pollution* 235: 739–749.

https://doi.org/10.1016/j.envpol.2017.12.109

Cabral, A.C. and C.C. Martins. 2018. Insights about sources, distribution, and degradation of sewage and biogenic molecular markers in surficial sediments and suspended particulate matter from a human-impacted subtropical estuary. *Environmental Pollution* 241: 1071-1081.

https://doi.org/10.1016/j.envpol.2018.06.032

Cabral, A.C., M.M. Wilhelm, R.C.L. Figueira and C.C. Martins. 2019. Tracking the historical sewage input in South American subtropical estuarine systems based on faecal sterols and bulk organic matter stable isotopes ($\delta^{13}C$ and $\delta^{15}N$). *Science of the Total Environment* 655: 855-864.

https://doi.org/10.1016/j.scitotenv.2018.11.150

Cabral, A.C., A.L.L. Dauner, F.C.B. Xavier, M.R.D. Garcia, M.M. Wilhelm, V.C.G. Santos, S.A. Netto and C.C. Martins. 2020. Tracking the sources of allochthonous organic matter along a subtropical fluvial-estuarine gradient using molecular proxies in view of land uses. *Chemosphere* 251: 126435.

https://doi.org/10.1016/j.chemosphere.2020.126435

Cai, W., M.J. McPhaden, A.M. Grimm, R.R. Rodrigues, A.S. Taschetto, R.D. Garreaud, B. Dewitte, G. Poveda, Y-G. Ham, A. Santoso, B. Ng, W. Anderson, G. Wang, T. Geng, H-S. Jo, J.A. Marengo, L.M. Alves, M. Osman, , S. Li, L. Wu, C. Karamperidou, K. Takahashi and C. Vera. 2020. Climate impacts of the El Niño–Southern Oscillation on South America. *Nature Reviews Earth & Environment* 1: 215–231.

https://doi.org/10.1038/s43017-020-0040-3

Camilloni, I.A. and V.R. Barros. 2000. The Parana River response to El Nino 1982 – 83 and 1997 – 98 Events. *Journal of Hydrometeorology* 1: 412–430.

https://doi.org/10.1175/1525-7541(2000)001<0412:TPRRTE>2.0.CO;2

Canuel, E.A. and A.K. Hardison. 2016. Sources, ages, and alteration of organic matter in estuaries. *Annual Review of Marine Science* 8: 409–434.

https://doi.org/10.1146/annurev-marine-122414-034058

Cardoso, F.D., A.L.L.Dauner and C.C. Martins. 2016. A critical and comparative appraisal of polycyclic aromatic hydrocarbons in sediments and suspended particulate material from a large South American subtropical estuary. Environmental Pollution 214: 219–229.

http://dx.doi.org/10.1016/j.envpol.2016.04.011

Carreira, R.S., A.L. Wagener, J.W. Readman, T.W. Fileman, S.A. Macko, A. Veiga. 2002. Changes in the sedimentary organic carbon pool of a fertilized tropical estuary, Guanabara Bay, Brazil: an elemental, isotopic and molecular marker approach. *Marine Chemistry* 79: 207-227.

https://doi.org/10.1016/S0304-4203(02)00065-8

Chemin, M. and C.M.S. Abrahão. 2014. Territorial integration of the coast of Paraná State

(Brazil): Transport, resort development and patrimonialization in the formation and dynamics of tourist spaces. RA'E GA – O Espaço Geográfico em Análise 32: 212–239.

Chikaraishi, Y. 2013. $^{13}C/^{12}C$ signatures in plants and algae. Treatise on Geochemistry: 2nd Edition. Elsevier Ltd.

Combi, T., S. Taniguchi, R.C.L. Figueira, M.M., Mahiques and C.C. Martins. 2013. Spatial distribution and historical input of polychlorinated biphenyls (PCBs) and organochlorine pesticides (OCPs) in sediments from a subtropical estuary (Guaratuba Bay, SW Atlantic). *Marine Pollution Bulletin* 70, 247–252.

https://doi.org/10.1016/j.marpolbul.2013.02.022

Costa, E.S., C.F. Grilo, G.A. Wolff, A. Thompson, R.C.L. Figueira, F. Sá and R.R. Neto. 2016. Geochemical records in sediments of a tropical estuary (Southeastern coast of Brazil). *Regional Studies in Marine Science* 6: 49–61.

https://doi.org/10.1016/j.rsma.2016.03.008

Dauner, A.L.L. and C.C. Martins. 2015. Spatial and temporal distribution of aliphatic hydrocarbons and linear alkylbenzenes in the particulate phase from a subtropical estuary (Guaratuba Bay, SW Atlantic) under seasonal population fluctuation. *Science of the Total Environment* 536: 750–760.

https://doi.org/10.1016/j.scitotenv.2015.07.091

Dauner, A.L.L., T.H. Dias, F.K. Ishii, B.G. Libardoni, R.A. Parizzi and C.C. Martins. 2018. Ecological risk assessment of sedimentary hydrocarbons in a subtropical estuary as tools to select priority areas for environmental management. *Journal of Environmental Management* 223: 417–425.

https://doi.org/10.1016/j.jenvman.2018.06.024

Duarte, C. M., J.J. Middelburg and N. Caraco. 2005. Major role of marine vegetation on the oceanic carbon cycle. *Biogeosciences* 2: 1-8.

https://doi.org/10.5194/bg-2-1-2005

Eglinton, G. and R.J. Hamilton. 1967. Leaf epicuticular waxes. *Science* 156: 1322–1335.

https://doi.org/10.1126/science.156.3780.1322

Egres, A.G., C.C. Martins, V.M. Oliveira, P.C. Lana. 2012. Effects of an experimental in situ diesel oil spill on the benthic community of unvegetated tidal flats in a subtropical estuary (Paranaguá Bay, Brazil). *Marine Pollution Bulletin* 64: 2681-2691.

https://doi.org/10.1016/j.marpolbul.2012.10.007

Ficken, K.J., B. Li, D.L. Swain and G. Eglinton. 2000. An *n*-alkane proxy for the sedimentary input of submerged/floating freshwater aquatic macrophytes. *Organic Geochemistry* 31: 745–749.

https://doi.org/10.1016/S0146-6380(00)00081-4

Folk, R. and W. Ward. 1957. Brazos river bar: A study in the significance of grain size parameters. *Journal of Sedimentary Petrology* 27: 3–27.

https://doi.org/10.1306/74D70646-2B21-11D7-8648000102C1865D

Freeman, K.H. and R.D. Pancost. 2013. *Biomarkers for terrestrial plants and climate*. Treatise on Geochemistry: 2nd Edition. Elsevier Ltd.

785 Gabriel, K.R. 1971. The biplot graphic display of matrices with application to principal
786 component analysis. *Biometrika* 58: 453–467.

787 https://doi.org/10.1093/biomet/58.3.453

788 Grimm, A.M., S.E. Ferraz and J. Gomes. 1998. Precipitation anomalies in southern Brazil
789 associated with El Niño and La Niña events. *Journal of Climate* 11: 2863-2880.

790 https://doi.org/10.1175/1520-0442(1998)011<2863:PAISBA>2.0.CO;2

791 Grimm, A.M. and R.G. Tedeschi. 2009. ENSO and extreme rainfall events in South America.
792 *Journal of Climate* 22: 1589-1609.

793 https://doi.org/10.1175/2008JCLI2429.1

794 Hu, L., Z. Guo, J. Feng, Z. Yang and M. Fang. 2009. Distributions and sources of bulk organic
795 matter and aliphatic hydrocarbons in surface sediments of the Bohai Sea, China. Marine
796 Chemistry 113: 197–211.

797 https://doi.org/10.1016/j.marchem.2009.02.001

798 IBGE (Instituto Brasileiro de Geografia e Estatística), 2017. Censos demográficos de 1872 -
799 2010. Available in: http://biblioteca.ibge.gov.br. (in Portuguese). Accessed in
800 February/2017.

801 Jafarabadi, A.R., M. Dashtbozorg, A.R. Bakhtiari, M. Maisano and T. Cappello. 2019.
802 Geochemical imprints of occurrence, vertical distribution and sources of aliphatic
803 hydrocarbons, aliphatic ketones, hopanes and steranes in sediment cores from ten
804 Iranian Coral Islands, Persian Gulf. *Marine Pollution Bulletin* 144: 287–298.

805 https://doi.org/10.1016/j.marpolbul.2019.05.014

806 Jolliffe, I.T. and J. Cadima. 2016. Principal component analysis: A review and recent
807 developments. *Philosophical Transactions of The Royal Society: A Mathematical*
808 *Physical and Engineering Sciences* 374: 20150202.

809 https://doi.org/10.1098/rsta.2015.0202

810 Lacey, J.H., M.J. Leng, C.H. Vane, A.D. Radbourne, H. Yang and D.B. Ryves. 2018. Assessing
811 human impact on Rostherne Mere, UK, using the geochemistry of organic matter.
812 *Anthropocene* 21: 52-65.

813 https://doi.org/10.1016/j.ancene.2018.02.002

814 Lamour, M.R. and C.R. Soares. 2007. *Histórico das atividades de dragagem e taxas de*
815 *assoreamento nos canais de navegação aos portos costeiros paranaenses*. In:
816 Dragagens portuárias no Brasil : Licenciamento e monitoramento ambiental. 312p.

817 Lana, P.C., E. Marone, R.M. Lopes and E.C. Machado. 2001. *The Subtropical Estuarine*
818 *Complex of Paranaguá Bay, Brazil*. In: Seeliger U., Kjerfve B. (eds) Coastal Marine
819 Ecosystems of Latin America. Ecological Studies (Analysis and Synthesis), vol 144.
820 Springer, Berlin, Heidelberg.

821 Leonard, L.L. and M.E. Luther. 1995. Flow hydrodynamics in tidal marsh canopies. *Limnology*
822 *and Oceanography* 40: 1474-1484.

823 https://doi.org/10.4319/lo.1995.40.8.1474

824 Logan, G.A., C.J. Smiley and G. Eglinton. 1995. Preservation of fossil leaf waxes in association
825 with their source tissues, Clarkia, Northern Idaho, USA. *Geochimica et Cosmochimica*
826 *Acta* 59: 751–763.

https://doi.org/10.1016/0016-7037(94)00362-P

Mantovanelli, A., E. Marone, E.T. da Silva, L.F. Lautert, M.S. Klingenfuss, V.P. Prata Jr., M.A. Noernberg, B.A. Knoppers and R.J. Angulo. 2004. Combined tidal velocity and duration asymmetries as a determinant of water transport and residual flow in Paranaguá Bay estuary. *Estuarine, Coastal and Shelf Science* 59: 523–537.

https://doi.org/10.1016/j.ecss.2003.09.001

Marone, E., E.C. Machado, R.M. Lopes and E.T. Silva. 2005. Land-ocean fluxes in the Paranaguá Bay Estuarine System, southern Brazil. *Brazilian Journal of Oceanography* 53: 169–181

Marone, E., M.A. Noernberg, I. Dos Santos, L.F. Lautert, O.R. Andreoli, H. Buba and H.D. Fill. 2006. Hydrodynamic of Guaratuba Bay, PR, Brazil. *Journal of Coastal Research* 38: 1879–1883.

http://www.jstor.org/stable/25743087.

Martins, C.C., M.C. Bícego, M.M. Mahiques, R.C.L. Figueira, M.G. Tessler, and R.C. Montone. 2010. Depositional history of sedimentary linear alkylbenzenes (LABs) in a large South American industrial coastal area (Santos Estuary, Southeastern Brazil). *Environmental Pollution* 158: 3355-3364.

https://doi.org/10.1016/j.envpol.2010.07.040

Martins, C.C., M.E. Doumer, W.C. Gallice, A.L.L. Dauner, A.C. Cabral, F.D. Cardoso, N.N. Dolci, L.M. Camargo, P.A.L Ferreira, R.C.L. Figueira and A.S. Mangrich. 2015. Coupling spectroscopic and chromatographic techniques for evaluation of the depositional history of hydrocarbons in a subtropical estuary. *Environmental Pollution* 205: 403–414.

https://doi.org/10.1016/j.envpol.2015.07.016.

Meyers, P.A. 1997. Organic geochemical proxies of paleoceanographic, plaeolimnologic, and plaeoclimatic processes. *Organic Geochemistry* 27: 213–250.

https://doi.org/10.1016/S0146-6380(97)00049-1

Mcleod, E., G.L. Chmura, S. Bouillon, R. Salm, M. Björk, C.M. Duarte, C.E. Lovelock, W.H. Schlesinger and B.R. Silliman. 2011. A blueprint for blue carbon: toward an improved understanding of the role of vegetated coastal habitats in sequestering CO_2. *Frontiers in Ecology and the Environment* 9: 552-560.

https://doi.org/10.1890/110004

Middelburg, J.J., J. Nieuwenhuize, R.K. Lubberts and O. van de Plassche. 1997. Organic carbon isotope systematics of coastal marshes. *Estuarine, Coastal and Shelf Science* 45: 681-687.

https://doi.org/10.1006/ecss.1997.0247

Mudge, S.M. and D.G. Lintern. 1999. Comparison of sterol biomarkers for sewage with other measures in Victoria Harbour, B.C., Canada. *Estuarine, Coastal and Shelf Science* 48: 27–38.

https://doi.org/10.1006/ecss.1999.0406

Peters, K.E., C.C. Walters and J.M. Moldowan. 2005. *The biomarker guide: biomarkers and isotopes in the environment and human history*. Cambridge Universty Press, UK.

869 Pierri, N., R.J. Angulo, M.C. Souza and M. Kim. 2006. A ocupação e o uso do solo no litoral
870 paranaense: condicionantes, conflitos e tendências. *Desenvolvimento e Meio Ambiente*
871 13: 137–167.

872 Pietzsch, R.; S.R. Patchineelam and J.P.M. Torres. 2010. Polycyclic aromatic hydrocarbons in
873 recent sediments from a subtropical estuary in Brazil. *Marine Chemistry* 118: 56–66.

874 https://doi.org/10.1016/j.marchem.2009.10.004

875 Pires, P.T.L., A.L. Zilli and C.T. Blum. 2005. *Atlas da Floresta Atlantica no Paraná.* 104p.

876 Queen, J.P., G.P. Quinn and M.J. Keough. 2002. *Experimental Design and Data Analysis for*
877 *Biologists*. Cambridge University Press, UK.

878 R Core Team (2020). R: A language and environment for statistical computing. R Foundation
879 for Statistical Computing, Vienna, Austria. URL https://www.R-project.org/.

880 Reboita, M.S., M.A. Gan, R.P.D. Rocha and T. Ambrizzi. 2010. Regimes de precipitação na
881 América do Sul: uma revisão bibliográfica. *Revista Brasileira de Meteorologia* 25: 185-
882 204.

883 https://doi.org/10.1590/S0102-77862010000200004

884 Reimann, C., P. Filzmoser, R. Garrett and R. Dutter. 2011. *Statistical Data Analysis Explained:*
885 *Applied Environmental Statistics with R*. John Wiley & Sons, Ltd, New York. 384 pp.

886 Robbins, J.A. and D.N. Edgington. 1975. Determination of recent sedimentation rates in Lake
887 Michigan using Pb-210 and Cs-137. *Geochimica et Cosmochimica Acta* 39: 285–304.
888 https://doi.org/10.1016/0016-7037(75)90198-2

889 Rullkötter, J. 2006. *Organic matter: The driving force for early diagenesis*. In: Schulz, H.D.,
890 Zabel, M. (eds). Marine Geochemistry. Springer, Berlin, Heidelberg.

891 Sikes, E.L., M.E. Uhle, S.D. Nodder and M.E. Howard. 2009. Sources of organic matter in a
892 coastal marine environment: Evidence from n-alkanes and their $\delta^{13}C$ distributions in the
893 Hauraki Gulf, New Zealand. *Marine Chemistry* 113: 149–163.

894 https://doi.org/10.1016/j.marchem.2008.12.003

895 Sutilli, M., T. Combi, M.R.D. Garcia and C.C. Martins. 2020. One century of historical
896 deposition and flux of hydrocarbons in a sediment core from a South Atlantic RAMSAR
897 subtropical estuary. *Science of the Total Environment* 706: 136017.

898 https://doi.org/10.1016/j.scitotenv.2019.136017

899 Timoszczuk, C.T., F.R. dos Santos, L.D. Araújo, S. Taniguchi, R.A. Lourenço, M.M. de
900 Mahiques, P.A.L. Ferreira, R.C.L. Figueira, P.A. Neves, D. Prates and M.C. Bícego.
901 2021. Historical deposition of PAHs in mud depocenters from the Southwestern Atlantic
902 continental shelf: The influence of socio-economic development and coal consumption
903 in the last century. *Environmental Pollution* 284: 117469.

904 https://doi.org/10.1016/j.envpol.2021.117469

905 Vanhoni, F. and F. Mendonça. 2008. O clima do litoral do Estado do Paraná. *Revista Brasileira*
906 *de Climatologia* 3: 49-63.

907 http://dx.doi.org/10.5380/abclima.v3i0.25423

908 Wisnieski, E., L.M.M. Ceschim and C.C. Martins. 2016. Validação de um método analítico
909 para determinação de marcadores orgânicos geoquímicos em amostras de sedimentos
910 marinhos. *Quimica Nova* 39: 1007–1014.

https://doi.org/10.5935/0100-4042.20160103

Yang, G., Z. Song, X. Sun, C. Chen, S. Ke and J. Zhang. 2020. Heavy metals of sediment cores in Dachan Bay and their responses to human activities. *Marine Pollution Bulletin* 150: 110764.

https://doi.org/10.1016/j.marpolbul.2019.110764

Zheng, Y., S. Xie, X. Liu, W. Zhou and P.A. Meyers. 2009. *N*-alkanol ratios as proxies of paleovegetation and paleoclimate in a peat-lacustrine core in southern China since the last deglaciation. *Frontiers of Earth Science in China* 3: 445–451.

https://doi.org/10.1007/s11707-009-0052-2

5 CONSIDERAÇÕES FINAIS

Este estudo investigou a distribuição da MO em sedimentos superficiais e testemunhos sedimentares no Complexo Estuarino de Paranaguá utilizando como ferramentas biogeoquímicas os marcadores moleculares, a composição elementar e isotópica para verificar à influência humana ou natural em relação ao aporte de MO nos estuários. A influência antrópica foi significativa, com atividades agrícolas, turísticas, portuárias e devido a transposição do rio Capivari para geração de energia, contribuindo para o aumento da carga de nutrientes, na mudança da composição da MO e no tamanho de grão dos sedimentos. As mudanças ambientais também desempenharam um papel significativo na hidrodinâmica do estuário controlando a deposição e o retrabalhamento de MO.

A MO sedimentar no CEP é oriunda de uma mistura complexa de material orgânico de origem terrígena e marinha, predominando fontes terrígenas em quase todo o estuário, mas há evidências de influência marinha, especialmente no sedimento superficial e nas camadas superficiais dos testemunhos sedimentares. A variação nas concentrações dos marcadores moleculares após a década de 1950, pode estar associada ao aumento da ocupação humana e as atividades portuárias. Já os esteróis se mostraram proxies promissores para identificar mudanças na contribuição autóctone da MO sedimentar. Isso significa que os esteróis podem ser usados para rastrear a origem da MO sedimentar e identificar impactos humanos.

Em relação aos eventos climáticos (ENSO), não parecem ter causado mudanças perceptíveis na MO sedimentar durante o último século. Isso é indicado pelos valores das razões diagnóstico desprovidas de correlação em todos os testemunhos e pela ausência de alterações substanciais no aporte de material terrígeno para os estuários.

O presente estudo fornece evidências de que a MO sedimentar do Complexo Estuarino de Paranaguá é influenciada por uma variedade de fatores, incluindo atividades humanas, mudanças ambientais que controlam a composição e a entrada de fontes distintas de MO no estuário. O estudo identificou áreas propensas ao acúmulo de nutrientes, o que pode levar a problemas ambientais futuros, como eutrofização e proliferação de algas. Essas informações podem ajudar na tomada de decisões, visando tomar medidas mitigatórias para reduzir a carga de nutrientes no estuário, e orientar políticas públicas, para a conservação desse ecossistema, além de contribuir para o cumprimento dos Objetivos de Desenvolvimento Sustentável.

Este estudo é uma contribuição significativa para o campo da Ciência Ambiental. Ele usa uma abordagem multiproxy para investigar mudanças ambientais em estuários subtropicais, incluindo mudanças climáticas e antrópicas, além de considerar fatores de diferentes escalas, desde características locais até eventos globais.

6 REFERÊNCIAS

Aboul-Kassim, T.A.T. and B.R.T. Simoneit. 1996. Lipid geochemistry of surficial sediments from the coastal environment of Egypt I. Aliphatic hydrocarbons-characterization and sources. *Marine Chemistry* 54: 135–158.https://doi.org/10.1016/0304-4203(95)00098-4

Abreu-Mota, M.A., C.A.M. Barboza, M.C. Bícego and C.C. Martins. 2014. Sedimentary biomarkers along a contamination gradient in a human-impacted sub-estuary in Southern Brazil: A multi-parameter approach based on spatial and seasonal variability. *Chemosphere* 103: 156–163.

Albergaria-Barbosa, A.C.R., Schefuß, E., Taniguchi, S., Santos, P.S., Cunha-Lignon, M., Tassoni-Filho, M., Figueira, R.C.L., Mahiques, M.M., Bícego, M.C., 2023. Characterization of the organic matter produced by Atlantic Rainforest plants and its influence in the surface sediments deposited in a protected subtropical Estuarine–Lagoon system. Regional Studies in Marine Science, 57, 102728

Alfaro, A.C., Thomas, F., Sergent, L., & Duxbury, M. 2006. Identification of trophic interactions within an estuarine food web (northern New Zealand) using fatty acid biomarkers and stable isotopes. *Estuarine, Coastal and Shelf Science*, *70*(1-2), 271-286. https://doi.org/10.1016/j.chemosphere.2013.11.052

Amorim, A.C.B., Scudelari, A.C., Cunha, C., Gonçalves, J.E., 2020. Eventos Extremos de Precipitação no Litoral do Paraná (Baía de Paranaguá). Revista Brasileira de Meteorologia, 35, 563-575.

ANA (Agência Nacional de Águas). 2017. Relatório de Alturas mensais de precipitação. Available in: http://www.sih-web.aguasparana.pr.gov.br/sih-web/gerarRelatorioAlturasAnuaisPrecipitacao.do?action=carregarInterfaceInicial. (in Portuguese). Accessed in March/2017.

Angeli, J.L.F., Trevizani, T.H., Nagai, R.H., Martins, C.C., Figueira, R.C.L., Mahiques, M.M., 2020. Geochemical mapping in a subtropical estuarine system influenced by large grain-shipping terminals: Insights using Metal/Metal ratios and multivariate analysis. Environmental Earth Sciences, 79, 1-15.

Angulo, R.J. 1999. Morphological characterization of the tidal deltas on the coast of the State of Paraná. *Anais da Academia Brasileira de Ciências* 71: 935-960.

Angulo, R.J. 2004. Mapa do Cenozóico do litoral do Estado do Paraná. *Boletim Paranaense de Geociências* 55: 25-42.

Angulo, R.J., C.R. Soares, E. Marone, M.C. Souza, L.L.R. Odreski, M.A. Noernberg. 2006. Paraná. *In*: Muehe, D., Erosão e progradação do litoral brasileiro. Brasília: Ministério do Meio Ambiente, 1, 475.

Azam, F., Fenchel, T., Field, J. G., Gray, J. S., Meyer-Reil, L. A., Thingstad, F. 1983. The ecological role of water-column microbes in the sea. *Marine ecology progress series*, 257-263.

Baldock, J.A., Masiello, C.A., Gelinas, Y., Hedges, J.I., 2004. Cycling and composition of organic matter in terrestrial and marine ecosystems. Marine Chemistry, 92, 39-64.

Barros, G.V., Martinelli, L.A., Novais, T.M.O., Ometto, J.P.H., Zuppi, G.M., 2010. Stable isotopes of bulk organic matter to trace carbon and nitrogen dynamics in an estuarine

ecosystem in Babitonga Bay (Santa Catarina, Brazil). Science of the Total Environment, 408, 2226-2232.

Belligotti, F.M., Carreira, R.S., Soares, M.L.G., 2007. Contribuição ao estudo do aporte de matéria orgânica em sistemas costeiros: hidrocarbonetos biogênicos em folhas de mangue. Geochimica Brasiliensis, 21, 71-85.

Bergamaschi, B.A., Tsamakis, E., Keil, R.G., Eglinton, T.I., Montluçon, D.B., Hedges, J.I., 1997. The effect of grain size and surface area on organic matter, lignin and carbohydrate concentration, and molecular compositions in Peru Margin sediments. Geochimica et Cosmochimica Acta, 61, 1247–1260.

Bern, C.R., K. Walton-Day and D.L. Naftz. 2019. Improved enrichment factor calculations through principal component analysis: Examples from soils near breccia pipe uranium mines, Arizona, USA. *Environmental Pollution* 248: 90–100. https://doi.org/10.1016/j.envpol.2019.01.122

Bet, R., M.C. Bícego and C.C. Martins. 2015. Sedimentary hydrocarbons and sterols in a South Atlantic estuarine/shallow continental shelf transitional environment under oil terminal and grain port influences. *Marine Pollution Bulletin* 95: 183-194. https://doi.org/10.1016/j.marpolbul.2015.04.024

Bianchi, T.S. and E.A. Canuel. 2011. *Chemical biomarkers in aquatic ecosystems*. Chemical Biomarker Applications to Ecology and Paleoecology. Princeton University Press, USA.

Bícego, M.C., Taniguchi, S., Yogui, G.T., Montone, R.C., da Silva, D.A.M., Lourenço, R.A., Martins, C.C., Sasaki, S.T., Pellizari, V.H., Weber, R.R., 2006. Assessment of contamination by polychlorinated biphenyls and aliphatic and aromatic hydrocarbons in sediments of the Santos and São Vicente Estuary System, São Paulo, Brazil. Marine Pollution Bulletin, 52, 1804-1816.

Bigarella, J.J. 2001. Contribuição ao estudo da planície litorânea do Estado do Paraná. *Brazilian Archives of Biology and Technology* Jubilee Volume (1946-2001): 65-110.

Bigarella, J.J., Klein R., Silva, J.L, Passos, E. 2008. A serra do Mar e planície costeira do Paraná: um problema de segurança ambiental e nacional. Florianópolis: UFSC/CFH/GCN.

Birch, G.F. 2011. Indicators of anthropogenic change and biological risk in coastal aquatic environments. Wolanski E, McLusky DS. Treatise on estuarine and coastal science. Ed. Waltham: Academic Press. Publisher: Elsevier, 235-270.

Borchers, H.W., 2019. pracma: Practical Numerical Math Functions. R package version 2.2.5.

Bourbonniere, R.A. and P.A. Meyers. 1996. Anthropogenic influences on hydrocarbon contents of sediments deposited in eastern Lake Ontario since 1800. *Environmental Geology* 28: 22–28.https://doi.org/10.1007/s002540050074

Bouloubassi, I., Saliot, A., 1993. Investigation of anthropogenic and natural organic inputs in estuarine sediments using hydrocarbon markers (NAH, LAB, PAH). Oceanologica Acta, 16, 145–161.

Branco, J.C., 2008. Variação morfológica dos ecossistemas de planície de maré na Foz do Rio Cachoeira, PR. Caminhos de Geografia, 9, 12–23.

Brandini, N., da Costa Machado, E., Sanders, C.J., Cotovicz Jr, L.C., Bernardes, M.C., Knoppers, B.A., 2022. Organic matter processing through an estuarine system:

Evidence from stable isotopes (δ13C and δ15N) and molecular (lignin phenols) signatures. Estuarine, Coastal and Shelf Science, 265, 107707.

Bray, E.E. and E.D. Evans. 1961. Distribution of n-paraffins as a clue to recognition of source beds. *Geochimica et Cosmochima Acta* 22: 2–15. https://doi.org/10.1016/0016-7037(61)90069-2.

Brownawell, B. J., Farrington, J. W. 1986. Biogeochemistry of PCBs in interstitial waters of a coastal marine sediment. *Geochimica et Cosmochimica Acta*, *50*(1), 157-169.

Bueno, C., Brugnoli, E., Bergamino, L., Muniz, P., García-Rodríguez, F., Figueira, R., 2018. Anthropogenic and natural variability in the composition of sedimentar organic matter of the urbanised coastal zone of Montevideo (Río de la Plata). Marine Pollution Bulletin, 126, 197–203.

Cabral, A.C., Stark, J.S., Kolm, H.E., Martins, C.C., 2018. An integrated evaluation of some faecal indicator bacteria (FIB) and chemical markers as potential tools for monitoring sewage contamination in subtropical estuaries. *Environmental Pollution* 235: 739–749. https://doi.org/10.1016/j.envpol.2017.12.109

Cabral, A.C. and C.C. Martins. 2018. Insights about sources, distribution, and degradation of sewage and biogenic molecular markers in surficial sediments and suspended particulate matter from a human-impacted subtropical estuary. *Environmental Pollution* 241: 1071-1081. https://doi.org/10.1016/j.envpol.2018.06.032

Cabral, A.C., M.M. Wilhelm, R.C.L. Figueira and C.C. Martins. 2019. Tracking the historical sewage input in South American subtropical estuarine systems based on faecal sterols and bulk organic matter stable isotopes ($\delta^{13}C$ and $\delta^{15}N$). *Science of the Total Environment* 655: 855-864. https://doi.org/10.1016/j.scitotenv.2018.11.150

Cabral, A.C., A.L.L. Dauner, F.C.B. Xavier, M.R.D. Garcia, M.M. Wilhelm, V.C.G. Santos, S.A. Netto and C.C. Martins. 2020. Tracking the sources of allochthonous organic matter along a subtropical fluvial-estuarine gradient using molecular proxies in view of land uses. *Chemosphere* 251: 126435. https://doi.org/10.1016/j.chemosphere.2020.126435

Cai, W., M.J. McPhaden, A.M. Grimm, R.R. Rodrigues, A.S. Taschetto, R.D. Garreaud, B. Dewitte, G. Poveda, Y-G. Ham, A. Santoso, B. Ng, W. Anderson, G. Wang, T. Geng, H-S. Jo, J.A. Marengo, L.M. Alves, M. Osman, , S. Li, L. Wu, C. Karamperidou, K. Takahashi and C. Vera. 2020. Climate impacts of the El Niño–Southern Oscillation on South America. *Nature Reviews Earth & Environment* 1: 215–231. https://doi.org/10.1038/s43017-020-0040-3

Calijuri, M. D. C., Cunha, D. G. F., Moccellin, J. 2013. Fundamentos ecológicos e ciclos naturais. *Engenharia Ambiental: Conceitos, Tecnologia e Gestão. São Paulo: Elsevier Editora Ltda.*

Camargo, M.G., 2006. Sysgran: um sistema de código aberto para análises granulométricas. Revista Brasileira de Geofísica, 2, 371–378.

Camilloni, I.A. and V.R. Barros. 2000. The Parana River response to El Nino 1982 – 83 and 1997 – 98 Events. *Journal of Hydrometeorology* 1: 412–430. https://doi.org/10.1175/1525-7541(2000)001<0412:TPRRTE>2.0.CO;2

Canuel, E.A. and A.K. Hardison. 2016. Sources, ages, and alteration of organic matter in estuaries. *Annual Review of Marine Science* 8: 409–434. https://doi.org/10.1146/annurev-marine-122414-034058

Cardoso, F.D., A.L.L.Dauner and C.C. Martins. 2016. A critical and comparative appraisal of polycyclic aromatic hydrocarbons in sediments and suspended particulate material from a large South American subtropical estuary. Environmental Pollution 214: 219–229. http://dx.doi.org/10.1016/j.envpol.2016.04.011

Carreira, R.S., A.L. Wagener, J.W. Readman, T.W. Fileman, S.A. Macko, A. Veiga. 2002. Changes in the sedimentary organic carbon pool of a fertilized tropical estuary, Guanabara Bay, Brazil: an elemental, isotopic and molecular marker approach. *Marine Chemistry* 79: 207-227. https://doi.org/10.1016/S0304-4203(02)00065-8

Carreira, R.S., Cordeiro, L.G.M.S., Bernardes, M.C., Hatje, V., 2016. Distribution and characterization of organic matter using lipid biomarkers: A case study in a pristine tropical bay in NE Brazil. Estuarine, Coastal and Shelf Science, 168, 1–9.

Cattani, P.E., Lamour, M.R., 2016. Considerations regarding sedimentation rates along the EW axis of the Paranaguá Estuarine Complex, Brazil: a bathymetric approach. Journal of Coastal Research, 32, 619-628.

Ceccopieri, M., Scofield, A.L., Almeida, L., Araújo, M.P., Hamacher, C., Farias, C.O., Soares, M.L.G., Wagner, A.L., 2021. Carbon isotopic composition of leaf wax n-alkanes in mangrove plants along a latitudinal gradient in Brazil. Organic Geochemistry, 161, 104299.

Chemin, M. and C.M.S. Abrahão. 2014. Territorial integration of the coast of Paraná State (Brazil): Transport, resort development and patrimonialization in the formation and dynamics of tourist spaces. RA'E GA – O Espaço Geográfico em Análise 32: 212–239.

Chevalier, N., Savoye, N., Dubois, S., Lama, M.L., David, V., Lecroart, P., Menach, K.L., Budzinski, H.J., 2015. Precise indices based on n-alkane distribution for quantifying sources of sedimentary organic matter in coastal systems. Organic Geochemistry, 88, 69–77.

Chikaraishi, Y. 2013. $^{13}C/^{12}C$ signatures in plants and algae. Treatise on Geochemistry: 2nd Edition. Elsevier Ltd.

Combi, T., S. Taniguchi, R.C.L. Figueira, M.M., Mahiques and C.C. Martins. 2013. Spatial distribution and historical input of polychlorinated biphenyls (PCBs) and organochlorine pesticides (OCPs) in sediments from a subtropical estuary (Guaratuba Bay, SW Atlantic). *Marine Pollution Bulletin* 70, 247–252. https://doi.org/10.1016/j.marpolbul.2013.02.022

Costa, E.S., C.F. Grilo, G.A. Wolff, A. Thompson, R.C.L. Figueira, F. Sá and R.R. Neto. 2016. Geochemical records in sediments of a tropical estuary (Southeastern coast of Brazil). *Regional Studies in Marine Science* 6: 49–61. https://doi.org/10.1016/j.rsma.2016.03.008

Cullen, P. 2008. Water in the landscape: The coupling of aquatic ecosystems and their catchments. *Managing and Designing Landscapes for Conservation: Moving from Perspectives to Principles*, 458.

Dan, S.F., Liu, S.M., Yang, B., 2020. Geochemical fractionation, potential bioavailability, and ecological risk of phosphorus in surface sediments of the Cross River estuary system and adjacent shelf, South East Nigeria (West Africa). Journal of Marine Systems, 201, 103244.

Daniel, M.H., Montebelo, A.A., Bernardes, M.C., Ometto, J.P., Camargo, P.B.D., Krusche, A.V., Ballester, M.V., Victoria, R.L., Martinelli, L.A., 2002. Effects of urban sewage

on dissolved oxygen, dissolved inorganic and organic carbon, and electrical conductivity of small streams along a gradient of urbanization in the Piracicaba River basin. Water, Air, and Soil Pollution, 136, 189-206.

Das, S.K., Routh, J., Roychoudhury, A.N., Klump, J.V., 2008. Elemental (C, N, H and P) and stable isotope ($\delta^{15}N$ and $\delta^{13}C$) signatures in sediments from Zeekoevlei, South Africa: a record of human intervention in the lake. Journal of Paleolimnology, 39, 349–360.

Dauner, A.L.L. and C.C. Martins. 2015. Spatial and temporal distribution of aliphatic hydrocarbons and linear alkylbenzenes in the particulate phase from a subtropical estuary (Guaratuba Bay, SW Atlantic) under seasonal population fluctuation. *Science of the Total Environment* 536: 750–760. https://doi.org/10.1016/j.scitotenv.2015.07.091

Dauner, A.L.L., T.H. Dias, F.K. Ishii, B.G. Libardoni, R.A. Parizzi and C.C. Martins. 2018. Ecological risk assessment of sedimentary hydrocarbons in a subtropical estuary as tools to select priority areas for environmental management. *Journal of Environmental Management* 223: 417–425. https://doi.org/10.1016/j.jenvman.2018.06.024

Dauner, A.L.L., Mollenhauer, G., Bícego, M.C., de Souza, M.M., Nagai, R.H., Figueira, R.C. L., Mahiques, M.M., Souza, S.H.M., Martins, C.C., 2019. Multi-proxy reconstruction of sea surface and subsurface temperatures in the western South Atlantic over the last~ 75 kyr. Quaternary Science Reviews, 215, 22-34.

De Leeuw, J.W., Largeau, C., 1993. A review of macromolecular organic compounds that comprise living organisms and their role in kerogen, coal, and petroleum formation. In: Organic Geochemistry, 23-72.

Defesa Civil do Paraná. 2011. Webpage: https://www.defesacivil.pr.gov.br/sites/defesa-civil/arquivos_restritos/files/documento/2019-05/desastre_de_2011_-_aguas_de_marco.pdf. Accessed on March 05, 2023.

Duarte, C. M., J.J. Middelburg and N. Caraco. 2005. Major role of marine vegetation on the oceanic carbon cycle. *Biogeosciences* 2: 1-8. https://doi.org/10.5194/bg-2-1-2005

Didyk, B. M., Simoneit, B. R. T., Brassell, S. T., Eglinton, G. 1978. Organic geochemical indicators of palaeoenvironmental conditions of sedimentation. *Nature*, *272*(5650), 216-222.

Eadie, B. J., Chambers, R. L., Gardner, W. S., Bell, G. L. 1984. Sediment trap studies in Lake Michigan: Resuspension and chemical fluxes in the southern basin. *Journal of Great Lakes Research*, *10*(3), 307-321.

Eganhouse, R.P., 1997. Molecular markers in environmental geochemistry. American Chemical Society Symposium Series 671.

Eglinton, G. and R.J. Hamilton. 1967. Leaf epicuticular waxes. *Science* 156: 1322–1335. https://doi.org/10.1126/science.156.3780.1322

Eglinton, T. I., Eglinton, G. 2008. Molecular proxies for paleoclimatology. *Earth and Planetary Science Letters*, *275*(1-2), 1-16.

Egres, A.G., C.C. Martins, V.M. Oliveira, P.C. Lana. 2012. Effects of an experimental in situ diesel oil spill on the benthic community of unvegetated tidal flats in a subtropical estuary (Paranaguá Bay, Brazil). *Marine Pollution Bulletin* 64: 2681-2691. https://doi.org/10.1016/j.marpolbul.2012.10.007

Farrington, J.W., Frew, N.M., Geshwend, P.M., Tripp, R.W., 1977. Hydrocarbons in cores of northwestern Atlantic coastal and continental margin sediments. Estuarine and Coastal Marine Science, 5, 793–808

Ficken, K.J., B. Li, D.L. Swain and G. Eglinton. 2000. An *n*-alkane proxy for the sedimentary input of submerged/floating freshwater aquatic macrophytes. *Organic Geochemistry* 31: 745–749. https://doi.org/10.1016/S0146-6380(00)00081-4

Filimonova, V., Goncalves, F., Marques, J. C., De Troch, M., Goncalves, A. M. 2016. Fatty acid profiling as bioindicator of chemical stress in marine organisms: a review. *Ecological indicators*, *67*, 657-672.

Freeman, K. H., Pancost, R. D. 2014. Biomarkers for terrestrial plants and climate. In *Organic Geochemistry* (pp. 395-416). Elsevier Inc..

Folk, R. and W. Ward. 1957. Brazos river bar: A study in the significance of grain size parameters. *Journal of Sedimentary Petrology* 27: 3–27. https://doi.org/10.1306/74D70646-2B21-11D7-8648000102C1865D

Freeman, K.H. and R.D. Pancost. 2013. *Biomarkers for terrestrial plants and climate*. Treatise on Geochemistry: 2nd Edition. Elsevier Ltd.

Gabriel, K.R. 1971. The biplot graphic display of matrices with application to principal component analysis. *Biometrika* 58: 453–467.https://doi.org/10.1093/biomet/58.3.453

Garcia, M.R., Cattani, A.P., Lana, P.C., Figueira, R.C.L., Martins, C.C., 2019. Petroleum biomarkers as tracers of low-level chronic oil contamination of coastal environments: A systematic approach in a subtropical mangrove. Environmental Pollution, 249, 1060-1070.

Garcia, M.R., Martins, C.C., 2021. A systematic evaluation of polycyclic aromatic hydrocarbons in South Atlantic subtropical mangrove wetlands under a coastal zone development scenario. Journal of Environmental Management, 277, 111421.

Gianesella, S.M.F., Saldanha-Corrêa, F.M.P. 2013. Oceanos e áreas costeiras. Engenharia Ambiental: Conceitos, Tecnologia e Gestão. São Paulo: Elsevier Editora Ltda.

Grimm, A.M., S.E. Ferraz and J. Gomes. 1998. Precipitation anomalies in southern Brazil associated with El Niño and La Niña events. *Journal of Climate* 11: 2863-2880. https://doi.org/10.1175/1520-0442(1998)011<2863:PAISBA>2.0.CO;2

Grimm, A.M. and R.G. Tedeschi. 2009. ENSO and extreme rainfall events in South America. *Journal of Climate* 22: 1589-1609. https://doi.org/10.1175/2008JCLI2429.1

Harwood, J. L., Russell, N. J. 1984. Lipids in plants and microbes Allen and Unwin.

Hedges, J.I., Keil, R.G., 1999. Organic geochemical perspectives on estuarine processes: sorption reactions and consequences. Marine Chemistry, 65, 55–65.

Hirst, A. J. 2004. Broad-scale environmental gradients among estuarine benthic macrofaunal assemblages of south-eastern Australia: implications for monitoring estuaries. Marine and Freshwater Research, 55(1), 79-92.

Hu, L., Z. Guo, J. Feng, Z. Yang and M. Fang. 2009. Distributions and sources of bulk organic matter and aliphatic hydrocarbons in surface sediments of the Bohai Sea, China. Marine Chemistry 113: 197–211. https://doi.org/10.1016/j.marchem.2009.02.001

IBGE (Instituto Brasileiro de Geografia e Estatística), 2017. Censos demográficos de 1872 - 2010. Available in: http://biblioteca.ibge.gov.br. (in Portuguese). Accessed in

February/2017.

IBGE (Instituto Brasileiro de Geografia e estatística). 2023. Densidade populacional estimada. Disponível em: https://cidades.ibge.gov.br. Acesso em: Out/2023.

IPARDES (Instituto Paranaense de Desenvolvimento Econômico e Social). 2001. Zoneamento da Área de Proteção Ambiental de Guaraqueçaba. Curitiba: IPARDES, p. 150.

Jafarabadi, A.R., M. Dashtbozorg, A.R. Bakhtiari, M. Maisano and T. Cappello. 2019. Geochemical imprints of occurrence, vertical distribution and sources of aliphatic hydrocarbons, aliphatic ketones, hopanes and steranes in sediment cores from ten Iranian Coral Islands, Persian Gulf. *Marine Pollution Bulletin* 144: 287–298. https://doi.org/10.1016/j.marpolbul.2019.05.014

Jolliffe, I.T. and J. Cadima. 2016. Principal component analysis: A review and recent developments. *Philosophical Transactions of The Royal Society: A Mathematical Physical and Engineering Sciences* 374: 20150202. https://doi.org/10.1098/rsta.2015.0202

Khan, N.S., Vane, C.H., Horton, B.P., Hillier, C., Riding, J.B., Kendrick, C.P., 2015. The application of $\delta^{13}C$, TOC and C/N geochemistry to reconstruct Holocene relative sea levels and paleoenvironments in the Thames Estuary, UK. Journal of Quaternary Science, 30, 417–433.

Killops, S.D., Killops, V.J. 1993. An introduction to organic geochemistry. New York: Longman Scientific &Technical,. 265 p..

Killops, V. J., Killops, S. D. 2005. Introduction to organic geochemistry. Blackwell Science Ltda, p.406.

Kowalewska-Kalkowska, H., Marks, R. 2015. Estuary, estuarine hydrodynamics. Encykl. Mar. Geosci, 1, 235-238.

Kuypers, M.M.M., Marchant, H.K., Kartal, B., 2018. The microbial nitrogen-cycling network. Nature Reviews Microbiology, 16, 263-276.

Lacey, J.H., M.J. Leng, C.H. Vane, A.D. Radbourne, H. Yang and D.B. Ryves. 2018. Assessing human impact on Rostherne Mere, UK, using the geochemistry of organic matter. *Anthropocene* 21: 52-65. https://doi.org/10.1016/j.ancene.2018.02.002

Lamour, M.R., Soares, C.R., Carrilho, J.C., 2004. Mapas de parâmetros texturais de sedimentos de fundo do complexo estuarino de Paranaguá PR. Boletim Paranaense de Geociências, 55, 77-82.

Lamour, M.R. and C.R. Soares. 2007. *Histórico das atividades de dragagem e taxas de assoreamento nos canais de navegação aos portos costeiros paranaenses*. In: Dragagens portuárias no Brasil : Licenciamento e monitoramento ambiental. 312p.

Lana, P.C., E. Marone, R.M. Lopes and E.C. Machado. 2001. *The Subtropical Estuarine Complex of Paranaguá Bay, Brazil*. In: Seeliger U., Kjerfve B. (eds) Coastal Marine Ecosystems of Latin America. Ecological Studies (Analysis and Synthesis), vol 144. Springer, Berlin, Heidelberg.

Leonard, L.L. and M.E. Luther. 1995. Flow hydrodynamics in tidal marsh canopies. *Limnology and Oceanography* 40: 1474-1484. https://doi.org/10.4319/lo.1995.40.8.1474

Lessa, G.C., Santos, F.M., Souza Filho, P.W., Corrêa-Gomes, L.C., 2018. Brazilian estuaries: A geomorphologic and oceanographic perspective. In: Brazilian Estuaries. Springer, Cham. pp. 1-37.

Libes, S. 2011. Introduction to marine biogeochemistry. Academic Press.

Liu, H., Liu, W. 2016. n-Alkane distributions and concentrations in algae, submerged plants and terrestrial plants from the Qinghai-Tibetan Plateau. Organic geochemistry, 99, 10-22.

Logan, G.A., C.J. Smiley and G. Eglinton. 1995. Preservation of fossil leaf waxes in association with their source tissues, Clarkia, Northern Idaho, USA. *Geochimica et Cosmochimica Acta* 59: 751–763. https://doi.org/10.1016/0016-7037(94)00362-P

Mahiques M. M., Fukumoto M. M., Silveira I. C. A., Figueira R. C. L., Bícego M. C., Lourenço R. A., et al. (2007). Sedimentary changes on the southeastern Brazilian upper slope during the last 35,000 years. Anais da Academia Brasileira de Ciências 79, 171–181.

Manahan, S.E. 2013. Química Ambiental. 9.ed. Porto Alegre: Bookman, 912 p.

Mantovanelli, A., E. Marone, E.T. da Silva, L.F. Lautert, M.S. Klingenfuss, V.P. Prata Jr., M.A. Noernberg, B.A. Knoppers and R.J. Angulo. 2004. Combined tidal velocity and duration asymmetries as a determinant of water transport and residual flow in Paranaguá Bay estuary. *Estuarine, Coastal and Shelf Science* 59: 523–537. https://doi.org/10.1016/j.ecss.2003.09.001

Marone, E., E.C. Machado, R.M. Lopes and E.T. Silva. 2005. Land-ocean fluxes in the Paranaguá Bay Estuarine System, southern Brazil. *Brazilian Journal of Oceanography* 53: 169–181

Marone, E., M.A. Noernberg, I. Dos Santos, L.F. Lautert, O.R. Andreoli, H. Buba and H.D. Fill. 2006. Hydrodynamic of Guaratuba Bay, PR, Brazil. *Journal of Coastal Research* 38: 1879–1883. http://www.jstor.org/stable/25743087.

Martins, C.C., M.C. Bícego, M.M. Mahiques, R.C.L. Figueira, M.G. Tessler, and R.C. Montone. 2010. Depositional history of sedimentary linear alkylbenzenes (LABs) in a large South American industrial coastal area (Santos Estuary, Southeastern Brazil). *Environmental Pollution* 158: 3355-3364. https://doi.org/10.1016/j.envpol.2010.07.040

Martins, C.C., Bícego, M.C., Figueira, R.C., Angelli, J.L.F., Combi, T., Gallice, W.C., Mansur, E.N., Rocha, M.L., Wisnieski, E., Ceschim, L.M.M., Ribeiro, A.P., 2012. Multi-molecular markers and metals as tracers of organic matter inputs and contamination status from an Environmental Protection Area in the SW Atlantic (Laranjeiras Bay, Brazil). Science of the Total Environment,417, 158-168.

Martins, C. C., Braun, J. A., Seyffert, B. H., Machado, E. C., Fillmann, G. 2010. Anthropogenic organic matter inputs indicated by sedimentary fecal steroids in a large South American tropical estuary (Paranaguá estuarine system, Brazil). *Marine Pollution Bulletin*, *60*(11), 2137-2143.

Martins, C.C., Seyffert, B.H., Braun, J.A., Fillmann, G., 2011. Input of organic matter in a large South American tropical estuary (Paranaguá Estuarine System, Brazil) indicated by sedimentary sterols and multivariate statistical approach. Journal of the Brazilian Chemical Society, 22, 1585-1594.

Martins, C.C., M.E. Doumer, W.C. Gallice, A.L.L. Dauner, A.C. Cabral, F.D. Cardoso, N.N. Dolci, L.M. Camargo, P.A.L Ferreira, R.C.L. Figueira and A.S. Mangrich. 2015. Coupling spectroscopic and chromatographic techniques for evaluation of the depositional history of hydrocarbons in a subtropical estuary. *Environmental Pollution* 205: 403–414. https://doi.org/10.1016/j.envpol.2015.07.016.

Martins, C. C., Adams, J. K., Yang, H., Shchetnikov, A. A., Di Domenico, M., Rose, N. L., & Mackay, A. W. 2023. Earthquake, floods and changing land use history: A 200-year overview of environmental changes in Selenga River basin as indicated by n-alkanes and related proxies in sediments from shallow lakes. *Science of The Total Environment*, *873*, 162245.

Mcleod, E., Chmura, G.L., Bouillon, S., Salm, R., Björk, M., Duarte, C.M., Lovelock, C.E., Schlesinger, W.H., Silliman, B.R., 2011. A blueprint for blue carbon: toward an improved understanding of the role of vegetated coastal habitats in sequestering CO_2. Frontiers in Ecology and the Environment, 9, 552-560.

Mertz, C., Kleber, M., Jahn, R., 2005. Soil organic matter stabilization pathways in clay sub-fractions from a time series of fertilizer deprivation. Organic. Geochemistry 36, 1311–1322.

Meyers, P. A. 1994. Preservation of elemental and isotopic source identification of sedimentary organic matter. *Chemical geology*, *114*(3-4), 289-302.

Meyers, P.A. 1997. Organic geochemical proxies of paleoceanographic, plaeolimnologic, and plaeoclimatic processes. *Organic Geochemistry* 27: 213–250. https://doi.org/10.1016/S0146-6380(97)00049-1

Meyers, P. A. 2003. Applications of organic geochemistry to paleolimnological reconstructions: a summary of examples from the Laurentian Great Lakes. *Organic geochemistry*, *34*(2), 261-289.

Meyers, P. A., Eadie, B. J. 1993. Sources, degradation and recycling of organic matter associated with sinking particles in Lake Michigan. *Organic Geochemistry*, *20*(1), 47-56.

Meyers, P. A., Ishiwatari, R. 1993. Lacustrine organic geochemistry—an overview of indicators of organic matter sources and diagenesis in lake sediments. *Organic geochemistry*, *20*(7), 867-900.

Meyers, P.A., Teranes, J.L., 2002. Sediment organic matter. In: Tracking environmental change using lake sediments. Springer, Dordrecht. pp. 239-269.

Middelburg, J.J., Herman, P.M.J., 2007. Organic matter processing in tidal estuaries. Marine Chemistry 106, 127–147.

Middelburg, J.J., J. Nieuwenhuize, R.K. Lubberts and O. van de Plassche. 1997. Organic carbon isotope systematics of coastal marshes. *Estuarine, Coastal and Shelf Science* 45: 681-687. https://doi.org/10.1006/ecss.1997.0247

Middelburg, J.J., Nieuwenhuize, J., 1998. Carbon and nitrogen stable isotopes in suspended matter and sediments from the Schelde Estuary. Marine Chemistry, 60, 217-225.

Mudge, S.M. and D.G. Lintern. 1999. Comparison of sterol biomarkers for sewage with other measures in Victoria Harbour, B.C., Canada. *Estuarine, Coastal and Shelf Science* 48: 27–38. https://doi.org/10.1006/ecss.1999.0406

Noernberg, M. A., Angelotti, R., Caldeira, G. A., & Ribeiro de Sousa, A. F. 2008. Determinação da sensibilidade do litoral paranaense à contaminação por óleo. Brazilian Journal of Aquatic Science and Technology, 12(2), 49-59.

Nagai R. H., Sousa S. H. M., Lourenço R. A., Bícego M. C., Mahiques M. M. (2010). Paleoproductivity changes during the late quaternary in the southeastern Brazilian upper

continental margin of the southwestern Atlantic. Brazilian Journal of Oceanography, 58, 31–41.

Netto, S.A., Lana, P.C., 1997. Influence of *Spartina alterniflora* on superficial sediment characteristics of tidal flats in Paranagua Bay (South-eastern Brazil). Estuarine, Coastal and Shelf Science, 44, 641-648.

Neto, J. B., Ponzi, V. R. A., Sichel, S. E. 2004. Introdução à geologia marinha. Editora Interciência, 279.

Odum, E.P., Barrett, G.W. 2015. Fundamentos de ecologia. São Paulo: Cengage Learning, p. 611.

Paladino, I.M., Mengatto, M.F., Mahiques, M.M., Noernberg, M.A., Nagai, R.H., 2022. End-member modeling and sediment trend analysis as tools for sedimentary processes inference in a subtropical estuary. Estuarine, Coastal and Shelf Science, 108126.

Patchineelam, S.M., Soares, C.R., Calliari, L.J. 2008. Assoreamento, aterros e dragagens. *Poluição Marinha.* Rio de Janeiro: Editora Interciência.

Paula, E.V., Paz, O.L.S., Pai, M.O., Oliveira, M., 2021. Sustaining port activities through nature conservation: the case of Paraná Coast in Southern Brazil. In: Practices in Regional Science and Sustainable Regional Development. https://doi.org/10.1007/978-981-16-2221-2_720

Peñuelas, J., Poulter, B., Sardans, J., Ciais, P., Van Der Velde, M., Bopp, L., Boucher, O., Godderis, Y., Hinsinger, P., Lusia, J., Nardin, E., Vicca, S., Obersteiner, M., Janssens, I.A., 2013. Human-induced nitrogen–phosphorus imbalances alter natural and managed ecosystems across the globe. Nature Communications, 4, 1-10.

Pérez-Fernández, B., Viñas, L., Besada, V. 2020. Concentrations of organic and inorganic pollutants in four Iberian estuaries, North Eastern Atlantic. Study of benchmark values estimation. *Marine Chemistry*, *224*, 103828.

Peters, K. E., Moldowan, J. M. 1993. The biomarker guide: interpreting molecular fossils in petroleum and ancient sediments.

Peters, K.E., C.C. Walters and J.M. Moldowan. 2005. *The biomarker guide: biomarkers and isotopes in the environment and human history*. Cambridge Universty Press, UK.

Pierri, N., R.J. Angulo, M.C. Souza and M. Kim. 2006. A ocupação e o uso do solo no litoral paranaense: condicionantes, conflitos e tendências. *Desenvolvimento e Meio Ambiente* 13: 137–167.

Pietzsch, R.; S.R. Patchineelam and J.P.M. Torres. 2010. Polycyclic aromatic hydrocarbons in recent sediments from a subtropical estuary in Brazil. *Marine Chemistry* 118: 56–66.

https://doi.org/10.1016/j.marchem.2009.10.004

Piola, R.F., Moore, S.K., Suthers, I.M., 2006. Carbon and nitrogen stable isotope analysis of three types of oyster tissue in an impacted estuary. Estuarine, Coastal and Shelf Science, 66, 255-266.

Pires, P.T.L., A.L. Zilli and C.T. Blum. 2005. *Atlas da Floresta Atlantica no Paraná.* 104p.

Pomeroy, L. R., WILLIAMS, P. J., Azam, F., Hobbie, J. E. 2007. The microbial loop. *Oceanography*, *20*(2), 28-33.

Queen, J.P., G.P. Quinn and M.J. Keough. 2002. *Experimental Design and Data Analysis for Biologists*. Cambridge University Press, UK.

R Core Team (2020). R: A language and environment for statistical computing. R Foundation for Statistical Computing, Vienna, Austria. URL https://www.R-project.org/.

Readman, J.W., Fillmann, G., Tolosa, I., Bartocci, J., Villeneuve, J.-P., Catinni, C., Mee, L.D., 2002. Petroleum and PAH contamination of the Black Sea. Marine Pollution Bulletin, 44, 48–62.

Reboita, M.S., M.A. Gan, R.P.D. Rocha and T. Ambrizzi. 2010. Regimes de precipitação na América do Sul: uma revisão bibliográfica. *Revista Brasileira de Meteorologia* 25: 185-204. https://doi.org/10.1590/S0102-77862010000200004

Reimann, C., P. Filzmoser, R. Garrett and R. Dutter. 2011. *Statistical Data Analysis Explained: Applied Environmental Statistics with R*. John Wiley & Sons, Ltd, New York. 384 pp.

Rivera-Monroy, V.H., Lee, S.Y., Kristensen, E., Twilley, R.R., 2017. Mangrove Ecosystems: A Global Biogeographic Perspective. Springer.

Robbins, J.A. and D.N. Edgington. 1975. Determination of recent sedimentation rates in Lake Michigan using Pb-210 and Cs-137. *Geochimica et Cosmochimica Acta* 39: 285–304. https://doi.org/10.1016/0016-7037(75)90198-2

Rullkötter, J. 2006. *Organic matter: The driving force for early diagenesis*. In: Schulz, H.D., Zabel, M. (eds). Marine Geochemistry. Springer, Berlin, Heidelberg.

Sachse, D., Radke, J., Gleixner, G., 2006. δD values of individual *n*-alkanes from terrestrial plants along a climatic gradient - implications for the sedimentary biomarker record. Organic Geochemistry, 37, 469–483.

Savage, C., Leavitt, P.R., Elmgren, R., 2010. Effects of land use, urbanization, and climate variability on coastal eutrophication in the Baltic Sea. Limnology and Oceanography, 55, 1033–1046.

Schulz, H.D.; Zabel, M. 2006. Marine Geochemistry. 2.ed. Berlin: Springer, p. 574.

Schwarzbauer, J., & Jovančićević, B. 2016. From biomolecules to chemofossils. Springer International Publishing.

Sikes, E.L., M.E. Uhle, S.D. Nodder and M.E. Howard. 2009. Sources of organic matter in a coastal marine environment: Evidence from n-alkanes and their $\delta^{13}C$ distributions in the Hauraki Gulf, New Zealand. *Marine Chemistry* 113: 149–163. https://doi.org/10.1016/j.marchem.2008.12.003

Soares, C. R., & Barcelos, J. H. 1995. Considerações sobre os sedimentos de fundo das baías de Laranjeiras e de Guaraqueçaba, Complexo Estuarino da Baía de Paranaguá (Paraná, Brasil). Boletim Paranaense de Geociências, 43, 41-60.

Suguio, K. 2003. Geologia sedimentar. Editora Blucher.

Sutilli, M., T. Combi, M.R.D. Garcia and C.C. Martins. 2020. One century of historical deposition and flux of hydrocarbons in a sediment core from a South Atlantic RAMSAR subtropical estuary. *Science of the Total Environment* 706: 136017. https://doi.org/10.1016/j.scitotenv.2019.136017

TCP (Terminal de Contêineres de Paranaguá). 2020. TCP quebra recordes de movimentações. Disponível em: <https://www.tcp.com.br/tcp-quebra-recordes-de-movimentacoes/>. Acesso em: Out/2020.

Timoszczuk, C.T., F.R. dos Santos, L.D. Araújo, S. Taniguchi, R.A. Lourenço, M.M. de Mahiques, P.A.L. Ferreira, R.C.L. Figueira, P.A. Neves, D. Prates and M.C. Bícego.

2021. Historical deposition of PAHs in mud depocenters from the Southwestern Atlantic continental shelf: The influence of socio-economic development and coal consumption in the last century. *Environmental Pollution* 284: 117469. https://doi.org/10.1016/j.envpol.2021.117469

Tremblay, L., & Gagné, J. P. 2009. Organic matter distribution and reactivity in the waters of a large estuarine system. Marine Chemistry, 116(1-4), 1-12.

Tolosa, I., Mesa-Albernas, M., Alonso-Hernandez, C.M., 2009. Inputs and sources of hydrocarbons in sediments from Cienfuegos bay, Cuba. Marine Pollution Bulletin, 58, 1624-1634.

UNESCO (United Nations Educational Scientific and Cultural Organization). 1999. Convention concerning the protection of the world cultural and natural heritage: Atlantic forest south/ east Brazil. Brazil, March, p. 257.

USEPA. (1996). Method 3050B. Acid digestion of sediments, sludges and soil. Revision 2, December, 1996.

USEPA. (2007). SW-846 test methods for evaluating solid waste, physical/chemical methods, method 6010C: Inductively coupled plasma-atomic emission spectrometry. Revision 3, February, 2007.

Vaalgamaa, S., Sonninen, E., Korhola, A., Weckström, K. 2013. Identifying recent sources of organic matter enrichment and eutrophication trends at coastal sites using stable nitrogen and carbon isotope ratios in sediment cores. Journal of Paleolimnology, 50, 191-206.

Vanhoni, F. and F. Mendonça. 2008. O clima do litoral do Estado do Paraná. *Revista Brasileira de Climatologia* 3: 49-63. http://dx.doi.org/10.5380/abclima.v3i0.25423

Vieira Filho, J.E.R., 2016. Expansão da fronteira agrícola no Brasil: desafios e perspectivas. IPEA. p. 1-28.

Villeneuve, J.P., de Mora, S.J., Cattini, C., Carvalho, F.P., 2000. Determination of organochlorinated compounds and petroleum hydrocarbons in sediment sample IAEA-408. Results from a world-wide intercalibration exercise. Journal of Environmental Monitoring, 2, 524-528.

Volkman, J.K., Holdsworth, D.G., Neill, G.P., Bavor Jr, H.J., 1992. Identification of natural, anthropogenic and petroleum hydrocarbons in aquatic sediments. Science of the Total Environment, 112, 203-219.

Volkman, J. K., Smittenberg, R. H. 2017. Lipid biomarkers as organic geochemical proxies for the paleoenvironmental reconstruction of estuarine environments. *Applications of paleoenvironmental techniques in estuarine studies*, 173-212.

Volkman, J. K. 2006. Lipid markers for marine organic matter. *Marine organic matter: biomarkers, isotopes and DNA*, 27-70.

Volkman, J. K., Barrett, S. M., Blackburn, S. I., Mansour, M. P., Sikes, E. L., Gelin, F. 1998. Microalgal biomarkers: a review of recent research developments. *Organic Geochemistry*, *29*(5-7), 1163-1179.

Voss, M., Emeis, K.-C., Hille, S., Neumann, T., Dippner, J.W., 2005. Nitrogen cycle of the Baltic Sea from an isotopic perspective. Global Biogeochemical Cycles, 19, 1–15, GB3001.

Wilhelm, M.M., Cabral, A.C., Dauner, A.L.L., Garcia, M.R., Figueira, R.C.L., Martins, C.C., 2023. Variability of sedimentary organic matter in subtropical estuarine systems due to anthropogenic and climatic events. Environmental Earth Sciences, 82, 22.

Wisnieski, E., L.M.M. Ceschim and C.C. Martins. 2016. Validação de um método analítico para determinação de marcadores orgânicos geoquímicos em amostras de sedimentos marinhos. *Quimica Nova* 39: 1007–1014. https://doi.org/10.5935/0100-4042.20160103

Yang, G., Z. Song, X. Sun, C. Chen, S. Ke and J. Zhang. 2020. Heavy metals of sediment cores in Dachan Bay and their responses to human activities. *Marine Pollution Bulletin* 150: 110764. https://doi.org/10.1016/j.marpolbul.2019.110764

Zhang, S., Liang, C., Xian, W., 2020. Spatial and temporal distributions of terrestrial and marine organic matter in the surface sediments of the Yangtze River estuary. Continental Shelf Research, 203, 104158.

Zheng, Y., S. Xie, X. Liu, W. Zhou and P.A. Meyers. 2009. *N*-alkanol ratios as proxies of paleovegetation and paleoclimate in a peat-lacustrine core in southern China since the last deglaciation. *Frontiers of Earth Science in China* 3: 445–451. https://doi.org/10.1007/s11707-009-0052-2

APÊNDICE 1 – MATERIAL SUPLEMENTAR DO CAPÍTULO I

Reagents and analytical contamination control

Solvents as ethanol (EtOH), hexanes (95% n-hexane), methanol (MeOH) and dichloromethane (DCM), with a high degree of purity (all with 99.9% minimum purity) were supplied by Riedel-de Haën/Honeywell®. The adsorbents as active aluminium oxide 90 (Al2O3 – 0.063-0.200 mm), silica gel (SiO2 – silica gel 60; 0.063 – 0.200 mm) and anhydrous sodium sulfate (Na2SO4) were supplied by Merck® with a purity of 99.9%.

The alumina and silica gel adsorbents were calcined in a high temperature furnace (at 400 °C) for 4 hs and stored in a vacuum desiccator until use. Copper was used to eliminate possible interferences in the instrumental analysis caused by sulphur, and it was treated for 30 minutes with HCl solution (2 mol L-1, prepared from a 37% P.A. solution – ACS, F. Maia), rinsed with distilled water, immersed in EtOH and, finally, in a mixture of MeOH: DCM (1:9; v:v). The KOH solution was prepared from solid KOH (85.0% P.A. – LabSynth), and H2O2 was 35% P.A (obtained from Exodus Cientifica).

All labiratory glasses used was adequately washed before used, after to have been immersed in a alkaline detergent Extran® (Merck) solution for approximately 12 hours. After drying in an oven at around 150 °C, the glasses was calcined at 400 °C for 4 hs. The volumetric material was dried at room temperature and washed three times with the solvents listed above at the time of use to minimize contamination by organic compounds.

The n-alkanes and isoprenoids (n-C10 to n-C40, pristane and phytane; DRH-008S-R2, 98.7-100.0% purity) were obtained from AccuStandard®. The n-alkanols n-C12-OH to n-C18-OH were obtained from Fluka® and the n-C19-OH to n-C30-OH from Sigma-Aldrich® (all with purity between 95.7 and 99.9 %). The internal standard 1-tetradecene (S-96219-A, 99.3% purity) and the subrogated standard 1-eicosene (S-96219–B, 97.5 - 99.1% purity) used in the determination of n-alkanes were obtained from AccuStandard®, while the subrogated standard 5α-androstanol (MBBB9521V, 97.0-99.0% purity) and the internal standard 5α-cholestane used in the determination of n-alkanols were obtained from Sigma-Aldrich®.

Quality assurance procedures

Extraction blanks containing 5 g of anhydrous sodium sulphate previously decontaminated (at 450 °C for 4 h) were performed for every 8 samples. Values greater than three times the instrumental limit of detection (LD, 0.020 μg g^{-1}) were subtracted. This value was defined from the lowest concentration of individual *n*-alkanes detectable in the GC/FID

(0.20 ng μL^{-1}), multiplied by the final volume of the extract (500 µL), divided by the mass of extracted dry material (5 g) (Wisnieski et al., 2016).

Spiked sediments were used to evaluate each analyte recovery of n-alkanes after laboratory procedure. The spiked samples were prepared with 1.5 g of a mixture of freeze-dried sediments from each of the 82 samples. From this composed sample, 5 g was weighed for each replica, and external standards of *n*-alkanes (*n*-C_{15} to *n*-C_{35}) with known quantities were added. These replicas were submitted to the same process of extraction, purification, and fractionation of the samples until injection.

The average recovery (duplicate) of the external standards (*n*-C_{15} to *n*-C_{35}) in the spiked samples varied between 50 and 101% (mean = 72 ± 3%) for at least 90% of the evaluated compounds. Repeatability was assessed by analysing an aleatory sediment in triplicate, and the relative standard deviation ranged between 1.4 and 8.9% (mean = 4.1 ± 2.1%) for the detected compounds. Surrogate recoveries ranged from 50 to 73% for 1-eicosene (mean: 60 ± 6).

Finally, the analytical procedures were also evaluated with reference materials (IAEA-408) from the International Atomic Energy Agency, with values within 95% confidence interval of the recommended ranges for the parameters: total n-alkanes, unresolved complex mixture (UCM), and total aliphatic hydrocarbons (Villeneuve et al., 2000).

Table S1. Grain size (% silt + clay), elementary and isotopic composition (TOC, TN, $\delta^{13}C$ and $\delta^{15}N$) and atomic ratios (C/N) in sediments from Paranaguá Estuarine System, South Atlantic. Samples 01 to 42. TOC: Total Organic Carbon; TN: Total Nitrogen; NA: not analysed.

Samples	silt +clay (%)	TOC (%)	TN (%)	C/N[1]	$\delta^{13}C$ (‰)	$\delta^{15}N$ (‰)
1	29.17	0.79	0.06	15.37	-26.80	8.82
2	11.07	0.37	0.04	10.79	-27.15	11.54
3	79.97	4.42	0.35	14.74	-26.57	4.14
4	94.85	3.24	0.27	14.00	-26.79	4.81
5	81.43	3.76	0.38	11.55	-26.10	4.09
6	87.91	3.88	0.42	10.78	-26.42	3.47
7	90.42	4.18	0.36	13.55	-26.55	3.59
8	65.99	3.61	0.32	13.17	-27.06	4.69
9	83.07	4.30	0.42	11.95	-26.09	4.83
10	96,80	3.77	0.44	10.00	-25.76	4.32
11	96.86	3.77	0.43	10.23	-25.52	4.63
12	31.92	1.18	0.10	13.77	-26.12	6.65
13	72.04	0.40	0.05	9.34	-25.90	9.41
14	38.30	1.42	0.11	15.06	-26.20	5.61
15	79.44	3.33	0.36	10.79	-25.38	5.47
16	77.03	2.13	0.27	9.21	-25.55	5.43
17	83.20	2.45	0.22	13.00	-25.55	5.81
18	29.87	1.30	0.10	15.17	-25.68	6.15
19	88.72	1.99	0.19	12.22	-25.44	6.50
20	38.51	1.14	0.10	13.30	-25.83	5.65
21	62.90	1.30	0.20	7.59	-25.07	7.00
22	23.60	0.71	0.09	9.21	-25,62	6.01
23	77.49	4.71	0.31	17.73	-26.41	3.21
24	16.54	0.50	0.06	9,73	-24.80	7.33
25	35.51	1.49	0.15	11.59	-24.90	4.66
26	14.47	0.57	0.05	13.30	-25.20	6.37
27	13.18	0.63	0.06	12.25	-25.41	5.94
28	0.00	2.13	0.19	13.08	-26.00	2.98
29	17.79	0.74	0.07	12.34	-26.56	3.75
30	14.85	0.65	0.06	12.64	-25.59	4.80
31	29.66	1.35	0.12	13.13	-25.83	4.15
32	57.18	2.62	0.20	15.29	-25.96	4.48
33	83.53	2.24	0.20	13.07	-25.72	5.22
34	30.79	1.16	0.10	13.54	-25.43	4.93
35	31.97	0.72	0.06	14.00	-25.71	5.76
36	62.49	1.94	0.15	15.09	-25.89	4.22
37	94.62	3.42	0.35	11.40	-25.30	4.04
38	19.70	0.84	0.07	14.00	-25.27	5.02
39	43.50	1.20	0.10	14.00	-25.28	5.92
40	21.83	0.97	0.10	11.32	-24.84	6.36
41	62.90	1.33	0.11	14.11	-25.89	5.98
42	21.33	0.80	0.06	15.56	-25.03	6.95

[1] The percentages of TOC and TN from the sediment samples are used to calculate the C/N ratio, which was multiplied by 1.167 (the balance of the atomic weight of N and C) (Meyers and Teranes, 2002).

Table S1 (continued). Samples 43 to 84.

Samples	silt +clay (%)	TOC (%)	TN (%)	C/N[1]	$d^{13}C$ (‰)	$d^{15}N$ (‰)
43	14.05	0.37	0.04	10.79	-24.30	7.02
44	79.85	3.29	0.25	15.36	-25.25	4.14
45	17.11	0.70	0.07	11.67	-24.70	3.28
46	3.72	0.14	0.03	5.45	-24.96	10.05
47	73.86	1.60	0.16	11.67	-24.35	5.03
49	13.27	2.44	0.22	12.94	-24.01	2.16
50	79.17	2.06	0.18	13.36	-23.96	5.22
51	63.47	0.92	0.08	13.42	-24.31	5.34
52	9.07	0.24	0.04	7.00	-25.16	2.88
53	5.17	0.21	0.03	8.17	-24.63	6.85
54	64.93	1.61	0.20	9.39	-24.87	3.02
55	13.58	0.44	0.06	8.56	-24.40	3.43
56	8.75	0.18	0.03	7.00	-24.04	8.27
57	11.71	0.27	0.04	7.88	-23.70	4.16
58	42.10	0.94	0.15	7.31	-23.59	3.18
59	30.53	0.76	0.13	6.82	-24.08	2.98
60	11.24	0.22	0.03	8.56	-23.39	4.96
61	18.04	0.42	0.06	8.17	-24.31	3.32
62	11.17	0.38	0.05	8.87	-24.45	2.94
63	6.69	0.14	0.02	8.17	-25.20	7.23
64	28.25	0.43	0.06	8.36	-23.81	3.10
66	7.05	0.10	0.02	5.84	-23.30	10.51
67	8.75	0.19	0.03	7.39	-23.96	6.47
68	8.75	0.18	0.03	7.00	-24.75	6.54
69	34.61	1.87	0.18	12.12	-26.33	3,70
70	45.13	2.45	0.23	12.43	-25.70	2.00
71	46.51	0.91	0.08	13.27	-25.36	3.03
72	19.87	0.58	0.07	9.67	-24.58	3.65
73	79.30	3.15	0.34	10.81	-25.75	3.34
74	83.51	3.01	0.37	9.49	-25.27	3.02
75	39.84	1.37	0.13	12.30	-25.45	3.48
76	16.80	0.60	0.06	11,67	-25.43	12.96
77	40.38	0.78	0.07	13.00	-23.78	4.02
78	76.09	2.05	0.18	13.29	-26.59	3.48
79	25.52	0.74	0.11	7.85	-22.88	2.91
80	20.19	0.73	0.10	8.52	-24.03	3.35
81	52.17	1.67	0.15	12.99	-24.76	9.29
82	82.87	3.19	0.31	12.01	-25.42	3.29
83	95.18	3.18	0.30	12.37	-25.42	4.71
84	99.05	3.47	0.34	11.91	-25.44	3.51

Table S2. Concentrations of individual *n*-alkanes (in µg g^{-1}) and related parameters in sediments from Paranaguá Estuarine System, South Atlantic. Samples 01 to 21. Total *n*-alk: total *n*-alkanes (C_{15}-C_{35}); ACL: Average Chain Length; TAR: Terrigenous-to-Aquatic Ratio; CPI: Preferential Carbon Index; P_{aq}: Aquatic proxy; UCM/*n*-alk: Unresolved Complex Mixture / Total *n*-alk. < LD: below detection limit; NC: not calculated, ND: UCM not detected.

	1	**2**	**3**	**4**	**5**	**6**	**7**	**8**	**9**	**10**	**11**	**12**	**13**	**14**	**15**	**16**	**17**	**18**	**19**	**20**	**21**
n-C_{15}	< LD	< LD	< LD	< LD	< LD	< LD	< LD	< LD	< LD	< LD	< LD	< LD	< LD	< LD	< LD	< LD	< LD	< LD	< LD	< LD	< LD
n-C_{16}	< LD	< LD	< LD	< LD	< LD	< LD	< LD	< LD	< LD	< LD	< LD	< LD	< LD	< LD	< LD	< LD	< LD	< LD	< LD	< LD	< LD
n-C_{17}	< LD	< LD	0.05	0.06	0.06	0.04	0.06	< LD	0.08	0.08	0.05	< LD	< LD	< LD	0.08	0.04	0.02	< LD	< LD	< LD	0.05
n-C_{18}	< LD	< LD	< LD	0.03	< LD	< LD	0.02	< LD	< LD	< LD	< LD	< LD	< LD	< LD	0.03	< LD	< LD	< LD	< LD	< LD	< LD
n-C_{19}	< LD	< LD	0.02	0.06	0.03	0.02	0.04	< LD	0.03	0.03	0.03	< LD	< LD	< LD	0.03	< LD	< LD	< LD	< LD	< LD	< LD
n-C_{20}	< LD	0.06	< LD	0.12	< LD	< LD	0.03	< LD	< LD	< LD	< LD	< LD	< LD	< LD	0.02	< LD	< LD	< LD	< LD	< LD	< LD
n-C_{21}	< LD	0.27	0.07	0.48	0.07	0.10	0.17	0.08	0.13	0.10	0.06	< LD	< LD	< LD	0.07	0.05	0.05	0.03	0.02	< LD	0.04
n-C_{22}	< LD	0.86	0.09	1.10	0.06	0.07	0.13	0.11	0.12	0.27	0.05	0.02	< LD	0.03	0.06	0.04	0.08	0.03	0.02	< LD	0.05
n-C_{23}	0.07	1.96	0.47	2.64	0.34	0.45	0.55	0.43	0.52	0.79	0.28	0.11	0.04	0.14	0.32	0.21	0.27	0.26	0.14	0.11	0.14
n-C_{24}	0.06	2.99	0.32	3.69	0.25	0.27	0.38	0.34	0.48	0.95	0.22	0.07	0.03	0.10	0.21	0.15	0.28	0.13	0.09	0.07	0.16
n-C_{25}	0.25	3.94	1.46	4.89	1.24	1.45	1.65	1.29	1.98	2.35	1.16	0.38	0.14	0.45	1.09	0.72	0.80	0.95	0.56	0.42	0.40
n-C_{26}	0.10	3.50	0.34	3.66	0.30	0.28	0.28	0.30	0.49	1.10	0.21	0.09	0.05	0.09	0.25	0.21	0.49	0.15	0.15	0.11	0.14
n-C_{27}	0.42	2.99	1.97	3.76	1.81	1.68	1.88	1.62	2.41	2.50	1.27	0.50	0.20	0.51	1.56	1.22	1.02	0.82	0.93	0.59	0.62
n-C_{28}	0.18	1.90	0.67	2.08	0.63	0.41	0.47	0.41	0.83	0.93	0.46	0.18	0.12	0.17	0.52	0.50	0.76	0.21	0.30	0.21	0.24
n-C_{29}	1.09	1.49	3.94	3.31	3.27	2.75	3.15	2.74	4.25	3.50	2.90	0.89	0.50	0.95	3.24	2.76	1.72	0.99	2.12	1.25	1.26
n-C_{30}	0.13	0.69	0.34	0.95	0.31	0.25	0.30	0.27	0.40	0.45	0.32	0.13	0.12	0.13	0.33	0.31	0.47	0.15	0.25	0.17	0.19
n-C_{31}	0.46	0.56	1.54	1.41	1.33	0.82	1.38	1.27	1.72	1.39	1.55	0.36	0.30	0.44	1.49	1.22	0.86	0.38	0.95	0.56	0.56
n-C_{32}	0.12	0.24	0.26	0.29	0.21	0.23	0.27	0.19	0.33	0.25	0.30	0.11	0.11	0.12	0.24	0.22	0.37	0.12	0.20	0.14	0.16
n-C_{33}	0.26	0.23	1.01	0.88	0.65	0.53	0.72	0.65	0.94	0.78	0.95	0.18	0.19	0.24	0.77	0.71	0.56	0.20	0.62	0.29	0.33
n-C_{34}	0.13	0.11	0.51	0.30	0.39	0.36	0.39	0.37	0.52	0.41	0.47	0.16	0.11	0.17	0.43	0.38	0.38	0.17	0.46	0.19	0.21
n-C_{35}	< LD	< LD	0.25	0.21	0.16	0.22	0.23	0.22	0.23	0.29	0.33	0.13	0.14	< LD	0.22	0.22	0.28	0.13	0.24	0.12	0.16
Total *n*-alk.	3.27	21.8	13.3	29.9	11.1	9.92	12.1	10.3	15.4	16.2	10.6	3.30	2.03	3.53	11.0	8.95	8.43	4.71	7.04	4.22	4.67
TAR	37.5	4.13	16.2	4.40	16.5	12.0	10.7	14.8	15.0	10.6	18.3	20.6	33.8	18.6	16.2	22.4	14.5	11.9	31.2	29.3	14.5
CPI	3.94	1.21	4.90	1.65	4.69	4.87	5.17	4.95	4.43	3.11	4.83	3.71	2.83	4.01	4.93	4.42	2.04	4.38	4.58	4.11	3.47
P_{aq}	0.17	0.74	0.26	0.61	0.26	0.35	0.33	0.30	0.29	0.39	0.24	0.28	0.18	0.30	0.23	0.19	0.29	0.47	0.19	0.22	0.23
ACL	29.0	26.9	28.7	27.5	28.6	28.3	28.5	28.6	28.5	28.2	29.0	28.5	29.3	28.6	28.8	29.0	28.7	27.8	29.1	28.8	28.9
UCM/*n*-alk	ND	0.20	1.60	0.10	1.09	0.17	2.45	1.01	0.84	ND	1.99	3.32	2.02	2.05	0.87	0.90	1.85	0.24	0.85	2.40	14.6

Table S2 (continued). Samples 22 to 42.

	22	**23**	**24**	**25**	**26**	**27**	**28**	**29**	**30**	**31**	**32**	**33**	**34**	**35**	**36**	**37**	**38**	**39**	**40**	**41**	**42**
n-C_{15}	< LD	< LD	< LD	< LD	< LD	< LD	< LD	< LD	< LD	< LD	< LD	< LD	< LD	< LD	< LD	< LD	< LD	< LD	< LD	< LD	< LD
n-C_{16}	< LD	< LD	< LD	< LD	< LD	< LD	< LD	< LD	< LD	< LD	< LD	< LD	< LD	< LD	< LD	< LD	< LD	< LD	< LD	< LD	< LD
n-C_{17}	< LD	0.06	0.04	0.06	0.03	< LD	0.07	0.11	0.02	< LD	0.05	0.05	< LD	< LD	0.05	0.08	< LD	< LD	< LD	< LD	0.02
n-C_{18}	< LD	< LD	< LD	< LD	< LD	< LD	< LD	< LD	< LD	< LD	0.02	< LD	< LD	< LD	< LD	< LD	< LD	< LD	< LD	< LD	< LD
n-C_{19}	< LD	0.04	< LD	< LD	< LD	< LD	0.02	< LD	< LD	< LD	0.03	< LD	< LD	< LD	< LD	0.03	< LD	< LD	< LD	< LD	< LD
n-C_{20}	< LD	< LD	< LD	< LD	< LD	< LD	0.03	0.02	< LD	< LD	0.03	< LD	< LD	< LD	< LD	< LD	< LD	< LD	< LD	< LD	< LD
n-C_{21}	< LD	0.17	< LD	0.03	0.02	< LD	0.10	0.11	0.08	< LD	0.20	0.03	0.05	< LD	0.05	0.08	0.02	< LD	< LD	< LD	< LD
n-C_{22}	0.02	0.11	< LD	0.07	0.06	0.04	0.18	0.28	0.24	0.03	0.48	0.04	0.14	< LD	0.10	0.09	0.06	0.03	0.02	0.02	< LD
n-C_{23}	0.08	0.96	0.05	0.23	0.16	0.09	0.49	0.65	0.62	0.12	1.26	0.20	0.36	0.09	0.29	0.36	0.17	0.14	0.11	0.12	0.09
n-C_{24}	0.09	0.51	0.04	0.29	0.24	0.12	0.69	1.06	0.96	0.11	1.82	0.14	0.43	0.07	0.27	0.28	0.18	0.10	0.10	0.07	0.06
n-C_{25}	0.24	3.00	0.22	0.68	0.48	0.39	1.28	1.51	1.44	0.50	3.13	0.67	0.80	0.36	0.85	1.14	0.49	0.47	0.33	0.46	0.45
n-C_{26}	0.06	0.40	0.05	0.31	0.26	0.11	0.69	1.17	1.09	0.12	2.08	0.18	0.39	0.08	0.24	0.31	0.18	0.13	0.13	0.11	0.08
n-C_{27}	0.23	2.68	0.28	0.68	0.50	0.23	1.13	1.37	1.33	0.67	2.63	1.00	0.80	0.41	0.82	1.84	0.57	0.71	0.47	0.64	0.40
n-C_{28}	0.12	0.67	0.14	0.30	0.28	0.12	0.56	0.78	0.82	0.32	1.25	0.36	0.32	0.17	0.28	0.63	0.23	0.28	0.22	0.25	0.18
n-C_{29}	0.42	4.25	0.69	1.09	0.76	0.37	1.62	1.44	1.53	1.49	2.53	2.21	1.33	0.85	1.31	3.92	1.12	1.62	1.01	1.49	0.85
n-C_{30}	0.10	0.39	0.12	0.19	0.17	0.10	0.28	0.39	0.40	0.20	0.57	0.25	0.21	0.15	0.19	0.45	0.18	0.25	0.17	0.19	0.15
n-C_{31}	0.22	1.31	0.35	0.45	0.36	0.16	0.61	0.62	0.63	0.64	1.15	1.08	0.67	0.45	0.66	1.79	0.55	0.82	0.52	0.69	0.45
n-C_{32}	0.07	0.26	0.11	0.15	0.12	0.06	0.19	0.21	0.19	0.17	0.33	0.21	0.17	0.13	0.17	0.32	0.15	0.18	0.14	0.17	0.14
n-C_{33}	0.18	0.86	0.20	0.33	0.24	0.14	0.30	0.32	0.35	0.37	0.57	0.79	0.39	0.24	0.53	0.94	0.33	0.55	0.34	0.47	0.37
n-C_{34}	0.13	0.37	0.10	0.27	0.13	0.11	0.21	0.15	0.16	0.18	0.33	0.39	0.19	0.12	0.25	0.50	0.18	0.23	0.18	0.25	0.15
n-C_{35}	< LD	0.26	0.13	0.17	0.15	< LD	0.16	< LD	0.14	0.15	0.22	0.28	0.21	0.14	0.19	0.35	0.17	0.17	0.16	0.19	0.14
Total *n*-alk.	1.95	16.3	2.52	5.29	3.92	2.02	8.61	10.2	10.0	5.06	18.7	7.89	6.46	3.25	6.24	13.1	4.57	5.67	3.90	5.12	3.53
TAR	16.2	9.87	19.0	10.1	11.3	14.6	7.34	6.08	7.33	30.1	6.51	20.1	9.71	26.8	10.7	17.7	16.0	30.0	23.9	30.8	22.2
CPI	2.78	5.62	3.54	2.61	2.32	2.59	2.32	1.71	1.75	3.87	1.93	4.61	2.88	3.70	3.67	4.57	3.36	4.15	3.38	4.32	3.86
P_{aq}	0.33	0.42	0.21	0.37	0.36	0.47	0.44	0.51	0.49	0.23	0.54	0.21	0.37	0.26	0.37	0.21	0.28	0.20	0.22	0.21	0.29
ACL	28.8	28.1	29.0	28.4	28.5	28.1	28.0	27.8	27.9	28.8	27.7	29.1	28.5	28.8	28.6	28.9	28.8	29.1	29.1	29.0	28.9
UCM/*n*-alk	13.9	ND	1.82	0.56	1.97	5.14	1.78	2.63	0.11	2.34	0.34	1.34	0.25	4.96	2.28	3.50	1.76	1.27	1.25	1.24	1.04

Table S2 (continued). Samples 43 to 63.

	43	**44**	**45**	**46**	**47**	**48**	**49**	**50**	**51**	**52**	**53**	**54**	**55**	**56**	**57**	**58**	**59**	**60**	**61**	**62**	**63**
n-C_{15}	< LD	< LD	< LD	< LD	< LD	-	< LD	< LD	< LD	< LD	< LD	< LD	< LD	< LD	< LD	< LD	< LD	< LD	< LD	< LD	< LD
n-C_{16}	< LD	< LD	< LD	< LD	< LD	-	< LD	< LD	< LD	< LD	< LD	< LD	< LD	< LD	< LD	< LD	< LD	< LD	< LD	< LD	< LD
n-C_{17}	< LD	0.13	0.04	< LD	0.06	-	0.15	0.11	0.03	< LD	< LD	0.08	< LD	< LD	< LD	0.10	0.05	0.07	< LD	< LD	< LD
n-C_{18}	< LD	< LD	< LD	< LD	0.03	-	0.08	0.07	< LD	< LD	< LD	0.03	< LD	< LD	< LD	< LD	< LD	< LD	< LD	< LD	< LD
n-C_{19}	< LD	0.04	< LD	< LD	0.02	-	0.04	0.04	< LD	< LD	< LD	0.02	< LD	< LD	< LD	< LD	< LD	< LD	< LD	< LD	< LD
n-C_{20}	< LD	< LD	< LD	< LD	0.02	-	< LD	0.02	< LD	< LD	0.03	< LD	< LD	< LD	< LD	< LD	< LD	< LD	< LD	< LD	< LD
n-C_{21}	< LD	0.04	< LD	< LD	0.10	-	0.04	0.13	0.06	0.04	0.18	0.04	< LD	< LD	< LD	0.02	0.04	< LD	< LD	< LD	< LD
n-C_{22}	< LD	0.04	< LD	0.05	0.22	-	0.04	0.34	0.16	0.13	0.57	0.13	< LD	< LD	0.04	< LD	0.11	< LD	< LD	< LD	< LD
n-C_{23}	0.04	0.31	0.14	0.11	0.57	-	0.20	0.91	0.41	0.30	1.26	0.30	0.02	< LD	0.10	0.07	0.31	0.03	0.05	0.05	< LD
n-C_{24}	0.04	0.27	0.11	0.14	0.79	-	0.13	1.36	0.58	0.45	2.06	0.36	0.02	< LD	0.11	0.05	0.45	0.04	0.05	0.05	< LD
n-C_{25}	0.14	2.50	0.81	0.20	1.32	-	0.62	2.14	0.84	0.62	2.50	0.57	0.11	0.04	0.22	0.27	0.72	0.10	0.19	0.15	0.04
n-C_{26}	0.07	0.24	0.15	0.14	0.90	-	0.19	1.61	0.61	0.51	2.34	0.20	0.06	0.03	0.13	0.09	0.50	0.07	0.09	0.07	0.03
n-C_{27}	0.24	1.84	0.77	0.17	1.28	-	0.92	1.99	0.75	0.49	2.05	0.60	0.20	0.09	0.24	0.45	0.73	0.14	0.27	0.25	0.07
n-C_{28}	0.13	0.65	0.24	0.13	0.62	-	0.37	1.17	0.41	0.31	1.45	0.26	0.13	0.07	0.14	0.22	0.39	0.11	0.15	0.14	0.07
n-C_{29}	0.60	3.75	1.26	0.23	1.70	-	2.07	2.29	0.94	0.46	1.23	1.46	0.47	0.25	0.52	1.08	1.07	0.34	0.60	0.67	0.17
n-C_{30}	0.14	0.34	0.18	0.12	0.33	-	0.29	0.54	0.24	0.19	0.63	0.19	0.14	0.09	0.12	0.16	0.24	0.12	0.14	0.14	0.08
n-C_{31}	0.39	1.29	0.52	0.20	0.84	-	1.20	1.19	0.50	0.30	0.60	0.71	0.29	0.19	0.32	0.59	0.57	0.25	0.36	0.42	0.16
n-C_{32}	0.13	0.28	0.14	0.08	0.24	-	0.27	0.32	0.18	0.13	0.30	0.18	0.13	0.12	0.14	0.18	0.17	0.11	0.13	0.14	0.10
n-C_{33}	0.26	0.77	0.33	0.16	0.48	-	1.01	0.72	0.34	0.17	0.24	0.64	0.17	0.13	0.24	0.52	0.45	0.16	0.28	0.32	0.12
n-C_{34}	0.13	0.36	0.15	< LD	0.31	-	0.45	0.38	0.21	0.11	0.15	0.33	0.14	0.11	0.16	0.26	0.21	0.11	0.13	0.14	0.09
n-C_{35}	0.15	0.28	0.17	< LD	0.23	-	0.40	0.34	0.19	< LD	< LD	0.25	< LD	< LD	< LD	0.22	0.20	< LD	0.15	0.14	< LD
Total *n*-alk.	2.45	13.1	4.98	1.73	10.1	-	8.46	15.7	6.44	4.21	15.6	6.34	1.89	1.11	2.48	4.27	6.22	1.66	2.58	2.67	0.91
TAR	43.0	19.6	20.7	8.59	7.39	-	13.5	6.96	6.73	6.05	4.59	8.98	51.7	NC	16.0	15.4	8.71	9.63	34.6	36.7	NC
CPI	3.04	5.58	4.45	1.89	2.15	-	4.19	1.87	1.86	1.44	1.17	3.41	2.33	1.91	2.32	3.64	2.19	2.06	2.86	3.13	1.80
P_{aq}	0.15	0.36	0.35	0.42	0.43	-	0.20	0.47	0.46	0.55	0.67	0.29	0.15	0.08	0.27	0.17	0.39	0.18	0.20	0.15	0.10
ACL	29.5	28.2	28.3	28.9	28.2	-	29.4	28.1	28.3	27.9	27.2	29.1	29.4	29.8	29.2	29.4	28.6	29.5	29.3	29.6	29.9
UCM/*n*-alk	0.48	0.90	ND	ND	0.86	-	1.40	0.08	ND	ND	1.07	5.51	1.57	2.60	4.78	2.95	ND	1.42	1.29	3.21	8.05

Table S2 (continued). Samples 64 to 84.

	64	**65**	**66**	**67**	**68**	**69**	**70**	**71**	**72**	**73**	**74**	**75**	**76**	**77**	**78**	**79**	**80**	**81**	**82**	**83**	**84**
n-C_{15}	< LD	-	< LD	< LD	< LD	< LD	< LD	< LD	< LD	< LD	< LD	< LD	< LD	< LD	< LD	< LD	< LD	< LD	< LD	< LD	< LD
n-C_{16}	< LD	-	< LD	< LD	< LD	< LD	< LD	< LD	< LD	< LD	< LD	< LD	< LD	< LD	< LD	< LD	< LD	< LD	< LD	< LD	< LD
n-C_{17}	< LD	-	< LD	< LD	< LD	0.12	0.10	0.03	< LD	0.09	0.10	< LD	< LD	< LD	< LD	0.09	0.04	0.05	0.08	0.08	0.08
n-C_{18}	< LD	-	< LD	< LD	< LD	0.03	< LD	< LD	< LD	0.03	0.02	< LD	< LD	0.02	< LD	< LD	0.02	< LD	< LD	< LD	< LD
n-C_{19}	< LD	-	< LD	< LD	< LD	0.06	0.03	< LD	< LD	0.04	0.03	< LD	< LD	0.05	< LD	< LD	0.04	< LD	0.02	0.03	0.05
n-C_{20}	< LD	-	< LD	< LD	< LD	0.11	< LD	< LD	< LD	0.05	0.02	< LD	< LD	0.07	< LD	< LD	0.13	< LD	< LD	0.02	0.05
n-C_{21}	< LD	-	< LD	< LD	< LD	0.43	0.07	0.02	< LD	0.24	0.10	0.02	< LD	0.07	0.04	0.07	0.53	0.03	0.05	0.09	0.26
n-C_{22}	< LD	-	< LD	< LD	< LD	1.27	0.05	< LD	< LD	0.47	0.20	0.03	< LD	0.08	0.03	0.18	1.63	0.04	0.05	0.17	0.58
n-C_{23}	0.03	-	< LD	< LD	< LD	3.10	0.19	0.08	0.08	1.16	0.55	0.19	0.05	0.13	0.25	0.46	3.99	0.27	0.36	0.62	1.54
n-C_{24}	0.02	-	< LD	< LD	< LD	5.20	0.16	0.06	0.05	1.52	0.66	0.15	0.04	0.12	0.19	0.66	6.66	0.26	0.25	0.67	2.26
n-C_{25}	0.11	-	0.03	0.06	0.04	7.19	0.69	0.36	0.31	2.35	1.22	0.62	0.21	0.30	0.84	0.90	8.52	1.10	1.26	1.70	3.37
n-C_{26}	0.05	-	0.03	0.04	0.03	5.36	0.17	0.08	0.07	1.36	0.63	0.17	0.07	0.15	0.21	0.70	7.71	0.31	0.25	0.66	2.35
n-C_{27}	0.23	-	0.05	0.11	0.06	5.13	0.88	0.37	0.31	1.83	1.21	0.84	0.35	0.45	1.33	0.83	6.69	1.25	1.86	2.34	3.60
n-C_{28}	0.13	-	0.06	0.09	0.06	3.45	0.43	0.17	0.15	0.83	0.53	0.33	0.17	0.25	0.48	0.49	4.54	0.45	0.60	0.87	1.75
n-C_{29}	0.59	-	0.13	0.28	0.12	4.13	1.87	0.72	0.67	2.13	1.77	1.77	0.91	1.03	3.35	1.24	4.21	2.15	4.20	4.83	5.53
n-C_{30}	0.13	-	0.08	0.12	0.08	1.53	0.26	0.13	0.14	0.39	0.27	0.22	0.15	0.24	0.34	0.29	2.02	0.26	0.42	0.55	0.91
n-C_{31}	0.40	-	0.15	0.24	0.12	1.59	0.80	0.36	0.37	0.79	0.72	0.88	0.51	0.63	1.65	0.70	1.41	1.00	1.86	2.43	2.76
n-C_{32}	0.13	-	0.10	0.11	0.10	0.70	0.27	0.13	0.13	0.29	0.22	0.21	0.14	0.25	0.29	0.20	0.87	0.23	0.36	0.44	0.58
n-C_{33}	0.30	-	0.13	0.18	0.11	0.79	0.85	0.28	0.32	0.65	0.89	0.63	0.39	0.58	1.01	0.54	0.80	0.78	1.51	2.02	2.12
n-C_{34}	0.15	-	< LD	0.11	0.10	0.38	0.35	0.19	0.17	0.46	0.50	0.38	0.17	0.29	0.39	0.21	0.27	0.26	0.59	0.67	0.72
n-C_{35}	0.18	-	< LD	0.14	< LD	0.24	0.36	0.21	0.13	0.25	0.26	0.28	0.16	0.21	0.35	0.23	0.24	0.27	0.46	0.57	0.56
Total *n*-alk.	2.43	-	0.76	1.47	0.80	40.8	7.51	3.17	2.89	14.9	9.88	6.74	3.30	5.77	10.8	7.78	50.3	8.70	14.6	19.2	29.4
TAR	64.9	-	NC	NC	NC	5.07	13.3	15.8	25.1	5.05	7.48	22.2	50.4	12.3	28.3	6.78	4.70	18.2	20.9	16.3	9.03
CPI	3.16	-	1.78	2.14	1.44	1.40	3.70	3.36	3.40	2.05	2.61	4.01	3.84	2.75	5.10	2.02	1.20	4.17	5.28	4.19	2.49
P_{aq}	0.12	-	0.10	0.10	0.13	0.64	0.25	0.29	0.27	0.55	0.42	0.23	0.16	0.20	0.18	0.41	0.69	0.30	0.21	0.24	0.37
ACL	29.7	-	30.2	29.9	30.0	27.3	29.1	28.8	29.1	27.9	28.6	29.0	29.4	29.5	29.2	28.6	27.1	28.7	29.1	29.1	28.6
UCM/*n*-alk	1.03	-	9.64	ND	2.83	ND	6.14	2.54	1.06	0.52	0.52	3.21	ND	0.63	0.78	ND	ND	2.07	0.86	0.83	ND

Table S3. Concentrations of individual *n*-alkanols (in μg g^{-1}) and related parameters in sediments from Paranaguá Estuarine System, South Atlantic. Samples 01 to 21. Total *n*-alk-OH: total *n*-alkanols (C_{14}-C_{34}); < LD: below detection limit.

	1	**2**	**3**	**4**	**5**	**6**	**7**	**8**	**9**	**10**	**11**	**12**	**13**	**14**	**15**	**16**	**17**	**18**	**19**	**20**	**21**
n-C_{14}-OH	0.01	0.20	0.07	0.15	0.25	0.13	0.48	0.64	0.21	0.22	1.10	0.19	0.12	0.99	0.08	0.20	0.12	0.08	0.05	0.05	0.20
n-C_{15}-OH	< LD	1.95	0.12	1.98	15.1	2.35	0.38	2.10	0.23	0.21	1.38	0.15	0.06	0.76	0.06	0.16	0.11	0.09	0.05	0.05	0.10
n-C_{16}-OH	0.03	0.21	0.46	0.59	2.72	0.19	2.72	7.84	0.46	0.51	2.86	0.56	0.36	0.22	0.36	1.07	0.44	0.41	0.17	0.31	0.78
n-C_{17}-OH	0.02	0.26	0.13	0.59	1.89	0.26	1.22	6.15	0.24	0.25	2.13	0.22	0.07	0.40	0.11	0.31	0.16	0.13	0.06	0.07	0.12
n-C_{18}-OH	0.03	1.02	0.23	0.62	1.84	0.44	1.35	9.89	0.34	0.36	2.35	0.39	0.20	1.08	0.13	0.47	0.26	0.15	0.08	0.11	0.60
n-C_{19}-OH	< LD	0.42	0.05	0.43	0.21	0.23	0.36	1.83	0.05	0.10	0.77	0.10	0.10	0.38	0.04	0.04	0.05	0.01	< LD	0.02	0.17
n-C_{20}-OH	0.06	0.57	0.18	0.51	2.08	0.48	2.70	2.49	0.39	0.53	2.76	0.50	0.14	0.23	0.15	0.34	0.17	0.14	0.14	0.16	0.20
n-C_{21}-OH	0.02	0.09	0.12	0.18	0.61	0.10	1.69	4.05	0.17	0.22	1.97	0.15	0.06	0.21	0.05	0.20	0.09	0.04	0.03	0.04	0.05
n-C_{22}-OH	0.16	0.85	0.97	0.48	4.89	0.22	5.28	10.5	1.86	0.97	3.01	0.90	0.29	0.77	0.60	1.31	0.55	0.53	0.35	0.25	0.58
n-C_{23}-OH	0.02	0.47	0.16	0.14	0.95	< LD	0.74	1.71	0.35	0.30	1.56	0.16	0.06	0.09	0.08	0.20	0.06	0.06	0.06	0.05	0.04
n-C_{24}-OH	0.17	0.96	0.86	1.02	3.83	0.64	3.62	10.8	1.96	1.78	6.46	1.30	0.17	0.75	0.50	1.47	0.37	0.63	0.37	0.42	0.39
n-C_{25}-OH	0.01	3.90	0.08	0.36	3.74	1.77	0.51	4.63	0.23	0.18	0.90	0.35	0.03	1.67	0.06	0.15	1.08	0.11	0.08	0.09	0.38
n-C_{26}-OH	0.27	2.88	0.73	1.44	2.56	1.06	3.53	28.1	2.85	2.27	4.98	0.99	0.29	0.37	0.95	2.18	0.30	0.69	0.52	0.41	0.41
n-C_{27}-OH	0.04	6.40	0.32	0.88	10.8	0.16	2.13	20.9	1.80	0.53	3.25	0.46	0.74	1.43	0.29	0.79	0.41	0.33	0.13	0.05	0.29
n-C_{28}-OH	0.95	12.4	1.51	13.7	7.94	9.71	13.5	132.1	3.88	4.26	21.3	3.46	3.10	23.9	1.99	5.22	4.90	2.17	1.26	1.30	18.9
n-C_{29}-OH	0.20	3.76	0.62	3.89	3.09	3.97	3.08	66.8	1.30	0.70	12.9	0.60	0.47	2.92	0.17	0.64	2.57	0.26	0.53	0.09	4.52
n-C_{30}-OH	3.94	33.3	10.7	37.2	29.6	54.2	52.7	636.1	19.7	22.8	266.6	19.9	15.8	61.1	5.96	24.3	18.2	10.7	6.16	5.9	22.0
n-C_{31}-OH	0.06	< LD	0.27	0.58	0.67	< LD	0.73	11.4	1.07	0.84	3.18	0.34	< LD	< LD	0.31	0.56	< LD	0.21	< LD	< LD	0.70
n-C_{32}-OH	0.54	22.3	0.26	8.63	12.2	10.2	10.2	229.9	0.89	0.46	11.0	2.01	1.51	14.9	0.34	1.02	1.71	0.84	0.72	0.27	2.10
n C_{33}-OH	0.04	< LD	0.04	0.38	0.39	< LD	0.47	5.84	0.20	0.18	1.83	0.22	< LD	0.08	0.14	0.43	0.30	0.05	< LD	0.02	0.32
n-C_{34}-OH	0.04	< LD	0.03	1.25	0.09	< LD	0.12	2.01	0.02	0.03	0.25	0.06	< LD	< LD	0.03	0.04	0.31	< LD	< LD	0.02	< LD
Phytol	0.58	1.10	3.24	0.92	2.33	1.6	31.1	75.7	0.03	10.2	32.5	12.2	0.18	1.44	4.10	4.20	5.30	1.44	1.42	2.16	5.24
Total *n*-alk-OH	7.19	93.0	21.2	75.9	107.8	87.7	138.6	1271.5	38.2	47.9	385.0	45.2	23.8	113.7	16.5	45.3	37.5	19.1	12.2	11.9	58.1

Table S3 (continued). Samples 22 to 42.

	22	**23**	**24**	**25**	**26**	**27**	**28**	**29**	**30**	**31**	**32**	**33**	**34**	**35**	**36**	**37**	**38**	**39**	**40**	**41**	**42**
n-C_{14}-OH	0.03	0.10	0.05	0.50	0.05	0.24	0.51	0.05	0.06	0.25	0.33	0.34	0.24	0.10	0.16	0.20	0.10	0.30	0.19	0.05	0.17
n-C_{15}-OH	0.04	0.07	0.04	0.53	0.07	0.37	0.23	0.05	0.08	0.14	0.10	0.07	0.12	0.05	0.07	0.09	0.09	0.21	0.13	0.03	0.29
n-C_{16}-OH	0.23	0.37	0.33	2.05	0.14	0.51	1.29	0.14	0.25	0.50	0.16	0.76	0.36	0.16	0.28	0.27	0.20	0.39	0.55	0.14	0.65
n-C_{17}-OH	0.05	0.08	0.09	0.63	0.10	0.11	0.30	0.07	0.07	0.20	0.10	0.18	0.06	0.07	0.12	< LD	0.10	0.07	0.21	0.05	0.30
n-C_{18}-OH	0.06	0.11	0.10	0.68	0.08	0.14	0.28	0.08	0.07	0.29	0.16	0.25	0.11	0.05	0.22	0.19	0.08	0.09	0.27	0.08	0.32
n-C_{19}-OH	< LD	0.06	0.02	0.16	0.01	0.03	0.06	0.04	0.02	0.08	0.02	0.11	0.05	0.03	0.02	0.04	0.02	0.01	0.06	0.02	0.60
n-C_{20}-OH	0.09	0.13	0.09	0.56	0.10	0.14	0.30	0.12	0.11	0.29	0.07	0.46	0.12	0.13	0.15	0.09	0.17	0.15	0.41	0.17	0.52
n-C_{21}-OH	0.04	0.08	0.02	0.30	0.08	0.07	0.23	0.03	0.04	0.08	0.08	0.14	0.03	0.01	0.03	0.02	0.03	0.09	0.09	0.06	0.13
n-C_{22}-OH	0.28	0.62	0.24	1.06	0.31	0.28	0.46	0.38	0.29	1.03	0.16	1.28	0.21	0.15	0.33	0.06	0.39	0.31	1.19	0.35	1.28
n-C_{23}-OH	0.04	0.14	0.03	0.18	0.04	0.04	0.12	0.04	0.05	0.11	0.02	0.19	0.04	0.02	0.05	0.03	0.05	0.04	0.20	0.11	0.20
n-C_{24}-OH	0.33	0.69	0.35	0.98	0.37	0.18	0.95	0.55	0.57	1.31	0.15	1.04	0.23	0.20	0.30	0.05	0.33	0.16	1.72	0.67	1.45
n-C_{25}-OH	0.06	0.05	0.16	0.27	0.08	0.62	0.43	0.03	0.06	0.27	0.20	0.67	< LD	0.08	0.02	0.01	0.01	0.66	0.26	0.08	0.24
n-C_{26}-OH	0.28	0.36	0.44	1.08	0.43	0.26	1.04	0.14	0.70	0.93	0.18	1.03	0.42	0.21	0.14	0.10	0.23	0.16	2.97	1.38	2.85
n-C_{27}-OH	0.10	0.22	0.11	0.50	0.09	0.22	0.13	0.02	0.03	0.47	0.09	0.77	0.43	0.08	0.13	0.09	0.07	0.15	0.31	0.21	0.39
n-C_{28}-OH	0.47	1.69	1.54	4.27	1.57	6.79	6.41	0.53	1.42	2.63	4.34	4.78	6.25	1.36	1.77	4.54	1.29	3.71	3.22	2.26	5.28
n-C_{29}-OH	< LD	0.26	0.16	1.58	0.62	2.61	2.05	< LD	0.07	0.21	0.56	0.88	2.29	0.07	1.12	1.00	< LD	< LD	0.41	0.15	0.57
n-C_{30}-OH	2.91	22.3	6.47	15.0	5.55	26.8	41.3	3.82	7.78	75.0	13.7	66.8	18.7	10.6	8.88	11.3	10.1	27.0	6.83	3.13	5.73
n-C_{31}-OH	0.03	0.12	0.22	0.31	< LD	< LD	0.52	< LD	0.08	< LD	< LD	0.56	< LD	0.09	< LD	0.04	0.10	< LD	0.16	0.10	0.20
n-C_{32}-OH	0.14	0.29	0.29	0.96	0.28	1.13	2.81	0.14	0.08	1.09	2.53	4.55	2.28	0.66	1.36	1.25	0.39	1.69	0.58	0.16	0.53
n C_{33}-OH	< LD	0.02	< LD	0.07	< LD	< LD	< LD	0.03	< LD	< LD	< LD	0.25	< LD	< LD	< LD	< LD	< LD	< LD	0.21	0.05	0.10
n-C_{34}-OH	< LD	< LD	< LD	0.04	< LD	0.08	< LD	< LD	< LD	< LD	< LD	0.03	< LD	< LD	< LD	< LD	< LD	< LD	< LD	0.03	< LD
Phytol	1.00	1.65	1.63	19.7	1.84	1.36	4.67	1.81	1.31	4.35	0.46	4.38	0.65	1.19	1.73	0.28	3.73	1.07	6.29	1.54	11.7
Total *n*-alk-OH	6.18	29.4	12.4	51.4	11.8	42.0	64.1	8.07	13.1	89.2	23.4	89.5	32.6	15.3	16.9	19.7	17.5	36.3	26.3	10.8	33.5

Table S3 (continued). Samples 43 to 63.

	43	**44**	**45**	**46**	**47**	**48**	**49**	**50**	**51**	**52**	**53**	**54**	**55**	**56**	**57**	**58**	**59**	**60**	**61**	**62**	**63**
n-C_{14}-OH	0.03	0.10	0.11	0.03	0.06	-	0.15	0.08	0.17	0.22	0.01	0.07	0.14	0.03	0.15	0.11	0.13	0.06	0.04	0.03	0.02
n-C_{15}-OH	0.02	0.11	0.11	0.02	0.03	-	0.12	0.10	0.14	0.24	0.02	0.09	0.36	0.05	0.21	0.11	0.14	0.12	0.03	0.03	0.02
n-C_{16}-OH	0.12	0.59	0.30	0.13	0.34	-	0.36	0.35	0.63	0.88	0.07	0.35	0.42	0.11	0.35	0.33	0.34	0.20	0.12	0.11	0.08
n-C_{17}-OH	0.03	0.23	0.15	0.06	0.05	-	0.16	0.11	0.16	4.61	0.02	0.11	0.15	0.05	0.16	0.12	0.08	0.07	0.06	0.05	0.04
n-C_{18}-OH	0.06	0.18	0.12	0.10	0.11	-	0.16	0.19	0.18	0.63	0.09	0.13	0.11	0.07	0.20	0.13	0.15	0.12	0.07	0.05	0.13
n-C_{19}-OH	< LD	0.06	0.03	< LD	0.01	-	0.04	0.03	0.04	1.10	< LD	0.01	0.01	< LD	0.03	0.02	0.03	< LD	< LD	< LD	< LD
n-C_{20}-OH	0.09	0.19	0.15	0.70	0.10	-	0.17	0.16	0.26	0.61	0.07	0.12	0.10	0.08	0.14	0.23	0.14	0.12	0.08	0.08	0.09
n-C_{21}-OH	0.01	0.05	0.03	< LD	0.04	-	0.05	0.05	0.08	0.13	0.01	0.03	0.02	< LD	0.02	0.03	0.03	0.02	0.01	< LD	< LD
n-C_{22}-OH	0.11	0.76	0.26	0.19	0.40	-	0.56	0.40	0.38	1.11	0.07	0.42	0.21	0.07	0.16	0.19	0.29	0.15	0.12	0.17	0.04
n-C_{23}-OH	0.02	0.06	0.08	0.02	0.06	-	0.10	0.13	0.09	0.25	< LD	0.07	0.02	< LD	0.03	0.04	0.02	0.01	0.02	0.02	< LD
n-C_{24}-OH	0.22	1.28	0.62	0.23	0.35	-	0.62	0.73	0.47	2.62	0.10	0.41	0.21	0.10	0.21	0.27	0.30	0.16	0.19	0.21	0.05
n-C_{25}-OH	0.02	0.14	0.08	0.06	0.06	-	0.07	0.08	0.07	1.28	0.03	0.04	0.02	< LD	0.01	0.06	0.02	0.01	< LD	0.03	0.05
n-C_{26}-OH	0.59	1.68	1.36	0.48	0.66	-	0.97	0.88	0.42	6.60	0.17	0.54	0.33	0.19	0.43	0.32	0.45	0.28	0.32	0.44	0.13
n-C_{27}-OH	0.03	0.79	0.09	0.02	0.07	-	0.12	0.15	0.15	2.81	< LD	0.07	0.01	< LD	0.02	0.05	0.04	0.01	0.01	0.01	< LD
n-C_{28}-OH	1.31	1.52	1.54	1.16	1.03	-	1.04	0.98	0.52	5.80	0.37	0.70	0.25	0.31	1.05	0.23	0.56	0.30	0.52	1.06	0.19
n-C_{29}-OH	0.05	0.65	0.09	0.05	0.08	-	0.16	0.09	0.06	1.25	0.02	0.07	< LD	0.02	0.05	0.03	0.03	0.02	0.02	0.05	< LD
n-C_{30}-OH	1.35	6.99	4.69	0.70	1.53	-	0.94	1.72	1.44	4.91	0.32	0.74	0.79	0.62	1.46	1.11	1.14	0.66	0.77	1.10	0.60
n-C_{31}-OH	0.07	0.29	0.07	0.05	0.07	-	0.08	0.05	0.12	1.97	0.02	0.07	0.06	0.03	0.06	0.05	0.06	0.05	0.04	0.03	< LD
n-C_{32}-OH	0.14	0.17	0.10	0.09	0.06	-	0.13	0.07	0.04	1.44	0.02	0.03	0.05	0.03	0.08	0.02	0.07	0.03	0.03	0.09	0.05
n C_{33}-OH	0.01	< LD	< LD	< LD	< LD	-	< LD	< LD	< LD	< LD	< LD	< LD	< LD	< LD	< LD	< LD	< LD	< LD	< LD	< LD	< LD
n-C_{34}-OH	< LD	< LD	< LD	< LD	< LD	-	< LD	< LD	< LD	< LD	< LD	< LD	< LD	< LD	< LD	< LD	< LD	< LD	< LD	< LD	< LD
Phytol	0.71	4.15	4.78	0.84	2.65	-	4.91	1.96	4.22	7.76	0.50	3.02	2.74	0.85	2.22	1.82	3.64	3.79	2.31	0.96	1.16
Total *n*-alk-OH	4.99	20.0	14.8	4.93	7.76	-	10.9	8.31	9.64	46.2	1.91	7.09	6.00	2.61	7.04	5.27	7.66	6.18	4.76	4.52	2.65

Table S3 (continued). Samples 64 to 84.

	64	**65**	**66**	**67**	**68**	**69**	**70**	**71**	**72**	**73**	**74**	**75**	**76**	**77**	**78**	**79**	**80**	**81**	**82**	**83**	**84**
n-C_{14}-OH	0.05	-	0.01	0.02	0.05	0.55	0.11	0.09	0.14	0.08	0.37	0.04	0.04	0.06	0.04	0.10	0.07	0.42	0.12	0.35	0.10
n-C_{15}-OH	0.04	-	< LD	0.01	0.02	0.58	0.08	0.08	0.16	0.07	0.18	0.05	0.02	0.11	0.06	0.29	0.07	0.69	0.12	0.19	0.08
n-C_{16}-OH	0.20	-	0.06	0.09	0.18	1.70	0.53	0.35	0.93	0.35	1.27	0.25	0.21	0.26	0.15	0.64	0.34	1.63	0.26	0.87	0.35
n-C_{17}-OH	0.09	-	0.02	0.03	0.03	0.76	0.12	0.08	0.16	0.08	0.39	0.07	0.05	0.17	0.06	0.27	0.10	0.62	0.14	0.38	0.11
n-C_{18}-OH	0.10	-	0.02	0.03	0.05	0.88	0.18	0.13	0.23	0.10	0.98	0.03	0.08	0.18	0.05	0.21	0.08	0.85	0.10	0.55	0.07
n-C_{19}-OH	0.01	-	< LD	< LD	< LD	0.23	0.05	0.02	0.02	0.03	0.08	0.02	0.01	0.07	< LD	0.05	0.03	0.08	0.04	0.06	0.02
n-C_{20}-OH	0.12	-	0.01	0.09	0.08	0.84	0.24	0.20	0.15	0.24	0.63	0.09	0.13	0.18	0.14	0.13	0.13	0.65	0.23	0.47	0.21
n-C_{21}-OH	0.02	-	< LD	< LD	< LD	0.33	0.05	0.04	0.04	0.10	0.23	0.06	0.03	0.04	0.05	0.03	0.04	0.17	0.11	0.24	0.06
n-C_{22}-OH	0.14	-	0.03	0.10	0.08	3.63	0.77	0.58	0.41	0.80	2.59	0.33	0.25	0.53	0.75	0.40	0.40	2.00	0.83	1.36	0.35
n-C_{23}-OH	0.02	-	< LD	< LD	< LD	0.59	0.13	0.10	0.06	0.14	0.22	0.08	0.05	0.07	0.10	0.06	0.06	0.42	0.15	0.35	0.04
n-C_{24}-OH	0.25	-	0.02	0.08	0.05	8.01	1.17	0.71	0.62	0.74	2.55	0.71	0.56	0.71	0.98	0.48	0.35	3.30	0.91	2.73	0.44
n-C_{25}-OH	0.03	-	0.04	0.01	< LD	0.59	0.08	0.09	0.05	0.08	0.22	0.06	0.08	0.08	0.10	0.03	0.06	0.36	0.11	0.32	0.07
n-C_{26}-OH	0.49	-	0.02	0.17	0.12	8.18	1.48	1.46	0.93	0.63	4.00	1.01	1.10	1.15	1.42	0.42	0.80	5.20	1.48	3.45	0.39
n-C_{27}-OH	0.02	-	< LD	< LD	< LD	1.89	0.32	0.16	0.03	0.21	2.21	0.20	0.07	0.08	0.26	0.07	0.08	1.13	0.68	1.10	0.48
n-C_{28}-OH	0.98	-	0.07	0.37	0.27	6.55	1.87	1.85	0.73	1.14	2.91	1.04	2.05	1.81	2.07	1.54	0.79	7.20	1.75	3.51	0.39
n-C_{29}-OH	0.04	-	< LD	0.02	< LD	2.28	0.19	0.13	0.06	0.23	1.81	0.14	0.09	0.10	0.31	0.07	0.11	1.28	1.03	1.68	0.09
n-C_{30}-OH	0.85	-	0.12	0.34	0.38	43.0	3.99	3.06	3.42	4.01	11.4	2.94	2.27	2.18	3.38	2.24	1.72	16.1	7.75	15.8	5.37
n-C_{31}-OH	0.06	-	0.01	0.01	0.03	1.16	0.29	0.08	0.04	0.10	1.30	0.08	0.11	0.11	0.16	0.12	0.09	0.68	0.32	1.06	0.13
n-C_{32}-OH	0.08	-	< LD	0.03	0.02	0.38	0.24	0.12	0.13	0.12	0.79	0.12	0.28	0.18	0.27	0.22	0.17	0.59	0.31	0.42	0.18
n C_{33}-OH	< LD	-	< LD	< LD	< LD	< LD	< LD	< LD	< LD	< LD	< LD	< LD	0.01	0.01	< LD	< LD	< LD	< LD	< LD	< LD	< LD
n-C_{34}-OH	< LD	-	< LD	< LD	< LD	< LD	< LD	< LD	< LD	< LD	< LD	< LD	0.02	0.02	< LD	< LD	< LD	< LD	< LD	< LD	< LD
Phytol	2.51	-	0.75	0.84	1.37	11.2	3.03	2.10	2.30	2.53	17.6	1.48	2.48	1.41	3.62	7.15	3.76	14.1	4.43	10.6	3.29
Total *n*-alk-OH	6.10	-	1.18	2.24	2.73	93.3	14.9	11.4	10.6	11.8	51.7	8.80	9.99	9.51	14.0	14.5	9.25	57.5	20.9	45.5	12.2

Table S4. Concentrations of total *n*-alkanes and aliphatic (in □g g^{-1}) from previous studies carried out in the Paranaguá Estuarine System (PES), South Atlantic, and the current study. SD = standard deviation.

Total *n*-alkanes (□g g^{-1})	**mean ± SD**	**Total aliphatic (□g g^{-1})**	**mean ± SD**	**Sampling date**	**Estimated population (inhabitants)**	**Specific site in PES**	**Reference**
0.01 – 0.64	0.27 ± 0.26	0.28 – 7.33	2.18 ± 2.70	2008	138.748	Cotinga Channel	Abreu-Motta et al. (2014)
0.06 – 1.23	0.46 ± 0.33	0.36 – 5.07	2.20 ± 1.48	2009			
0.10 – 6.06	2.03 ± 1.70	0.28 – 8.19	2.96 ± 2.23	2010	140.469	Laranjeiras Bay	Martins et al. (2012)
0.07 – 15.9	5.35 ± 5.43	0.41 – 39.3	13.9 ± 14.1	2011		Paranaguá Bay	Cardoso et al. (2016)
1.29 – 6.00	3.03 ± 1.20	10.8 – 34.5	17.9 ± 5.90	2015 – 2016	151.829	Cotinga Channel	Garcia et al. (2019)
0.64 – 11.9	4.11 ± 3.02	2.27 – 29.9	9.82 ± 7.97				
0.76 – 50.3	8.48 ± 8.40	4.51 – 82.4	27.0 ± 17.5	2018 – 2019	156.174	Paranaguá Estuarine System	Current study

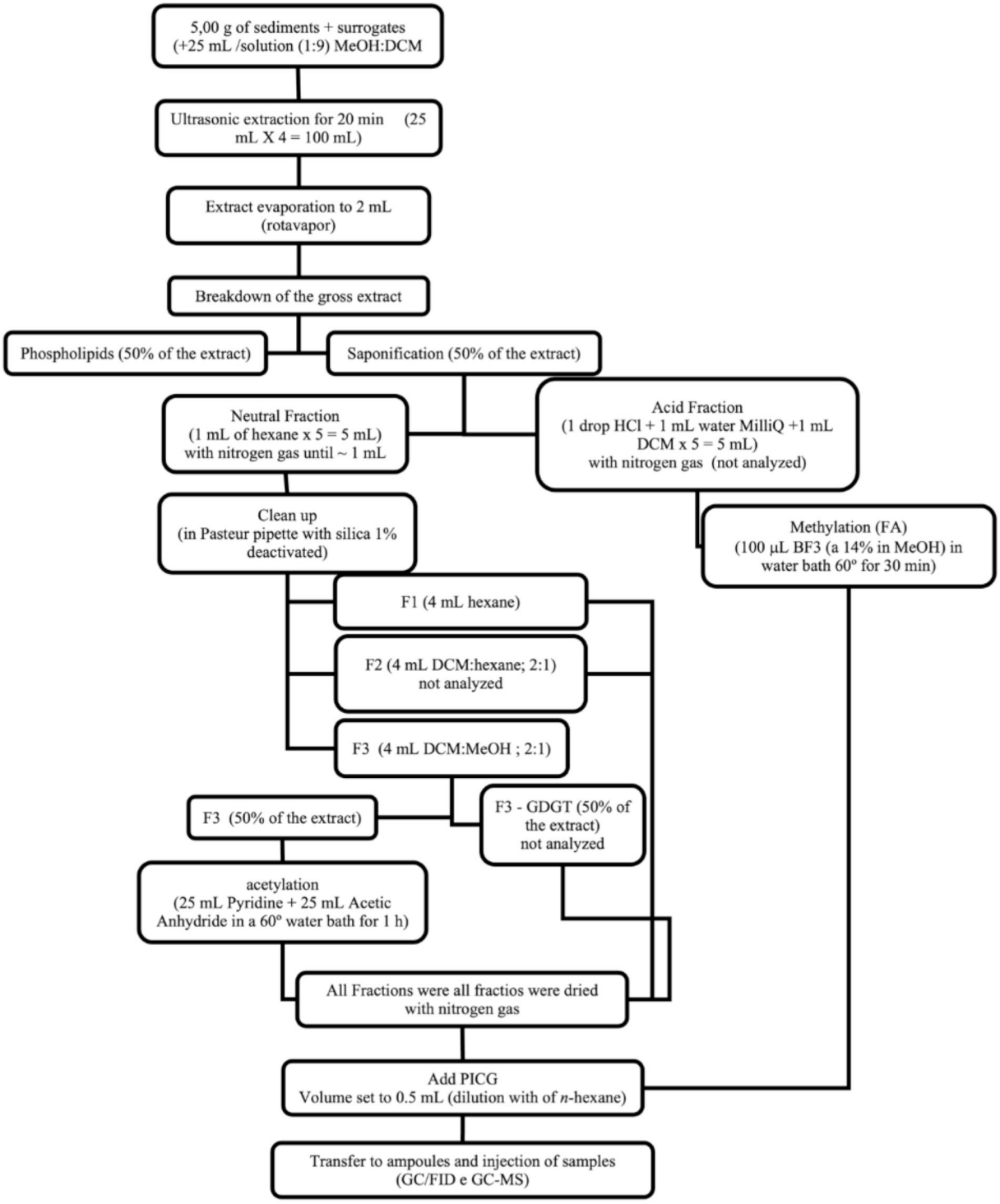

Fig. S1. Flowchart of the laboratory method used to determine the geochemical markers (*n*-alkanes and *n*-alkanols).

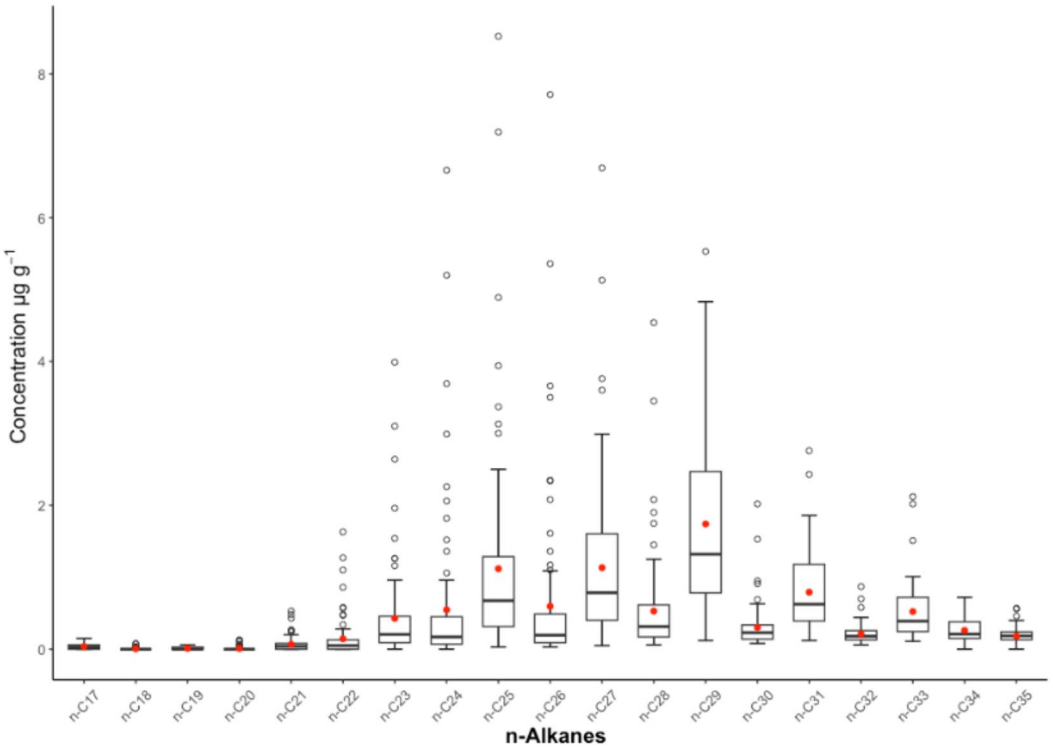

Fig. S2. Box plot of the distribution of *n*-alkanes analysed in the surficial sediments of the Paranaguá Estuarine System, South Atlantic. Open circle: outliers; Red circle: mean value.

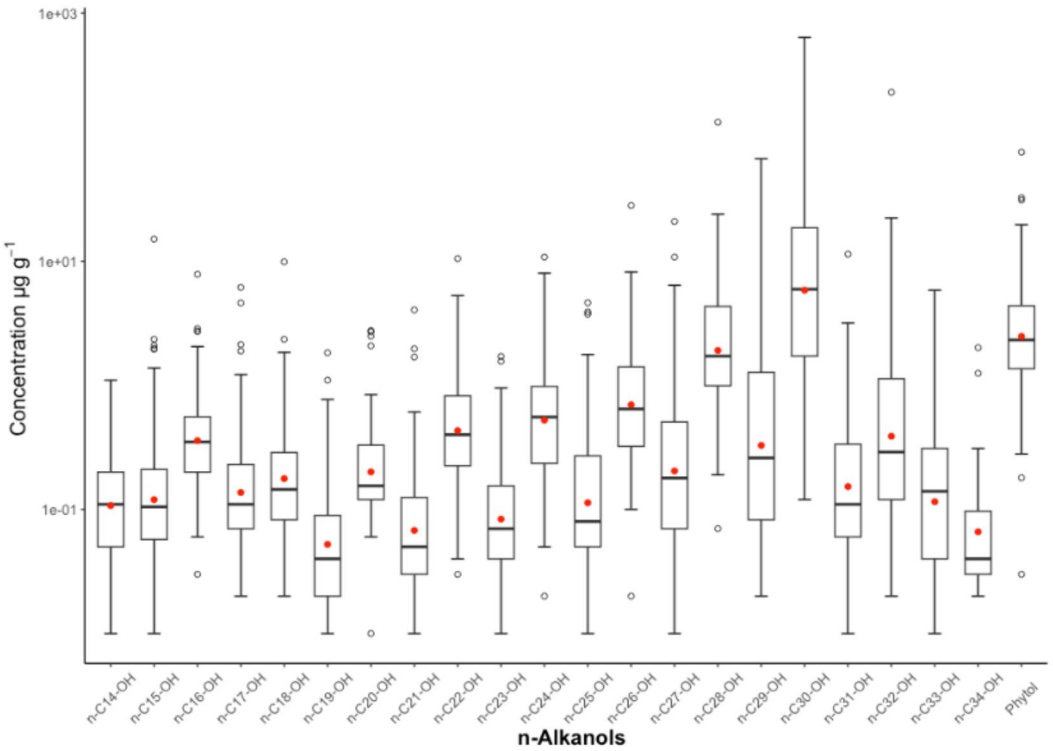

Fig. S3. Box plot of the distribution of *n*-alkanols analysed in the surficial sediments of the Paranaguá Estuarine System, South Atlantic. Open circle: outliers; Red circle: mean value.

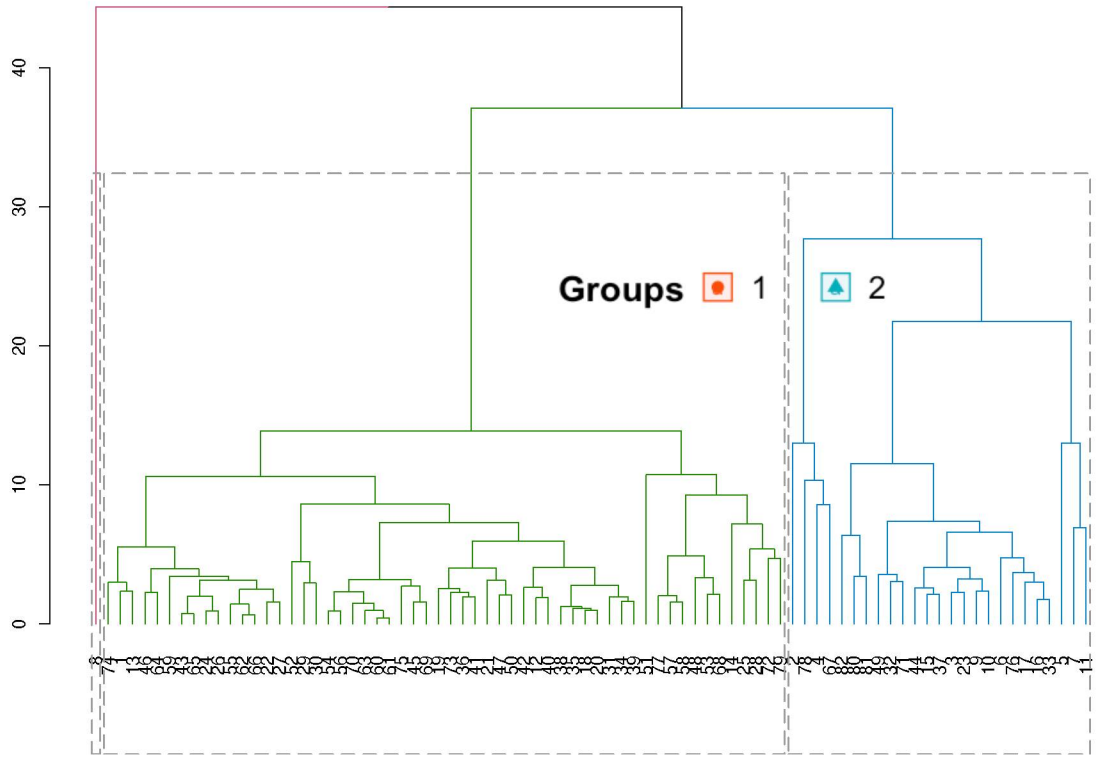

Fig. S4. Cluster analyses performed with full parameters in the surficial sediments of the Paranaguá Estuarine System, South Atlantic, to vectorization. Classes defined according to the cluster analysis: C1 = red; C2 = cyan.

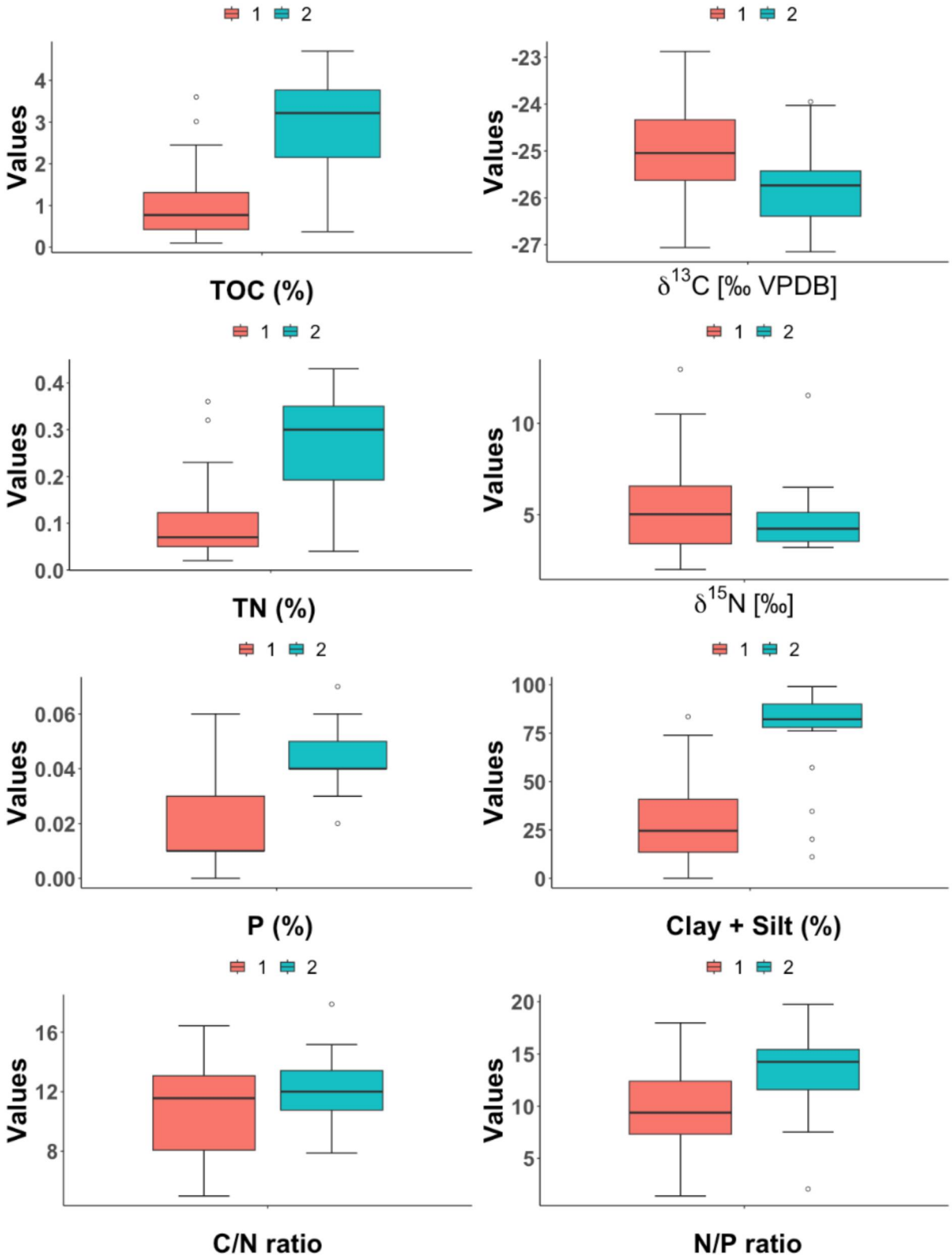

Fig. S5. Box plot of the distribution of TOC, $\delta^{13}C$, TN, $\delta^{15}N$, TP, % fine sediments, C/N and N/P ratios, analysed in the surficial sediments of the Paranaguá Estuarine System, South Atlantic. Classes defined according to the cluster analysis: C1 = red; C2 = cyan.

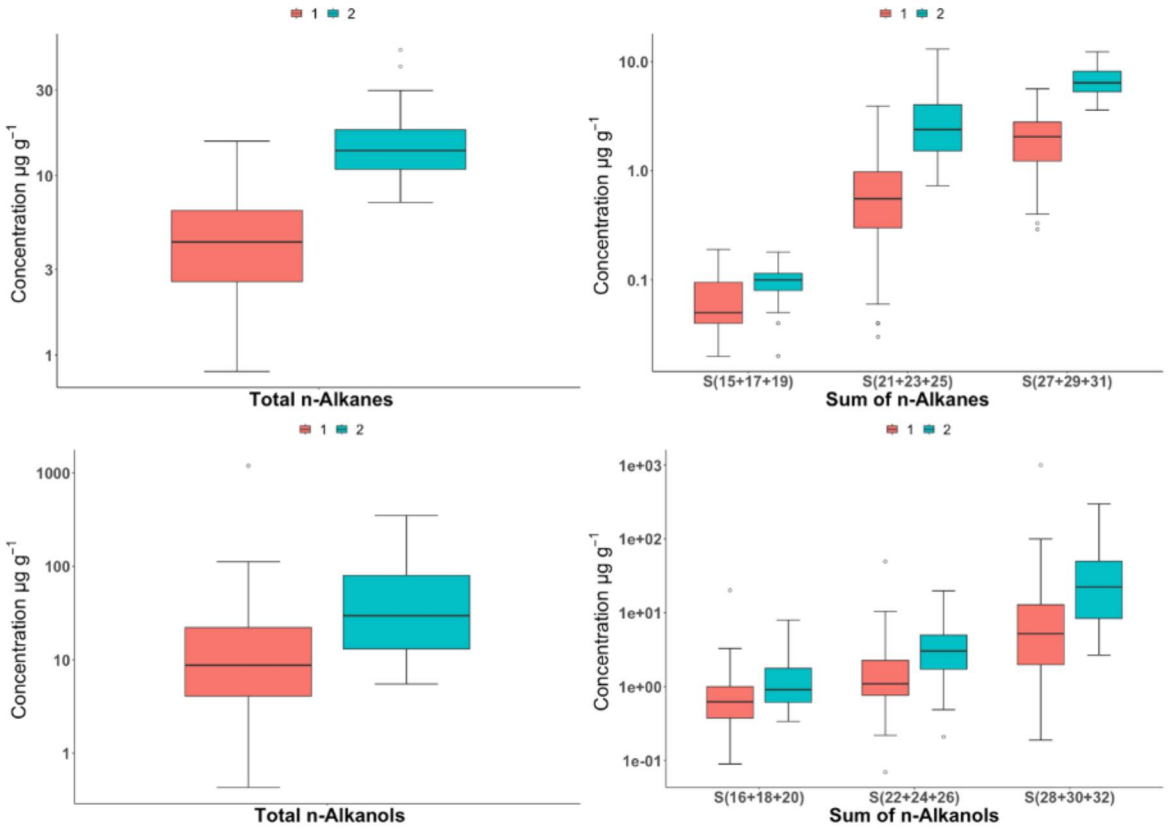

Fig. S6. Box plot of the distribution of the sum of molecular markers (in □g g^{-1}): total *n*-alkanes, short- (Σ *n*-C_{15} + *n*-C_{17} + *n*-C_{19}), mid- (Σ *n*-C_{21} + *n*-C_{23} + *n*-C_{25}) and long-chain (Σ *n*-C_{27} + *n*-C_{29} + *n*-C_{31}) *n*-alkanes, total *n*-alkanols, short- (Σ *n*-C_{16}-OH + *n*-C_{18}-OH + *n*-C_{20}-OH), mid- (Σ *n*-C_{22}-OH + *n*-C_{24}-OH + *n*-C_{26}-OH) and long chain (Σ *n*-C_{28}-OH + *n*-C_{30}-OH + *n*-C_{32}-OH) *n*-alkanols, analysed in the surficial sediments of the Paranaguá Estuarine System, South Atlantic. Open circle: outliers; Classes defined according to the cluster analysis: C1 = red; C2 = cyan.

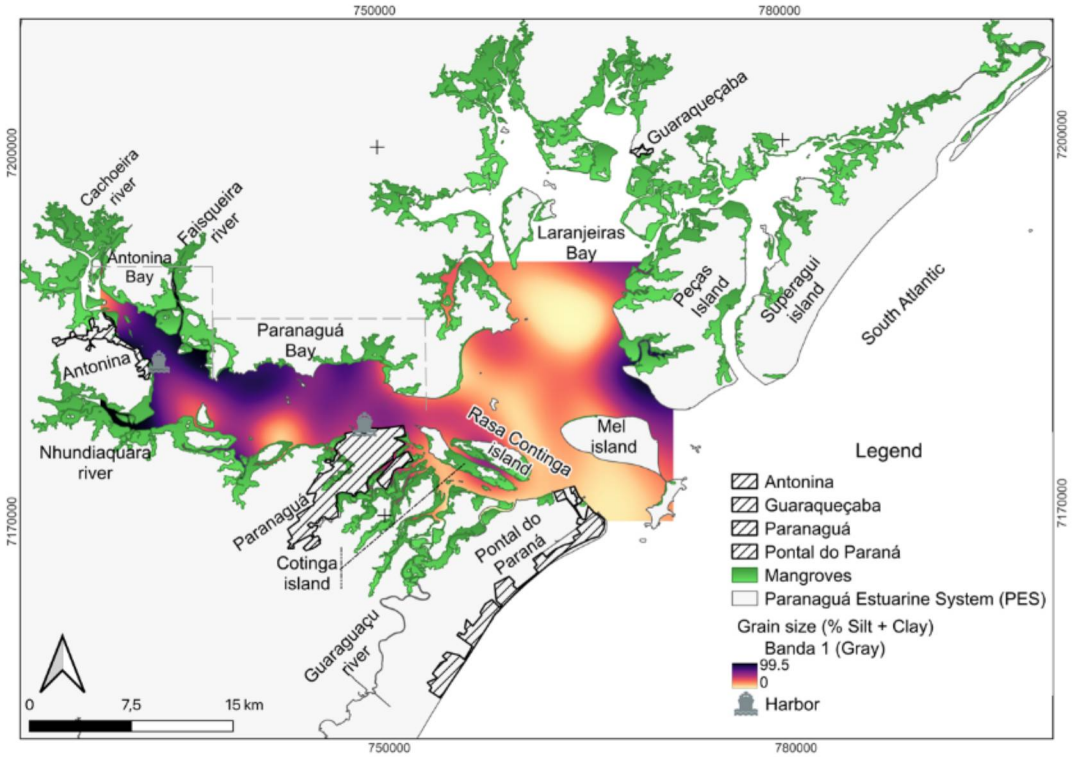

Fig. S7. Distribution map of the % fine sediments (silt + clay) in the surficial sediments of the Paranaguá Estuarine System, South Atlantic.

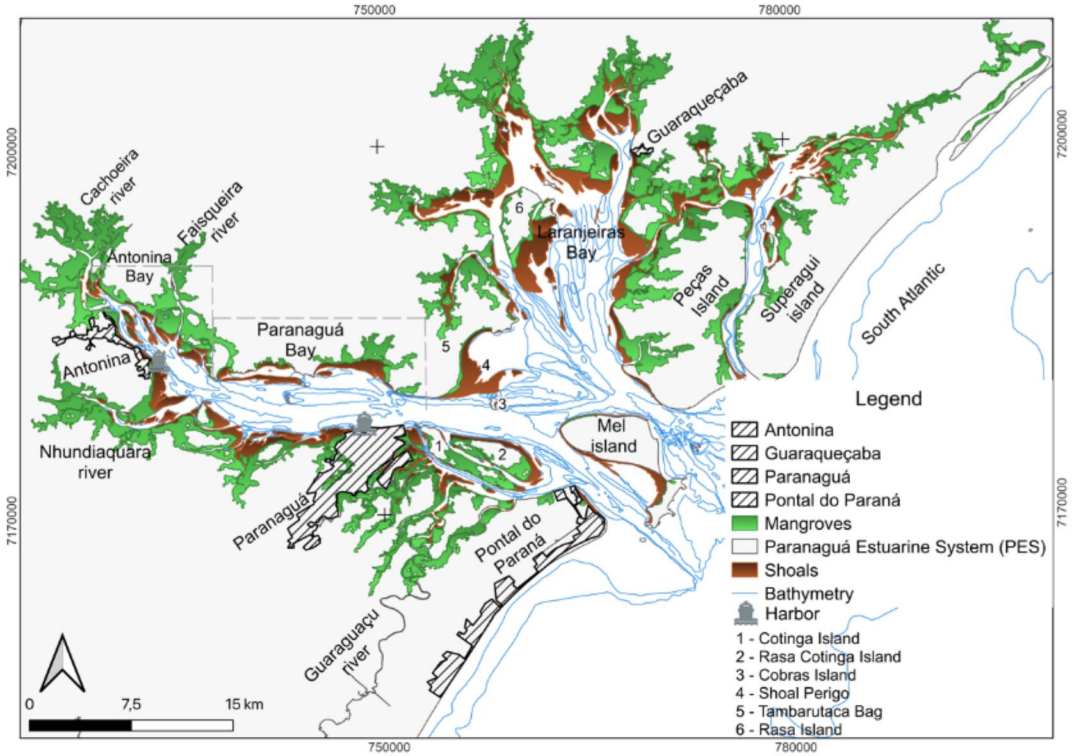

Fig. S8. Map of the location of shallows (brown) and bathymetric lines (blue), in the Paranaguá Estuarine System, South Atlantic.

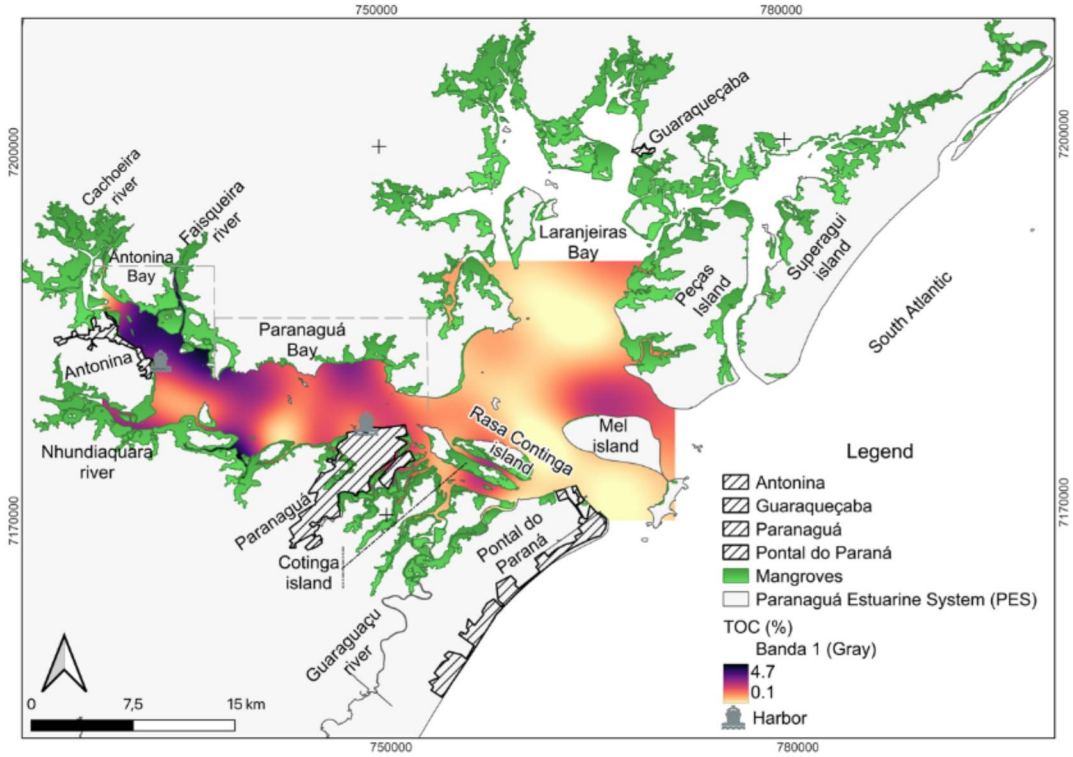

Fig. S9. Distribution map of the % TOC (total organic carbon) in the surficial sediments of the Paranaguá Estuarine System, South Atlantic.

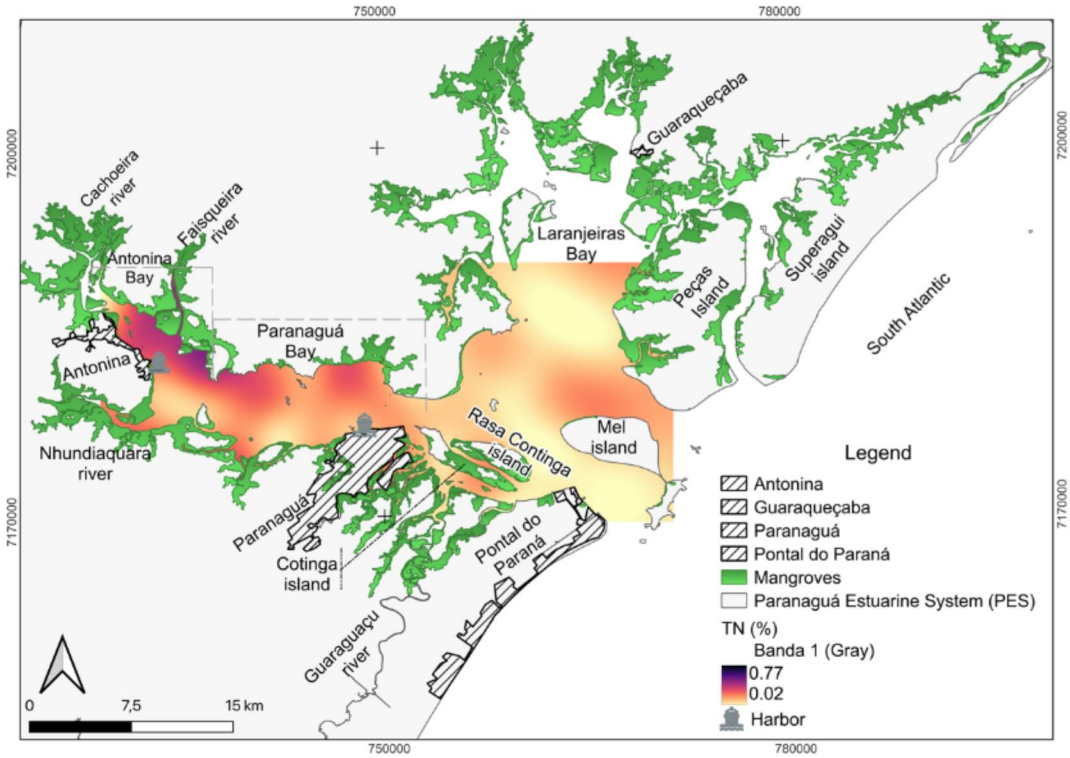

Fig. S10. Distribution map of the % TN (total nitrogen) in the surficial sediments of the Paranaguá Estuarine System, South Atlantic.

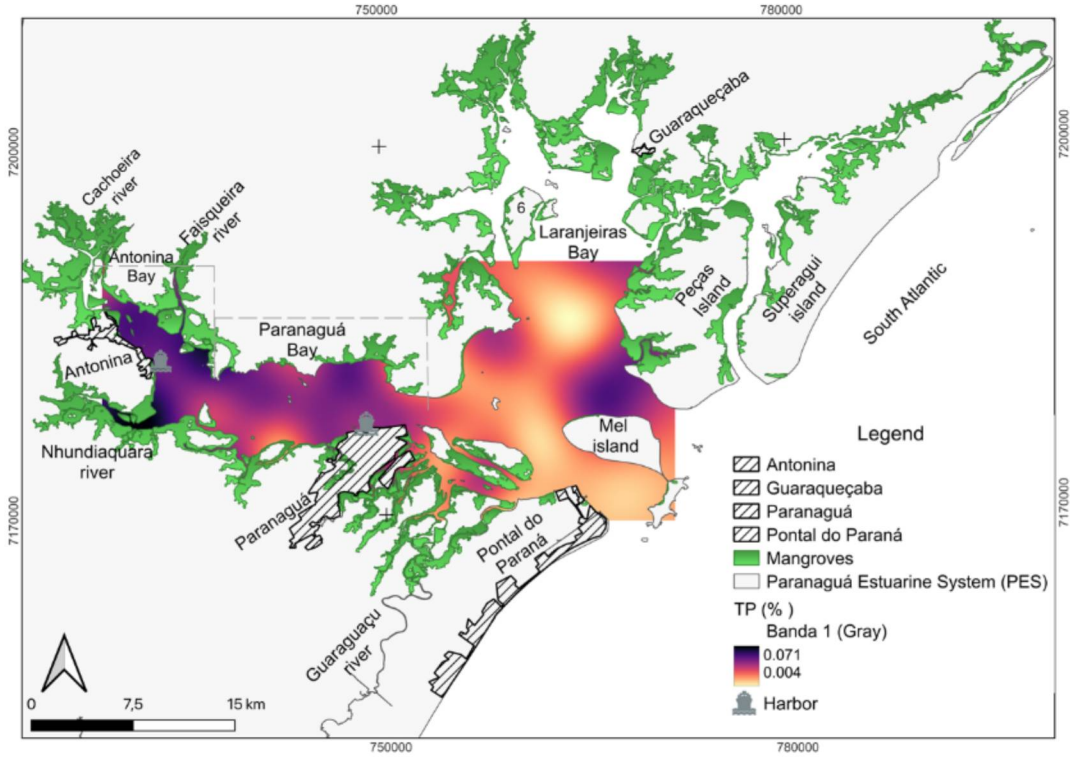

Fig. S11. Distribution map of the % TP (total phosphorus) in the surficial sediments of the Paranaguá Estuarine System, South Atlantic.

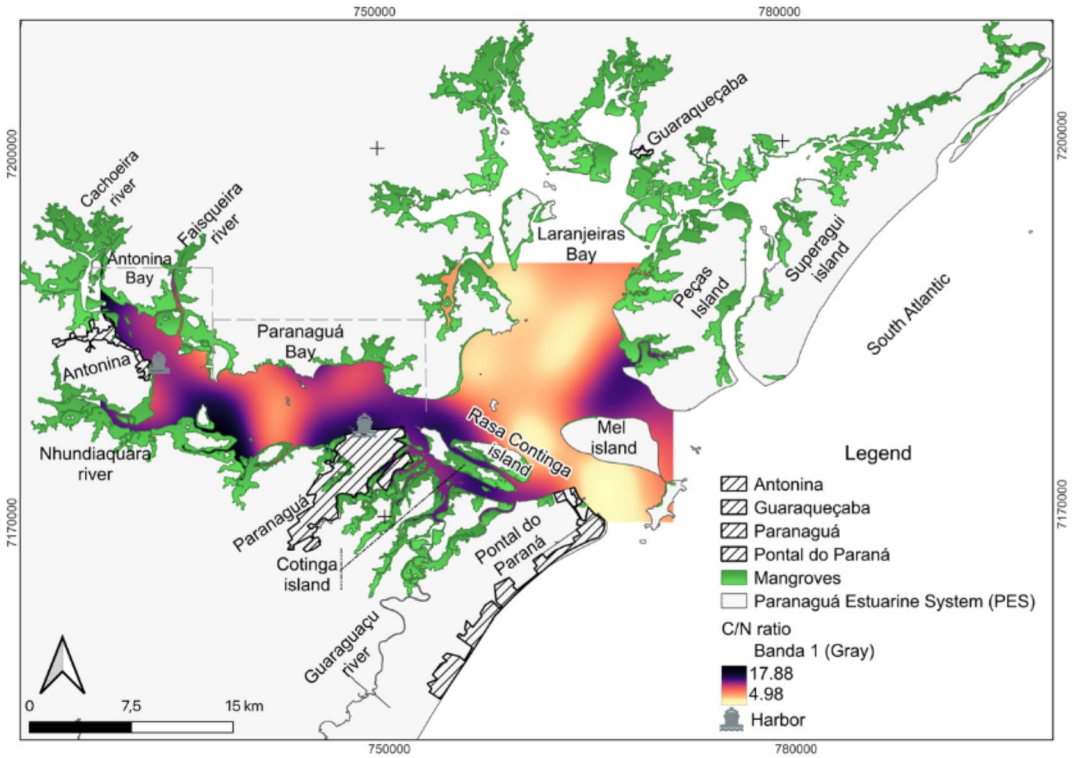

Fig. S12. Distribution map of the C/N ratio in the surficial sediments of the Paranaguá Estuarine System, South Atlantic.

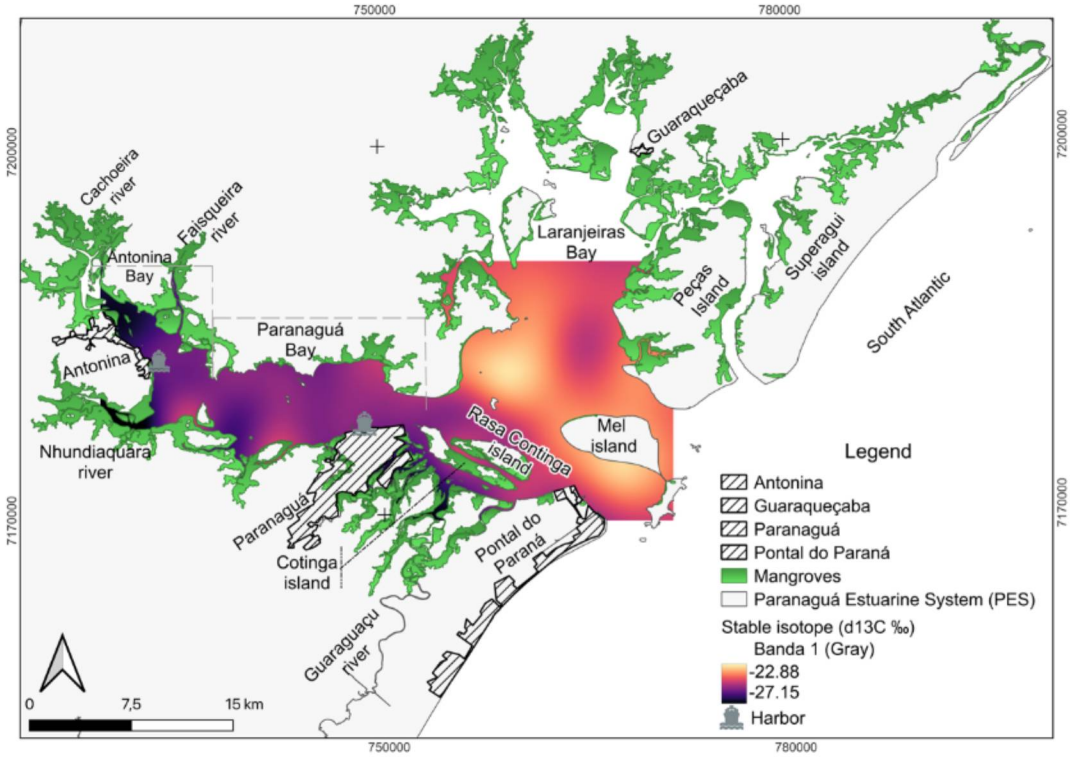

Fig. S13. Distribution map of the $\delta^{13}C$ in the surficial sediments of the Paranaguá Estuarine System, South Atlantic.

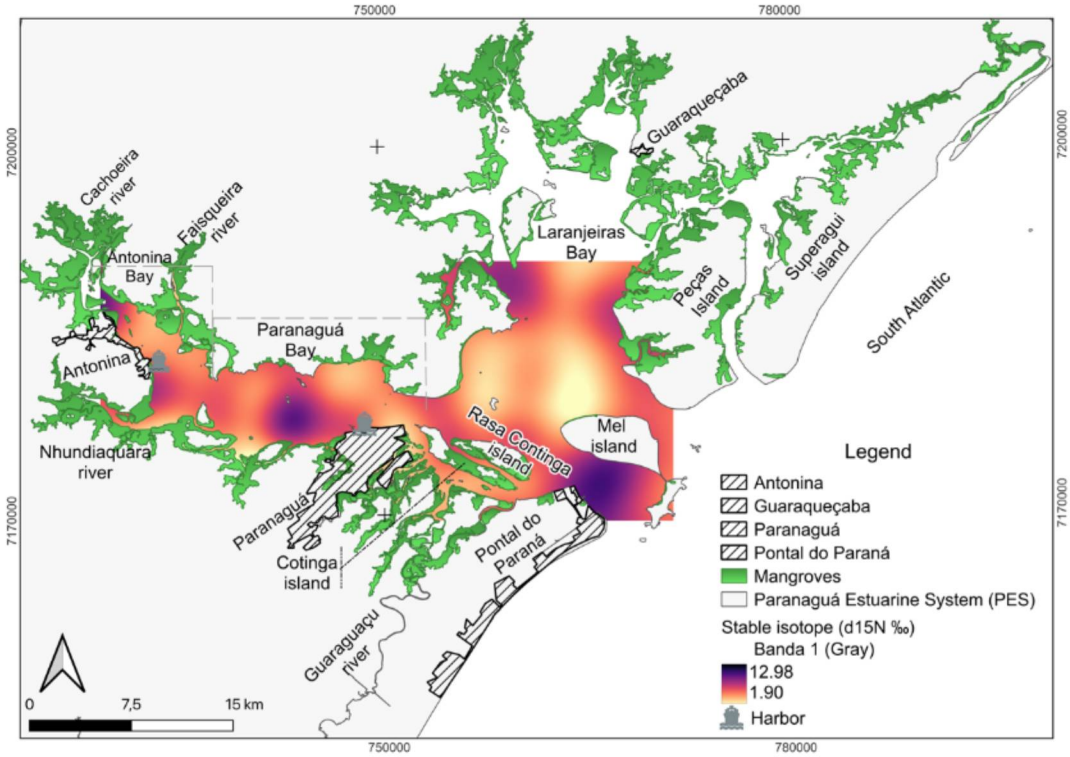

Fig. S14. Distribution map of the $\delta^{15}N$ in the surficial sediments of the Paranaguá Estuarine System, South Atlantic.

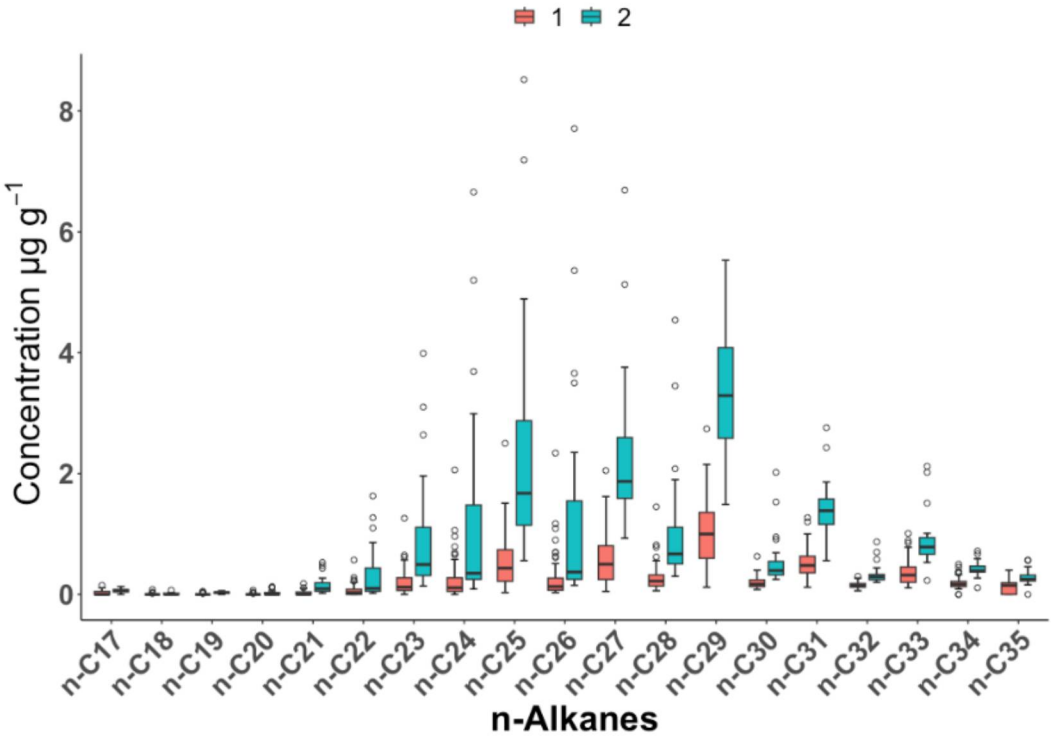

Fig. S15. Box plot of the distribution of individual *n*-alkanes (in □g g^{-1}), analysed in the surficial sediments of the Paranaguá Estuarine System, South Atlantic. Open circle: outliers; Classes defined according to the cluster analysis: C1 = red; C2 = cyan.

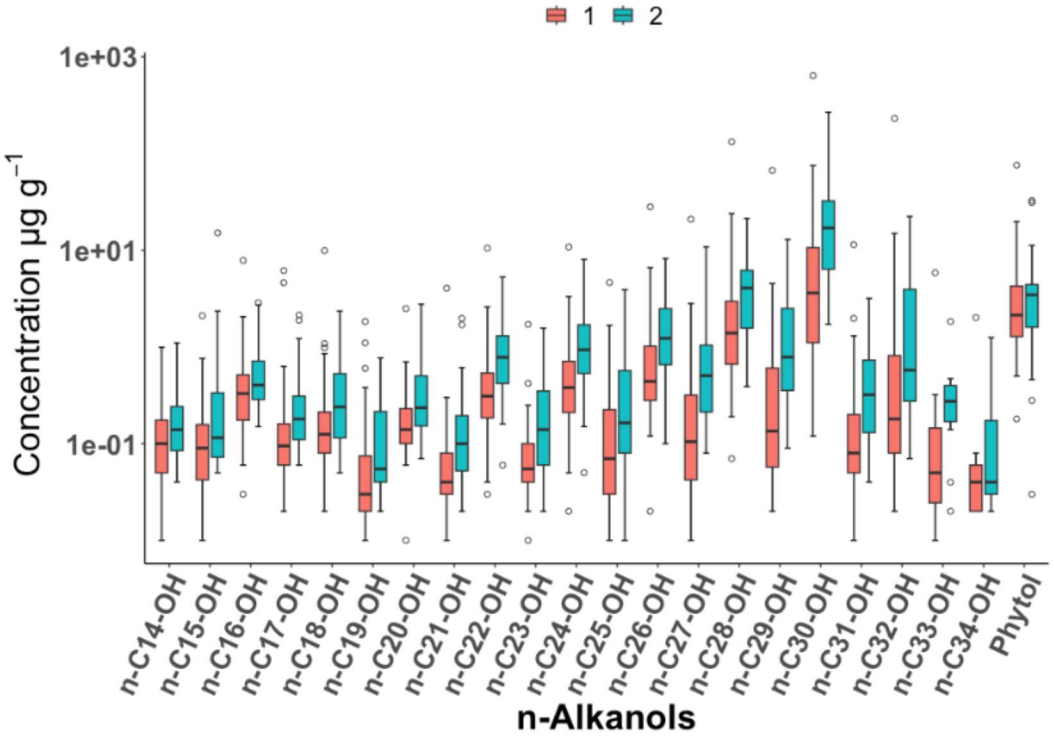

Fig. S16. Box plot of the distribution of individual *n*-alkanols (in □g g^{-1}), analysed in the surficial sediments of the Paranaguá Estuarine System, South Atlantic. Open circle: outliers; Classes defined according to the cluster analysis: C1 = red; C2 = cyan.

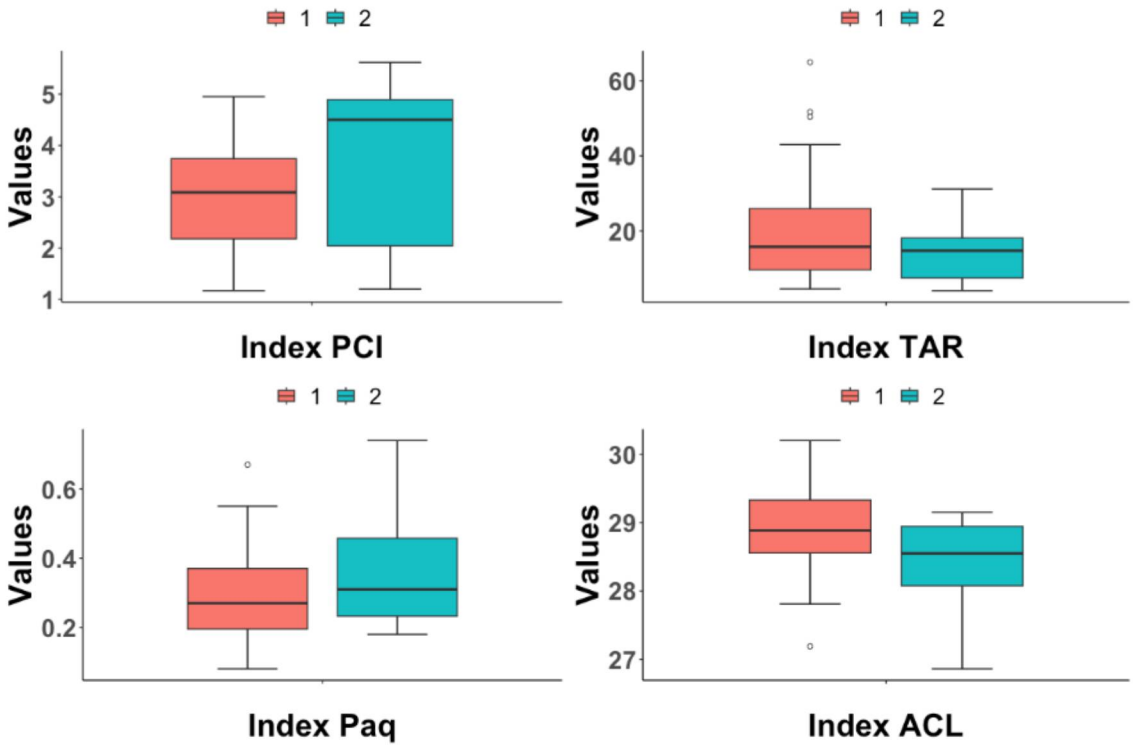

Fig. S17. Box plot of the distribution of diagnostic OM sources (CPI, TAR, P_{aq} and ACL), analysed in the surficial sediments of the Paranaguá Estuarine System, South Atlantic. Classes defined according to the cluster analysis: C1 = red; C2 = cyan.

APÊNDICE 2 – MATERIAL SUPLEMENTAR DO CAPÍTULO II

Table S1. Grain size (% silt + clay), elementary and isotopic composition (TOC, TN, Carbonate, $\delta^{13}C$ and $\delta^{15}N$) and atomic ratios (C/N) in sediments from Paranaguá Estuarine System, Brazil. T1 samples 0–2 to 82–84. TOC: Total Organic Carbon; TN: Total Nitrogen.

Depth (cm)	Estimated date	silt +clay (%)	TOC (%)	TN (%)	Carbonate (%)	C/N	$\delta^{13}C$ (‰)	$\delta^{15}N$ (‰)
0–2	2020	32.03	2.02	0.19	11.50	12.44	–24.57	1.52
2–4	2016	27.38	1.82	0.16	10.44	13.03	–25.90	4.04
4–6	2014	21.06	1.62	0.11	7.58	16.86	–26.21	6.75
6–8	2013	17.93	1.43	0.12	7.64	13.88	–26.25	3.44
8–10	2009	18.97	1.81	0.14	9.0	14.28	–26.41	4.57
10–12	2005	22.33	1.66	0.12	8.05	15.00	–26.36	3.48
12–14	2002	21.01	1.96	0.17	10.78	13.34	–26.03	3.72
14–16	1998	22.48	2.26	0.19	10.8	13.86	–26.22	2.41
16–18	1992	15.94	1.92	0.14	8.92	15.08	–26.09	4.58
18–20	1989	17.41	1.78	0.15	9.82	13.88	–26.23	3.61
20–22	1985	13.60	1.34	0.12	8.91	12.44	–26.04	3.75
22–24	1982	14.43	1.26	0.09	7.93	15.61	–26.55	3.20
24–26	1979	16.14	0.98	0.09	7.99	12.34	–26.29	2.00
26–28	1976	10.41	0.95	0.08	7.57	13.38	–26.33	3.75
28–30	1973	12.87	1.08	0.09	7.83	13.72	–26.48	5.57
30–32	1970	19.54	1.46	0.11	9.61	14.90	–26.18	4.03
32–34	1967	16.66	0.95	0.09	8.00	11.72	–26.21	4.25
34–36	1964	23.61	1.41	0.11	10.36	14.38	–25.68	4.21
36–38	1961	34.68	1.01	0.09	8.95	12.03	–25.50	4.42
38–40	1958	16.31	1.38	0.10	9.64	14.81	–26.02	3.55
40–42	1957	19.21	1.10	0.09	8.55	13.42	–25.97	1.45
42–44	1956	16.60	1.02	0.08	7.09	14.32	–26.26	1.33
44–46	1955	17.36	0.94	0.07	6.78	14.32	–26.27	3.10
46–48	1954	15.78	1.21	0.09	7.37	15.37	–26.47	3.42
48–50	1953	14.18	1.05	0.08	6.74	15.07	–26.00	2.71
50–52	1952	11.97	0.79	0.07	6.11	13.12	–26.49	2.94
52–54	1951	13.19	1.06	0.07	6.36	16.35	–26.32	2.40
54–56	1951	12.92	1.03	0.07	7.41	17.13	–26.08	7.74
56–58	1950	15.34	1.28	0.06	8.13	24.60	–26.32	8.96
58–60	1949	17.13	0.92	0.06	7.41	16.79	–26.00	9.08
60–62	1948	11.74	0.79	0.04	6.09	18.64	–26.18	9.52
62–64	1946	13.95	0.67	0.04	6.23	18.30	–25.88	9.34
64–66	1944	16.51	1.13	0.06	8.03	18.98	–26.01	6.13
66–68	1943	13.76	0.66	0.04	6.25	15.44	–25.89	8.28
68–70	1941	14.99	0.71	0.03	5.53	22.70	–25.97	13.74
70–72	1939	13.29	0.89	0.04	5.74	24.07	–26.01	10.69
72–74	1933	12.83	0.57	0.04	5.41	15.25	–25.95	10.47
74–76	1927	10.47	0.45	0.03	4.33	16.58	–25.92	14.19
76–78	1922	10.16	0.40	0.02	3.59	18.65	–26.30	13.83
78–80	1916	8.29	0.35	0.02	2.63	20.36	–26.09	19.99
80–82	1910	16.25	1.37	0.11	7.13	14.00	–26.15	3.82
82–84	1905	16.75	1.00	0.08	7.25	13.37	–26.03	4.55

Table S1 (continued). T1 samples 84–86 to 118–120.

Depth (cm)	Estimated date	silt +clay (%)	TOC (%)	TN (%)	Carbonate (%)	C/N	$\delta^{13}C$ (‰)	$\delta^{15}N$ (‰)
84–86	1901	12.62	0.76	0.06	0.06	13.85	–26.01	4.34
86–88	1896	11.64	0.68	0.05	0.05	13.65	–26.17	1.92
88–90	1891	8.79	0.58	0.04	0.04	14.64	–26.16	1.58
90–92	1886	5.73	0.29	0.02	0.02	11.49	–25.95	5.12
92–94	1882	4.15	0.29	0.03	0.03	11.3	–27.15	9.93
94–96	1877	0.00	0.12	0.01	0.01	8.34	–26.19	21.72
96–98	1872	0.00	0.12	0.01	0.01	8.91	–26.47	18.33
98–100	1868	0.00	0.09	0.01	0.01	9.83	–26.87	26.37
100–102	1863	0.00	0.20	0.01	0.01	18.69	–26.75	23.44
102–104	1858	0.00	0.10	0.01	0.01	9.96	–27.18	22.68
104–106	1854	1.56	0.11	0.01	0.01	9.33	–26.62	21.24
106–108	1849	0.00	0.16	0.01	0.01	10.65	–26.80	19.52
108–110	1844	0.00	0.20	0.01	0.01	13.02	–26.28	17.25
110–112	1839	5.90	0.27	0.03	0.03	10.05	–25.06	5.95
112–114	1835	6.34	0.47	0.03	0.03	13.95	–26.05	5.74
114–116	1830	7.16	0.57	0.05	0.05	12.59	–26.56	1.81
116–118	1825	10.12	0.87	0.05	0.05	17.77	–26.38	3.52
118–120	1821	13.35	1.15	0.06	0.06	21.04	–26.50	5.04

Table S2. Grain size (% silt + clay), elementary and isotopic composition (TOC, TN, Carbonate, $\delta^{13}C$ and $\delta^{15}N$) and atomic ratios (C/N) in sediments from Paranaguá Estuarine System, Brazil. T2 samples 0–2 to 82–84. TOC: Total Organic Carbon; TN: Total Nitrogen. NA: not analysed.

Depth (cm)	Estimated date	silt +clay (%)	TOC (%)	TN (%)	Carbonate (%)	C/N	$\delta^{13}C$ (‰)	$\delta^{15}N$ (‰)
0–2	2020	NA	2.66	0.26	18.39	11.68	–25.44	2.64
2–4	2019	94.89	2.35	0.29	24.26	9.26	–25.34	–0.78
4–6	2018	94.02	2.18	0.24	23.49	10.27	–25.45	2.59
6–8	2014	93.43	3.11	0.23	11.12	15.46	–26.26	3.38
8–10	2011	58.12	2.00	0.22	22.26	10.56	–25.56	3.84
10–12	2001	41.49	1.48	0.13	13.45	12.41	–26.43	2.46
12–14	1999	79.53	1.46	0.1	11.68	15.73	–26.18	5.72
14–16	1992	27.41	1.25	0.12	10.10	12.10	–26.77	3.00
16–18	1986	23.93	0.72	0.06	6.79	12.83	–26.52	4.28
18–20	1984	15.85	0.73	0.07	5.84	12.18	–27.00	1.35
20–22	1983	26.86	0.51	0.05	5.23	10.45	–26.32	3.01
22–24	1979	13.48	0.42	0.04	6.11	11.46	–26.29	8.27
24–26	1977	11.69	0.36	0.04	4.89	9.76	–25.84	9.43
26–28	1975	21.36	0.38	0.03	4.81	12.40	–25.8	9.69
28–30	1972	NA	0.44	0.03	5.11	13.89	–26.14	11.91
30–32	1970	NA	0.36	0.04	4.95	10.70	–26.02	10.79
32–34	1967	NA	0.45	0.04	4.72	12.83	–26.49	7.50
34–36	1967	NA	0.36	0.04	5.39	9.74	–25.92	9.81
36–38	1966	NA	0.34	0.04	5.43	8.59	–25.68	4.01
38–40	1965	NA	0.46	0.06	5.71	8.93	–26.10	–0.06
40–42	1961	NA	0.41	0.04	5.29	10.05	–25.81	5.83
42–44	1958	NA	0.41	0.03	4.83	12.42	–25.90	6.87
44–46	1957	NA	0.37	0.04	4.32	10.02	–25.78	9.83
46–48	1956	NA	0.31	0.03	6.23	9.74	–25.77	7.00
48–50	1955	NA	0.35	0.04	6.75	8.69	–25.62	8.99
50–52	1954	NA	0.42	0.04	7.98	11.34	–25.98	12.24
52–54	1953	NA	0.25	0.04	5.37	7.55	–25.81	–2.15
54–56	1952	NA	0.22	0.02	5.99	12.36	–25.30	18.22
56–58	1950	54.71	1.04	0.07	10.03	15.22	–26.49	4.45
58–60	1948	67.26	0.76	0.07	9.15	11.39	–25.81	6.83
60–62	1947	67.06	0.80	0.07	8.47	12.92	–25.93	2.97
62–64	1945	42.59	0.97	0.08	10.81	13.05	–26.37	2.63
64–66	1943	37.43	1.28	0.10	12.84	14.93	–26.39	5.70
66–68	1940	NA	1.22	0.12	11.83	11.81	–26.09	8.20
68–70	1938	78.27	1.82	0.15	16.61	13.39	–26.36	4.12
70–72	1935	84.38	2.13	0.20	18.31	12.43	–26.32	1.76
72–74	1933	46.38	2.13	0.19	17.57	12.81	–26.27	6.49
74–76	1929	84.45	2.14	0.18	19.34	13.42	–26.21	4.71
76–78	1924	82.63	2.66	0.21	20.22	14.43	–26.37	3.58
78–80	1920	82.61	2.49	0.19	18.02	14.97	–26.37	4.87
80–82	1916	68.25	2.11	0.19	18.09	12.53	–26.25	3.98
82–84	1911	69.95	1.97	0.15	17.81	15.10	–26.34	6.62

Table S2 (continued). T2 samples 84–86 to 118–120.

Depth (cm)	Estimated date	silt +clay (%)	TOC (%)	TN (%)	Carbonate (%)	C/N	$\delta^{13}C$ (‰)	$\delta^{15}N$ (‰)
84–86	1903	84.06	2.41	0.21	20.62	13.15	–26.26	2.85
86–88	1895	88.20	2.32	0.20	21.72	13.03	–25.90	7.08
88–90	1887	91.20	2.45	0.25	22.48	11.31	–25.65	2.80
90–92	1878	91.14	2.07	0.22	21.61	10.97	–25.56	3.20
92–94	1870	89.13	2.14	0.20	20.51	12.15	–25.89	4.91
94–96	1862	86.81	2.07	0.21	20.10	11.47	–25.78	4.60
96–98	1854	90.52	2.20	0.22	20.91	11.30	–25.70	3.52
98–100	1845	92,00	2.33	0.24	22.68	10.90	–25.63	6.15
100–102	1837	95.64	2.24	0.24	21.28	10.79	–25.49	4.35
102–104	1829	86.44	3.47	0.28	21.68	14.44	–26.35	3.90
104–106	1821	84.21	2.34	0.19	20.30	13.79	–25.90	5.50
106–108	1812	85.63	1.75	0.18	20.24	11.11	–25.89	3.77
108–110	1804	79.31	2.56	0.21	20.88	13.87	–26.26	2.55
110–112	1796	75.43	2.21	0.23	21.28	10.77	–26.26	–0.53
112–114	1788	91.47	2.77	0.24	22.75	13.30	–26.18	3.51
114–116	1779	85.27	4.17	0.26	24.23	18.57	–26.68	–0.14
116–118	1771	92.68	3.67	0.27	22.94	15.79	–26.71	–0.37
118–120	1763	90.60	3.43	0.23	22.31	16.95	–26.10	4.42

Table S3. Grain size (% silt + clay), elementary and isotopic composition (TOC, TN, Carbonate, $\delta^{13}C$ and $\delta^{15}N$) and atomic ratios (C/N) in sediments from Paranaguá Estuarine System, Brazil. T3 samples 0–2 to 82–84. TOC: Total Organic Carbon; TN: Total Nitrogen.

Depth (cm)	Estimated date	silt +clay (%)	TOC (%)	TN (%)	Carbonate (%)	C/N	$\delta^{13}C$ (‰)	$\delta^{15}N$ (‰)
0–2	2020	85.10	2.36	0.25	23.54	10.99	–26.33	4.40
2–4	2018	81.09	1.40	0.12	17.79	13,00	–25.99	5.51
4–6	2017	72.90	1.53	0.16	20.30	10.63	–25.67	4.92
6–8	2013	70.76	1.54	0.16	20.38	10.94	–26.02	5.71
8–10	2010	70.57	1.58	0.14	16.78	12.82	–25.88	5.55
10–12	2007	43.13	1.33	0.12	16.55	12.45	–25.80	7.18
12–14	2004	55.57	1.16	0.11	14.57	11.70	–26.10	6.29
14–16	2000	76.64	1.18	0.12	17.57	11.07	–25.75	5.61
16–18	1999	94.28	2.11	0.24	24.71	10.11	–25.89	3.20
18–20	1996	93.12	2.54	0.28	26.37	10.45	–25.87	3.45
20–22	1991	80.53	2.2	0.24	25.18	10.67	–25.93	4.85
22–24	1991	86.55	2.57	0.28	25.8	10.50	–25.98	4.41
24–26	1990	94.43	2.52	0.26	25.74	11.05	–25.91	4.49
26–28	1990	94.11	2.84	0.31	26.63	10.71	–25.95	4.03
28–30	1990	93.59	2.55	0.28	26.02	10.54	–25.87	3.99
30–32	1989	95.97	2.66	0.31	26.65	9.99	–25.95	3.22
32–34	1989	95.46	2.69	0.30	25.21	10.44	–25.93	3.73
34–36	1988	95.41	2.23	0.28	34.99	9.21	–25.98	3.59
36–38	1988	96.92	2.16	0.25	24.87	10.12	–25.90	3.03
38–40	1987	94.95	2.74	0.30	26.47	10.58	–25.95	2.75
40–42	1986	96.79	2.51	0.27	27.21	10.56	–25.89	3.04
42–44	1985	92.30	2.58	0.29	28.35	10.21	–25.67	4.60
44–46	1984	95.73	2.61	0.29	25.82	10.30	–25.86	1.67
46–48	1983	97.34	2.55	0.27	26.36	10.72	–25.68	4.47
48–50	1982	96.87	2.64	0.29	25.49	10.51	–25.94	4.97
50–52	1981	94.56	2.38	0.29	26.31	9.56	–25.72	4.28
52–54	1981	92.35	2.35	0.24	27.09	11.23	–25.83	5.66
54–56	1978	82.74	2.13	0.21	23.81	11.65	–25.71	6.40
56–58	1975	84.65	2.06	0.20	21.86	11.57	–25.58	6.51
58–60	1973	89.37	2.63	0.24	22.64	12.79	–26.07	6.28
60–62	1970	86.01	1.48	0.13	15.34	12.57	–26.44	6.66
62–64	1969	16.45	0.40	0.04	6.91	10.60	–26.23	6.04
64–66	1969	17.41	0.24	0.02	5.45	11.45	–26.11	17.17
66–68	1968	72.34	0.80	0.07	15.85	11.90	–25.40	5.11
68–70	1967	28.22	0.30	0.02	7.23	12.98	–26.11	11.60
70–72	1966	18.23	0.34	0.03	9.23	10.27	–26.21	11.33
72–74	1965	28.77	0.55	0.05	9.53	12.38	–25.83	5.75
74–76	1963	23.43	0.22	0.02	6.16	10.27	–26.01	13.22
76–78	1962	31.03	0.51	0.06	10.72	9.72	–25.72	4.27
78–80	1961	52.79	0.65	0.05	11.89	13.39	–25.13	7.99
80–82	1959	46.24	0.79	0.04	7.72	18.82	–27.11	6.64
82–84	1957	18.98	0.28	0.02	6.49	13.38	–25.82	20.10

Table S3 (continued). T3 samples 84–86 to 118–120.

Depth (cm)	Estimated date	silt +clay (%)	TOC (%)	TN (%)	Carbonate (%)	C/N	$\delta^{13}C$ (‰)	$\delta^{15}N$ (‰)
84–86	1955	37.51	0.35	0.03	6.93	12.55	–25.59	14.60
86–88	1952	30.04	0.34	0.03	8.02	10.59	–25.13	12.39
88–90	1950	36.15	0.29	0.03	7.01	11.15	–25.49	8.77
90–92	1948	13.08	0.24	0.03	6.83	9.16	–25.84	12.19
92–94	1946	21.31	0.38	0.03	7.75	12.96	–25.02	7.81
94–96	1944	NA	0.35	0.03	8.53	10.65	–25.32	8.34
96–98	1941	16.18	0.47	0.04	8.51	13.17	–25.52	7.75
98–100	1939	16.88	0.82	0.05	11.86	18.94	–26.04	9.29
100–102	1937	31.63	0.57	0.04	10.8	14.22	–25.80	9.05
102–104	1935	50.86	0.46	0.04	9.61	12.52	–26.16	6.53
104–106	1933	29.79	0.66	0.03	10.70	22.03	–25.83	16.95
106–108	1930	37.19	0.24	0.01	6.37	25.64	–25.76	36.34
108–110	1928	22.66	0.43	0.02	8.51	20.47	–25.94	22.46
110–112	1926	59.24	0.92	0.04	16.74	23,00	–25.69	10.44
112–114	1924	86.25	1.41	0.08	21.89	20.63	–25.22	9.88
114–116	1922	53.49	0.70	0.04	15.76	20.55	–25.14	16.53
116–118	1919	11.69	0.19	0.01	7.39	22.34	–25.94	41.12
118–120	1917	13.61	0.29	0.01	5.25	20.33	–25.80	27.62

Table S4. Grain size (% silt + clay), elementary and isotopic composition (TOC, TN, Carbonate, $\delta^{13}C$ and $\delta^{15}N$) and atomic ratios (C/N) in sediments from Paranaguá Estuarine System, Brazil. T4 samples 0–2 to 82–84. TOC: Total Organic Carbon; TN: Total Nitrogen. NA: not analysed.

Depth (cm)	Estimated date	silt +clay (%)	TOC (%)	TN (%)	Carbonate (%)	C/N	$\delta^{13}C$ (‰)	$\delta^{15}N$ (‰)
0–2	2020	NA	3.87	0.33	21.40	13.64	–25.61	5.27
2–4	2018	99.54	3.92	0.33	23.11	13.60	–25.85	5.41
4–6	2017	99.62	3.97	0.33	22.42	13.70	–25.73	5.53
6–8	2016	99.58	4.10	0.33	21.70	14.11	–25.78	5.46
8–10	2014	99.72	4.19	0.34	21.41	13.98	–25.82	5.25
10–12	2012	99.27	3.77	0.32	20.28	13.37	–25.58	5.24
12–14	2010	99.42	3.80	0.33	23.17	13.24	–25.46	5.73
14–16	2008	99.39	3.70	0.33	23.54	12.87	–25.56	5.54
16–18	2004	99.56	3.80	0.34	22.27	12.97	–25.57	5.62
18–20	2000	98.97	3.71	0.31	22.49	13.69	–25.58	5.68
20–22	1996	99.89	3.46	0.31	22.59	12.74	–25.79	5.57
22–24	1990	99.89	3.34	0.29	27.65	13.34	–25.95	5.18
24–26	1984	99.92	2.06	0.23	19.26	10.11	–25.79	4.44
26–28	1980	94.69	2.60	0.18	17.79	16.14	–26.10	6.75
28–30	1977	73.82	2.88	0.18	19.01	17.84	–26.05	8.17
30–32	1976	61.14	1.85	0.12	18.29	17.76	–25.88	10.16
32–34	1974	53.90	1.29	0.08	24.41	17.46	–25.57	12.62
34–36	1973	60.38	1.97	0.12	20.89	18.24	–25.68	9.50
36–38	1972	55.84	1.83	0.12	18.94	17.01	–25.77	8.02
38–40	1971	71.28	1.35	0.09	13.85	17.38	–25.75	8.94
40–42	1970	61.44	1.10	0.08	13.64	15.62	–25.24	10.1
42–44	1969	52.20	0.88	0.07	14.05	13.45	–25.27	8.19
44–46	1968	46.58	0.83	0.07	13.52	13.39	–24.83	2.28
46–48	1966	67.31	1.11	0.06	15.10	20.58	–23.80	7.50
48–50	1964	58.60	1.03	0.07	17.20	15.08	–24.77	6.62
50–52	1963	70.67	1.17	0.07	17.38	17.45	–24.77	8.00
52–54	1961	69.97	1.07	0.08	17.47	15.42	–24.47	7.41
54–56	1959	81.10	1.27	0.07	17.45	18.73	–25.06	6.85
56–58	1956	68.90	1.07	0.08	18.32	15.68	–24.53	5.92
58–60	1954	87.65	1.21	0.08	18.88	16.45	–24.37	7.07
60–62	1952	87.56	1.27	0.08	18.47	18.31	–24.56	5.85
62–64	1949	85.16	1.14	0.06	18.36	20.64	–24.39	6.31
64–66	1947	71.96	1.17	0.06	19.55	21.00	–24.42	5.24
66–68	1944	77.03	1.38	0.10	18.92	16.09	–24.63	7.28
68–70	1942	80.31	1.40	0.10	18.71	16.04	–24.56	4.53
70–72	1940	60.21	1.27	0.10	18.62	13.78	–24.66	5.37
72–74	1937	59.17	1.31	0.10	19.70	14.95	–24.69	7.06
74–76	1935	86.58	1.23	0.09	18.08	14.43	–24.59	7.33
76–78	1933	64.69	1.18	0.09	19.23	14.29	–24.41	7.30
78–80	1930	77.58	1.24	0.10	18.34	13.65	–24.54	4.91
80–82	1928	72.06	1.33	0.10	19.48	15.14	–24.49	7.51
82–84	1926	74.14	1.27	0.09	17.47	16.40	–24.63	8.08

Table S4 (continued). T4 samples 84–86 to 118–120.

Depth (cm)	Estimated date	silt +clay (%)	TOC (%)	TN (%)	Carbonate (%)	C/N	$\delta^{13}C$ (‰)	$\delta^{15}N$ (‰)
84–86	1923	71.13	1.05	0.08	17.65	14.70	–24.58	7.98
86–88	1921	60.55	1.36	0.07	19.02	20.48	–25.00	5.29
88–90	1918	66.07	0.96	0.06	16.18	18.03	–24.56	6.26
90–92	1916	73.48	0.92	0.06	15.04	17.37	–24.48	8.58
92–94	1912	82.23	1.10	0.06	18.18	20.02	–24.45	8.77
94–96	1908	74.46	1.01	0.07	18.40	16.35	–24.35	4.52
96–98	1904	73.95	1.12	0.06	17.16	19.16	–25.04	7.52
98–100	1900	94.49	0.83	0.06	14.55	15.54	–24.61	6.21
100–102	1896	85.77	0.97	0.07	15.68	16.19	–24.65	7.03
102–104	1900	83.12	1.10	0.08	15.33	15.72	–25.10	5.27
104–106	1896	65.02	1.04	0.08	16.86	14.35	–24.67	5.89
106–108	1893	69.17	1.19	0.10	18.72	13.79	–25.02	2.60
108–110	1889	59.15	0.99	0.08	17.05	14.46	–24.76	5.55
110–112	1885	66.23	0.96	0.07	15.60	14.49	–25.03	5.59
112–114	1881	52.81	1.07	0.07	18.68	16.16	–25.61	6.90
114–116	1877	52.12	1.14	0.09	18.73	14.36	–24.65	4.34
116–118	1873	73.06	1.06	0.09	18.05	12.55	–24.64	2.66
118–120	1869	69.28	0.75	0.07	13.64	12.05	–25.16	1.81

Table S5. Grain size (% silt + clay), elementary and isotopic composition (TOC, TN, Carbonate, $\delta^{13}C$ and $\delta^{15}N$) and atomic ratios (C/N) in sediments from Paranaguá Estuarine System, Brazil. T5 samples 0–2 to 82–84. TOC: Total Organic Carbon; TN: Total Nitrogen. NA: not analysed.

Depth (cm)	Estimated date	silt +clay (%)	TOC (%)	TN (%)	Carbonate (%)	C/N	$\delta^{13}C$ (‰)	$\delta^{15}N$ (‰)
0–2	2020	11.45	1.52	0.09	5.53	18.93	–26.36	5.00
2–4	2018	20.60	0.98	0.08	5.39	13.68	–25.80	5.68
4–6	2017	21.98	0.98	0.07	6.01	15.79	–25.61	5.58
6–8	2015	13.54	0.76	0.06	4.35	13.87	–25.50	5.72
8–10	2013	20.15	0.93	0.06	4.67	16.46	–25.54	6.57
10–12	2010	23.18	0.86	0.05	4.69	17.94	–25.14	5.63
12–14	2008	19.01	0.94	0.07	5.59	15.10	–25.27	6.90
14–16	2007	12.06	0.84	0.05	4.47	16.96	–25.14	6.31
16–18	2006	22.12	0.92	0.05	4.95	20.43	–25.81	6.77
18–20	2005	16.35	0.81	0.06	4.61	15.63	–25.71	6.03
20–22	2004	15.47	0.83	0.05	4.53	18.73	–25.73	5.70
22–24	2004	20.88	0.80	0.07	4.49	12.82	–25.71	3.69
24–26	2003	16.08	0.78	0.05	4.37	15.46	–25.85	4.33
26–28	2002	38.63	0.93	0.05	4.69	20.27	–26.06	6.64
28–30	2001	14.23	0.76	0.04	4.43	19.06	–25.44	7.60
30–32	1998	12.59	0.96	0.07	4.73	16.15	–25.98	4.54
32–34	1994	27.45	0.91	0.05	5.13	18.96	–25.95	6.36
34–36	1991	34.56	0.74	0.04	4.39	17.74	–25.78	7.47
36–38	1989	15.21	0.93	0.05	4.99	19.81	–25.92	6.40
38–40	1986	23.06	1.04	0.06	4.81	17.65	–26.11	5.03
40–42	1985	10.24	1.64	0.05	4.61	34.92	–27.69	6.35
42–44	1984	18.56	1.10	0.07	4.91	17.13	–26.36	6.14
44–46	1982	16.97	1.35	0.05	4.95	26.80	–26.43	6.28
46–48	1981	14.84	1.26	0.06	4.65	24.14	–26.50	5.42
48–50	1980	8.31	1.49	0.06	5.09	29.15	–26.60	6.46
50–52	1979	8.87	1.46	0.05	5.09	30.52	–26.85	5.89
52–54	1978	13.52	1.23	0.05	4.95	26.16	–26.70	6.31
54–56	1976	23.16	0.98	0.05	5.53	21.60	–26.54	6.35
56–58	1975	9.87	0.96	0.04	4.45	26.08	–26.55	7.49
58–60	1974	22.63	0.65	0.03	4.09	20.75	–26.14	8.35
60–62	1973	7.75	0.72	0.03	4.07	24.17	–26.11	8.84
62–64	1971	9.35	0.66	0.03	4.05	24.14	–26.01	8.42
64–66	1970	7.40	0.85	0.03	4.59	29.41	–25.92	8.35
66–68	1968	7.81	0.61	0.03	4.59	20.21	–26.18	7.52
68–70	1966	9.02	0.65	0.03	4.09	21.8	–25.77	8.27
70–72	1965	8.06	0.56	0.03	4.11	18.67	–25.89	7.23
72–74	1962	6.49	0.54	0.03	4.45	19.37	–25.73	8.48
74–76	1960	6.95	0.57	0.04	3.87	14.98	–25.94	9.87
76–78	1958	11.36	0.69	0.03	4.31	20.88	–26.10	6.51
78–80	1956	11.16	0.64	0.03	4.29	22.20	–25.88	7.50
80–82	1954	9.77	0.71	0.04	4.37	19.45	–26.17	9.01
82–84	1949	7.31	0.50	0.04	3.95	13.78	–25.63	10.43

Table S5 (continued). T5 samples 84–86 to 118–120.

Depth (cm)	Estimated date	silt +clay (%)	TOC (%)	TN (%)	Carbonate (%)	C/N	$\delta^{13}C$ (‰)	$\delta^{15}N$ (‰)
84–86	1945	13.17	0.49	0.03	3.95	16.81	–26.02	9.18
86–88	1941	11.47	0.60	0.04	4.01	17.50	–25.60	8.19
88–90	1937	8.42	0.49	0.03	3.91	17.05	–25.54	8.74
90–92	1933	7.11	0.51	0.03	3.87	15.81	–25.63	7.78
92–94	1929	9.54	0.57	0.03	3.97	17.62	–25.98	7.13
94–96	1925	7.22	0.55	0.03	4.01	19.11	–25.69	7.01
96–98	1921	11.78	0.49	0.03	3.73	18.08	–25.79	8.08
98–100	1917	6.64	0.44	0.03	3.67	14.36	–25.07	10.63
100–102	1913	9.57	0.63	0.03	4.03	20.51	–26.03	9.66
102–104	1909	9.09	0.53	0.03	4.59	17.97	–25.74	8.70
104–106	1905	12.55	0.51	0.03	4.13	18.24	–25.24	8.68
106–108	1901	9.88	0.49	0.03	3.75	16.47	–25.13	8.75
108–110	1897	14.79	0.69	0.03	4.07	20.91	–25.68	7.32
110–112	1893	7.02	0.65	0.03	3.73	23.95	–25.41	9.62
112–114	1888	9.06	0.65	0.03	3.93	24.73	–25.39	8.78
114–116	1884	8.71	0.57	0.02	3.57	23.09	–25.20	8.94
116–118	1880	10.21	0.60	0.03	3.43	22.13	–25.67	9.11
118–120	1876	8.66	0.65	0.02	4.03	26.47	–25.74	10.14

Table S6. Data from the dating of T1, T2, T3, T4 and T5 cores collected in the Paranaguá Estuarine System, Brazil. Samples 0–2 to 92–94.

Depth (cm)	T1	T2	T3	T4	T5
	Year				
0–2	2020	2020	2020	2020	2020
2–4	2016	2019	2018	2018	2018
4–6	2014	2018	2017	2017	2017
6–8	2013	2014	2013	2016	2015
8–10	2009	2011	2010	2014	2013
10–12	2005	2001	2007	2012	2010
12–14	2002	1999	2004	2010	2008
14–16	1998	1992	2000	2008	2007
16–18	1992	1986	1999	2004	2006
18–20	1989	1984	1996	2000	2005
20–22	1985	1983	1991	1996	2004
22–24	1982	1979	1991	1990	2004
24–26	1979	1977	1990	1984	2003
26–28	1976	1975	1990	1980	2002
28–30	1973	1972	1990	1977	2001
30–32	1970	1970	1989	1976	1998
32–34	1967	1967	1989	1974	1994
34–36	1964	1967	1988	1973	1991
36–38	1961	1966	1988	1972	1989
38–40	1958	1965	1987	1971	1986
40–42	1957	1961	1986	1970	1985
42–44	1956	1958	1985	1969	1984
44–46	1955	1957	1984	1968	1982
46–48	1954	1956	1983	1966	1981
48–50	1953	1955	1982	1964	1980
50–52	1952	1954	1981	1963	1979
52–54	1951	1953	1981	1961	1978
54–56	1951	1952	1978	1959	1976
56–58	1950	1950	1975	1956	1975
58–60	1949	1948	1973	1954	1974
60–62	1948	1947	1970	1952	1973
62–64	1946	1945	1969	1949	1971
64–66	1944	1943	1969	1947	1970
66–68	1943	1940	1968	1944	1968
68–70	1941	1938	1967	1942	1966
70–72	1939	1935	1966	1940	1965
72–74	1933	1933	1965	1937	1962
74–76	1927	1929	1963	1935	1960
76–78	1922	1924	1962	1933	1958
78–80	1916	1920	1961	1930	1956
80–82	1910	1916	1959	1928	1954
82–84	1905	1911	1957	1926	1949
84–86	1901	1903	1955	1923	1945
86–88	1896	1895	1952	1921	1941
88–90	1891	1887	1950	1918	1937
90–92	1886	1878	1948	1916	1933
92–94	1882	1870	1946	1912	1929

Table S6 (continued). Samples 94–96 to 118–120.

Depth (cm)	T1	T2	T3	T4	T5
	Year				
94–96	1877	1862	1944	1908	1925
96–98	1872	1854	1941	1904	1921
98–100	1868	1845	1939	1900	1917
100–102	1863	1837	1937	1896	1913
102–104	1858	1829	1935	1900	1909
104–106	1854	1821	1933	1896	1905
106–108	1849	1812	1930	1893	1901
108–110	1844	1804	1928	1889	1897
110–112	1839	1796	1926	1885	1893
112–114	1835	1788	1924	1881	1888
114–116	1830	1779	1922	1877	1884
116–118	1825	1771	1919	1873	1880
118–120	1821	1763	1917	1869	1876

Table S7. Comparison of TOC, TN, ratio C/N and $d^{13}C$ parameters from different estuaries in Brazil.

Location	**TOC**	**TN**	**C/N**	**$\delta^{13}C$**	**Reference**
Guanabara Bay (RJ), Brazil	2.0–7.5		14.0–22.0	–27.0 to –23.0	Monteiro et al. (2012)
Caravelas Estuary (BA), Brazil	0.7–2.1	0.05–0.10	11.9–24.9	–25.7 to –23.0	Souza et al. (2014)
Santos Estuary (SP), Brazil	0.8–3.5	0.08–0.14	4.0–28.0	–28.0 to –23.0	de Jesus et al. (2020)
Guaratuba Bay (PR), Brazil	0.05–0.35	0.03–0.27	10.0–20.0	–28.0 to –27.0	Brandini et al. (2022)
Paranaguá Estuarine System (PR), Brazil	0.09–4.19	0.01–0.34	7.5–34.9	–27.7 to –23.8	Current study

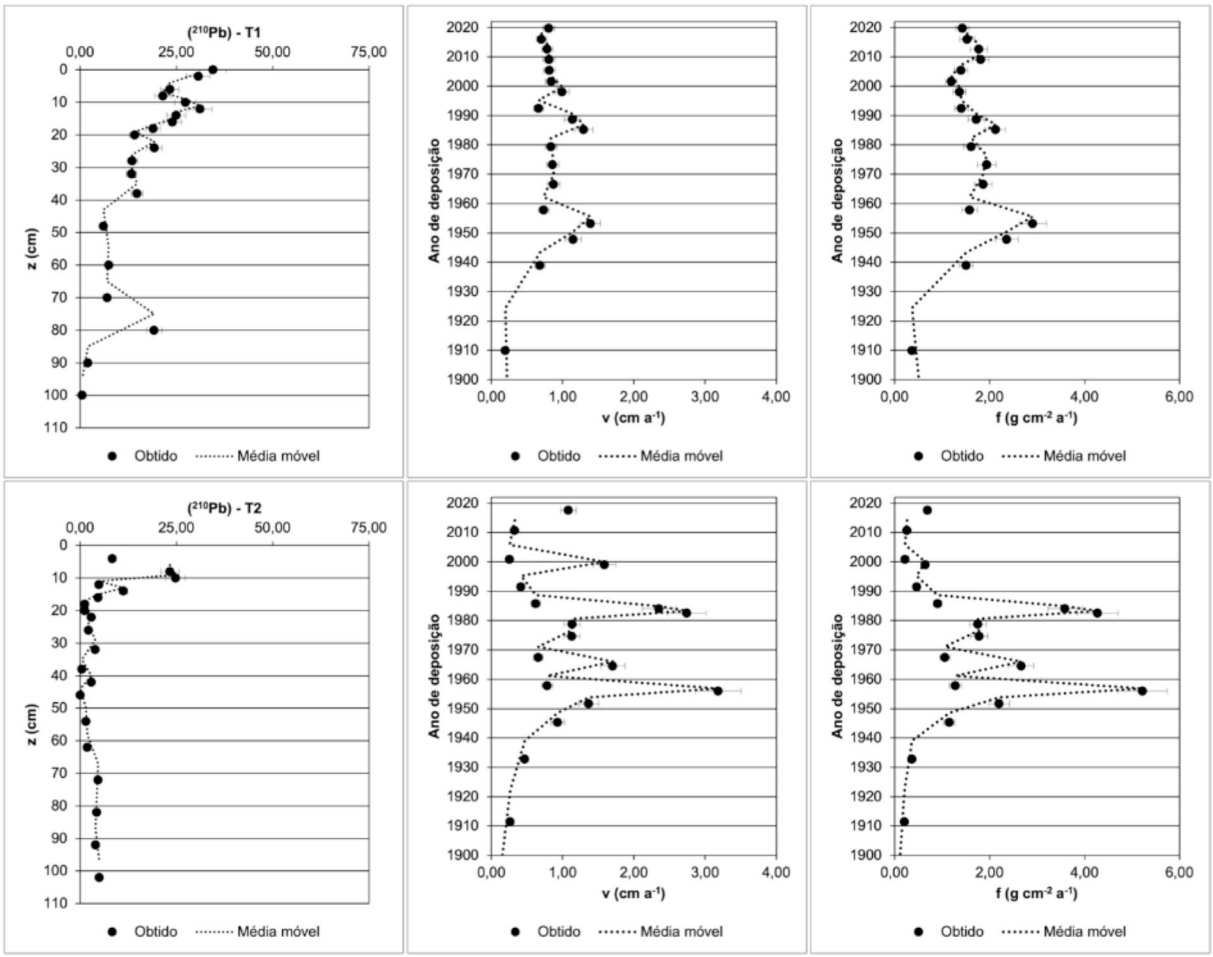

Figure S1 – ^{210}Pb CRS geochronological models used in the dating of cores T1 and T2.

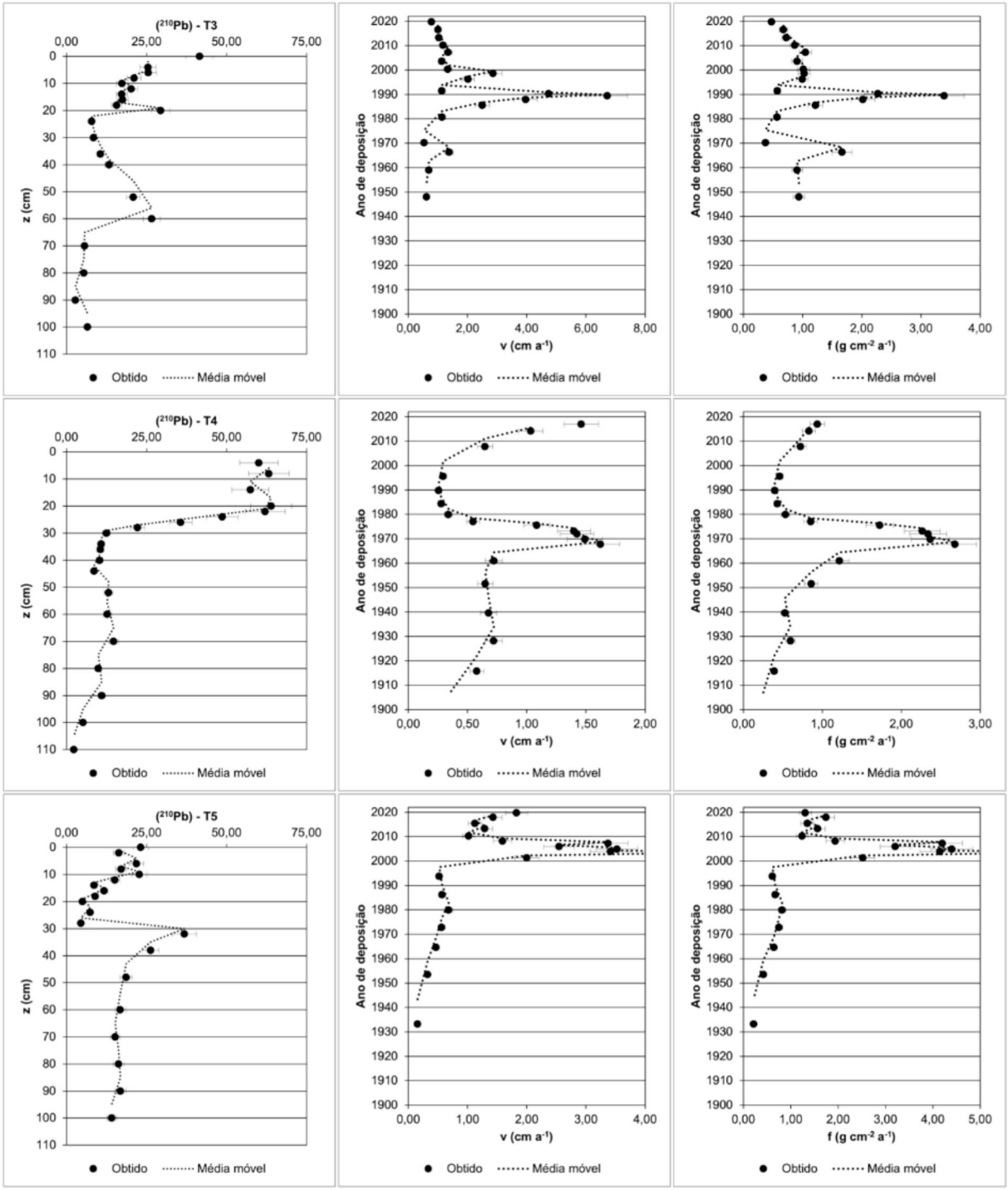

Figure S2 – ^{210}Pb CRS geochronological models used in the dating of cores T3, T4 and T5.

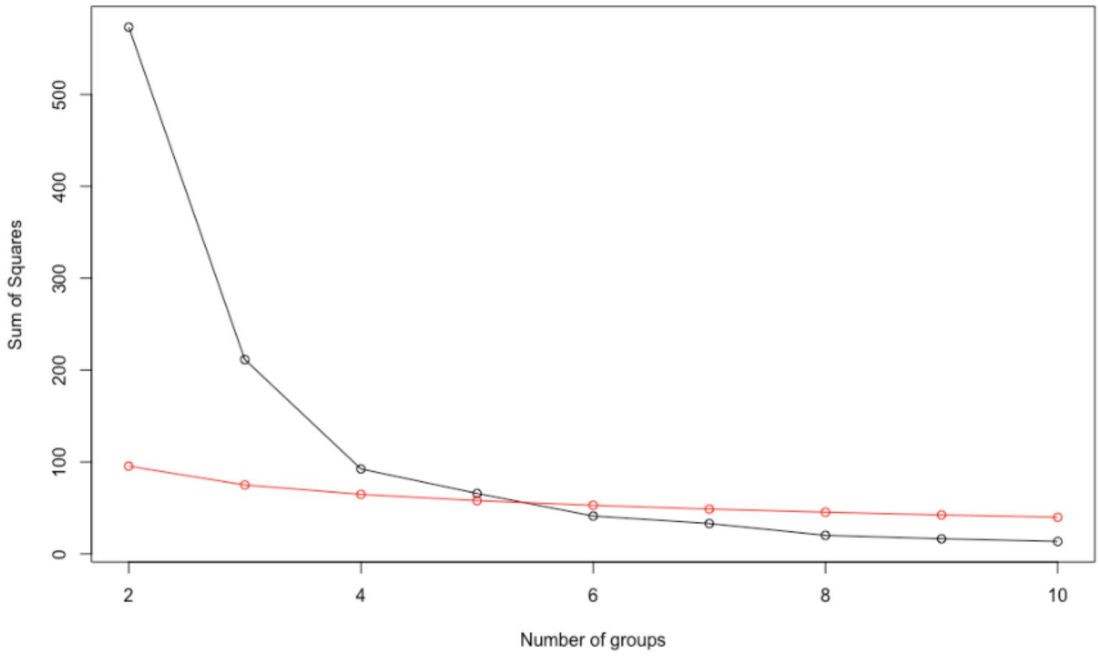

Figure S3 – The Brokenstick package was used to define the number of cluster groupings that best explained the sampled data. Example of T2, which according to Brokenstick the ideal number of groups is 4.

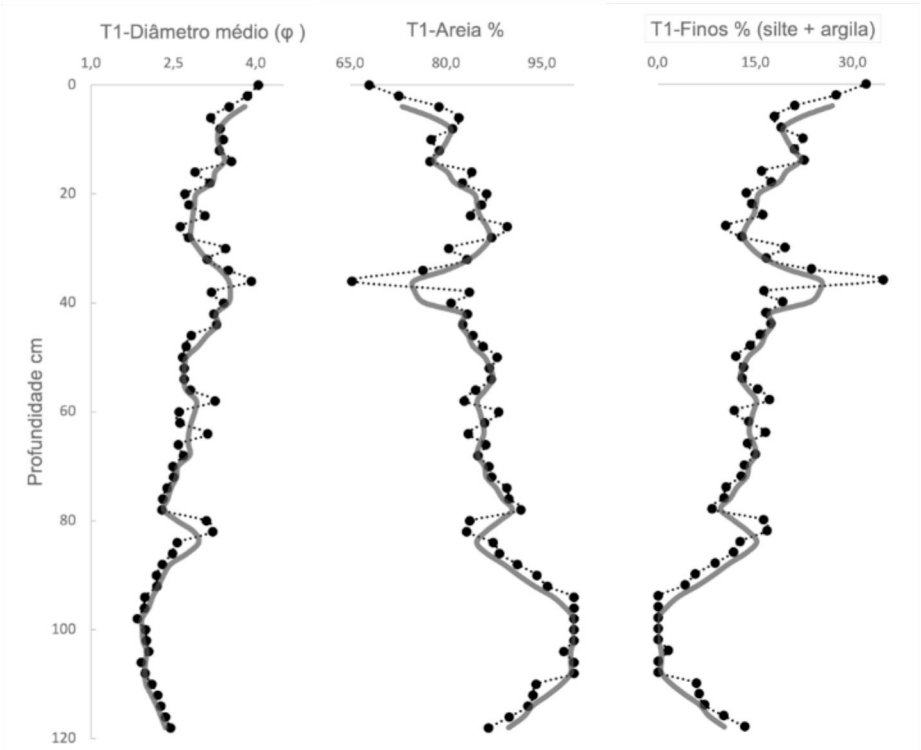

Figura S4 – Testemunho T1: Diâmetro médio do grão (ϕ) e conteúdo (%) de areia e finos (silte + argila) ao longo do perfil do testemunho. Os pontos ligados pela linha pontilhada preta foram os valores encontrados para cada parâmetro, e a linha cheia cinza representa a média móvel entre 3 pontos.

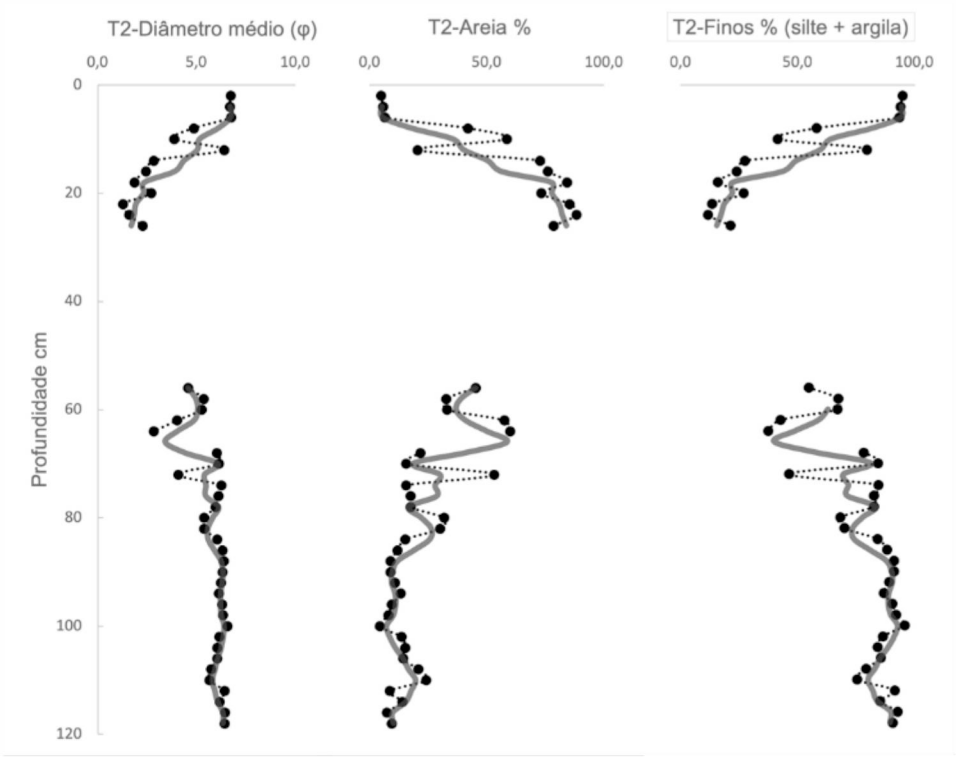

Figura S5 – Testemunho T2: Diâmetro médio do grão (ϕ) e conteúdo (%) de areia e finos (silte + argila) ao longo do perfil do testemunho. Os pontos ligados pela linha pontilhada preta foram os valores encontrados para cada parâmetro, e a linha cheia cinza representa a média móvel entre 3 pontos.

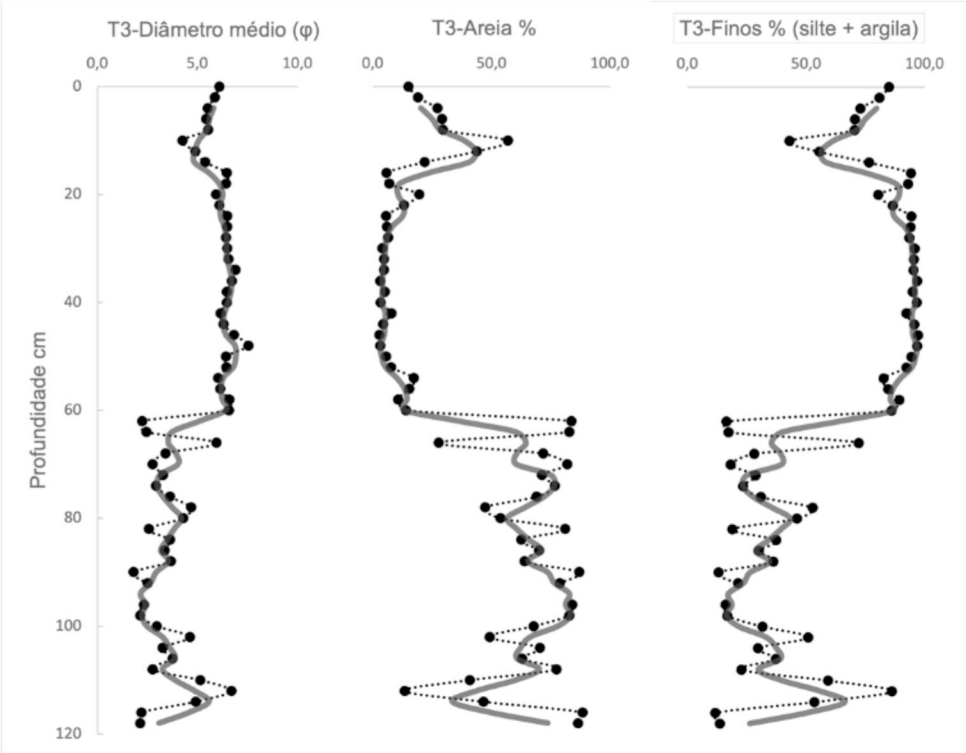

Figura S6 – Testemunho T3: Diâmetro médio do grão (ϕ) e conteúdo (%) de areia e finos (silte + argila) ao longo do perfil do testemunho. Os pontos ligados pela linha pontilhada preta foram os valores encontrados para cada parâmetro, e a linha cheia cinza representa a média móvel entre 3 pontos.

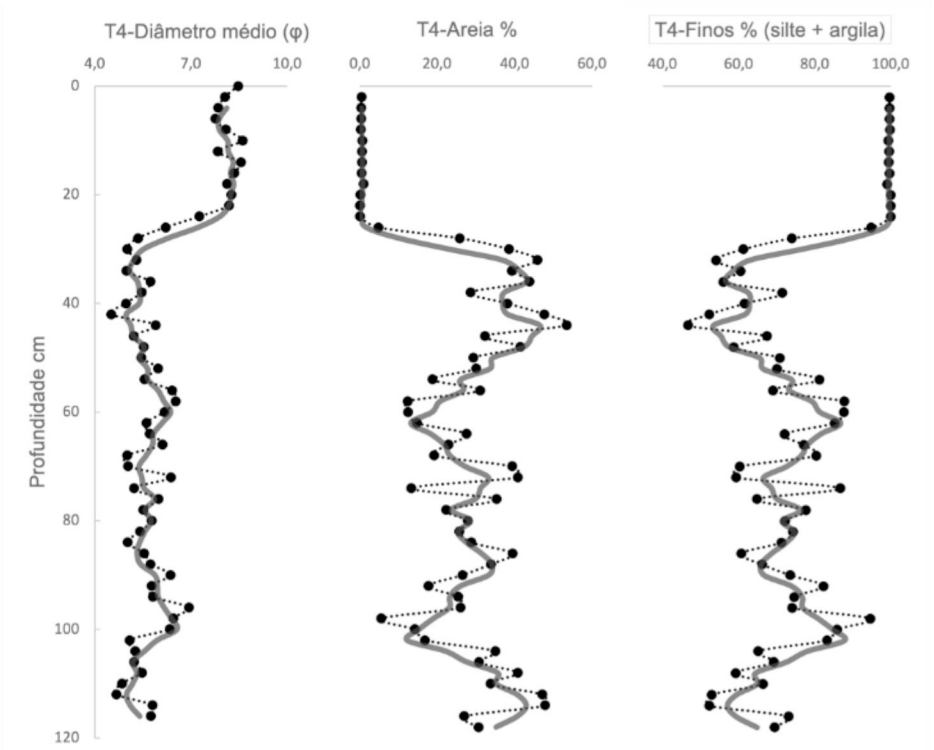

Figura S7– Testemunho T4: Diâmetro médio do grão (ϕ) e conteúdo (%) de areia e finos (silte + argila) ao longo do perfil do testemunho. Os pontos ligados pela linha pontilhada preta foram os valores encontrados para cada parâmetro, e a linha cheia cinza representa a média móvel entre 3 pontos.

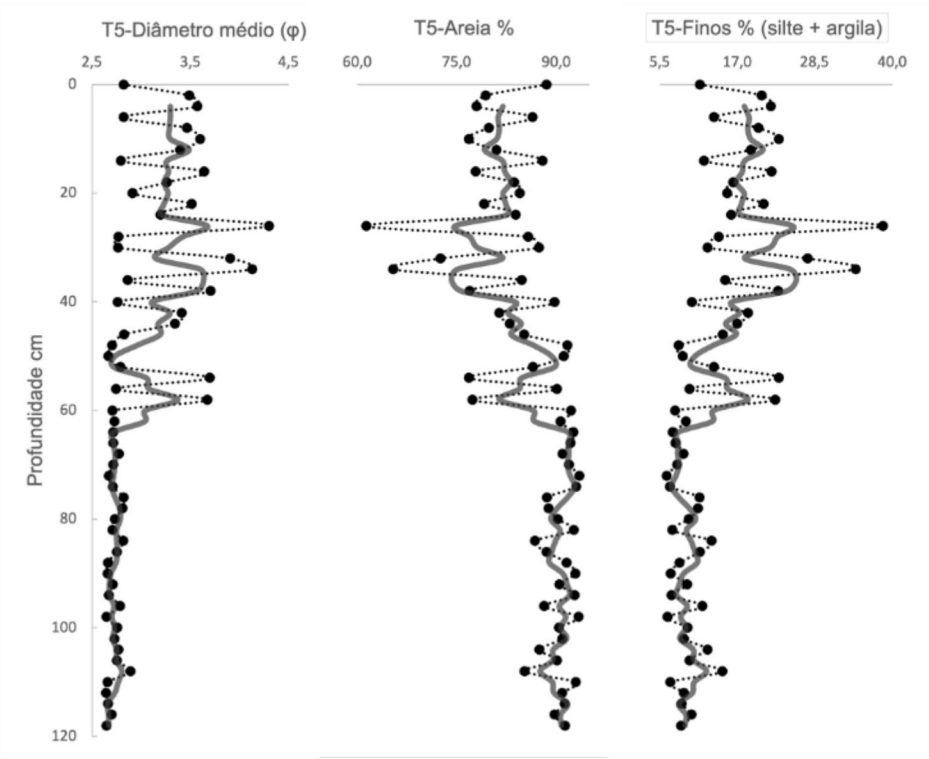

Figura S8– Testemunho T5: Diâmetro médio do grão (ϕ) e conteúdo (%) de areia e finos (silte + argila) ao longo do perfil do testemunho. Os pontos ligados pela linha pontilhada preta foram os valores encontrados para cada parâmetro, e a linha cheia cinza representa a média móvel entre 3 pontos.

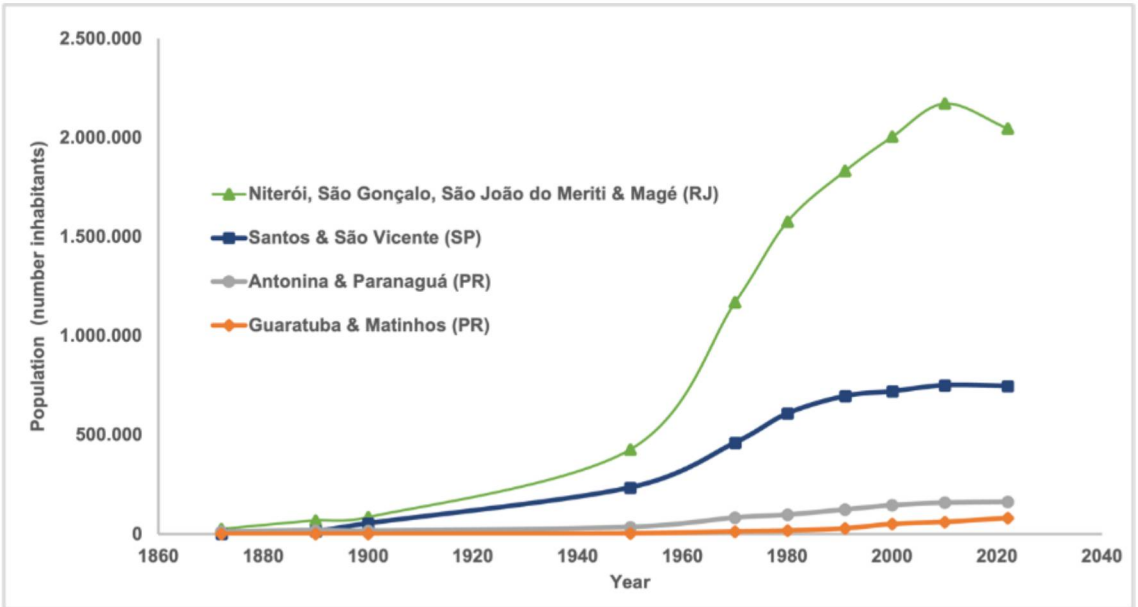

Figura S9– Crescimento populacional (em número de habitantes), comparando a população das principais cidades do entorno da Baía de Guanabara, RJ (Niterói, São Gonçalo, São João do Meriti e Magé), estuário de Santos, SP (cidades de Santos e São Vicente), Baía de Paranaguá, PR (municípios de Paranaguá e Antonina) e Baía de Guaratuba, PR (municípios de Guaratuba e Matinhos), obtidos do IBGE (Instituto Brasileiro de Geografia e Estatística), 2023.

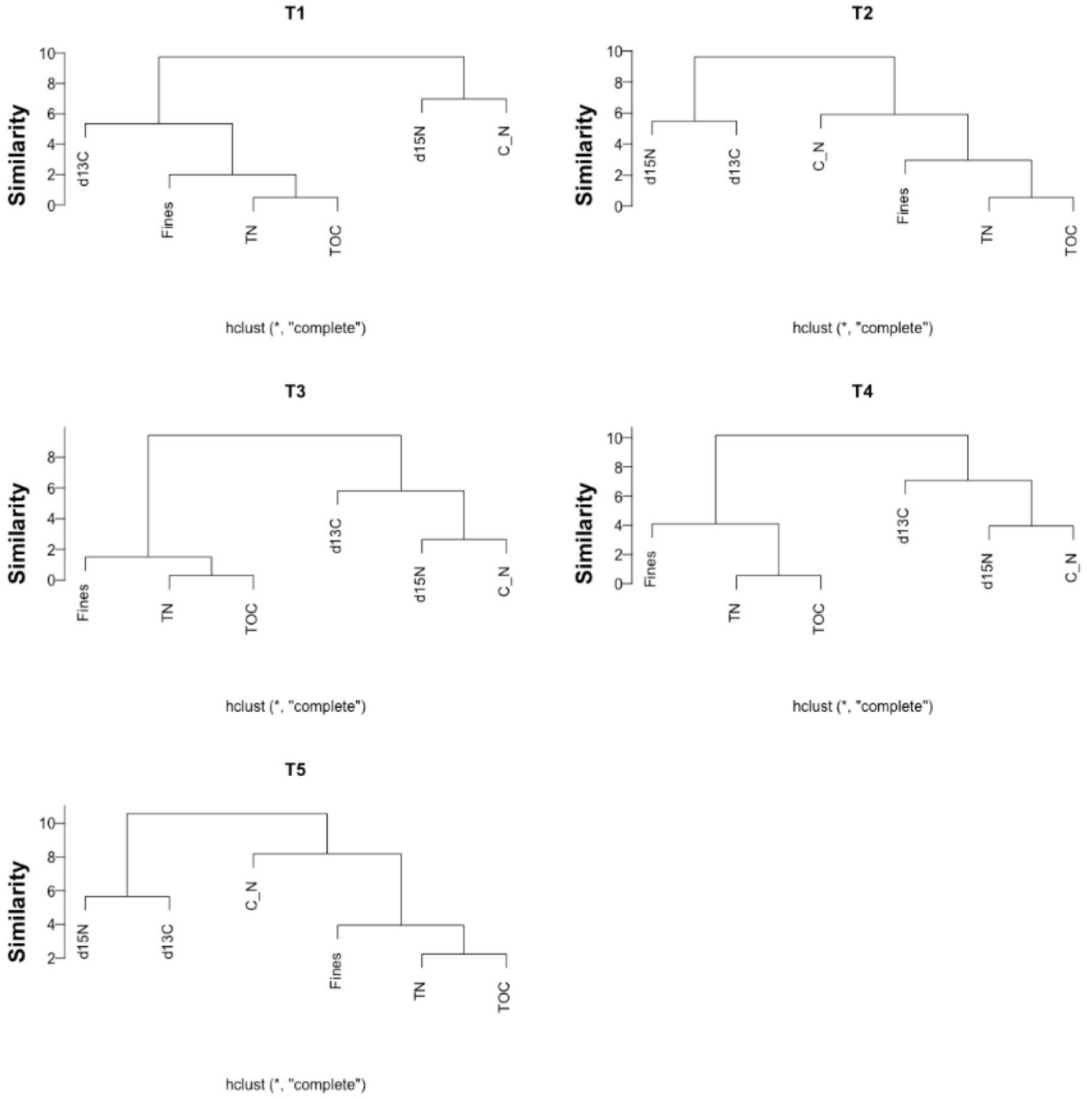

Figure S10 – The SAX (Symbolic Aggregate Approximation) representation of the 'TSclust' package used to create the dissimilarity matrix for each sedimentary record.

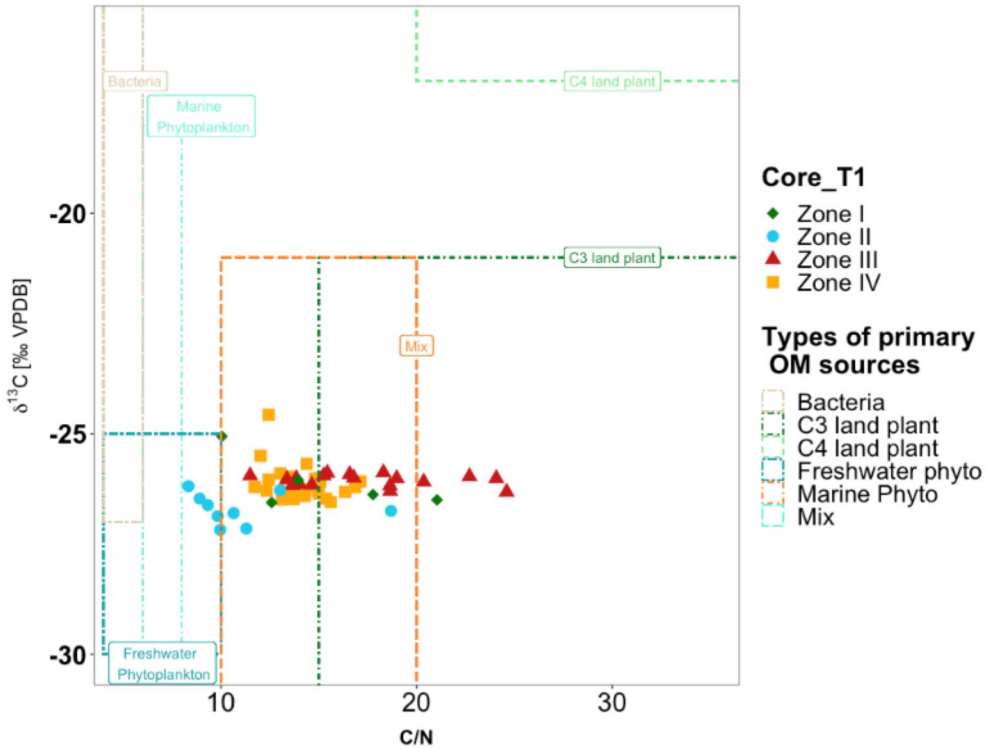

Figura S11– Distribuição espacial das principais fontes de MO presente no testemunho T1 em relação $\delta^{13}C$ *vs* C/N.

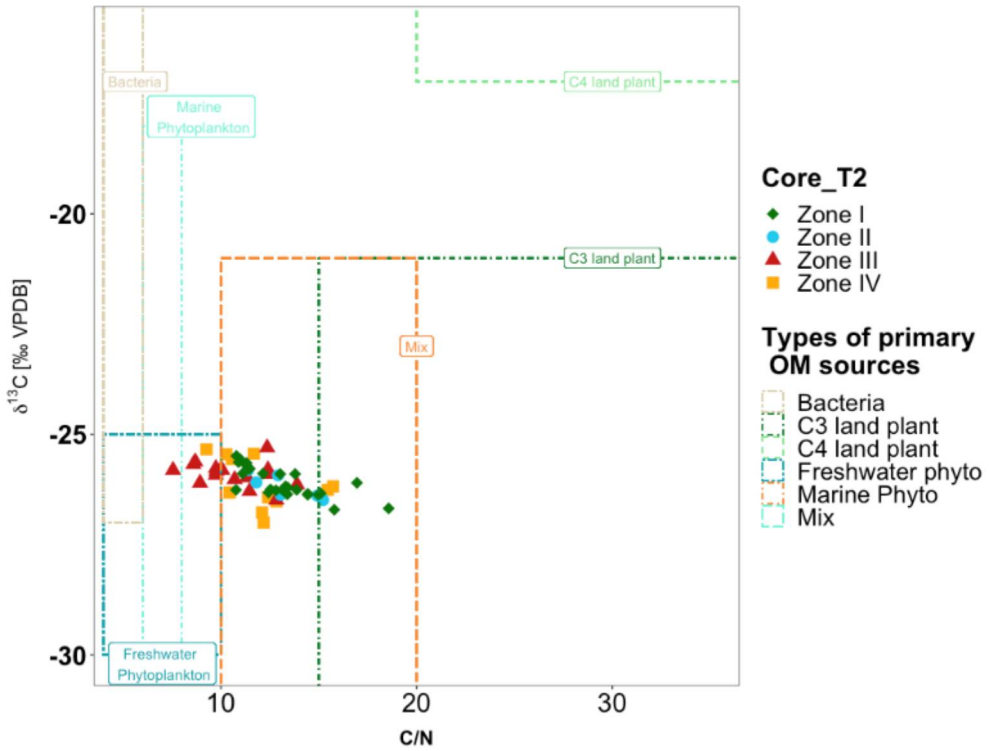

Figura S12– Distribuição espacial das principais fontes de MO presente no testemunho T2 em relação $\delta^{13}C$ *vs* C/N.

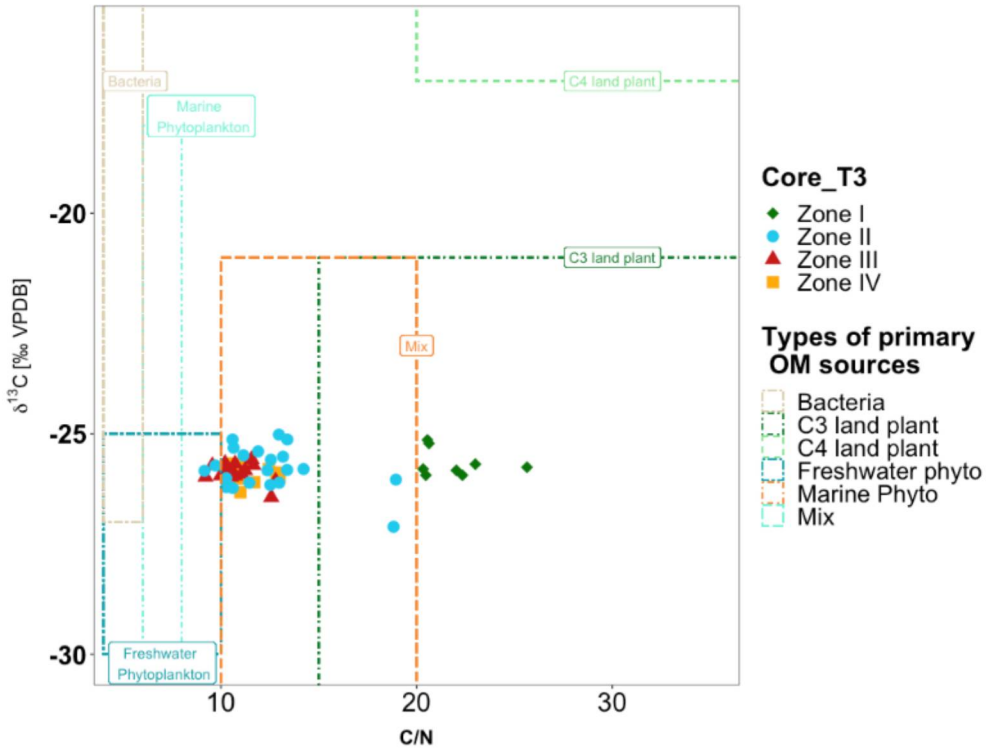

Figura S13– Distribuição espacial das principais fontes de MO presente no testemunho T3 em relação $\delta^{13}C$ *vs* C/N.

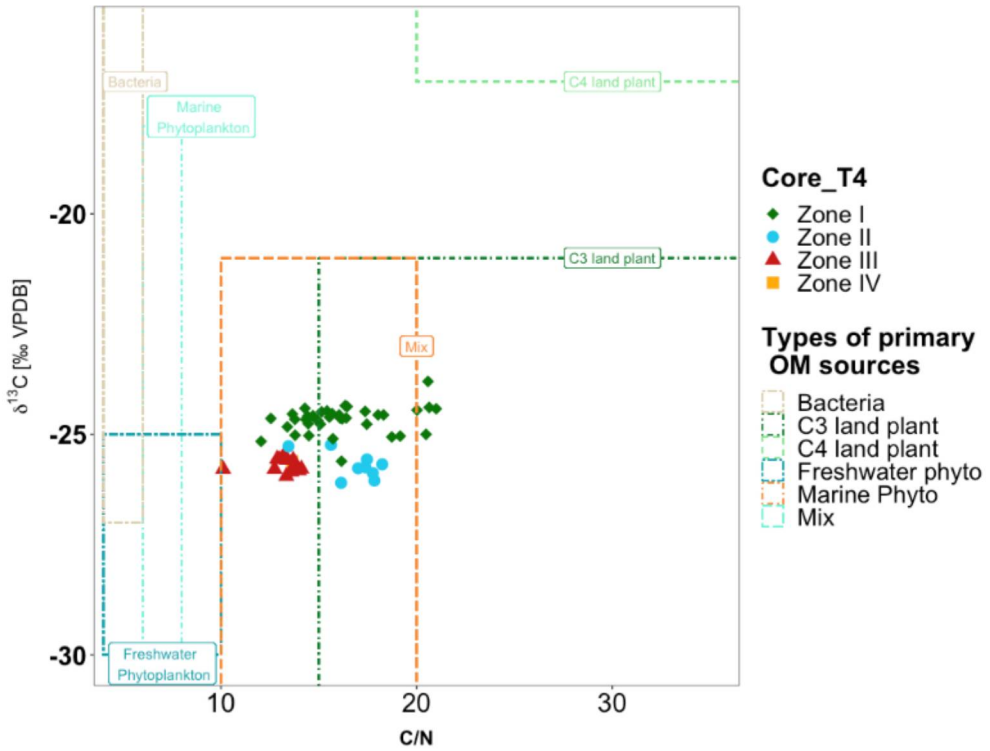

Figura S14 – Distribuição espacial das principais fontes de MO presente no testemunho T4 em relação $\delta^{13}C$ *vs* C/N.

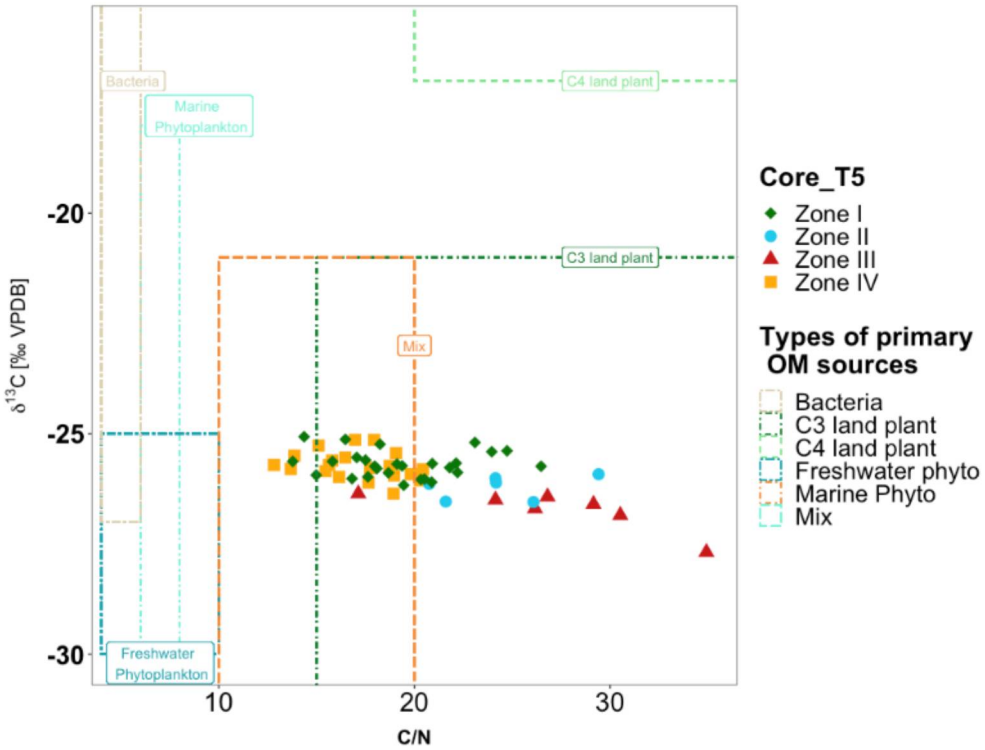

Figura S15– Distribuição espacial das principais fontes de MO presente no testemunho T5 em relação $\delta^{13}C$ *vs* C/N.

APÊNDICE 3 – MATERIAL SUPLEMENTAR DO CAPÍTULO III

Material and Methods

Instrumental analysis of molecular markers

For the instrumental analyses of the selected molecular markers analysed, 1 μL of the final extracts was injected into a gas chromatograph (Agilent GC System 7890A Series) equipped with a flame ionization detector (FID), in splitless mode using hydrogen as the carrier gas. The chromatographic columns used were a HP-5 Agilent 19091J-413 (30.0 m x 0.32 mm x 0.25 μm) for *n*-alkanes and a HP-5 Agilent 19091J-015 (50.0 m x 0.32 mm x 0.17 μm) for *n*-alkanols and sterols.

The HP Enhanced Chemstation G2070BA program was used to perform the measurements. Compounds were identified by matching retention times with results from standard mixtures of *n*-alkanes, *n*-alkanols and sterols. For the sample quantification, it was considered the peak area of each compound multiplied by its own response factor, present in calibration curve, in relation to the mass/area ratio of surrogate standards added before extraction. Detailed instrumental analyses were previously presented by Dauner et al. (2017), Cabral et al. (2019) and Sutilli et al. (2020).

References

Cabral, A.C., Wilhelm, M.M., Figueira, R.C.L., Martins, C.C., 2019. Tracking the historical sewage input in South American subtropical estuarine systems based on faecal sterols and bulk organic matter stable isotopes (δ13C and δ15N). Sci. Total Environ. 655, 855-864.

Dauner, A.L.L., MacCormack, W.P., Hernández, E.A., Martins, C.C., 2017. Sources and distribution of biomarkers in surficial sediments from a polar marine ecosystem (Potter Cove, King George Island, Antarctica). Polar Biol. 40, 2015-2025

Sutilli, M., Combi, T., Garcia, M.R.D., Martins, C.C. 2020. One century of historical deposition and flux of hydrocarbons in a sediment core from a South Atlantic RAMSAR subtropical estuary. Sci. Total Environ. 706, 136017.

Table S1. Elementary and isotopic composition (TOC, TN, $\delta^{13}C$ and $\delta^{15}N$) and diagnostic ratios for *n*-alkanes. *n*-alkanols and sterols in the sediment cores from Paraná coast. TOC: Total Organic Carbon; NT: Total Nitrogen; TAR: Terrigenous-to-Aquatic Ratio; CPI: Preferential Carbon Index. P_{aq}: Aquatic proxy. AC: Antonina core; PC: Paranaguá core; GC: Guaratuba core.

	Estimated date	**Depth (cm)**	**TOC %**	**TN %**	**$\delta^{13}C$ (‰)**	**$\delta^{15}N$ (‰)**	**Silt + clay (%)**	**TAR [1]**	**CPI [2]**	**P_{aq} [3]**	**C_{22}/C_{24} [4]**	**C_{24}/C_{26} [5]**	**C_{26}/C_{30} [6]**
	2012	*0-2*	3.97	0.31	-26.22	2.69	34.6	26.4	5.50	0.19	0.39	0.64	0.46
	2008	*2-4*					28.3	50.7	6.14	0.20	0.33	0.59	0.45
	2004	*4-6*	3.71	0.30	-26.35	2.82	31.8	20.5	5.46	0.24	0.33	0.61	0.42
	2000	*6-8*					33.4	68.2	5.92	0.17	0.33	0.52	0.57
	1996	*8-10*	3.62	0.30	-26.38	2.65	30.4	59.1	5.69	0.17	0.33	0.60	0.43
AC	1989	*11-13*	3.73	0.30	-26.49	3.00	33.8	50.3	5.95	0.17	0.33	0.59	0.57
	1983	*14-16*	3.60	0.31	-26.35	3.45	30.0	50.9	5.54	0.16	0.33	0.59	0.42
	1977	*17-19*	3.51	0.30	-26.23	3.47	77.9	70.3	5.61	0.16	0.33	0.60	0.47
	1971	*20-22*	3.58	0.30	-26.13	3.74	27.8	97.4	5.55	0.16	0.32	0.60	0.44
	1965	*23-25*	3.54	0.31	-26.24	3.47	30.7	58.6	5.68	0.17	0.33	0.60	0.52
	1960	*26-27*	3.57	0.31	-26.37	3.66	76.6	43.8	5.91	0.18	0.33	0.64	0.34
	2010	*0-2*	1.09	0.18	-24.98	3.93	18.2	5.22	5.66	0.20	0.38	0.53	0.27
	2002	*2-4*	1.19	0.17	-25.08	3.50	22.5	13.5	6.08	0.20	0.38	0.53	0.25
	1995	*4-6*	0.96	0.15	-25.09	1.94	19.4	7.63	5.55	0.22	0.39	0.53	0.28
	1987	*6-8*	0.97	0.16	-25.06	2.31	31.7	10.5	5.79	0.23	0.35	0.52	0.33
	1979	*8-10*	1.23	0.14	-25.58	2.55	31.0	15.7	5.72	0.21	0.37	0.54	0.27
PC	1968	*11-13*	0.79	0.13	-25.38	1.84	15.1	19.3	5.78	0.19	0.36	0.57	0.27
	1956	*14-16*	0.94	0.15	-25.57	2.28	24.2	6.86	4.76	0.31	0.34	0.55	0.26
	1945	*17-19*	0.71	0.13	-25.37	1.31	14.2	7.07	4.33	0.31	0.25	0.53	0.27
	1933	*20-22*	0.72	0.10	-25.10	1.65	7.80	13.9	5.56	0.14	0.30	0.52	0.26
	1922	*23-25*	0.71	0.09	-25.03	2.70	16.8	104.7	4.82	0.15	0.24	0.44	0.22
	1912	*26-27*	0.81	0.12	-25.53	1.91	20.9	214.2	4.80	0.17	0.25	0.49	0.28

Table S1 (continued).

	Estimated date	Depth (cm)	TOC %	TN %	$\delta^{13}C$ (‰)	$\delta^{15}N$ (‰)	Silt + clay (%)	TAR [1]	CPI [2]	P_{aq} [3]	C_{22}/C_{24} [4]	C_{24}/C_{26} [5]	C_{26}/C_{30} [6]
GC	2008	*0-2*	1.19	0.14	-26.59	2.77	39.2	36.2	6.37	0.17	0.39	0.49	0.40
	2003	*2-4*	0.81	0.11	-27.09	1.58	26.8	72.5	6.72	0.16	0.36	0.47	0.30
	1997	*4-6*	0.90	0.08	-26.94	2.65	37.0	69.2	6.76	0.16	0.30	0.45	0.31
	1991	*6-8*	0.86	0.11	-27.04	1.38	35.6	73.2	6.88	0.17	0.35	0.48	0.33
	1986	*8-10*	1.06	0.14	-27.33	0.46	38.1	69.0	6.89	0.17	0.33	0.41	0.27
	1980	*10-12*	1.25	0.14	-27.05	1.67	39.1	115.1	7.24	0.17	0.36	0.50	0.47
	1975	*12-14*	1.08	0.12	-27.42	1.69	17.0	74.9	8.31	0.16	0.38	0.50	0.36
	1969	*14-16*	1.11	0.13	-27.22	2.73	26.7	86.9	6.94	0.16	0.36	0.48	0.33
	1964	*16-18*	1.16	0.14	-26.96	1.07	37.6	112.2	6.55	0.17	0.37	0.48	0.45
	1958	*18-20*	1.16	0.12	-27.09	1.31	16.7	131.2	6.70	0.17	0.36	0.47	0.47
	1953	*20-22*	0.83	0.14	-26.95	1.27	24.1	70.2	7.07	0.17	0.35	0.47	0.31
	1947	*22-24*	1.19	0.14	-27.36	2.27	7.23	117	7.12	0.17	0.36	0.46	0.47
	1941	*24-26*	1.19	0.13	-27.26	2.65	27.5	70.5	7.20	0.19	0.34	0.47	0.60
	1936	*26-28*	1.06	0.11	-27.16	1.66	38.4	85.0	7.49	0.18	0.33	0.47	0.49
	1930	*28-30*	0.90	0.11	-27.02	2.42	30.0	114.8	7.32	0.18	0.34	0.47	0.48
	1925	*30-32*	1.01	0.12	-27.03	2.17	28.8	68.6	7.29	0.19	0.36	0.49	0.60

[1] **TAR** = ((n-C_{27}+n-C_{29}+n-C_{31}) / (n-C_{15}+n-C_{17}+n-C_{19}));
[2] **CPI** = {0.5 * [(n-C_{25}+n-C_{27}+n-C_{29}+n-C_{31}+n-C_{33}) / (n-C_{24}+n-C_{26}+n-C_{28}+n-C_{30}+n-C_{32}) + (n-C_{25}+n-C_{27}+n-C_{29}+n-C_{31}+n-C_{33}) / (n-C_{26}+n-C_{28}+n-C_{30}+n-C_{32}+n-C_{34})]};
[3] $\mathbf{P_{aq}}$ = ((n-C_{23}+n-C_{25}) / (n-C_{23}+n-C_{25}+n-C_{29}+n-C_{31}))
[4] $\mathbf{C_{22}/C_{24}}$ = (n-C_{22}-OH) / (n-C_{24}-OH);
[5] $\mathbf{C_{24}/C_{26}}$ = (n-C_{24}-OH) / (n-C_{26}-OH);
[6] $\mathbf{C_{26}/C_{30}}$ = (n-C_{26}-OH) / (n-C_{30}-OH).

Table S2. Concentration of *n*-alkanes, pristane and phytane (in µg g^{-1}) along each section (in cm) of the Antonina core. < LD: below the limit of detection.

Antonina core - *n*-alkanes											
Estimated date	**2012**	**2008**	**2004**	**2000**	**1996**	**1989**	**1983**	**1977**	**1971**	**1965**	**1960**
Depth	*0-2*	*2-4*	*4-6*	*6-8*	*8-10*	*11-13*	*14-16*	*17-19*	*20-22*	*23-25*	*26-27*
***n*-C_{10}**	< LD	< LD	< LD	< LD	< LD	< LD	< LD	< LD	< LD	< LD	< LD
***n*-C_{11}**	< LD	< LD	< LD	< LD	< LD	< LD	< LD	< LD	< LD	0.01	< LD
***n*-C_{12}**	< LD	< LD	< LD	< LD	< LD	< LD	< LD	< LD	< LD	0.01	< LD
***n*-C_{13}**	0.01	< LD	0.01	< LD	< LD	< LD	0.01	0.01	< LD	0.01	0.01
***n*-C_{14}**	0.04	0.01	0.05	< LD	0.01	0.02	0.03	0.02	0.02	0.03	0.03
***n*-C_{15}**	0.11	0.06	0.11	0.03	0.04	0.04	0.05	0.04	0.03	0.06	0.06
***n*-C_{16}**	0.08	0.04	0.21	0.02	0.03	0.04	0.05	0.05	0.03	0.07	0.08
***n*-C_{17}**	0.40	0.24	0.82	0.18	0.19	0.29	0.24	0.16	0.12	0.20	0.27
***n*-C_{18}**	0.07	0.05	0.21	0.04	0.04	0.06	0.05	0.05	0.03	0.06	0.08
***n*-C_{19}**	0.11	0.10	0.23	0.08	0.08	0.10	0.08	0.07	0.05	0.09	0.09
***n*-C_{20}**	0.09	0.03	0.20	0.02	0.02	0.06	0.03	0.02	0.01	0.03	0.09
***n*-C_{21}**	0.19	0.22	0.64	0.15	0.13	0.19	0.15	0.15	0.15	0.16	0.16
***n*-C_{22}**	0.34	0.21	1.33	0.16	0.15	0.22	0.18	0.12	0.13	0.16	0.31
***n*-C_{23}**	0.85	0.98	2.19	0.77	0.72	0.85	0.74	0.68	0.73	0.81	0.87
***n*-C_{24}**	0.37	0.49	1.30	0.40	0.35	0.47	0.37	0.35	0.38	0.42	0.50
***n*-C_{25}**	2.09	2.91	3.64	2.44	2.22	2.51	2.13	2.14	2.37	2.60	2.34
***n*-C_{26}**	0.52	0.58	0.87	0.55	0.51	0.63	0.53	0.53	0.58	0.60	0.53
***n*-C_{27}**	3.62	4.69	5.41	4.37	3.99	4.70	4.06	4.16	4.50	4.67	4.09
***n*-C_{28}**	1.16	1.26	1.47	1.32	1.43	1.40	1.50	1.55	1.63	1.65	1.13
***n*-C_{29}**	8.07	10.1	11.8	9.77	9.01	10.8	9.44	9.72	10.3	10.5	9.08
***n*-C_{30}**	1.12	1.32	1.60	1.25	1.18	1.39	1.28	1.30	1.35	1.40	1.24
***n*-C_{31}**	4.63	5.68	6.57	5.50	5.03	6.14	5.25	5.46	5.59	5.98	5.09
***n*-C_{32}**	0.64	0.73	0.89	0.70	0.65	0.79	0.68	0.69	0.72	0.77	0.66
***n*-C_{33}**	2.25	2.76	3.01	2.55	2.84	3.08	2.91	3.05	2.65	3.26	2.56
***n*-C_{34}**	0.25	0.26	0.29	0.27	0.23	0.27	0.24	0.24	0.24	0.26	0.22
***n*-C_{35}**	0.51	0.59	0.67	0.55	0.55	0.66	0.54	0.56	0.53	0.61	0.49
***n*-C_{36}**	0.10	0.08	0.09	0.07	0.06	0.07	0.07	0.05	0.07	0.06	0.06
***n*-C_{37}**	0.16	0.14	0.15	0.13	0.13	0.15	0.13	0.13	0.12	0.14	0.12
***n*-C_{38}**	0.09	0.08	0.07	0.07	0.07	0.06	0.06	0.06	0.07	0.07	0.06
***n*-C_{39}**	0.16	0.12	0.14	0.11	0.11	0.11	0.12	0.11	0.12	0.13	0.10
***n*-C_{40}**	0.11	0.08	0.06	0.07	0.07	0.07	0.06	0.06	0.07	0.07	0.05
Pristane	0.11	0.04	0.25	0.03	0.03	0.06	0.05	0.03	0.02	0.04	0.08
Phytane	0.11	0.05	0.33	0.03	0.04	0.07	0.05	0.03	0.02	0.04	0.10
Total n-alkanes	28.1	33.7	44.0	31.6	29.8	35.1	31.0	31.5	32.6	34.9	30.4

Table S3. Concentration of *n*-alkanes, pristane and phytane (in μg g^{-1}) along each section (in cm) of the Paranaguá core. < LD: below the limit of detection.

Paranaguá core - *n*-alkanes											
Estimated date	**2010**	**2002**	**1995**	**1987**	**1979**	**1968**	**1956**	**1945**	**1933**	**1922**	**1912**
Depth	*0-2*	*2-4*	*4-6*	*6-8*	*8-10*	*11-13*	*14-16*	*17-19*	*20-22*	*23-25*	*26-27*
***n*-C_{10}**	< LD	< LD	< LD	< LD	< LD	< LD	< LD	< LD	< LD	< LD	< LD
***n*-C_{11}**	< LD	< LD	< LD	< LD	< LD	< LD	< LD	< LD	< LD	< LD	< LD
***n*-C_{12}**	0.01	< LD	< LD	< LD	< LD	< LD	< LD	< LD	< LD	< LD	< LD
***n*-C_{13}**	< LD	< LD	< LD	< LD	< LD	< LD	< LD	< LD	< LD	< LD	< LD
***n*-C_{14}**	0.03	0.02	0.02	0.02	0.01	< LD	0.02	0.01	< LD	0.01	< LD
***n*-C_{15}**	0.14	0.06	0.05	0.05	0.04	0.02	0.05	0.03	0.23	0.02	< LD
***n*-C_{16}**	0.11	0.06	0.06	0.05	0.03	0.02	0.07	0.04	0.00	< LD	0.00
***n*-C_{17}**	0.49	0.30	0.35	0.31	0.24	0.15	0.48	0.28	0.02	0.01	0.01
***n*-C_{18}**	0.28	0.13	0.15	0.11	0.05	0.04	0.15	0.12	< LD	< LD	< LD
***n*-C_{19}**	0.36	0.18	0.19	0.11	0.06	0.04	0.13	0.12	0.01	0.01	0.01
***n*-C_{20}**	0.32	0.14	0.17	0.11	0.05	0.04	0.10	0.13	< LD	< LD	< LD
***n*-C_{21}**	0.20	0.14	0.16	0.11	0.07	0.07	0.23	0.12	0.02	0.02	0.02
***n*-C_{22}**	0.29	0.18	0.29	0.21	0.18	0.12	0.53	0.34	0.02	0.01	0.01
***n*-C_{23}**	0.33	0.40	0.37	0.36	0.34	0.24	0.69	0.48	0.11	0.12	0.14
***n*-C_{24}**	0.17	0.15	0.23	0.19	0.18	0.13	0.62	0.46	0.06	0.06	0.06
***n*-C_{25}**	0.69	1.01	0.64	0.74	0.73	0.52	0.90	0.60	0.37	0.43	0.50
***n*-C_{26}**	0.18	0.24	0.17	0.18	0.18	0.13	0.23	0.19	0.11	0.13	0.13
***n*-C_{27}**	1.09	1.68	1.01	1.11	1.18	0.88	1.08	0.70	0.75	0.80	0.82
***n*-C_{28}**	0.34	0.48	0.30	0.32	0.37	0.27	0.33	0.25	0.28	0.33	0.34
***n*-C_{29}**	2.66	3.71	2.28	2.47	2.68	2.08	2.33	1.58	1.91	1.94	2.00
***n*-C_{30}**	0.34	0.46	0.29	0.31	0.33	0.26	0.30	0.20	0.25	0.30	0.32
***n*-C_{31}**	1.39	1.88	1.20	1.28	1.38	1.07	1.15	0.78	0.98	1.03	1.04
***n*-C_{32}**	0.17	0.24	0.15	0.16	0.18	0.13	0.15	0.09	0.13	0.16	0.17
***n*-C_{33}**	0.70	1.00	0.58	0.69	0.72	0.54	0.58	0.41	0.51	0.56	0.54
***n*-C_{34}**	0.06	0.08	0.05	0.06	0.06	0.05	0.05	0.04	0.05	0.07	0.06
***n*-C_{35}**	0.16	0.22	0.13	0.15	0.17	0.12	0.13	0.09	0.11	0.12	0.11
***n*-C_{36}**	0.02	0.03	0.02	0.02	0.02	0.01	0.01	0.01	0.01	0.03	0.02
***n*-C_{37}**	0.04	0.06	0.04	0.04	0.04	0.03	0.03	0.02	0.03	0.03	0.03
***n*-C_{38}**	0.01	0.03	0.01	0.02	0.02	0.01	0.02	0.01	0.01	0.02	0.01
***n*-C_{39}**	0.05	0.07	0.03	0.04	0.05	0.04	0.04	0.03	0.04	0.04	0.03
***n*-C_{40}**	0.03	0.03	0.02	0.02	0.03	0.03	0.03	0.02	0.03	0.03	0.03
Pristane	0.18	0.11	0.12	0.11	0.06	0.04	0.13	0.07	< LD	< LD	< LD
Phytane	0.22	0.12	0.17	0.14	0.08	0.05	0.22	0.11	< LD	< LD	< LD
Total *n*-alkanes	10.7	13.0	8.91	9.20	9.37	7.03	10.4	7.16	6.04	6.27	6.39

Table S4. Concentration of *n*-alkanes, pristane and phytane (in μg g^{-1}) along each section (in cm) of the Guaratuba core. < LD: below the limit of detection.

Guaratuba core - *n*-alkanes																
Estimated date	**2008**	**2003**	**1997**	**1991**	**1986**	**1980**	**1975**	**1969**	**1964**	**1958**	**1953**	**1947**	**1941**	**1936**	**1930**	**1925**
Depth	*0-2*	*2-4*	*4-6*	*6-8*	*8-10*	*10-12*	*12-14*	*14-16*	*16-18*	*18-20*	*20-22*	*22-24*	*24-26*	*26-28*	*28-30*	*30-32*
***n*-C_{10}**	< LD	< LD	< LD	< LD	< LD	< LD	< LD	< LD	< LD	< LD	< LD	< LD	< LD	< LD	< LD	< LD
***n*-C_{11}**	< LD	< LD	< LD	< LD	< LD	< LD	< LD	< LD	< LD	< LD	< LD	< LD	< LD	< LD	< LD	< LD
***n*-C_{12}**	< LD	< LD	< LD	< LD	< LD	< LD	< LD	< LD	< LD	< LD	< LD	< LD	< LD	< LD	< LD	< LD
***n*-C_{13}**	< LD	< LD	< LD	< LD	< LD	< LD	< LD	< LD	< LD	< LD	< LD	< LD	< LD	< LD	< LD	< LD
***n*-C_{14}**	< LD	< LD	< LD	< LD	< LD	< LD	< LD	< LD	0.01	< LD	< LD	< LD	0.01	0.01	< LD	0.01
***n*-C_{15}**	0.03	0.01	0.01	0.01	0.01	0.01	0.01	0.01	0.02	0.01	0.02	0.01	0.02	0.02	0.01	0.02
***n*-C_{16}**	0.03	< LD	< LD	< LD	< LD	< LD	< LD	< LD	< LD	< LD	0.02	< LD	0.02	0.02	< LD	0.03
***n*-C_{17}**	0.05	0.02	0.02	0.02	0.02	0.02	0.02	0.02	0.02	0.02	0.03	0.02	0.04	0.03	0.02	0.03
***n*-C_{18}**	0.03	0.01	0.01	0.01	0.01	0.01	0.01	0.01	0.01	0.01	0.03	0.01	0.02	0.02	0.01	0.02
***n*-C_{19}**	0.02	0.01	0.01	0.01	0.01	0.01	0.01	0.01	0.01	0.01	0.02	0.01	0.03	0.01	0.01	0.02
***n*-C_{20}**	0.01	< LD	< LD	< LD	< LD	< LD	< LD	< LD	< LD	< LD	< LD	< LD	0.01	< LD	< LD	< LD
***n*-C_{21}**	0.02	0.01	0.02	0.01	0.02	0.02	0.01	0.02	0.03	0.02	0.02	0.02	0.04	0.02	0.02	0.02
***n*-C_{22}**	0.02	0.01	0.01	0.01	0.02	0.02	0.01	0.02	0.02	0.02	0.02	0.02	0.03	0.01	0.02	0.03
***n*-C_{23}**	0.11	0.08	0.08	0.08	0.10	0.12	0.09	0.10	0.18	0.18	0.16	0.17	0.20	0.16	0.14	0.18
***n*-C_{24}**	0.05	0.04	0.04	0.04	0.05	0.06	0.04	0.05	0.08	0.09	0.08	0.08	0.10	0.08	0.07	0.09
***n*-C_{25}**	0.41	0.31	0.31	0.32	0.38	0.48	0.36	0.38	0.69	0.68	0.61	0.67	0.78	0.64	0.56	0.70
***n*-C_{26}**	0.10	0.07	0.07	0.07	0.09	0.10	0.09	0.09	0.16	0.14	0.14	0.15	0.16	0.14	0.12	0.14
***n*-C_{27}**	0.85	0.64	0.65	0.65	0.77	0.96	0.78	0.82	1.41	1.37	1.25	1.34	1.49	1.26	1.11	1.30
***n*-C_{28}**	0.24	0.15	0.16	0.15	0.17	0.19	0.18	0.19	0.36	0.35	0.25	0.28	0.30	0.24	0.21	0.25
***n*-C_{29}**	1.70	1.28	1.36	1.29	1.52	1.86	1.55	1.70	2.73	2.70	2.39	2.63	2.80	2.38	2.10	2.41

Table S4 (continued).

Guaratuba core - *n*-alkanes																
Estimated date	**2008**	**2003**	**1997**	**1991**	**1986**	**1980**	**1975**	**1969**	**1964**	**1958**	**1953**	**1947**	**1941**	**1936**	**1930**	**1925**
Depth	*0-2*	*2-4*	*4-6*	*6-8*	*8-10*	*10-12*	*12-14*	*14-16*	*16-18*	*18-20*	*20-22*	*22-24*	*24-26*	*26-28*	*28-30*	*30-32*
***n*-C_{30}**	0.20	0.15	0.16	0.15	0.17	0.20	0.17	0.18	0.31	0.30	0.26	0.29	0.30	0.26	0.23	0.27
***n*-C_{31}**	0.93	0.70	0.76	0.69	0.82	0.98	0.82	0.87	1.46	1.44	1.27	1.41	1.49	1.29	1.15	1.37
***n*-C_{32}**	0.11	0.09	0.09	0.08	0.10	0.11	0.00	0.10	0.17	0.16	0.14	0.16	0.16	0.14	0.12	0.15
***n*-C_{33}**	0.40	0.30	0.34	0.30	0.35	0.40	0.35	0.37	0.60	0.60	0.52	0.60	0.62	0.49	0.47	0.56
***n*-C_{34}**	0.03	0.02	0.02	0.02	0.02	0.02	0.02	0.02	0.04	0.03	0.03	0.04	0.04	< LD	0.03	0.04
***n*-C_{35}**	0.07	0.05	0.05	0.05	0.06	0.06	0.06	0.06	0.09	0.09	0.08	0.09	0.10	0.07	0.07	0.07
***n*-C_{36}**	0.01	0.01	0.01	0.01	0.02	0.01	0.02	0.01	< LD	< LD	0.01	0.01	0.01	< LD	< LD	< LD
***n*-C_{37}**	0.02	0.02	0.02	0.02	0.02	0.02	0.02	0.02	0.03	0.02	0.03	0.03	0.03	0.02	0.02	0.02
***n*-C_{38}**	0.01	0.01	0.01	0.01	0.02	0.01	0.01	0.01	0.01	< LD	0.02	0.01	0.01	< LD	< LD	< LD
***n*-C_{39}**	0.02	0.02	0.02	0.02	0.02	0.02	0.01	0.02	0.03	0.02	0.03	0.02	0.03	0.03	0.03	0.02
***n*-C_{40}**	< LD	< LD	< LD	< LD	< LD	< LD	< LD	< LD	< LD	< LD	< LD	< LD	< LD	< LD	< LD	< LD
Pristane	0.02	< LD	< LD	< LD	< LD	< LD	< LD	< LD	< LD	< LD	< LD	< LD	< LD	< LD	< LD	< LD
Phytane	0.01	< LD	< LD	< LD	< LD	< LD	< LD	< LD	< LD	< LD	< LD	< LD	0.01	< LD	< LD	< LD
Total *n*-alkanes	5.43	4.00	4.23	4.02	4.73	5.69	4.64	5.07	8.47	8.27	7.45	8.07	8.84	7.34	6.52	7.75

Table S5. Concentration of *n*-alkanols and phytol (in µg g^{-1}) along each section (in cm) of the Antonina core. < LD: below the limit of detection.

Antonina core - *n*-alkanols											
Estimated date	**2012**	**2008**	**2004**	**2000**	**1996**	**1989**	**1983**	**1977**	**1971**	**1965**	**1960**
Depth	*0-2*	*2-4*	*4-6*	*6-8*	*8-10*	*11-13*	*14-16*	*17-19*	*20-22*	*23-25*	*26-27*
***n*-C_{12}-OH**	0.10	0.09	0.13	0.08	0.08	0.08	0.09	0.08	0.07	0.09	0.08
***n*-C_{13}-OH**	0.10	0.09	0.08	0.09	0.10	0.10	0.14	0.12	0.12	0.14	0.08
***n*-C_{14}-OH**	0.09	0.09	0.09	0.08	0.08	0.09	0.10	0.10	0.10	0.10	0.07
***n*-C_{15}-OH**	1.41	0.32	0.10	0.08	0.03	1.16	0.44	0.46	0.27	0.12	0.03
***n*-C_{16}-OH**	0.12	0.17	0.07	0.10	0.08	0.16	0.10	0.12	0.12	0.13	0.08
***n*-C_{17}-OH**	0.03	0.03	0.02	0.03	0.03	0.03	0.04	0.05	0.05	0.04	0.02
***n*-C_{18}-OH**	0.19	0.06	0.05	0.04	0.05	0.06	0.05	0.06	0.06	0.06	0.04
***n*-C_{19}-OH**	0.03	0.02	0.07	0.02	0.02	0.02	0.02	0.02	0.02	0.03	0.02
***n*-C_{20}-OH**	0.18	0.16	0.11	0.13	0.14	0.14	0.14	0.14	0.15	0.16	0.11
***n*-C_{21}-OH**	0.10	0.11	0.09	0.09	0.09	0.09	0.11	0.09	0.10	0.11	0.07
***n*-C_{22}-OH**	0.99	1.05	0.78	0.85	0.80	0.90	0.79	0.80	0.87	0.86	0.62
***n*-C_{23}-OH**	0.27	0.32	0.24	0.24	0.25	0.26	0.26	0.26	0.28	0.29	0.21
***n*-C_{24}-OH**	2.51	3.19	2.34	2.61	2.43	2.75	2.38	2.43	2.72	2.62	1.87
***n*-C_{25}-OH**	0.53	0.67	0.50	0.55	0.56	0.61	0.55	0.54	0.61	0.64	0.41
***n*-C_{26}-OH**	3.90	5.43	3.82	4.98	4.04	4.69	4.03	4.04	4.53	4.36	2.92
***n*-C_{27}-OH**	0.97	1.18	0.90	1.08	0.90	1.07	1.01	0.98	1.05	1.05	0.72
***n*-C_{28}-OH**	10.2	13.5	9.82	11.7	9.49	10.7	10.1	9.92	11.1	10.1	7.46
***n*-C_{29}-OH**	0.81	1.05	0.83	0.80	0.90	0.82	0.96	0.84	0.98	0.87	0.84
***n*-C_{30}-OH**	8.51	12.0	9.06	8.69	9.46	8.17	9.59	8.51	10.4	8.33	8.70
***n*-C_{31}-OH**	0.40	0.46	0.40	0.39	0.42	0.39	0.48	0.44	0.41	0.47	0.41
***n*-C_{32}-OH**	4.24	5.26	4.35	4.27	4.46	3.90	4.81	4.45	4.33	4.50	4.22
Phytol	0.57	0.25	0.19	0.21	0.09	0.14	0.07	0.12	0.1	0.07	0.05
Total n-alkanols	34.5	43.7	32.6	35.7	33.1	35.0	34.8	33.2	37.0	33.7	27.7

Table S6. Concentration of *n*-alkanols and phytol (in μg g^{-1}) along each section (in cm) of the Paranaguá core. < LD: below the limit of detection.

Paranaguá core - *n*-alkanols											
Estimated date	**2010**	**2002**	**1995**	**1987**	**1979**	**1968**	**1956**	**1945**	**1933**	**1922**	**1912**
Depth	*0-2*	*2-4*	*4-6*	*6-8*	*8-10*	*11-13*	*14-16*	*17-19*	*20-22*	*23-25*	*26-27*
***n*-C_{12}-OH**	0.05	0.03	0.05	0.05	0.04	0.04	0.08	0.06	0.06	< LD	< LD
***n*-C_{13}-OH**	0.06	0.03	0.03	0.04	0.03	0.03	0.03	0.02	0.04	0.02	< LD
***n*-C_{14}-OH**	0.08	0.05	0.07	0.08	0.07	0.06	0.08	0.05	0.03	0.03	0.02
***n*-C_{15}-OH**	0.52	0.01	0.16	0.13	< LD	0.09	0.31	0.07	0.04	0.12	0.09
***n*-C_{16}-OH**	0.14	0.05	0.09	0.09	0.08	0.08	0.08	0.04	0.05	< LD	0.03
***n*-C_{17}-OH**	0.02	0.01	< LD	0.02	0.02	< LD	0.02	< LD	< LD	0.02	< LD
***n*-C_{18}-OH**	0.09	0.04	0.05	0.06	0.05	0.05	0.05	0.03	0.04	0.02	0.03
***n*-C_{19}-OH**	< LD	< LD	0.02	0.02	0.02	0.02	0.05	0.02	< LD	< LD	< LD
***n*-C_{20}-OH**	0.09	0.05	0.05	0.05	0.05	0.04	0.03	0.03	0.04	0.03	0.03
***n*-C_{21}-OH**	0.04	0.02	0.02	0.03	0.03	0.02	0.02	0.02	0.02	< LD	< LD
***n*-C_{22}-OH**	0.32	0.18	0.24	0.28	0.28	0.20	0.24	0.13	0.11	0.10	0.11
***n*-C_{23}-OH**	0.10	0.06	0.06	0.08	0.08	0.06	0.08	0.05	0.04	0.05	0.04
***n*-C_{24}-OH**	0.84	0.47	0.62	0.79	0.76	0.56	0.71	0.51	0.37	0.42	0.44
***n*-C_{25}-OH**	0.20	0.11	0.14	0.18	0.16	0.12	0.16	0.11	0.09	0.12	0.11
***n*-C_{26}-OH**	1.59	0.88	1.16	1.51	1.41	0.99	1.30	0.97	0.71	0.95	0.89
***n*-C_{27}-OH**	0.44	0.22	0.28	0.36	0.33	0.24	0.30	0.21	0.17	0.24	0.21
***n*-C_{28}-OH**	4.81	2.77	3.33	4.34	4.21	2.81	3.94	2.85	2.11	3.53	3.03
***n*-C_{29}-OH**	0.54	0.28	0.35	0.38	0.40	0.32	0.39	0.27	0.22	0.29	0.22
***n*-C_{30}-OH**	5.87	3.58	4.19	4.63	5.15	3.69	5.08	3.66	2.68	4.28	3.20
***n*-C_{31}-OH**	0.12	0.05	0.07	0.07	0.22	0.05	0.05	0.04	0.05	0.05	0.09
***n*-C_{32}-OH**	1.35	0.68	0.88	0.87	2.79	0.64	0.72	0.48	0.64	0.67	1.30
Phytol	0.11	0.03	0.11	0.12	0.09	0.05	0.07	0.03	< LD	0.02	< LD
Total n-alkanols	16.6	9.24	11.4	13.6	15.6	9.74	13.3	9.31	7.24	10.6	9.53

Table S7. Concentration of *n*-alkanols and phytol (in μg g^{-1}) along each section (in cm) of the Guaratuba core. < LD: below the limit of detection.

Guaratuba core - *n*-alkanols																
Estimated date	**2008**	**2003**	**1997**	**1991**	**1986**	**1980**	**1975**	**1969**	**1964**	**1958**	**1953**	**1947**	**1941**	**1936**	**1930**	**1925**
Depth	*0-2*	*2-4*	*4-6*	*6-8*	*8-10*	*10-12*	*12-14*	*14-16*	*16-18*	*18-20*	*20-22*	*22-24*	*24-26*	*26-28*	*28-30*	*30-32*
***n*-C_{12}-OH**	0.07	0.04	0.03	0.05	0.06	0.07	0.07	0.05	0.06	0.05	0.08	0.06	0.06	0.07	0.05	0.07
***n*-C_{13}-OH**	0.04	0.03	0.02	0.03	0.03	0.04	< LD	0.02	0.04	0.02	0.03	0.03	0.02	0.02	< LD	0.02
***n*-C_{14}-OH**	0.10	0.04	0.03	0.05	0.05	0.04	0.05	0.04	0.04	0.04	0.07	0.04	0.05	0.05	0.04	0.05
***n*-C_{15}-OH**	0.08	0.05	< LD	0.03	0.03	0.07	0.05	0.06	< LD	< LD	< LD	< LD	< LD	< LD	< LD	< LD
***n*-C_{16}-OH**	0.41	0.09	0.07	0.24	0.06	0.06	0.19	0.12	0.09	0.09	0.28	0.09	0.16	0.25	0.11	0.17
***n*-C_{17}-OH**	0.05	0.02	< LD	0.02	0.02	0.02	0.02	0.02	0.02	0.02	< LD	< LD	0.02	0.02	0.02	< LD
***n*-C_{18}-OH**	0.08	0.03	0.02	0.05	0.03	0.03	0.04	0.04	0.04	0.04	0.05	0.04	0.04	0.05	0.04	0.04
***n*-C_{19}-OH**	< LD	< LD	< LD	< LD	< LD	< LD	< LD	< LD	< LD	< LD	< LD	< LD	< LD	< LD	< LD	< LD
***n*-C_{20}-OH**	0.07	0.04	0.03	0.05	0.05	0.05	0.05	0.05	0.06	0.05	0.06	0.05	0.07	0.05	0.05	0.05
***n*-C_{21}-OH**	0.03	0.02	< LD	0.02	0.03	0.02	0.02	0.03	0.03	0.03	0.03	0.03	0.03	0.02	0.02	0.03
***n*-C_{22}-OH**	0.23	0.18	0.13	0.18	0.21	0.22	0.23	0.24	0.27	0.26	0.23	0.25	0.28	0.21	0.20	0.21
***n*-C_{23}-OH**	0.06	0.05	0.04	0.06	0.06	0.06	0.06	0.06	0.07	0.07	0.07	0.07	0.08	0.06	0.06	0.06
***n*-C_{24}-OH**	0.59	0.50	0.43	0.52	0.63	0.61	0.60	0.67	0.73	0.73	0.65	0.69	0.83	0.64	0.59	0.59
***n*-C_{25}-OH**	0.13	0.12	0.11	0.12	0.16	0.14	0.14	0.16	0.17	0.18	0.16	0.17	0.20	0.15	0.14	0.14
***n*-C_{26}-OH**	1.20	1.06	0.96	1.09	1.52	1.23	1.19	1.40	1.53	1.56	1.39	1.49	1.76	1.36	1.26	1.21
***n*-C_{27}-OH**	0.27	0.24	0.22	0.25	0.35	0.29	0.27	0.30	0.35	0.35	0.32	0.34	0.39	0.29	0.27	0.27
***n*-C_{28}-OH**	3.78	3.60	3.43	3.57	5.47	3.87	3.94	4.51	5.15	4.95	4.97	4.57	5.72	4.64	4.00	3.57
***n*-C_{29}-OH**	0.85	0.69	0.29	0.68	0.79	1.07	0.68	1.11	1.14	1.20	1.00	1.04	1.09	0.89	0.81	0.84
***n*-C_{30}-OH**	3.00	3.58	3.11	3.35	5.54	2.64	3.32	4.21	3.39	3.33	4.52	3.16	2.94	2.80	2.64	2.01
***n*-C_{31}-OH**	0.29	0.20	0.06	0.23	0.20	0.73	0.29	0.43	0.50	0.58	0.28	0.49	0.72	0.39	1.76	0.56
***n*-C_{32}-OH**	1.02	1.05	0.59	1.15	1.43	1.79	1.42	1.64	1.48	1.60	1.28	1.50	1.95	1.24	5.72	1.35
Phytol	0.05	0.02	< LD	0.02	0.02	0.02	0.02	0.02	0.02	0.02	0.03	0.02	0.03	0.02	0.02	0.02
Total n-alkanols	12.1	11.4	9.51	11.5	16.5	12.3	12.3	14.7	14.7	14.6	15.2	13.6	15.7	12.8	16.0	10.7

Table S8. Concentration of sterols (in μg g^{-1}) along each section (in cm) of the Antonina core. < LD: below the limit of detection.

Antonina core - sterols											
Estimated date	**2012**	**2008**	**2004**	**2000**	**1996**	**1989**	**1983**	**1977**	**1971**	**1965**	**1960**
Depth	*0-2*	*2-4*	*4-6*	*6-8*	*8-10*	*11-13*	*14-16*	*17-19*	*20-22*	*23-25*	*26-27*
$27\Delta^{5,22E}$	1.70	0.55	0.06	0.05	0.04	0.02	0.04	0.02	0.03	0.01	0.04
$27\Delta^{5}$	2.56	2.13	0.62	0.56	0.58	0.45	0.48	0.31	0.34	0.35	0.77
$27\Delta^{0}$	1.28	0.66	0.50	0.50	0.53	0.49	0.49	0.39	0.39	0.41	0.77
$28\Delta^{5,22E}$	1.66	0.58	0.16	0.13	0.14	0.14	0.11	0.10	0.09	0.05	0.20
$28\Delta^{5}$	0.64	0.35	0.14	0.14	0.14	0.13	0.11	0.07	0.08	0.07	0.09
$29\Delta^{5,22E}$	2.03	3.01	3.66	1.54	1.58	1.54	1.14	0.92	1.06	0.97	2.18
$29\Delta^{5}$	2.55	2.66	2.22	1.68	1.93	1.73	1.64	1.14	1.37	1.55	1.19
$29\Delta^{0}$	0.79	0.99	0.83	0.73	0.86	0.78	0.69	0.57	0.63	0.69	0.51
$30\Delta^{22E}$	0.05	0.07	0.05	0.06	0.06	0.07	0.06	0.04	0.06	0.07	0.07
Total sterols	13.3	11.0	8.24	5.39	5.86	5.35	4.76	3.56	4.05	4.17	5.82

Table S9. Concentration of sterols (in μg g^{-1}) along each section (in cm) of the Paranaguá core. < LD: below the limit of detection.

Paranaguá core - sterols											
Estimated date	**2010**	**2002**	**1995**	**1987**	**1979**	**1968**	**1956**	**1945**	**1933**	**1922**	**1912**
Depth	*0-2*	*2-4*	*4-6*	*6-8*	*8-10*	*11-13*	*14-16*	*17-19*	*20-22*	*23-25*	*26-27*
$27\Delta^{5,22E}$	0.27	0.23	0.12	0.09	0.09	0.04	0.02	< LD	0.01	< LD	< LD
$27\Delta^{5}$	1.54	1.42	0.78	0.67	0.55	0.34	0.27	0.15	0.15	0.11	0.14
$27\Delta^{0}$	0.35	0.64	0.48	0.38	0.31	0.18	0.17	0.07	0.05	0.04	0.02
$28\Delta^{5,22E}$	0.52	0.63	0.26	0.24	0.24	0.14	0.09	0.04	0.06	0.02	0.01
$28\Delta^{5}$	0.33	0.47	0.29	0.25	0.22	0.15	0.09	0.03	0.03	0.02	0.02
$29\Delta^{5,22E}$	0.86	1.83	0.82	0.72	0.68	0.71	0.98	0.51	0.20	0.19	0.25
$29\Delta^{5}$	1.05	1.66	1.16	0.95	0.95	0.80	0.67	0.44	0.43	0.42	0.41
$29\Delta^{0}$	0.38	0.68	0.49	0.39	0.41	0.32	0.29	0.14	0.16	0.15	0.10
$30\Delta^{22E}$	0.03	0.03	0.03	0.03	0.03	0.03	0.03	0.03	0.02	0.02	0.02
Total sterols	5.33	7.59	4.43	3.72	3.48	2.71	2.61	1.41	1.11	0.97	0.97

Table S10. Concentration of sterols (in µg g^{-1}) along each section (in cm) of the Guaratuba core. < LD: below the limit of detection. na: not analysed.

Guaratuba core - sterols																
Estimated date	**2008**	**2003**	**1997**	**1991**	**1986**	**1980**	**1975**	**1969**	**1964**	**1958**	**1953**	**1947**	**1941**	**1936**	**1930**	**1925**
Depth	*0-2*	*2-4*	*4-6*	*6-8*	*8-10*	*10-12*	*12-14*	*14-16*	*16-18*	*18-20*	*20-22*	*22-24*	*24-26*	*26-28*	*28-30*	*30-32*
$27\Delta^{5,22E}$	0.02	0.02	0.04	0.03	0.03	0.25	0.04	0.04	0.03	0.04	0.04	0.05	0.05	0.07	0.03	0.04
$27\Delta^{5}$	0.35	0.14	0.12	0.11	0.11	0.11	0.10	0.10	0.10	0.09	0.08	0.10	0.08	0.08	0.08	0.08
$27\Delta^{0}$	0.09	0.07	0.07	0.05	0.06	0.06	0.05	0.06	0.07	0.06	0.06	0.06	0.05	0.05	0.06	0.04
$28\Delta^{5,22E}$	na	na	na	na	na	na	na	na	na	na	na	na	na	na	na	na
$28\Delta^{5}$	0.08	0.07	0.09	0.07	0.07	0.08	0.07	0.08	0.12	0.11	0.11	0.10	0.10	0.09	0.10	0.07
$29\Delta^{5,22E}$	0.24	0.23	0.20	0.20	0.23	0.23	0.21	0.25	0.24	0.22	0.20	0.22	0.21	0.20	0.23	0.22
$29\Delta^{5}$	0.46	0.38	0.38	0.37	0.43	0.44	0.39	0.40	0.50	0.47	0.43	0.48	0.41	0.41	0.45	0.47
$29\Delta^{0}$	0.10	0.08	0.10	0.10	0.09	0.08	0.09	0.11	0.10	0.10	0.10	0.12	0.11	0.09	0.18	0.11
$30\Delta^{22E}$	na	na	na	na	na	na	na	na	na	na	na	na	na	na	na	na
Total sterols	1.34	0.99	1.00	0.93	1.02	1.25	0.95	1.04	1.16	1.09	1.02	1.13	1.01	0.99	1.13	1.03

Table S11. Spearman correlations to the parameters analysed in Antonina core (AC). Parameters: fine sediments (silt + clay; fine), total organic carbon (TOC), $\delta^{13}C$, total nitrogen (TN), $\delta^{15}N$, long chain *n*-alkanes (Alk_L), mid-chain *n*-alkanes (Alk_M), short chain *n*-alkanes (Alk_S), long chain *n*-alkanols (OH_L), mid-chain *n*-alkanols (OH_M), short chain *n*-alkanols (OH_S), dehydrocholesterol ($27\Delta^{\square\square\square}$), cholesterol ($27\Delta^5$), campesterol ($28\Delta^5$), stigmasterol ($29\Delta^{5,22}$), sitosterol ($29\Delta^5$), population (pop) and total annual precipitation (prec). Bold values represent significant ρ-value ($\alpha < 0.05$).

AC	*fine*	*TOC*	*$\delta^{13}C$*	*TN*	*$\delta^{15}N$*	*Alk_L*	*Alk_M*	*Alk_S*	*OH_L*	*OH_M*	*OH_S*	*$27\Delta^{5,22}$*	*$27\Delta^5$*	*$28\Delta^5$*	*$29\Delta^{5,22}$*	*$29\Delta^5$*	*pop*	*prec*
fine																		
TOC	-0.16																	
$\delta^{13}C$	-0.29	0.00																
TN	-0.06	0.06	0.23															
$\delta^{15}N$	0.09	**-0.75**	0.17	0.03														
Alk_L	-0.24	0.07	-0.02	-0.29	0.17													
Alk_M	-0.17	0.35	-0.06	0.12	-0.09	**0.74**												
Alk_S	0.26	0.57	-0.29	0.35	-0.37	0.15	0.52											
OH_L	**-0.81**	0.35	0.48	-0.06	-0.31	0.06	0.03	-0.35										
OH_M	-0.33	0.45	0.32	-0.12	-0.22	0.32	0.24	-0.27	0.48									
OH_S	-0.13	0.40	0.51	0.32	-0.16	0.05	0.01	0.06	0.12	0.64								
$27\Delta^{5,22}$	-0.08	**0.73**	0.20	0.23	-0.65	-0.27	0.17	0.47	0.44	0.02	0.00							
$27\Delta^5$	0.05	0.68	-0.05	0.46	-0.63	-0.31	0.33	0.68	0.11	-0.10	0.01	**0.87**						
$28\Delta^5$	-0.10	**0.92**	-0.02	0.09	**-0.87**	-0.17	0.22	0.53	0.38	0.24	0.18	**0.89**	**0.83**					
$29\Delta^{5,22}$	-0.01	0.66	-0.19	0.17	-0.55	0.02	0.55	**0.73**	0.10	-0.15	-0.20	**0.79**	**0.89**	**0.76**				
$29\Delta^5$	-0.28	**0.91**	0.01	0.12	**-0.87**	0.10	0.41	0.58	0.40	0.32	0.33	**0.73**	**0.71**	**0.92**	**0.70**			
pop	0.17	0.69	0.05	-0.55	-0.52	0.24	0.31	0.24	0.00	0.24	0.24	0.59	0.19	0.61	0.33	0.62		
prec	-0.15	**0.78**	-0.12	0.12	**-0.86**	-0.43	-0.05	0.34	0.41	0.16	0.34	**0.79**	**0.74**	**0.92**	0.57	**0.78**	0.48	

Table S12. Spearman correlations to the parameters analysed in Paranaguá core (PC). Parameters: fine sediments (silt + clay; fine), total organic carbon (TOC), $\delta^{13}C$, total nitrogen (TN), $\delta^{15}N$, long chain *n*-alkanes (Alk_L), mid-chain *n*-alkanes (Alk_M), short chain *n*-alkanes (Alk_S), long chain *n*-alkanols (OH_L), mid-chain *n*-alkanols (OH_M), short chain *n*-alkanols (OH_S), dehydrocholesterol ($27\Delta^{5,22}$), cholesterol ($27\Delta^{5}$), campesterol ($28\Delta^{5}$), stigmasterol ($29\Delta^{5,22}$), sitosterol ($29\Delta^{5}$), population (pop) and total annual precipitation (prec). Bold values represent significant ρ-value ($\alpha < 0.05$).

PC	*fine*	*TOC*	*$\delta^{13}C$*	*TN*	*$\delta^{15}N$*	*Alk_L*	*Alk_M*	*Alk_S*	*OH_L*	*OH_M*	*OH_S*	*$27\Delta^{5,22}$*	*$27\Delta^{5}$*	*$28\Delta^{5}$*	*$29\Delta^{5,22}$*	*$29\Delta^{5}$*	*pop*	*prec*
fine																		
TOC	**0.75**																	
$\delta^{13}C$	-0.17	-0.01																
TN	0.55	**0.78**	0.28															
$\delta^{15}N$	0.52	0.52	0.49	0.56														
Alk_L	**0.75**	**0.96**	0.07	**0.81**	**0.76**													
Alk_M	0.56	0.54	0.08	**0.86**	0.40	0.62												
Alk_S	0.31	0.53	0.26	**0.86**	0.40	0.55	**0.83**											
OH_L	0.68	0.59	0.05	0.43	0.65	0.60	0.31	0.34										
OH_M	0.55	0.62	0.11	**0.75**	0.45	0.63	0.63	0.68	**0.79**									
OH_S	0.42	0.69	0.19	**0.78**	0.35	0.65	0.49	0.68	0.58	**0.87**								
$27\Delta^{5,22}$	0.40	**0.83**	0.34	**0.87**	0.61	**0.84**	0.55	**0.72**	0.40	0.65	**0.84**							
$27\Delta^{5}$	0.39	**0.81**	0.32	**0.92**	0.52	**0.80**	0.63	**0.77**	0.35	0.68	**0.85**	**0.98**						
$28\Delta^{5}$	0.40	**0.80**	0.33	**0.91**	0.54	**0.81**	0.65	**0.74**	0.30	0.63	**0.79**	**0.97**	**0.99**					
$29\Delta^{5,22}$	0.50	0.68	0.09	**0.91**	0.45	**0.75**	**0.89**	**0.84**	0.26	0.59	0.63	**0.78**	**0.82**	**0.83**				
$29\Delta^{5}$	0.40	**0.77**	0.28	**0.86**	0.51	**0.78**	0.63	**0.73**	0.28	0.61	**0.76**	**0.94**	**0.96**	**0.98**	**0.81**			
pop	0.03	0.67	**0.75**	**0.84**	**0.72**	0.68	0.36	0.58	0.27	0.47	0.70	**0.97**	**0.98**	**0.97**	0.60	**0.93**		
prec	0.40	0.52	0.60	**0.81**	0.52	0.52	0.57	0.60	0.19	0.17	0.29	**0.72**	**0.79**	**0.79**	0.62	**0.81**	**0.82**	

Table S13. Spearman correlations to the parameters analysed in Guaratuba core (GC). Parameters: fine sediments (silt + clay; fine), total organic carbon (TOC), $\delta^{13}C$, total nitrogen (TN), $\delta^{15}N$, long chain *n*-alkanes (Alk_L), mid-chain *n*-alkanes (Alk_M), short chain *n*-alkanes (Alk_S), long chain *n*-alkanols (OH_L), mid-chain *n*-alkanols (OH_M), short chain *n*-alkanols (OH_S), dehydrocholesterol ($27\Delta^{5,22}$), cholesterol ($27\Delta^{5}$), campesterol ($28\Delta^{5}$), stigmasterol ($29\Delta^{5,22}$), sitosterol ($29\Delta^{5}$), population (pop) and total annual precipitation (prec). Bold values represent significant ρ-value ($\alpha < 0.05$).

GC	*fine*	*TOC*	*$\delta^{13}C$*	*TN*	*$\delta^{15}N$*	*Alk_L*	*Alk_M*	*Alk_S*	*OH_L*	*OH_M*	*OH_S*	*$27\Delta^{5,22}$*	*$27\Delta^{5}$*	*$28\Delta^{5}$*	*$29\Delta^{5,22}$*	*$29\Delta^{5}$*	*pop*	*prec*
fine																		
TOC	0.13																	
$\delta^{13}C$	0.44	-0.26																
TN	0.06	0.60	-0.08															
$\delta^{15}N$	0.01	0.30	0.08	-0.16														
Alk_L	-0.19	0.53	-0.05	0.38	-0.01													
Alk_M	-0.12	0.47	-0.02	0.38	-0.04	**0.98**												
Alk_S	0.27	0.16	0.37	0.30	0.17	0.50	0.56											
OH_L	-0.23	0.07	-0.33	0.37	-0.29	0.31	0.28	-0.08										
OH_M	-0.25	0.58	-0.39	0.58	-0.22	**0.75**	0.70	0.17	**0.72**									
OH_S	0.00	-0.07	0.15	0.06	0.15	0.17	0.18	0.66	-0.03	-0.01								
$27\Delta^{5,22}$	-0.16	0.43	-0.39	0.09	0.15	0.46	0.42	0.04	0.03	0.35	-0.05							
$27\Delta^{5}$	0.35	0.04	0.15	0.05	0.07	**-0.70**	**-0.72**	-0.34	-0.44	-0.45	-0.36	-0.47						
$28\Delta^{5}$	-0.19	0.26	0.26	0.24	-0.07	**0.72**	0.63	0.24	0.45	0.63	0.02	0.25	-0.45					
$29\Delta^{5,22}$	0.19	0.39	0.03	0.45	0.15	0.01	0.02	-0.08	0.19	0.20	-0.24	-0.40	0.31	-0.04				
$29\Delta^{5}$	-0.01	0.52	0.15	0.59	-0.10	**0.74**	**0.75**	0.29	0.19	0.53	-0.05	0.07	-0.30	0.52	0.42			
pop	0.42	-0.02	0.22	-0.46	0.47	**-0.73**	**-0.78**	-0.36	-0.38	-0.60	-0.23	-0.39	**0.94**	-0.04	0.03	-0.54		
prec	-0.29	0.38	-0.60	0.28	0.21	0.36	0.30	-0.41	0.69	0.50	-0.48	**0.80**	-0.60	0.25	0.34	0.19	-0.60	

Table S14. Description of dimension of PCA. Population (pop), total annual precipitation (prec), fine sediment (silt + clay; fine), short-chain *n*-alkanes (Alk_S), long-chain *n*-alkanes (Alk_L), short-chain *n*-alkanols (OH_S), long-chain *n*-alkanols (OH_L), terrigenous sterols (Sitoe_Stige; $29\Delta^{5,22}$ and $29\Delta^{5}$), marine sterols (Dehye_Chole, $27\Delta^{5,22}$ and $27\Delta^{5}$), $\delta^{13}C$, $\delta^{15}N$, CPI (Preferential Carbon Index) and the sterol ratio Sitoe_Chole_Sitoe ($29\Delta^{5}/27\Delta^{5} + 29\Delta^{5}$).

	Antonina core		**Paranaguá core**		**Guaratuba core**	
	PC1	*PC2*	*PC1*	*PC2*	*PC1*	*PC2*
pop	0.68		0.89			-0.55
prec	0.78					
fine	-0.60			0.75		
Alk_S		0.69	0.72		0.56	
Alk_L		0.73	0.86			0.90
OH_S	0.75		0.72		0.62	
OH_L						
Sitoe_Stige	0.72		0.84			0.81
Dehye_Chole	0.81		0.97		0.67	
$\delta^{13}C$				-0.68	0.90	
$\delta^{15}N$	-0.73		0.84			
CPI			0.70		-0.56	
Sitoe_Chole_Sitoe				0.80		0.71

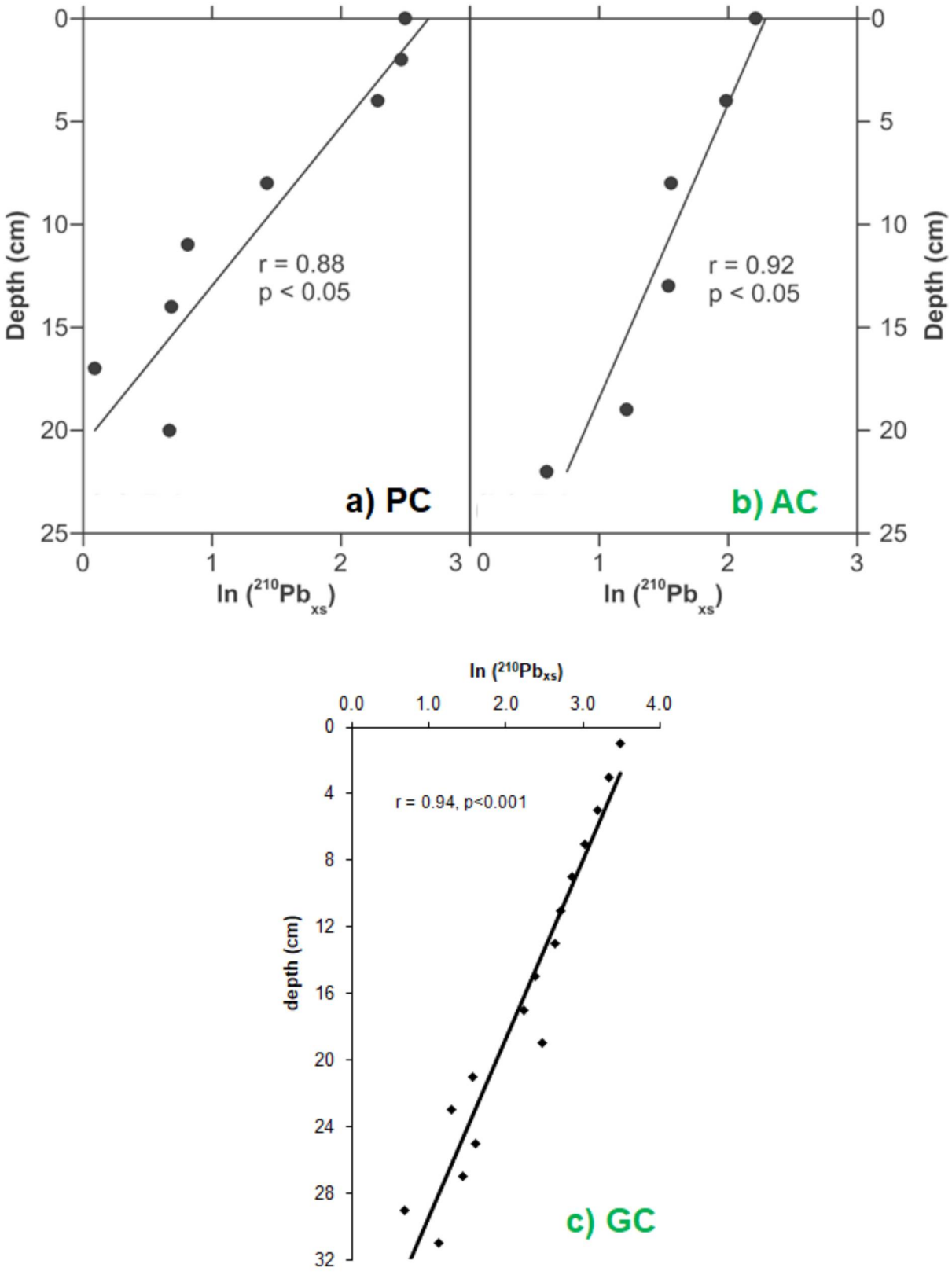

Fig. S1. CIC (Constant Initial Concentration) model applied to the vertical profiles of Lead-210 (as ln ($^{210}Pb_{xs}$)) in the studied sediment cores. (a) Paranaguá Core - PC, (b) Antonina Core - AC, (c) Guaratuba Core - GC.

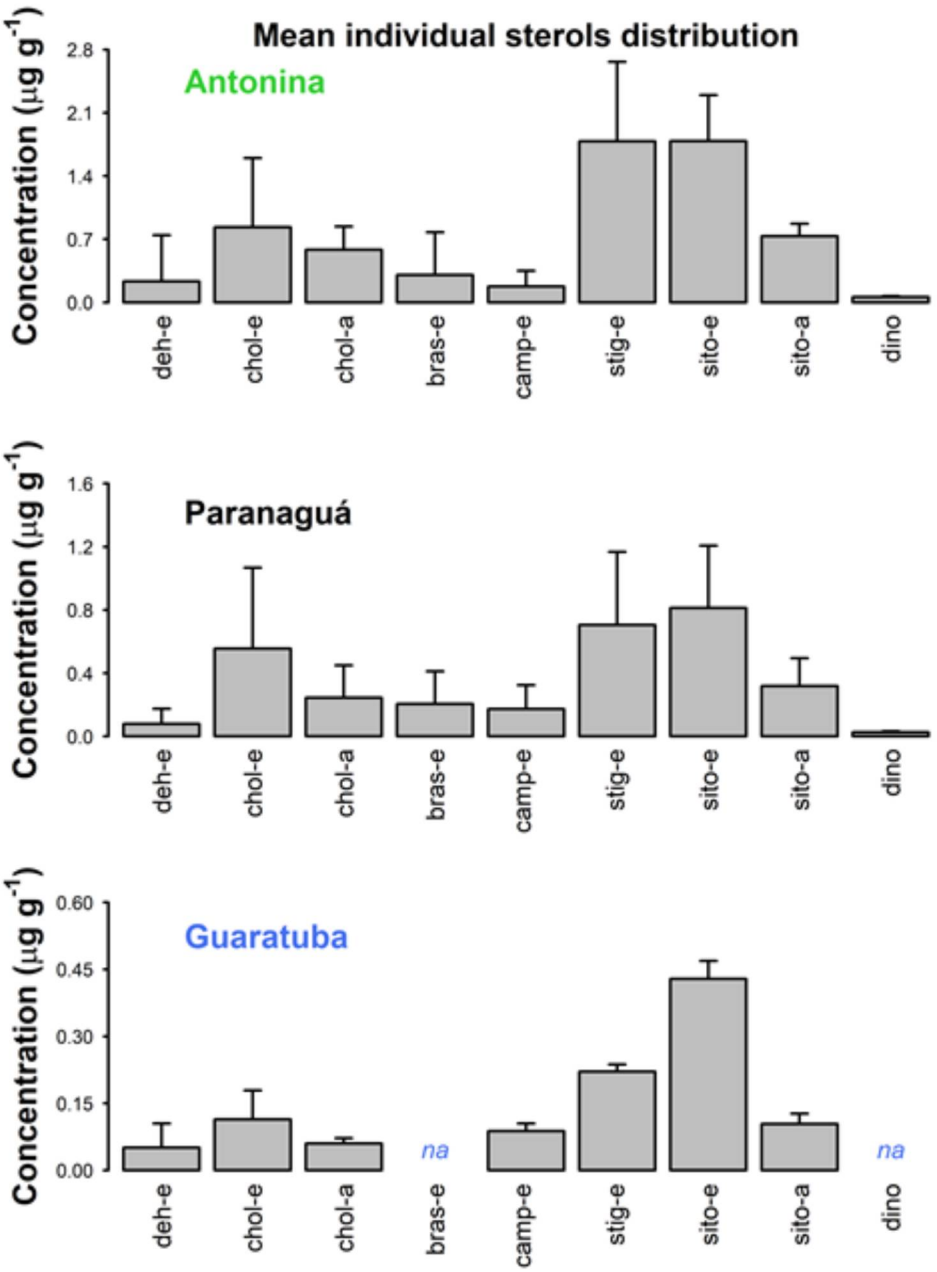

Fig. S2. Mean concentrations of individual sterols, both in µg g^{-1}. The error bars reflect the standard deviations of the compounds among the depths from each sediment core. Abbreviations: deh-e: dehydrocholesterol ($27\Delta^{5,22E}$); chol-e: cholesterol ($27\Delta^{5}$); chol-a: cholestanol ($27\Delta^{0}$); bras-e: brassicasterol ($28\Delta^{5,22E}$); camp-e: campesterol ($28\Delta^{5}$); stig-e: stigmasterol ($29\Delta^{5,22E}$); sito-e: sitosterol ($29\Delta^{5}$); dino: dinosterol ($30\Delta^{22E}$).

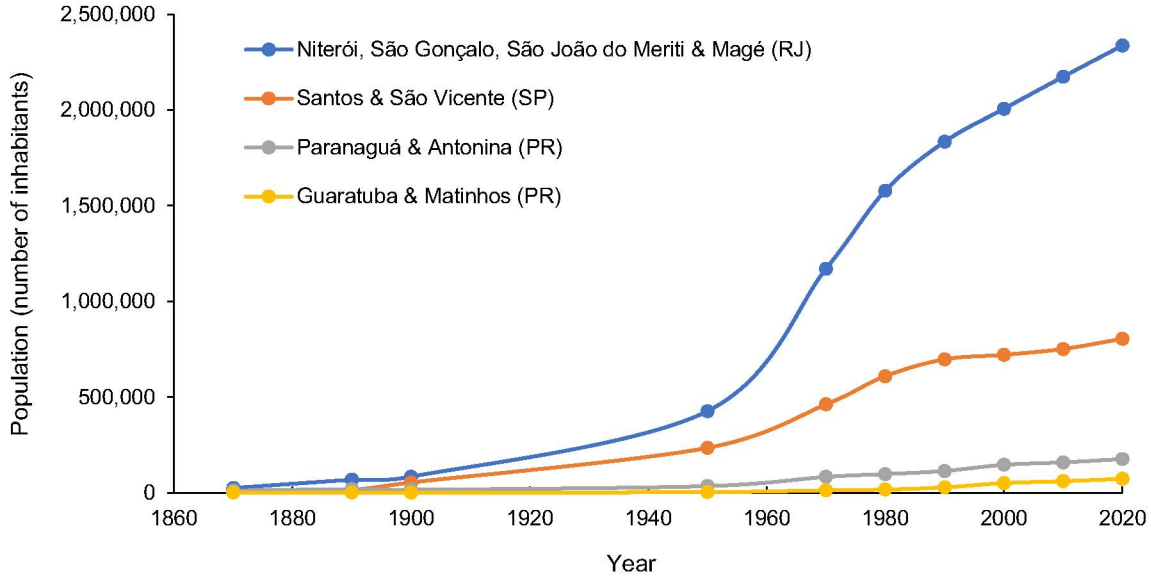

Fig. S3. Population growth (in number of inhabitants) in the last century comparing the population of main cities around Guanabara Bay, RJ (Niterói, São Gonçalo, São João do Meriti and Magé cites), Santos estuary, SP (Santos and São Vicente cities), Paranaguá Bay, PR (Paranaguá and Antonina cities) and Guaratuba Bay, PR (Guaratuba and Matinhos cities), obtained from IBGE (Instituto Brasileiro de Geografia e Estatística), 2022. Censos demográficos de 1870 – 2020. Data between 1900 and 1950 and 1950 and 1970 are not available.

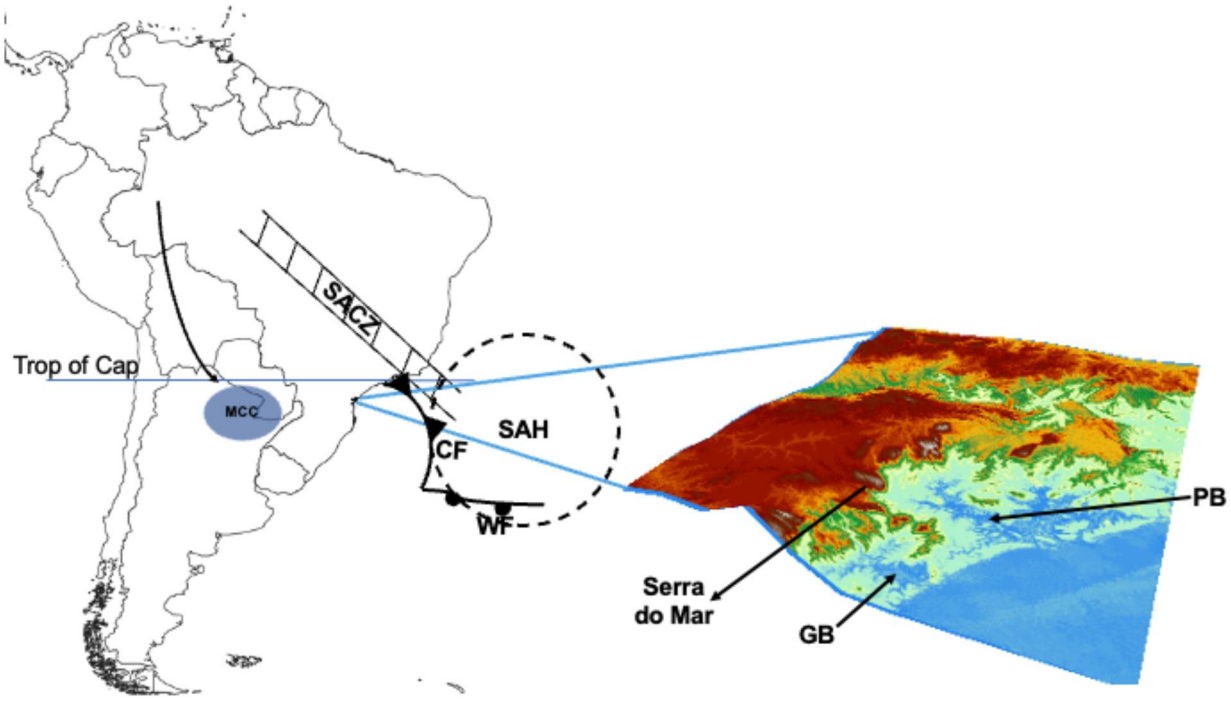

Figure S4. Schematic representation of the atmospheric systems acting on the areas of Paranaguá estuarine system (PB) and Guaratuba Bay (GB) during austral summer (adapted from Reboita et al., 2010). SAH: South Atlantic High, MCC: mesoscale convective complex, CF: cold fronts, WF: warm fronts, Trop of Cap: Tropic of Capricorn, SACZ: South Atlantic Convergence Zone.